EXHIBIT C30

IN THE UNITED STATES DISTRICT COURT
FOR THE DISTRICT OF NEW JERSEY

IN RE: JOHNSON & JOHNSON TALCUM POWDER PRODUCTS MARKETING, SALES PRACTICES AND PRODUCTS LIABILITY LITIGATION ***THIS DOCUMENT RELATES TO ALL CASES***	**MDL NO. 16-2738 (FLW) (LHG)**

EXPERT REPORT OF M. DARBY DYAR, PHD FOR GENERAL CAUSATION *DAUBERT* HEARING

Date: February 25, 2019

M. Darby Dyar

M. Darby Dyar, Ph.D.

TABLE OF CONTENTS

Page

I. EXECUTIVE SUMMARY

To confirm the presence of asbestos in talcum powder, there are three questions to consider:

1. **Mineralogy**: Are the mineral species present among those that include asbestos?

2. **Physical properties (habit)**: Do the minerals have an "asbestiform" habit, occurring as particles that are lengthwise separable into flexible fibers?

3. **Concentration**: What are the abundances of the minerals?

The expert reports dated November 14, 2018, January 15, 2019 and February 2, 2019 from plaintiffs' experts William E. Longo and Mark W. Rigler (the "Longo/Rigler MDL Reports") fail to demonstrate that **any** of these three requirements is true of the impurities allegedly occurring in the tested talcum powder. Instead, they (or more specifically, their five analysts) applied a methodology that was inherently designed to achieve the results they desired for purposes of this litigation.

As an initial matter, many minerals have very similar chemical formulas, and many minerals occur with fibrous shapes, but not all of these minerals are "asbestos." Asbestos minerals have both a specific chemical composition and a unique 'habit' or morphology. Asbestos is defined as one of six particular minerals exhibiting the characteristics of an asbestiform habit, meaning they can be separated into flexible fibers with high tensile strength. Drs. Longo and Rigler confuse "counting criteria" with this definition, using a disingenuous distinction between what they call the "geological definition" and what they wrongly invent as the "regulatory definition." This is not scientifically proper.

- **EDS (mineral chemistry)**. Drs. Longo and Rigler opine on tests run by their analysts using Energy Dispersive Spectroscopy ("EDS") to identify the chemistry of certain particles that they have isolated in the samples tested. EDS, properly used, can somewhat measure the chemistry of a mineral, or at least narrow down the possible chemistries, even if it cannot tell a scientist whether that mineral's shape is asbestiform or not. But the analysts do not follow generally accepted scientific methodology in their EDS analysis. For example:

  - They "eyeball" the EDS spectra and rely only on the images generated by an EDS analysis to evaluate the chemical composition of each mineral.

  - They visually compare their spectra to "reference standards" apparently belonging to their lab only, which standards are not in the published literature, which likely represent only asbestiform minerals and which Drs. Longo and Rigler did not produce (such that it cannot be determined if these standards have any scientific validity whatsoever).

  - In doing so, they deliberately choose not to generate **quantitative numbers** that would more accurately determine chemical compositions, which is the very purpose of an EDS analysis of an unknown mineral. The quantitative data is necessary to make scientifically valid conclusions, and their conclusions are therefore unsupportable.

As a result, Drs. Longo and Rigler and their analysts used a flawed methodology that resulted in wildly inconsistent results across different analysts and over time. In science, proof involves demonstrating that a result is replicable. Consequently, the particles that they identify as "anthophyllite" may actually be talc, cummingtonite or other minerals. The particles that they identify as "tremolite" could be other amphiboles[1], diopside (pyroxene) or other minerals.

Finally, confirming the lack of reproducibility in their methodologies, I have analyzed the EDS interpretations of each of the five separate analysts used by Drs. Longo and Rigler. Although there should be parallel results across analysts, there is clear evidence of personal biases, which is unsurprising given the unscientific and subjective nature of the methodologies employed.

- **SAED (crystal structure)**. Drs. Longo and Rigler opine on tests run by their analysts using selected area electron diffraction (SAED) to identify the crystal structure of selected particles in the samples tested. Again, they do not follow generally accepted scientific methodology in their SAED analysis. For example:

  - A majority of the patterns they generate are of poor quality, making them impractical or impossible to interpret.

  - For an accurate identification of an unknown mineral, at least two (and preferably more) SAED patterns must be taken with the sample oriented along a "zone axis."[2] Yet for those minerals identified as "tremolite," they use only one SAED pattern, resulting in inconclusive data that would be consistent with many other minerals, including those that have no asbestiform habit. Similarly, for those minerals that they identify as "anthophyllite," the analysts took two SAED patterns for only two samples, and these are insufficient to uniquely identify anthophyllite.

  - A fundamental part of analyzing SAED results is to calculate the "*d*-spacings" between layers of atoms, which may be diagnostic of each mineral species. It appears that Drs. Longo and Rigler and their analysts did not initially use *d*-spacings at all, once again adopting qualitative "eyeball" methodologies found nowhere in the literature over quantitative, accepted science. **After** generating their first report, they used a small number of *d*-spacing measurements to "verify" their prior conclusions. Yet those "verifications" show *d*-spacings that are consistent with **25% of all common rock-forming minerals**. Even Drs. Longo and Rigler concede they do not uniquely identify any one mineral.

  - Some of the Longo/Rigler *d*-spacing interpretations even have impossible values, demonstrating significant flaws in the methodology used.

[1] Amphibole is the group name of a group of hydrous silicate minerals that include, among other individual minerals, tremolite, actinolite and anthophyllite.

[2] The zone axis is the direct crystal axis that is parallel to the electron beam at the orientation when the SAED pattern is recorded

- The EPA "Yamate III" protocol for analyzing talc for impurities – which Drs. Longo and Rigler say they followed – requires two SAED zone axis determinations. Yet, of the more than 70 bottles tested, Drs. Longo and Rigler only did this for **two** bottles.

As a result, what Drs. Longo and Rigler identify as anthophyllite or tremolite in the samples analyzed may actually be hundreds of other possible minerals or individual crystal structures.

- **TEM visual inspection**. The analysts in the Longo/Rigler MDL Reports purport to find the concentration of "asbestos" using visual inspection techniques under TEM. They do not, however, follow generally accepted scientific methodology in this analysis. For example:

  - Use of TEM images to **visually** distinguish non-asbestiform amphiboles and asbestiform amphiboles is scientifically invalid, as stated by the very protocols upon which Drs. Longo and Rigler rely.

    - Indeed, Drs. Longo and Rigler and their analysts did not apply objective criteria for distinguishing between cleavage fragments, bundles and fibers, as demonstrated by the inconsistent results of their analysts.

    - Moreover, the results reported in the Longo/Rigler MDL Reports are inconsistent from analyst to analyst, highlighting the unreliability of their method of visual identification using TEM.

  - The analysts used by Drs. Longo and Rigler utilized the concept of "aspect ratio" – the ratio of a particle's length to width – and counted all particles greater than 0.5 μm in length that have substantially parallel sides and an aspect ratio greater than 5:1. Yet, as Drs. Longo and Rigler admit, a particle that is non-asbestiform **can also have an aspect ratio greater** than 5:1. This means that the Longo/Rigler MDL Reports do not distinguish asbestiform minerals from non-asbestiform minerals (e.g., "cleavage fragments") in this regard.

  - This is scientifically invalid because, based on peer-reviewed studies, it is known that size distributions for non-asbestiform particles are different than those for asbestiform particles. Using statistical methods – methods not used by Drs. Longo and Rigler – asbestiform and non-asbestiform populations can readily be distinguished. **However, Drs. Longo and Rigler deliberately did not compile data in the low aspect ratio range, making a valid particle analysis impossible**.

  - To the extent analysis is possible of the aspect ratio size population they did measure, statistical tests of aspect ratio populations establish that the particles measured by the analysts used by Drs. Longo and Rigler belong to the population represented by **non-asbestiform tremolite**.

- **PLM (mineral identification)**. The analysts used polarizing light microscope (PLM) images to identify the nature of any asbestos in the tested samples and the concentration. They did not, however, follow generally accepted scientific methodology in their PLM analysis. For example:

- The analysts purported to follow the methodology found in a peer-reviewed article by Su (2003). But Su sets forth a particular methodology to do dispersion staining, an absolutely critical step of the analysis, which was not followed.

- Otherwise, the PLM images from the Longo/Rigler MDL Reports are in many cases ambiguous because talc and amphiboles have overlapping and similar optical properties, and they can easily be confused for each other.

- The analysts doing the PLM work purported to use two methodologies to determine concentration of asbestos contaminants – "ISO" PLM and "Blount" PLM – which should have consistent results. All tests using the former were either negative or under 0.1% by weight percentage (consistent with the absence of asbestos). Ten of the tests using the latter were positive at concentrations up to seven times the results of the former, which indicates a complete lack of reliability and reproducibility in this PLM testing.

- Dr. Longo and Rigler's "concentration" analysis did not use "point counting," which is the standard method to estimate concentration of phases by PLM. Rather, Drs. Longo and Rigler's analysts used, once again, visual reference charts that appear to be unique to their lab, are not in the peer-reviewed literature, and are not produced (such that it cannot be determined if these standards have any scientific validity whatsoever).

In summary, the results in the Longo/Rigler MDL Reports are the product of fundamentally flawed methodologies and are **not the result of work done according to generally accepted scientific standards and methodologies.** Despite producing lengthy, descriptive reports and undertaking extensive measurements according to government protocols, Drs. Longo and Rigler did not properly train their personnel for the task of characterizing impurities in talc, where the possible mineralogy is unconstrained. Thus, they lack the background to understand or interpret their results, especially where, as here, the impurities are tiny, and many possible minerals can be present.

The Longo/Rigler MDL Reports simply fail to demonstrate that *any* asbestos minerals are present in the material Drs. Longo and Rigler tested in *any* concentration with *any* asbestiform shapes.[3] Indeed, every methodological error in their testing results in false positive findings of asbestos, but not false negatives. Given that Drs. Longo and Rigler's testing can only be described as a series of errors, each of which acts to amplify the errors preceding it, the results of Drs. Longo and Rigler's testing cannot be considered scientifically valid.

All opinions in this report are stated to a reasonable degree of scientific certainty, and the methods used are among those that I employ in my professional work as a mineralogist.

[3] IARC (2012) defines the minerals that can be asbestos as follows: "the generic commercial designation for a group of naturally occurring mineral silicate fibres of the serpentine and amphibole series. These include the serpentine mineral chrysotile [], and the five amphibole minerals – actinolite, amosite [], anthophyllite, crocidolite [], and tremolite." International Agency for Research on Cancer (2012), *Monographs on the Evaluation of Carcinogenic Risks to Humans Vol. 100C: Asbestos (Chrysotile, Amosite, Crocidolite, Tremolite, Actinolite and Anthophyllite)*, 219.

II. BACKGROUND AND QUALIFICATION

I studied geology at Wellesley College, where my thesis involved field work to create a geologic map of the nearby Broadmoor Wildlife Sanctuary. I received my Ph.D. from the Massachusetts Institute of Technology in geochemistry and mineralogy. My Ph.D. thesis, entitled "Crystal chemistry and statistical analysis of iron in mineral standards, micas, and glasses," focused on minerals from a cross-section of geological problems. I was next a member of the Research Faculty at the California Institute of Technology, before holding faculty positions in the Department of Geological Sciences at the University of Oregon, Department of Geology and Astronomy at West Chester University, and most recently, at Mount Holyoke College, where I began in the Department of Geology and Geography before moving to chair the Department of Astronomy. I now hold an endowed chair as Kennedy-Schelkunoff Professor of Astronomy. I am also a member of the graduate faculty at the University of Massachusetts in Amherst, and a Senior Scientist at the Planetary Science Institute.

Over the course of my years in academia, I have taught mineralogy at least 20 times, including as a teaching assistant at MIT and at all three academic institutions where I have been a faculty member. I have supported public outreach related to mineralogy through the creation of two software programs used in many US states for teaching mineralogy to K-12 students. They include *The Study of Minerals* (1997) and *Hands-On Mineral Identification* (1999). I have also authored two textbooks: *Mineralogy and Optical Mineralogy: A Three-Dimensional Approach* with Mickey E. Gunter (first published in 2008, now in its 2nd edition and also available as an iBook) and *Geostatistics Explained, An Introductory Guide for Earth Scientists* with Steven McKillip (2010).

My research has resulted in more than 250 papers published in peer-reviewed journals, and it spans a number of different topics in mineralogy. Areas of interest have included metamorphic rocks from western Maine, tourmaline mineralogy from worldwide occurrences, mineralogy of rocks (xenoliths) from 90 km below Earth's surface (brought up by volcanoes), and many other rock types. The study of amphibole minerals has been a constant theme throughout my career, starting with a chapter in my thesis, extending to studies of its chemical variation that continue to this day.[4] I have also published several papers relating to the mineralogy of asbestiform minerals, including papers on serpentine and amphibole asbestiform minerals.[5]

---

[4] *See* Dyar (1984) *American Mineralogist*, **69**, 1127-1144; Dyar et al. (1996), in Dyar et al., EDXA, *Mineral Spectroscopy: A Tribute to Roger G. Burns*, Special Publication #5, Geochemical Society, 273-289. Delaney et al. (1996), in Dyar et al., EDXA, *Mineral Spectroscopy: A Tribute to Roger G. Burns*, Special Publication #5, Geochemical Society, 170-177; King et al. (2000) *Earth and Planetary Science Letters*, **178**, 97-112. Gunter et al. (2003) *American Mineralogist*, **88**, 1944-1952; Minitti et al. (2008) *Earth and Planetary Science Letters*, **266**, 46-60; Minitti et al. (2008) *Earth and Planetary Science Letters*, **266**, 288-302; Sanchez et al. (2008) *European Journal of Mineralogy*, **20**, 1043-1053; Lupulescu et al. (2009) *Canadian Mineralogist*, **47**, 909-916; McCanta et al. (2009) *Geochimica et Cosmochimica Acta*, **72**, 5757-5780; Gunter et al. (2011) *American Mineralogist*, **96**, 1414-1417; Dyar et al. (2016) *American Mineralogist*, **101**, 1171-1189; Chan et al. (2016) *Canadian Mineralogist*, **54**, 337-351; Mueller et al. (2017) *European Journal of Mineralogy*, **29**, 167-180; Di Guiseppe et al. (submitted) *Toxicology and Applied Pharmacology*.

[5] O'Hanley and Dyar (1993) *American Mineralogist*, **78**, 391-404; O'Hanley and Dyar (1998) *Canadian Mineralogist*, **36**, 727-739; Gunter et al. (2003) *American Mineralogist*, **88**, 1944-1952; Gunter et al. (2011) *American*

The unifying theme of my research is developing and using analytical techniques to solve geological problems, most of which involve identifying and quantifying minerals in mixtures. NASA is especially interested in this problem because many techniques that are used on planetary surfaces and in orbits involve acquiring signatures of rocks and then extracting individual mineralogy from those mixed signals. For example, in my work as a Participating Scientist on the science team for the Mars Exploration Rover *Curiosity*, we studied the problem of identifying individual minerals based on rock measurements.[6] I studied meteorites from Mars and examined the spectra signatures of individual minerals and also the rock from which they were separated.[7] We sometimes even create "fake rocks" from mineral mixtures and then make measurements of the mixtures to try to understand how to determine abundances of those minerals.[8] My research depends heavily on the use of robust statistical analyses, and I often utilize machine learning techniques to solve problems in an unambiguous way.[9]

I work hard to uphold the standards of my profession by reviewing research proposals and journal publications continuously. I have been an Associate Editor for the *American Mineralogist* since 2000, handling up to 30 papers each year. I have edited one book for the Geochemical Society and one special volume of the *American Mineralogist*. I personally review at least a dozen manuscripts for a wide variety of journals every year, as well as many research proposals. I serve on review panels for the National Science Foundation and NASA almost every year, in which capacity I sometimes review as many as 18 proposals per year. As such, I am an experienced reviewer of scientific reports.

My research has been recognized with both national and international awards. I am a Fellow of the Mineralogical Society of America, the Geochemical Society and the Geological Society of America (GSA). I received the 2017 G. K. Gilbert award from the GSA for my outstanding contributions to planetary science and the 2018 Eugene Shoemaker Distinguished Scientist medal from NASA for "a scientist who has significantly contributed to the field of lunar and/or asteroid science throughout the course of their scientific career." I received the Hawley Medal from the Mineralogical Association of Canada in 2017, and currently hold the position of Helmholtz International Fellow with the German Aerospace Center (Deutsches Zentrum für Luft- und Raumfahrt).

A copy of my current curriculum vitae is attached hereto as Exhibit A. My hourly rate for this work has been $500 per hour.

Mineralogist, **96**, 1414-1417; Evans et al. (2012) *American Mineralogist*, **97**, 184-196; Swayze et al. (2018) *American Mineralogist*, **103**, 517-549; Di Guiseppe et al. (submitted) *Toxicology and Applied Pharmacology*.

[6] Dyar et al. (2013) *Geological Society of American Annual Meeting*, Denver, Abstract #6-5; Dyar et al. (2014). *Lunar Planet. Sci.* **XLV**, Lunar Planet. Inst., Houston, CD-ROM #1788 (abstr.).

[7] Dyar (2002) *LPI Conf.*, Houston, #6011; Dyar (2003) *Meteoritics and Planetary Science*, **38**, 1733-1752.

[8] Carey et al. (2016) *Lunar Planet. Sci.* **XLVII**, Lunar Planet. Inst., Houston, (abstr.) #2626.

[9] Boucher et al. (2015) *Journal of Chemometrics*, doi: 10.1002/cem.2727; Dyar et al. (2016) *Spectrochimica Acta B.*, **126**, 53-64; Boucher et al. (2015) *Spectrochimica Acta B*, **107**, 1-10; Carey et al. (2015) *Journal of Raman Spectroscopy*, **46**, 894-903; Boucher et al. (2017) *Journal of Chemometrics*, **31**, e2877; and Giguere et al. (2017) *Applied. Spectroscopy*, **71**, 1457-1470.

III. BACKGROUND: WHAT IS AN ASBESTIFORM MINERAL?

The definition of asbestos involves three different characteristics of a particle: **chemical composition, crystal structure and physical properties**.

By way of overview, the asbestiform nature of asbestos minerals is seen in **Figure 1**, which shows photomicrographs of tremolite and anthophyllite – two of the amphibole minerals that will form the basis for much discussion in this report.

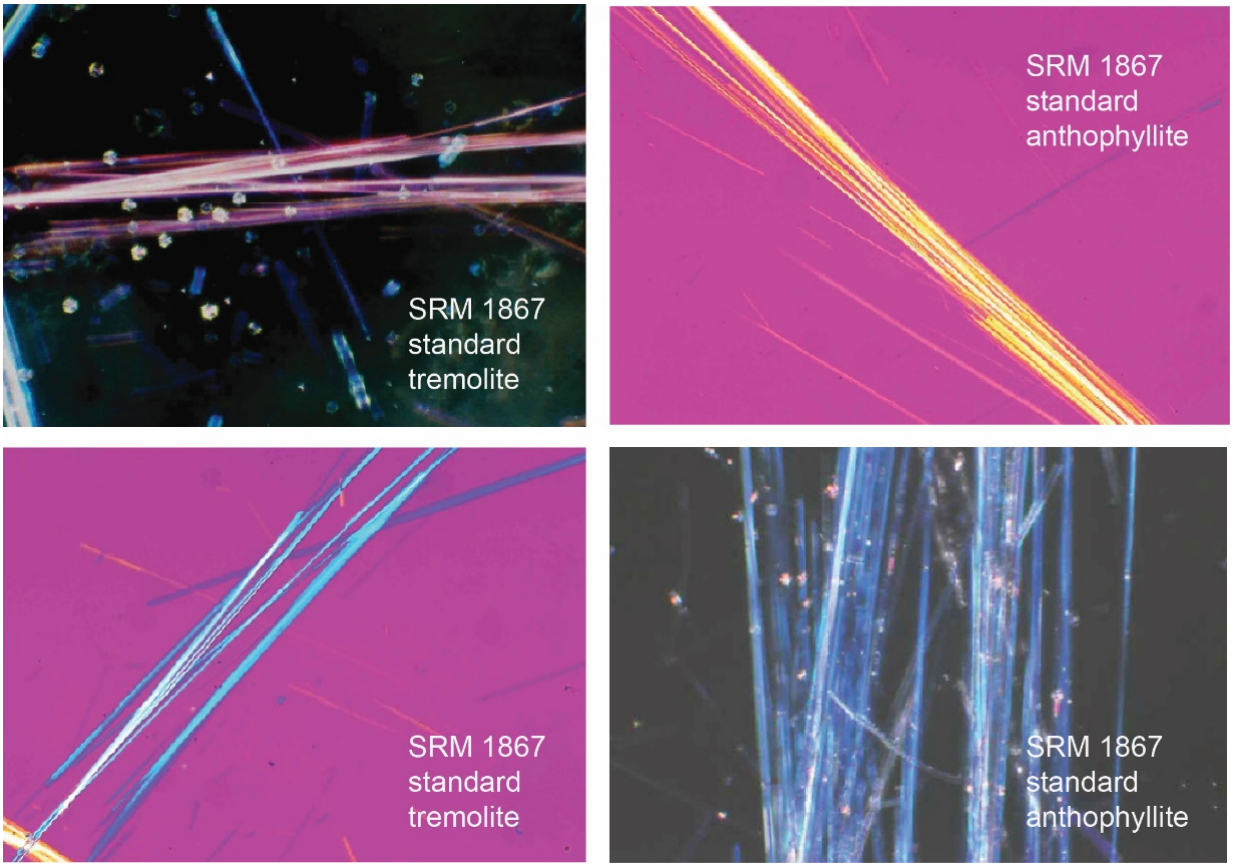

Figure 1. *Microscopic images of tremolite (left) and anthophyllite (right) asbestos reference standards from the U.S. National Institute of Standards and Technology. All of these particles meet the standard definition of "asbestiform" articulated in Gunter (2010) and can "be separated lengthwise into fibers." Images from ISO 22262-1, Figures D.23, D.25, D.32, and D.34.*

Each of these minerals has a specific chemical composition, crystal structure and physical properties. This is what makes them asbestos.

Thus, this Introduction explains the criteria relevant to the study of potentially asbestiform minerals in talcum powder. There are three issues to consider:

1. **Mineralogy**: Are the mineral species among those that include asbestos?

2. **Physical properties (habit)**: Do the minerals have an 'asbestiform' habit – in other words, is this the asbestiform version of a mineral and not the non-asbestiform version?

3. **Concentration**: What are the abundances of the minerals?

A. Mineral Species Identification

Summary: Many minerals have very similar chemical formulas, and many minerals occur with fibrous shapes, but "asbestos" minerals have *both* a specific chemical composition and a unique 'habit' or morphology.

The strict definition of a mineral species is that it (1) occurs in nature, (2) is stable at room temperature, (3) is generally produced by inorganic processes, (4) can be represented by a **chemical formula**, and (5) has a **specific, ordered arrangement of atoms**. The last two of these are especially important to this report.

Mineralogists use very specific mineral species names, regulated by an international committee, to assure that minerals with the same name have all five of these characteristics in common. There are currently ~5,500 known mineral species, and many more are found every year.[10] Mineral classification is hierarchical, like biological classifications. Instead of the familiar "kingdom, phylum…genus, species" used in biology, mineralogists use mineral class, type, group and species. Species names are unique and highly specific. While there are **only six regulated asbestiform mineral species,** shown in red in **Table 1**, there are many other minerals related to them.

[**Table 1** on next page.]

[10] Mineral species names and compositions are certified by the Commission on New Minerals and Mineral Names (CNMMN) of the International Mineralogical Association.

Table 1. Minerals Similar to Talc that Contain Si, Mg, Fe, Ca, Na, H and O*

Mineral Species	Mineral Class	Chemical Formula	(Mg,Fe) : Si
Anthophyllite	Amphibole	$Mg_7Si_8O_{22}(OH)_2$	7 : 8
Antigorite	Serpentine	$Mg_3Si_2O_5(OH)_4$	3 : 2
Chesterite	inosilicate >1 chain	$Mg_{17}Si_{20}O_{54}(OH)_6$	17 : 20
Chrysotile	Serpentine	$Mg_3Si_2O_5(OH)_4$	3 : 2
Clinohumite	Nesosilicate	$(Mg,Fe)_9(SiO_4)_4(OH)_2$	9 : 16
(clino)jimthompsonite	inosilicate >1 chain	$Mg_5Si_6O_{16}(OH)_2$	5 : 6
Enstatite	Pyroxene	$Mg_2Si_2O_6$	1 : 1
Grunerite	Amphibole	$Fe_7Si_8O_{22}(OH)_2$	7 : 8
Hydroxylclinohumite	Nesosilicate	$Mg_9(SiO_4)_4(OH)_2$	9 : 16
Cummingtonite	Amphibole	$Mg_7Si_8O_{22}(OH)_2$	7 : 8
Minnesotaite	sheet silicate	$(Fe,Mg)_3Si_4O_{10}(OH)_2$	3 : 4
Sepiolite	modulated layers	$Mg_4Si_6(OH)_{26}H_2O$	4 : 6
Talc	sheet silicate	$Mg_3Si_4O_{10}(OH)_2$	3 : 4
Tremolite	Amphibole	$Ca_2Mg_5Si_8O_{22}(OH)_2$	5 : 8
Actinolite	Amphibole	$Ca_2(Mg,Fe)_5Si_8O_{22}(OH)_2$	5 : 8
Ferrowinchite	Amphibole	$CaNaFe_4(Al,Fe)Si_8O_{22}(OH)_2$	5 : 8
Richterite	Amphibole	$Na(CaNa)Mg_5Si_8O_{22}(OH)_2$	5 : 8
Ferrorichterite	Amphibole	$Na(CaNa)Fe_5Si_8O_{22}(OH)_2$	5:8
Riebeckite	Amphibole	$Na_2Fe^{2+}{}_3Fe^{3+}{}_2Si_8O_{22}(OH)_2$	5:8
Magnesioriebeckite	Amphibole	$Na_2Mg_3Fe^{3+}{}_5Si_8O_{22}(OH)_2$	5:8
Aegirine-augite	Pyroxene	$(Ca,Na)(Mg,Fe,Al,Ti)(Si,Al)_2O_6$	1 : 1
Diopside	Pyroxene	$CaMgSi_2O_6$	1 : 1
Hedenbergite	Pyroxene	$CaFeSi_2O_6$	1 : 1

Table 1. *Formulas from the approved IMA "List of minerals" (http://nrmima.nrm.se/). Species names in red are termed "asbestos" when they occur in an asbestiform morphology. Shaded species in gray contain Na or Ca.*

As shown above, these minerals all contain Si and cations such as Mg, Fe and Ca. Each has a particular ratio of Si to the other cations (the far-right column), which is important in the context of an energy-dispersive X-ray (EDXA) analysis (discussed below).

The mineral species significant to this report are those that combine the elements silicon (Si), magnesium (Mg), iron (Fe), calcium (Ca) and sodium (Na) along with hydrogen (H) and oxygen (O). Notice that the minerals are grouped in two groups, with Ca- and Na-bearing samples in the bottom half of the table. Many minerals have closely related (in some cases, identical) formulas; yet only those highlighted in red are mineral species that are regulated. Thus, it becomes critically important to discriminate these minerals carefully by chemistry and by crystal structure. Tools for these analyses fall into these two groups: tests of mineral composition (the chemical formula criterion noted above) and tests of determination of crystal structure (atomic arrangement). In addition, a particle must have a fibrous morphology to be considered asbestos.

B. Asbestiform Habit

Summary: Asbestos is defined as one of six particular minerals exhibiting the characteristics of an asbestiform habit, meaning they can be separated into flexible fibers with high tensile strength. Drs. Longo and Rigler confuse "counting criteria" with this definition, using a disingenuous distinction between what they call the "geological definition" and what they wrongly invent as the "regulatory definition."

Asbestos is a **noun** describing a specific material with a distinctive shape that is **asbestiform** (**adjective**), which means the crystal can be separated into flexible fibers with high tensile strength.

IARC (2012) defines the minerals that can be asbestos as follows: "the generic commercial designation for a group of naturally occurring mineral silicate fibres of the serpentine and amphibole series. These include the serpentine mineral chrysotile [], and the five amphibole minerals – actinolite, amosite [], anthophyllite, crocidolite [], and tremolite." IARC (2012), p. 222, also states: "Asbestos fibres tend to possess good strength properties (e.g. high tensile strength, weak and friction characteristics); flexibility (e.g. the ability to be woven); excellent thermal properties (e.g. heat stability, thermal, electrical and acoustic insulation); absorption capacity; and, resistance to chemical, thermal and biological degradation." Thus, there is agreement in the scientific community that asbestos exhibits fibrosity, high tensile strength and flexibility. This is repeated over and again in the published literature, for example:

> Zoltai, T., "*Amphibole Asbestos Mineralogy*," Reviews in Mineralogy & Geochemistry, (1981) 9(5): 237-278 (stating "the individual asbestos fibers and acicular cleavage fragments are strikingly different. The fibers are extremely strong and flexible, while the acicular cleavage fragments are weak and brittle.").
>
> Zoltai, T., "*Amphibole Asbestos Mineralogy*," Reviews in Mineralogy & Geochemistry (1981) 9(5): 237-278, at 272 (concluding that "cleavage fragments of amphibole crystals should yield the opposite strength-diameter effect than that observed in asbestos fibers").
>
> McCrone, W.C., *The Asbestos Particle Atlas 36* (1980) (describing chrysotile as having "distinctive fine flexible fibrils").
>
> Gary, M., McAfee, R., and Wolf, C., Eds., (1974) *Glossary of Geology* ("Asbestos is a commercial term applied to a group of silicate minerals that readily separates into long, thin, strong fibers that have sufficient flexibility to be woven, are heat resistant and chemically inert, are electrical insulators, and are therefore suitable for uses … where incombustible, nonconducting, or chemically resistant material is required.").
>
> Veblen D.R. and Wylie A. (1993) Reviews in Mineralogy, 28, 61-138 ("the asbestiform habit has a number of characteristics that differentiate it from other habits, but the main differences are the fibrillar structure and the fiber flexibility and strength").

Dyar and Gunter (2008) *Mineralogy and Optical Mineralogy* ("there are several types of minerals than can have asbestiform habits, which are distinguished by their fibrillar structure and the flexibility and strength of the fibers."

Asbestos Fibers and Other Elongate Mineral Particles: State of the Science and Roadmap for Research, (2011) U.S. Dept. of Health & Human Services, NIOSH, Current Intelligence Bulletin 62 at 6 (stating that "[t]he fibers of all varieties of asbestos are long, thin and usually flexible when separated"), 9 (stating that "[i]t has been suggested that crystals grown in an 'asbestiform' habit can be distinguished by certain characteristics, such as parallel or radiating growth of very thin and elongate crystals that are to some degree flexible, the presence of bundles of fibrils, and, for amphiboles, a particular combination of twinning, stacking faults, and defects"), 34 (describing chrysotile fibers as "consist[ing] of aggregates of long, thin, flexible fibrils that resemble scrolls or cylinders"), 36 (stating that "[a]sbestiform amphibole fibers consist of aggregates of long, thin, flexible fibrils that separate along grain boundaries between the fibrils").

Asbestiform Fibers: Nonoccupational Health Risks, National Research Council (1984) at 33 (stating that asbestos particles that have sufficiently small diameters have great strength and flexibility, and that the tensile strength of commercial quality asbestos fibers is 20 to 50 times greater than that of the non-asbestiform crystals of the same minerals), 38 (noting that the flexibility of asbestos fibers enables them to bend without breaking, which facilitates their passage through the respiratory tract into the deep lung), 41 (explaining that, "Asbestiform fibers, including asbestos fibers, are mineral fibers that are characterized by a specific set of interdependent physical properties, including fiber-like shape, enhanced strength and flexibility, increased durability, strong and defect-free surface structure, and the dependence of these properties on conditions of growth. The fiber properties that have been considered for possible association with deleterious health effects are respirability (i.e., fibers <3 μm diameter), size and aspect ratio, durability, flexibility and tensile strength, chemical composition, surface area, and surface charge.").

Gunter, M., *Defining Asbestos: Differences between the Built and Natural Environments*, 60 CHIMIA No. 10, 747, 748 (2010) (stating that a mineralogist would require that a fiber would need to exhibit a certain set of physical properties, i.e., be curved and flexible, in order to be classified as asbestos).

This usage is echoed in other documents, such as the methodology standards upon which Drs. Longo and Rigler purport to rely:[11]

ISO 22262-1, -2, -3: defining asbestiform as a "specific type of mineral fibrosity in which the fibres and fibrils possess high tensile strength and flexibility." ISO 22262-1 (2012) at 2; ISO 22262-2 (2014) at 8; ISO 22262-3 (2016) at 2.

[11] *See* 40 C.F.R. Ch. I (7-1-03 Edition) (defining asbestiform as "a specific type of mineral fibrosity in which the fibers and fibrils possess high tensile strength and flexibility"); 40 C.F.R. 763.83 (defining asbestos as the "asbestiform varieties of" six minerals).

> ISO 13794: defining asbestiform as a "specific type of mineral fibrosity in which the fibres and fibrils possess high tensile strength and flexibility." ISO 13794 (1999) at 2.
>
> ISO 10312: defining asbestiform as a "specific type of mineral fibrosity in which the fibres and fibrils possess high tensile strength and flexibility." ISO 10312 (1995) at 2.
>
> AHERA: defining asbestiform as a "specific type of mineral fibrosity in which the fibers and fibrils possess high tensile strength and flexibility." 40 CFR Ch. 1, Pt. 763 Subpt. E, App. A, 728 (July 1, 2013).
>
> ASTM D5755: defining asbestiform as "a special type of fibrous habit in which the fibers are separable into thinner fibers and ultimately into fibrils. This habit accounts for greater flexibility and higher tensile strength than other habits of the same mineral." ASTM D5755 – 09 at 518-19.
>
> ASTM D5756: defining asbestiform as "a special type of fibrous habit in which the fibers are separable into thinner fibers and ultimately into fibrils. This habit accounts for greater flexibility and higher tensile strength than other habits of the same mineral." ASTM D5756 – 02 (2008) at 532-33.

Further, if a particle is deemed to be fibrous, it does not mean it is asbestiform, as noted, for example, in Campbell et al. (1997), which recognizes that "the term fibrous has been used … to describe all kinds of minerals that crystallize in habits resembling organic fibers… asbestiform is a specific type of fibrosity."[12]

Drs. Longo and Rigler appear to agree that asbestos has these qualities, although Dr. Longo calls this a "mineralogical definition."[13] Dr. Longo then distinguishes this from what he calls a "regulatory definition." That is misleading, because in reality, Drs. Longo and Rigler are referring to the **counting criteria** in regulatory documents, not what asbestos is or is not. Indeed, some of the very documents that they use to draw this disingenuous distinction expressly **define** asbestos according to what Drs. Longo and Rigler want to call the "mineralogical definition," *e.g.*, ISO 22262. Along the same lines, there are other criteria used under air sampling methodology (EPA

---

[12] Campbell et al. (1997) *Information Circular 8751*. U.S. Bureau of Mines.

[13] 01/07/19 Longo Depo. 79:4-11 ("[asbestos] has to have high tensile strength, flexible splayed fibers, for asbestiform, and that's a geological definition."); 10/31/18 Longo Depo. 43:16-20 ("Q. And some of the features of asbestos growing in the asbestiform habit, as a geologist would use the term, have to do with tensile strength and flexibility; correct? A. That is the geological definition"); 10/24/18 Longo Depo. 269:13-23 ("Q. So I believe you said that the definition of asbestiform habit that you just gave is not your definition, is that what you said? A. That's correct. I mean, it's the standard definition, it's fibrous. Now, what it also says for asbestiform, that it has to have high tensile strength, it has to have splayed ends, it has to have this, it has to have that. That's a geological definition . . ."); 2/05/2019 Longo Depo. 222:2-17 ("Q. Do you agree with ISO 13794 that this method cannot discriminate between individual fibers of the asbestos and nonasbestos analogs of the same amphibole material? A. … but, no, it does not meet the geological definition for asbestos, high tensile strength, flexible, and so on and so forth.").

Asbestos Hazard Emergency Response Act, AHERA[14] and EPA 600/R-93[15]) to describe fibers. In those documents, mean aspect ratios for populations of asbestos particles range from 20:1 to 100:1, which is inconsistent with the findings from Drs. Longo and Rigler. Certain protocols may look to whether the aspect ratios of detected particles are at least 3:1 for measurements by polarizing light microscopes[16] and at least 5:1 for TEM measurements.[17,18]

In other words, these aspect ratio dimensions alone do not imply that the observed particles are asbestos – there are non-asbestiform amphiboles and many other minerals that have aspect ratios above 3:1 or 5:1. Drs. Longo and Rigler confirmed this in their depositions.[19] This is discussed in more depth below in Section VII.

C. Measurements of Concentration

Summary: An appropriate analytical technique must be used to determine the degree to which there is asbestos in a talc sample, depending on the level of any impurity.

If asbestos minerals are present in talcum powder, it is important to be able to assess their abundance. There are spectroscopic methods, such as visible, Raman, and infrared spectroscopies, that work well on such powders, but they cannot detect minor phases that are <~1%. Particles that are present in very low abundances (such as parts per million) are nearly impossible to quantify. The measurement of small amounts of asbestos as an impurity in talc in greater detail in Section V, below.

---

[14] US Code Title 15, Chapter 53, Subchapter II. Asbestos Hazard Emergency Response, https://www.govinfo.gov/content/pkg/USCODE-2011-title15/pdf/USCODE-2011-title15-chap53-subchapII.pdf.

[15] EPA/600/R-93/116, https://tinyurl.com/y4z765xp.

[16] 40 C.F.R. 763, Subpart E, https://www.govinfo.gov/content/pkg/CFR-2009-title40-vol30/pdf/CFR-2009-title40-vol30-part763.pdf.

[17] EPA/600/R-93/116, https://tinyurl.com/y4z765xp.

[18] 40 C.F.R. 763, Subpart E, https://www.govinfo.gov/content/pkg/CFR-2009-title40-vol30/pdf/CFR-2009-title40-vol30-part763.pdf.

[19] 2/5/19 Longo Depo. 246:5-15 ("Q. Okay. Is there anything in the published literature that you've seen that suggests that there are cleavage fragments with a greater than 5-to-1 aspect ratio? A. There's been a number of published articles that state things like that, yes. Q. Are there any published articles that state that there are cleavage fragments that have greater than 3-to-1 aspect ratio? A. Yes, there is publications that state that."); 2/6/19 Rigler Depo. 191:21-193:4 ("Q. Using a geological definition of asbestos, can you have a cleavage fragment that is greater than 5-to-1 aspect ratio? A. In my opinion, the answer to that is yes. Q. Okay. And using the geological definition of asbestos as you have used it, there can be an asbestiform particle that has an aspect ratio of below 3-to-1? A. Are you talking about what kind of particle? Q. Asbestiform particle. A. Smaller than 3-to-1? Q. Yeah. … in most cases of that size, you know, you may see some that are in that range, but you have to use the PLM to see them, probably.").

IV. MINERAL IDENTIFICATION USING CHEMICAL COMPOSITION: EDS

Drs. Longo and Rigler opine on the results of analyses done by their five analysts using electron dispersive spectroscopy (EDS or EDXA for x-ray spectroscopy).[20] This section discusses the use of EDS to the identification of mineral compositions.

A. How EDS Works

Summary: EDS, when properly used, can provide a limited analysis of the *chemical makeup* of certain mineralogical samples.

In this technique, an electron source is used to produce high-energy electrons that are focused onto a tiny spot on a sample. The electrons interact with the atoms in the crystal structure, causing a low-energy inner shell electron to be ejected from the atom. Higher-energy electrons from higher shells in that atom quickly drop down to fill the void, and in doing so, they release energy in the form of x-rays. The energy is characteristic of each element and reflects the spacing of the two shells involved, which is unique to each element. A detector counts how many electrons are scattered and at what energies. This produces a graph of energy (x axis) vs. counts (y axis) as shown in **Figure 2**.

[**Figure 2** on next page.]

[20] Both Drs. Longo and Rigler testified that they did not personally run any of the experiments on which they opine in their reports. Instead, they were involved in various levels of oversight and supervision. *See* 2/6/2019 Rigler Depo. 13:6-15 ("Q. Did you ever use a PLM for the purposes of this report? A. No, I did not. Q. Did you ever use a TEM for the purposes of this report? A. Not for the purposes of this report. Q. Did you ever use an XRD device for the purposes of this report? A. We do not have the XRD device or that type of device at our laboratory."); 11/27/18 Longo Depo. 447:6-10 ("Q. Okay. For any of the analyses that were done for the November 14, 2018, report, were you the analyst that reported the findings on the bench sheets? A. No."). There were five such analysts: four at Drs. Longo and Rigler's laboratory, and one at J3, a laboratory not formally affiliated with Drs. Longo and Rigler. *See* 2/5/19 Longo Depo. 258:16-18 ("Q: [T]here were four people doing analysis in the MDL report; right? A: Correct."); February 1, 2019 Report, at 4 ("MAS [i.e., Longo and Rigler] sent a number of historical J&J samples to J^3 Resources for both PLM and XRD analysis using ISO 22262-1 and ISO 22262-3 protocols.").

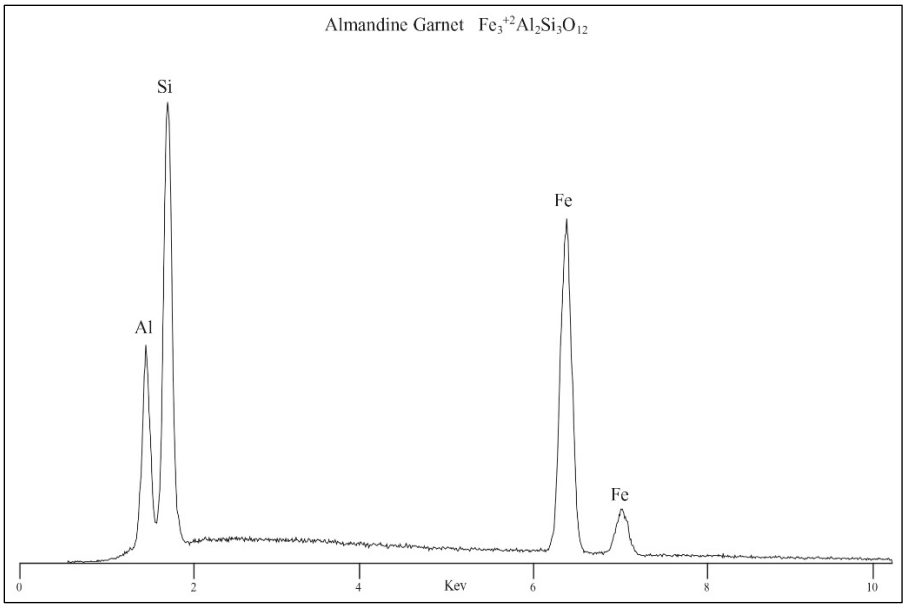

***Figure 2**. EDS spectrum of the mineral species almandine ($Fe_3Al_2Si_3O_{12}$) from the classic book by Severin (1984).*[21]

Peaks in the EDS plots arise from individual elements, and the areas of the peaks are roughly proportional to the amounts present (e.g., Severin, 1984). In the example above, the mineral is almandine, which has a nominal formula of $Fe_3Al_2Si_3O_{12}$. There are three formula units of Si and three formula units of Fe. Notice how the total area of the Fe peaks is roughly comparable to the total are of the single Si peak because both elements are present in roughly equal proportions. There are only two formula units of Al, and that peak is thus somewhat smaller.

This example was purposely chosen to be simple. But in most EDS spectra, the correspondence between peak areas and elemental abundances is not so direct due to a host of factors[22] (see Section B below). There are ways to correct for them, and every TEM instrument sold today includes a software package based on the same physical principles that can make the appropriate corrections via detailed calculations. Such calibrations are used to convert the areas to true (albeit semi-quantitative) elemental percentages in the mineral. Independent software is also available for this purpose (e.g., Desktop Spectrum Analyzer II[23] or XIDENT[24]), which allows a user to import spectral files with a standard format and extract quantitative information from them.

Depending on the x-ray intensity and the type of detector used, some elements are difficult to measure by EDS. EDS **cannot** be used to quantify either hydrogen (H) or oxygen (O) accurately.

---

[21] Severin (1984) *Energy Dispersive Spectrometry of Common Rock-Forming Minerals*, Kluwer.

[22] Deriving quantitative information from an EDS spectrum is a complicated process due to instrumental (such as the type of window on the detector), experimental (which energy was used), and physical (absorption and fluorescence) factors. A nice summary of this is given at https://cstl.nist.gov/div837/837.02/epq/dtsa2/.

[23] https://cstl.nist.gov/div837/837.02/epq/dtsa2/.

[24] Rhoades (1976) *XIDENT – A computer technique for the direct indexing of electron diffraction spot patterns* (Research Report 70/76), https://ir.canterbury.ac.nz/handle/10092/11515.

Therefore, distinguishing among the minerals in talcum powder similar to talc (**Table 1**) requires that magnesium (Mg), iron (Fe), calcium (Ca) and silicon (Si) be distinctive for each phase and have x-ray peaks in the right energy region (0-10 keV), as seen in **Figure 2** above. EDS analyses are generally considered to be semi-quantitative for chemical analyses, with errors of about ±5% relative for major elements (Si, Al, Ti, Mg, Fe, Ca, Na, and K).[25,26] **Attaining such accuracy requires use of a calibration and ideal experimental conditions.**

B. Factors Affecting Accuracy of EDS

Summary: EDS can distinguish many minerals from one another, but it has significant limitations when minerals from completely different groups have similar chemistries. For example, EDS cannot accurately distinguish anthophyllite *amphibole* from talc *sheet silicate* (or even enstatite *pyroxene*), or tremolite *amphibole* from diopside *pyroxene*.

Mineral identification based on EDS data alone is quite dependent on coaxing the best possible chemical data out of a semi-quantitative instrument. To a first order, the areas of each peak in an EDS spectrum reflect the concentration of that element.[27] But as noted above, other factors, such as particle geometry, spectrometer model, type of detector,[28] detector sensitivity, and the efficiency of x-ray generation, come into play as well to affect the peak areas, requiring sophisticated calibration to obtain interpretable results. **Figure 3** shows the EDS pattern of cummingtonite from the classic book of EDS patterns by Severin (1984). This mineral has a composition of $(Mg,Fe)_7Si_8O_{22}(OH)_2$.[29] Even though this sample has more Mg than Fe atoms, the peak areas are radically different due to the factors noted above: 5% for Mg and 26% for Fe. **In other words, the peak areas are not directly proportional to the abundances of the elements.**

[**Figure 3** on next page.]

[25] Newbury and Rotchie (2015) *Journal of Material Sciences*, **50**, 493-518; Miller and Mirtič (2013) *Geologija*, **56**, 5-17.

[26] Hafner, *Energy Dispersive Spectroscopy on the SEM: A Primer*, http://www.charfac.umn.edu/instruments/eds_on_sem_primer.pdf.

[27] Severin (2004) *Energy Dispersive Spectrometry of Common Rock Forming Minerals*. Springer, Kluwer.

[28] As noted by Dr. Longo in deposition, EDS instruments can have Si-drifted, Li-drifted, or windowless detectors. 2/5/19 Longo Depo. 101:8-23. He continues: "if it's a light element detector, the magnesium can be a little higher, the silicon will be your primary peak, somewhere in the 25-30 percent of the magnesium for a non-light element detector. And the calcium peaks and the magnesium peaks are usually very similar in size." 2/5/19 Longo Depo. 77:17-78:6.

[29] The ideal "end member" composition of cummingtonite is $Mg_7Si_8O_{22}(OH)_2$, but it forms a continuous series with grunerite ($Fe_7Si_8O_{22}(OH)_2$) so it can contain up to 3.5 formula units of Fe. In the formula given above, the "Mg,Fe" is a notation that indicates that there is more Mg than Fe.

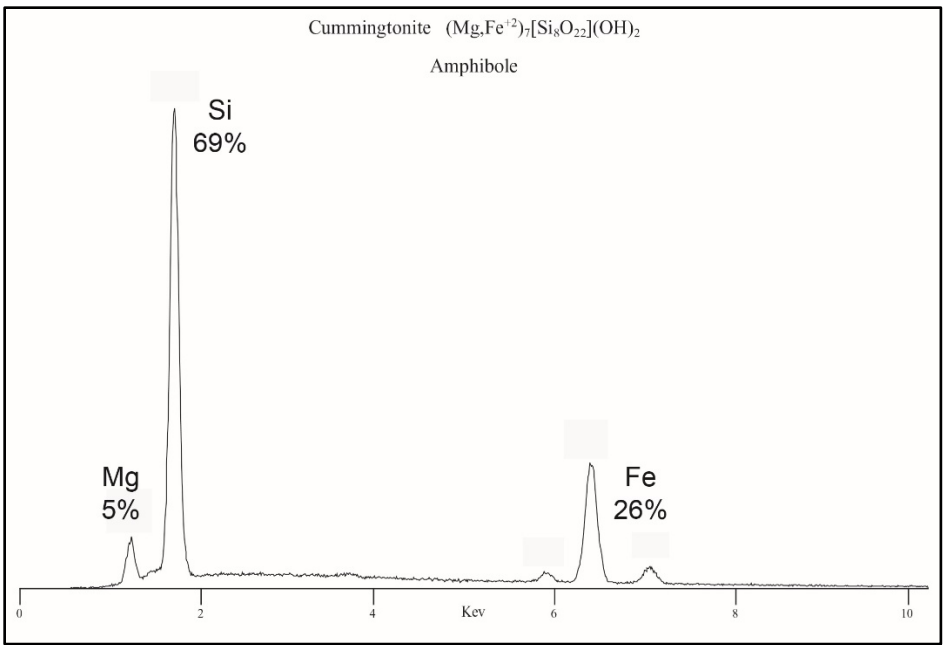

Figure 3. *EDS spectrum of the mineral species cummingtonite, $(Mg,Fe)_7Si_8O_{22}(OH)_2$, from Severin (1984).*[30]

When proper calibrations are used, EDS has ±5% or larger error bars, making it only semi-quantitative under the best of protocols (i.e., not sensitive enough for subtle chemical differences).[31] This can be a significant limitation on the usefulness of EDS in many contexts. For example, one way scientists use EDS readouts to roughly determine the chemical makeup of a sample is to use the ratio of the peak areas of the elements (e.g., Mg+Fe) to Si.[32] The right-hand column of **Table 1** shows these ratios in some rock-forming minerals containing Si, Mg, Fe and Ca. Those data suggest that only accurate analyses will allow these minerals to be distinguished on the basis of chemistry alone, given the error bars of EDS. The most accurate methods (such as electron probe microanalysis, EPMA, which has a beam size ~1000-20,000 nm) can measure mineral chemistry well enough to tell these minerals apart, but these methods lack the excellent spatial resolution of EDS on a TEM, which is roughly 0.5 nm (~1000× smaller than EPMA). Therefore, studies of asbestos-bearing rocks generally use EDS for chemical analyses, sacrificing accuracy for the ability to focus the beam on a tiny particle.

By way of specific example, **Figure 4** shows the Mg/Si ratios for selected **Table 1** minerals, along with propagated error bars of 5%, which are generally accepted best accuracies for analyses

---

[30] As noted on the previous page, the ideal "end member" composition of cummingtonite is $Mg_7Si_8O_{22}(OH)_2$, but it forms a continuous series with grunerite ($Fe_7Si_8O_{22}(OH)_2$) so it can contain up to 3.5 formula units of Fe. In the formula given above, the "Mg,Fe" is a notation that indicates that there is more Mg than Fe. Figure from Severin (1984) *Energy Dispersive Spectrometry of Common Rock-Forming Minerals*, Kluwer.

[31] Newbury and Ritchie (2015) *Journal of Material Sciences*, 50, 493-518; Miller and Mirtič (2013) *Geologija*, 56, 5-17.

[32] Severin (1984) 23 (it is possible to "determine the approximate relative concentrations of the element. The number of characteristic X-rays is, to a first order, related to the number of atoms of a particular element in the sample…").

of particles and rough surfaces.[31] The **dashed** purple line in **Figure 4** shows that anthophyllite and enstatite are identical within the error bars. The **dotted** purple line shows that talc and sepiolite are indistinguishable. Within these error bars, talc and anthophyllite are also identical because their error bars overlap (thick purple shaded line).

The analogous conclusions can be drawn from the diagram at right for tremolite (amphibole) and diopside (pyroxene), where the *y* axis is now (Mg+Ca)/Si. Again, these minerals have completely different crystal structures, yet their formulas are quite similar. The purple shaded bar here indicates how much these two minerals overlap. These two minerals would be indistinguishable to EDS, **even though they belong to completely different mineral groups** (amphibole and pyroxene, respectively) with very distinct properties.

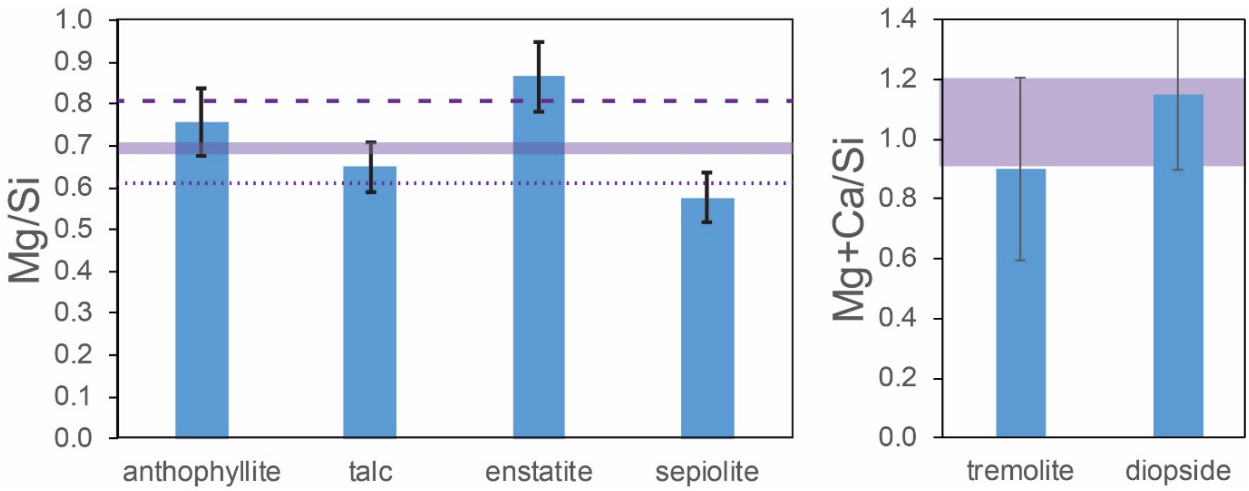

***Figure 4**. Ratios of the weight percentage of magnesium (Mg) to silicon (Si) along with propagated 5% errors on each measurement.[33] Formulas from webmineral.com with 5% errors added.*

Further, the EDS results in the Longo/Rigler MDL Reports labelled as "tremolite" may very well be consistent with minerals other than diopside. Drs. Longo and Rigler have never produced their quantitative data and, accordingly, this analysis cannot be completed.[34]

[33] For example, anthophyllite contains 28.78 wt.% Si and 21.79 wt.% Mg. EDS determines these values to within ±5%, i.e., 28.78±1.44 and 21.79±1.09. So Mg/Si = 0.65 and the propagated error on Mg/Si is ±0.08. The same calculation is done here for talc, enstatite, sepiolite, tremolite, and diopside.

[34] For example, these may include at least monticellite, bredigite, merwinite and rondorfite, which are other minerals that contain only Si, Mg and Ca. Many more common mineral species would be included in this list if Fe and Na were allowed as possible chemical constituents.

C. The Analysts Used By Drs. Longo And Rigler Do Not Use EDS In A Way Accepted By The Scientific Community, Resulting In Unsupportable Conclusions

Summary: The "eyeball" method of estimating EDS data employed by Drs. Longo and Rigler is not considered reliable by the scientific community. Drs. Longo and Rigler do not report the quantitative data one needs to make scientifically valid conclusions, and their conclusions are therefore unsupportable.

It is clear that Dr. Longo does not understand the limitations of EDS results that are explained above. He states, "I believe every spectra in here is quantitative EDS analysis" (2/5/19 Longo Depo. 72:22-23). He explains how his analysts use peak ratios (like those above) to identify minerals based on EDS spectra. To identify tremolite from anthophyllite, "[y]ou have a magnesium and calcium peak that are pretty close. Typically the calcium peak can be a little lower. … the magnesium can be a little higher, the silicon will be your primary peak, somewhere in the 25 to 30 percent of the magnesium … [a]nd the calcium peaks and the magnesium peaks are usually very similar in size. And then we look at the amount of iron to see if we're going to call it actinolite or tremolite. And not aware of any other minerals out there that have those ratios, so that's how I call it tremolite." (2/5/19 Longo Depo. 77:14-78:6).

It is apparent from these remarks that Dr. Longo, who admits he has never taken any courses in mineralogy (2/5/19 Longo Depo. 16:2-3), is unaware of the breadth of other possible minerals that can match these EDS patterns within the known analytical errors. His methodologies are contrary to those that are accepted in the scientific community.

D. EDS Data from Drs. Longo And Rigler Show Great Variabilty

Turning now to EDS data in the Longo/Rigler MDL Reports, **Figure 5** shows several different talc spectra. Note the variable amounts of Fe in the sample, and the varying ratio between the intensities of the Mg and Si peaks. Do these grains really have different compositions, or are the variations from analytical imprecision? It would only be possible to make this determination with calibrated data.

[**Figure 5** on next page.]

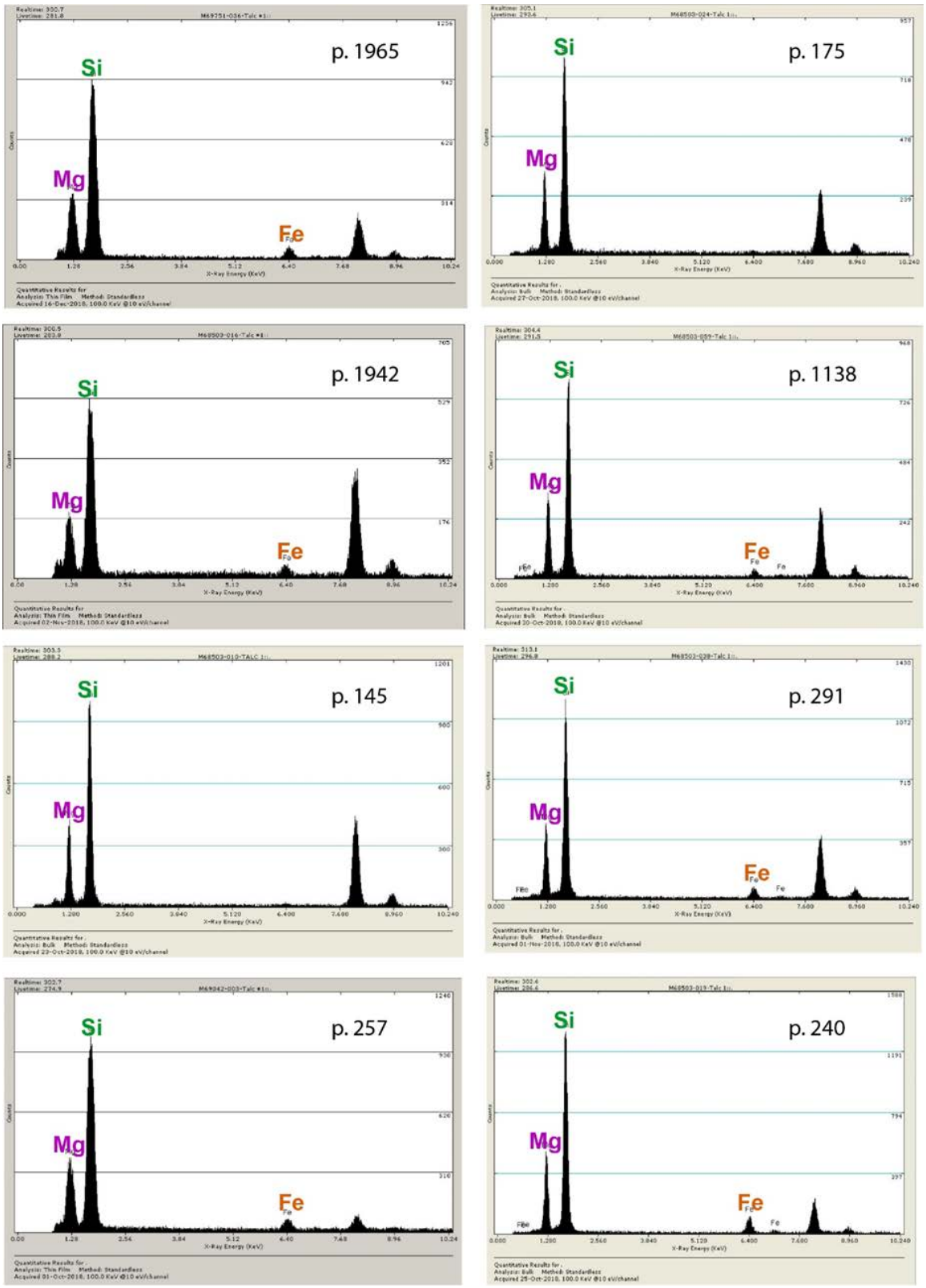

Figure 5. *Talc spectra in the January 2019 Longo/ Rigler MDL report, showing variable ratios between the intensity/area of the Mg and Si peaks. Note also the varying amounts of Fe in these talcs.*

Similarly, **Figure 6** shows a number of different anthophyllite spectra from the January 2019 MDL Report. Although these are all identified as "anthophyllite," they could be almost any mineral containing Mg and Fe but no Ca (cf. top portion of **Table 1**).

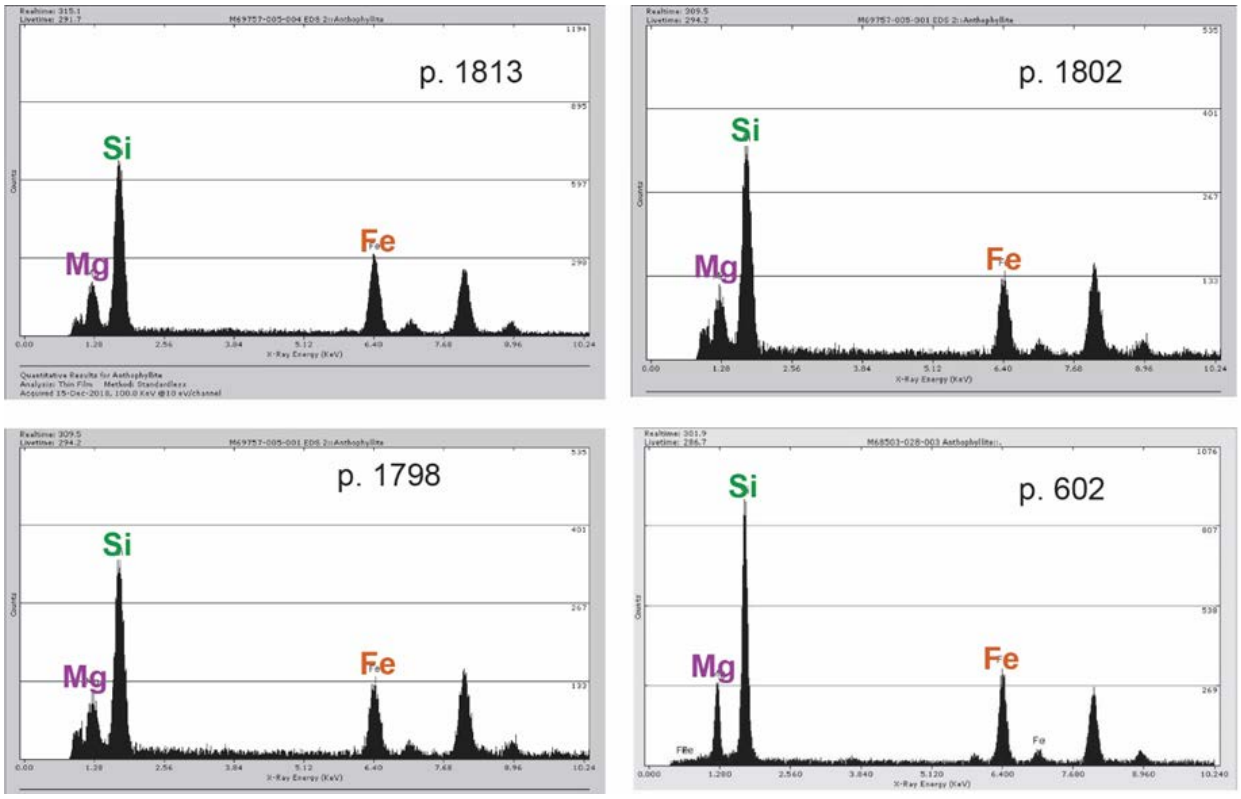

Figure 6. *Anthophyllite spectra in the January 2019 Longo/ Rigler MDL report showing Fe peaks that are larger than Mg peaks.*

In fact, these spectra in **Figure 6** closely resemble the spectrum of cummingtonite shown in **Figure 3**. Without a calibration to correct the peak areas for experimental variables, it is quite difficult to determine which minerals are present. Moreover, the formula of anthophyllite, $(Mg,Fe)_7Si_8O_{22}(OH)_2$) should have much more Mg than Fe, which is clearly not the case here.

It is **nearly impossible to tell some of these spectra apart** solely by visual inspection of their EDS patterns. Calibrations are needed to produce optimal, albeit semi-quantitative, results. These graphs show why the calibration procedure to convert from peak areas to elemental concentrations is routinely part of the software that comes with a TEM instrument.[35] It is irresponsible for Drs. Longo and Rigler to choose not to employ calibration software to assist with their mineral identifications.

[35] This calibration is done using first principles calculations or by comparison with spectra of a small number of standards with known compositions, as described in Newbury (1995) "Standardless" quantitative electronic probe microanalysis with energy-dispersive x-ray spectrometry: Is it worth it? *Anal. Chem.*, **67**, 1866-1871.

E. Drs. Longo And Rigler And Their Analysts Appear to Have Deliberately Avoided Reporting The Data That Would Actually Be Useful Here

Summary: EDS instruments and their accompanying standard software are capable of produce numerical data on chemical composition. Drs. Longo and Rigler appear to have deliberately avoided producing or reporting those data.

The more information extracted from an EDS analysis, the more a scientist can narrow down the composition of the subject mineral. A typical EDS output is shown in **Figure 7**, with each peak identified on the screen and the quantitative analysis given below the spectrum. Results include a listing of each element in weight %, the standard deviation of that number based on repeat analyses,[36] atomic %, and cations (positively charged ions), along with the total weight % of the summed elements.

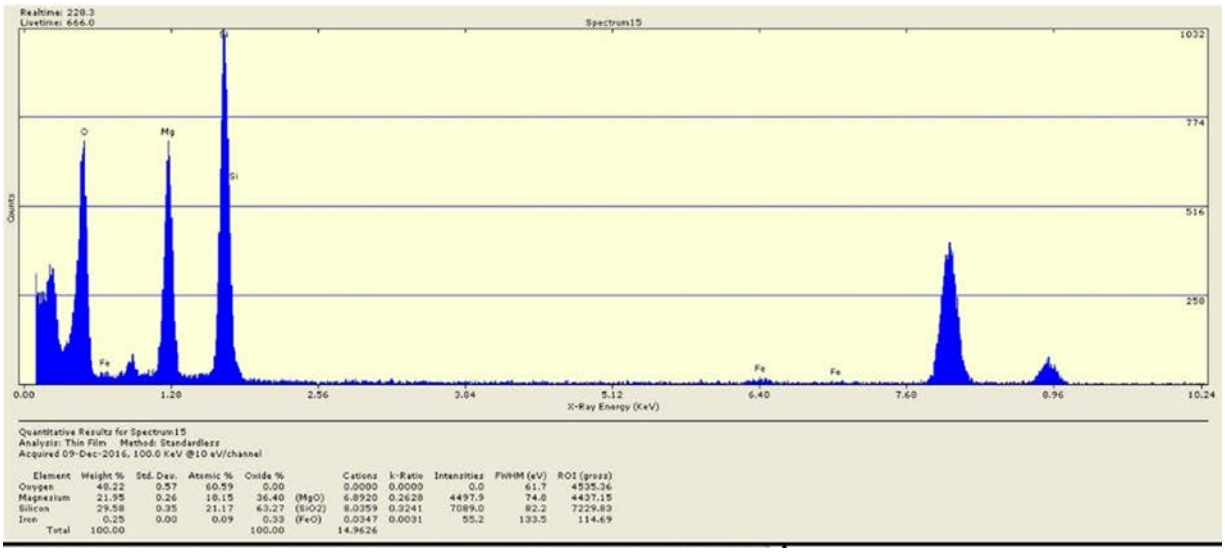

Quantitative Results for Spectrum15
Analysis: Thin Film Method: Standardless
Acquired 09-Dec-2016, 100.0 KeV @10 eV/channel

Element	Weight %	Std. Dev.	Atomic %	Oxide %		Cations	k-Ratio	Intensities	FWHM (eV)	ROI (gross)
Oxygen	48.22	0.57	60.59	0.00		0.0000	0.0000	0.0	61.7	4535.36
Magnesium	21.95	0.26	18.15	36.40	(MgO)	6.8920	0.2628	4497.9	74.8	4437.15
Silicon	29.58	0.35	21.17	63.27	(SiO2)	8.0359	0.3241	7089.0	82.2	7229.83
Iron	0.25	0.00	0.09	0.33	(FeO)	0.0347	0.0031	55.2	133.5	114.69
Total	100.00			100.00		14.9626				

Figure 7. *Mostly amphibole EDS spectrum from the Connecticut Geological Society using the eZAF Smart Quant calibration, from their web site at https://www.geologicalsocietyct.org/geoconnections-articles/recent-analyses-of-connecticut-amphiboles.*

Asked whether their EDS tools could produce this information, Dr. Rigler agreed. Looking at the precise readout that is in **Figure 7** above, he testified:

[36] Notice that accuracy is not given in the output – only precision ("Std. Dev." in the table below the figure).

> Q. Okay. It is from your report. So is that what an EDXA spectra looks like?
>
> A. Yes.
>
> Q. And you'll notice on the bottom left-hand corner it says elements and it has got some elements and it says total?
>
> A. Yes.
>
> **Q. Your software can generate information that fills in that; correct?**
>
> **A. Yes.**[37]

The quantitative data are conspicuously lacking from all the EDS patterns in the Longo/Rigler MDL Reports. It is also curious that the printouts of EDS patterns from the Longo/Rigler MDL Reports list the elements chosen by the analyst (Mg, Si, etc.), followed by the word "Total," which implies that a column of numbers to the right of the element list gives a listing of peak areas. In the more typical EDS analysis from another lab, as seen in **Figure 7**, the composition is given in cations as $Si_{8.04}Mg_{6.98}Fe_{0.03}$. It would be very difficult to obtain these numbers simply by looking at the graph.

Yet the EDS protocol in the lab of Drs. Longo and Rigler does exactly that – the analysts "eyeball" the spectra and decide which mineral is present based on the peak areas.[38] This practice cannot be justified because it is highly subjective. Compositions are not given for any of the EDS patterns produced by Drs. Longo and Rigler, even though their EDS is equipped to provide this data.

Dr. Longo states that the quantitative numbers are "not something that's required to render my opinion in this case."[39] He also states that "you can't look at the areas, but the peak ratios is what's important here."[40] This practice of identifying mineralogy by visual inspection of EDS data may be defensible in other applications undertaken at Drs. Longo and Rigler's lab **where the material being tested is already known**. In such cases, EDS is used simply to distinguish among the known minerals. But "eyeballing" of compositions is completely inappropriate in talc testing because of the many different minerals that could be present and how similar they may appear.

Mineral identifications (like those in **Figure 7**) might have been easier if quantitative peak area data had been presented in the Longo/Rigler MDL Reports. It is a standard capability of EDS software to generate elemental composition data (literally one click of a button), but those data are missing from the Longo/Rigler MDL Reports. Had the list of peak areas for individual elements been included in the reports, these data could have corroborated the mineral species identifications made by the other techniques (e.g., PLM by Lee Poye at J3 Resources, Inc.). But because those

---

37 2/6/19 Rigler Depo. 55:23-56:7 (emphasis added).

38 2/5/19 Longo Depo. 81:18-83:14; 2/6/19 Rigler Depo. 96:24-97:12.

39 2/5/19 Longo Depo. 83:15-20.

40 2/5/19 Longo Depo. 76:10-14.

data are missing, little useful information can be gleaned from the EDS plots beyond the presence/absence of Ca.

F. Lack Of Data On And Misuse Of Standards

Summary: Dr. Longo testified that his analysts used "reference standards" of asbestiform minerals in their analysis, but Drs. Longo and Rigler did not produce any, and no such standards exist that could match the Longo/Rigler "eyeball" methodology.

In his deposition, Dr. Longo stated that "they routinely check reference samples,"[41] although none of the reports say this.[42] This lack of data on reference standards makes it impossible to assess the accuracy of the SAED analyses in the Longo/Rigler MDL Reports. Dr. Longo further states that his lab has asbestos reference samples "on the TEM walls."[43] In other words, in the laboratory of Drs. Longo and Rigler, analysts match the asbestos EDS patterns on their screens to ones printed out and hanging on the walls. Because the only reference standards used by the analysts are for asbestos minerals, the confirmation bias is apparent. It virtually guarantees that a particle they identify on the basis of EDS patterns will be asbestos, regardless of whether it really is.

G. Species Identifications Vary By Date And By Analyst

Summary: The mineral species identifications in the Longo/Rigler MDL Reports are not only scientifically indefensible, they appear demonstrably biased according to the particular EDS operator.

Because the mineral species identifications in the Longo/Rigler MDL Reports were made by naked-eye review of the EDS spectra, it would likely be difficult for different analysts to produce comparable results, and in fact, it was. **Figure 8** shows the distribution of mineral species by analyst. Despite the fact that most of these individuals worked on the project over time from 2018-2019 and the samples were randomly selected,[44] the **results appear to be biased by each operator's perceptions of peak intensities**. For example, Lee Poye identifies only anthophyllite. Mehrdad Motamedi and Anthony Keaton consistently find more tremolite than anthophyllite, and Jayme Callan finds more anthophyllite. It is difficult to understand how this could happen if the samples they were testing were randomly distributed.

[**Figure 8** on next page.]

41 2/5/19 Longo Depo. 41:10-18.

42 2/5/19 Longo Depo. 45:9-12.

43 2/5/19 Longo Depo. 41:10-18.

44 2/5/19 Longo Depo. 45:13-20 ("Q: How does your lab distribute samples to individual analysts to test? Is it random? Is it like some analysts get a certain kind of sample? A: It's random. Q: Is that the same for J3? Did you give them random samples? A: Random samples.").

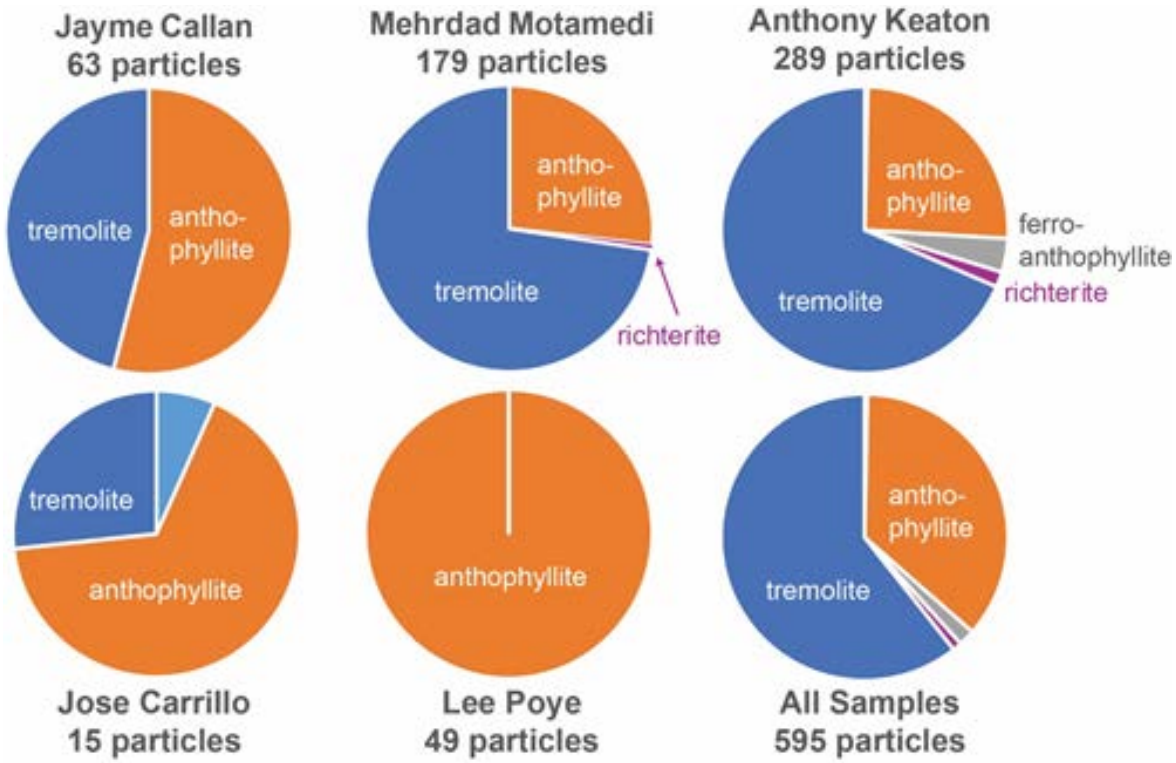

Figure 8. *Distribution of mineral species identifications sorted by analyst for all samples reported to date.*[45]

If all samples were assigned to analysts at random, then the distribution of mineral species should all be the same.

Perhaps the distribution of mineralogy seen in **Figure 8** was the result of which localities each analyst happened to receive? For example, data in the Longo/Rigler MAS Reports indicate that samples mined from Vermont appear to have ~75% anthophyllite and 25% tremolite. So both Lee Poye and Jose Carrillo, who analyzed only Vermont samples (**Figure 9**), should have identical 75/25 ratios of anthophyllite/tremolite, and they do not.

[**Figure 9** on next page.]

[45] This compilation includes all grains for which mineral species were identified with dimensions (i.e., TEM data) in each of four of the reports: 1) *Supplemental Expert Report & Analysis of Johnson and Johnson Baby Powder and Valeant Shower to Shower Talc Products for Amphibole Asbestos* March 11, 2018, 2) *Analysis of Historical Johnson's Baby Powder M69042 October 2018*, 3) *The Analysis of Johnson & Johnson's Historical Baby Powder & Shower to Shower Products from the 1960's to the Early 1990's for Amphibole Asbestos* November 14, 2019, and 4) *The Analysis of Johnson & Johnson's Historical Product Containers and Imerys's Historical Railroad Car Samples from the 1960's to the Early 2000's for Amphibole Asbestos* January 15, 2019. This analysis thus includes data on 163 samples, with some repetition.

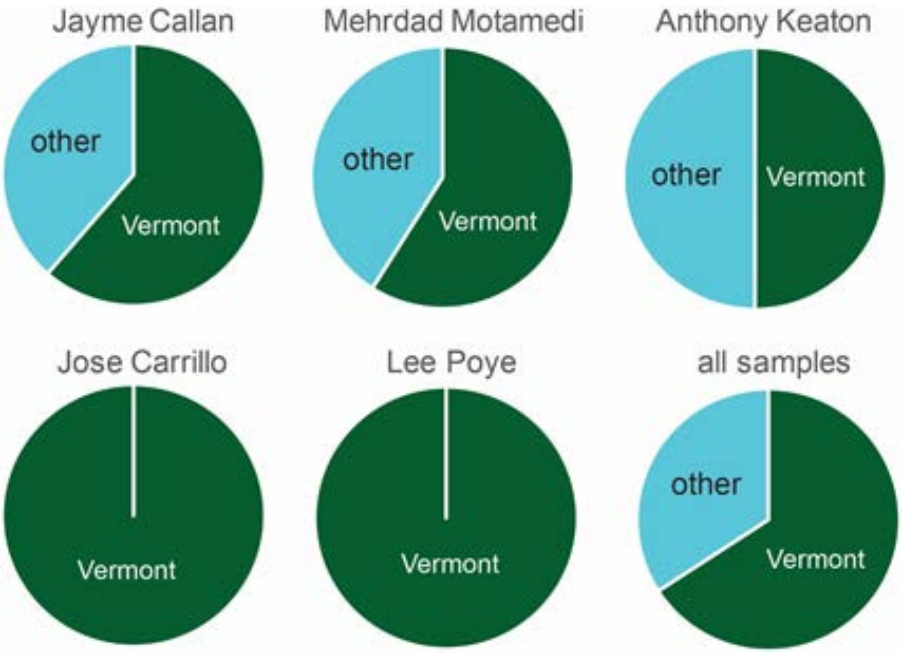

Figure 9. *Distribution of mineral species identifications from Vermont vs. all other localities, sorted by analyst for all samples reported to date.*

In other words, there is no justifiable explanation for why some analysts find different numbers of each mineral species. The logical conclusion is that the mineral species identifications are inconsistent and non-repeatable.

Furthermore, **Figure 10** shows that species identifications also appear to change over time.

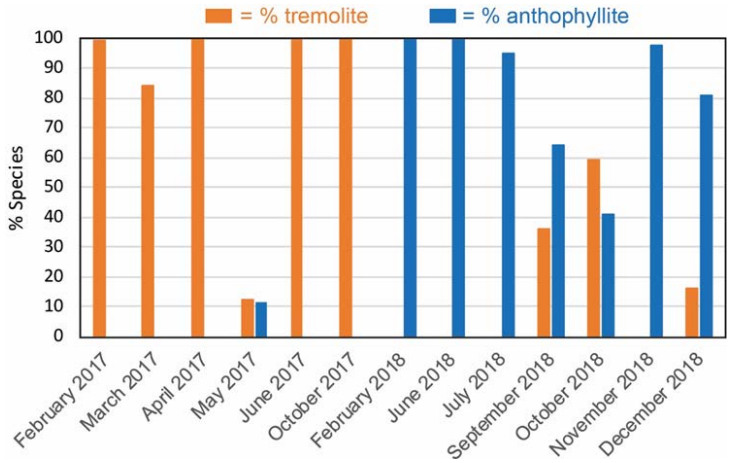

Figure 10. *Comparison of the identification of mineral species by the analytical team of Drs. Longo and Rigler over time. Colors and data sources as in* ***Figure 8****.*

Most of the mineral species identified in 2017 were tremolite, while most of the sample species identified in 2018 were anthophyllite. This could only happen if the samples analyzed in 2017 were all from the same tremolite-bearing locality. But this would be unlikely if all samples were randomly tested.

These variations cast doubt over *all* EDS-based species assignments made by this team, and therefore make it unlikely that any asbestos mineral species could be identified on the basis of these EDS data. This conclusion is of no surprise given the analytical uncertainties of the technique, as explained above.

H. Conclusions Regarding EDS

- **The generally accepted error bars on EDS chemical analysis indicate that it is impossible to easily discriminate amphibole (or any other minerals with similar compositions) species from talc using this technique.** The compositions of a wide range of Si-Mg-Si minerals are so similar that EDS, especially qualitative EDS as used here, cannot distinguish among them.

- **EDS spectral printouts alone are insufficient to discriminate any particular mineral species.** It is impossible to tell anything quantitative about these compositions without calibrated results, which could easily have been produced by Drs. Longo and Rigler or their assistants using software already built into their instruments. Instead, the analysts "eyeballed" the mineral identifications, and compared their spectra only to known asbestos minerals without considering other possible phases that could have similar EDS data.

- **Drs. Longo and Rigler and their analysts thus used a flawed methodology that resulted in wildly inconsistent results across different analysts and over time.** In science, proof involves demonstrating that a result is replicable. Because the Longo/Rigler MDL Reports show no actual data (i.e., percentages of each element derived from a calibration) of any kind to substantiate their mineral species assignments, these results are not credible and cannot be scientifically considered.

- **EDS patterns alone cannot determine the morphology of a mineral particle.** Even if a EDS pattern can be matched with a specific mineral, this only identifies which mineral species is present. Such analysis cannot determine whether or not the mineral is asbestiform.

V. MINERAL IDENTIFICATION USING CRYSTAL STRUCTURE: SAED

The alternative to analyses from EDS is to identify minerals based on their crystal structure – i.e., the arrangement of the atoms. Analytical approaches to this problem generally exploit how energy in the form of light or x-rays passes through the arrangement of atoms in a crystal. The success of any technique in identifying a specific mineral species is dependent on the distinctiveness of each species' crystal structure.

A. Introduction To Selected Area Electron Diffraction (SAED)

Summary: SAED, when properly used, can be used to create patterns of dots. When properly analyzed, these patterns can identify the *crystal structure* of the sample. This is done using the "*d*-spacing," corresponding to spaces between the dots.

A transmission electron microscope (TEM), the same instrument used for EDS, is employed to acquire SAED patterns. For SAED, the waves of electrons pass through the crystal structure and interact with the atoms, which act as a diffraction grating. Some electrons travel straight through the sample and others are scattered by the atoms. By using each mineral's unique crystal structure, the amount by which the electrons are diffracted can be calculated. In the resultant pattern of dots (e.g., **Figure 11**), **spacings between dots are inversely proportional to the spacings between atoms**.[46] Thus, the arrangement of dots can be diagnostic of a mineral structure.

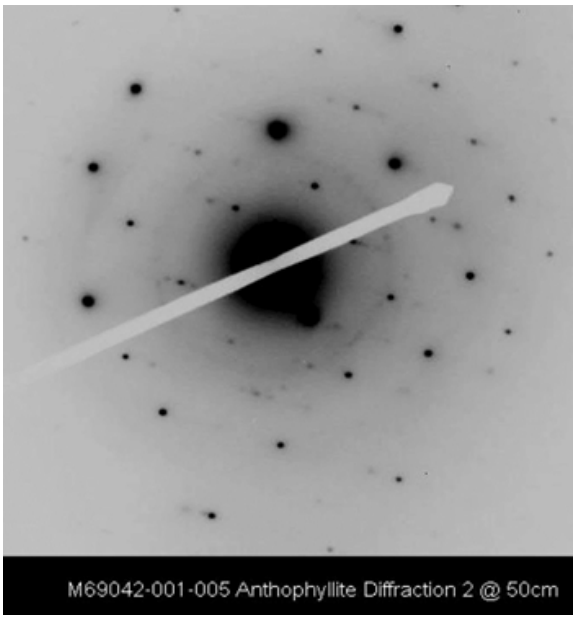

Figure 11. *SAED pattern of M9042-001-005 from page 64 of the 2019.1.16 Longo/Rigler MDL report.*

Optimal SAED patterns are acquired when the individual crystal happens to be lying with a zone axis parallel to the electron beam. This is most easily done when a crystal exhibits elongate (like an amphibole) or sheet-like (sheet silicates) morphology. To obtain these special

[46] Dyar and Gunter (2008) *Mineralogy and Optical Mineralogy*. Mineralogical Society of America.

orientations, most instruments allow the stage to be tilted to produce an optimal pattern, but this requires considerable skill and time.[47] In other words, the crystal must be oriented to obtain a zone axis pattern in which the reflections line up to produce an interpretable pattern.

B. To Uniquely Identify An Unknown Mineral, SAED Patterns Should Be Taken From Multiple Axes

Summary: Multiple SAED patterns along multiple "zone axes" are required to uniquely identify a mineral.

For an accurate identification of an unknown mineral, at least two (and preferably more) SAED patterns must be taken with the sample oriented along a known zone axis.[48] Consider this simplified analogy: imagine a cube, with an atom at every corner, and in the middle of each face (**Figure 12**).[49]

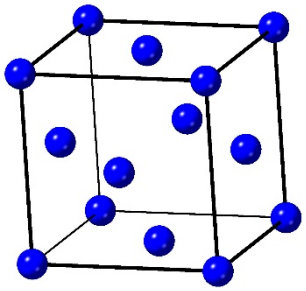

Figure 12. *Crystal structure of copper, which is simply a cube with atoms at the corners and in the middle of each face. Viewed at this angle, the pattern of atoms can be easily discerned.*

If the cube is held with only one side facing the viewer, the corners would line up, and it would look something like **Figure 13**, with its SAED pattern shown at right.

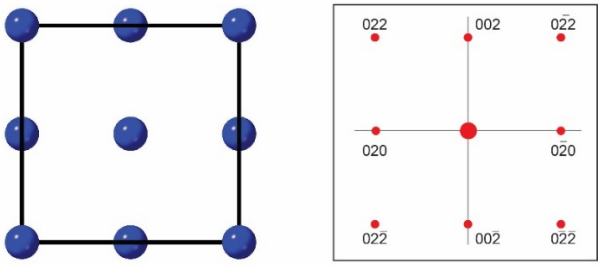

Figure 13. *Crystal structure of copper, with a face of the cube facing the viewer.*

The resultant SAED pattern of the orientation in **Figure 13** is shown to the right. From this perspective, it is impossible to tell where all the atoms are – do they lie on the edges and corners,

---

47 ISO 22262-1 document, page 65.

48 Yamate, EPA (1984).

49 This example happens to be the structure of pure copper, taken from Wyckoff R W G (1963) Second edition. Interscience Publishers, New York, New York, cubic closest packed structure. *Crystal Structures* 1:7 - 83.

or on faces and corners, or both? How tall is this shape? Is it a cube or a rectangle with a square end? Viewed from only one angle, these questions cannot be answered.

So a view from a different angle, as seen in **Figure 14**, is needed to confirm where all the atoms are located. Now it can be seen that this is a cube with atoms at the corners and in the center of each face.

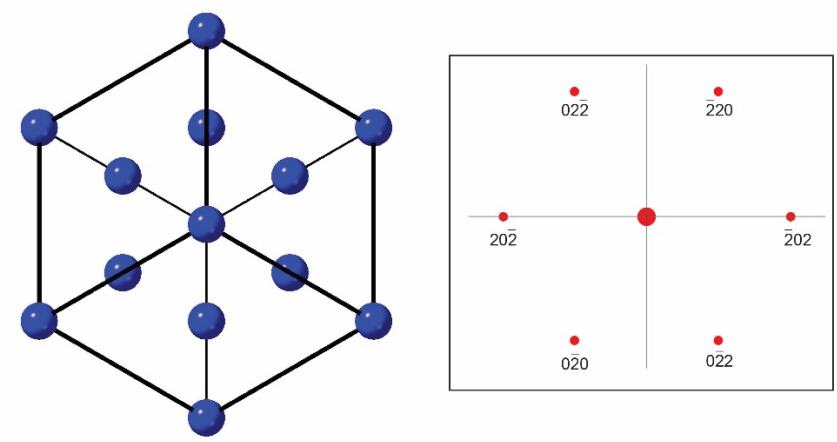

Figure 14. *Crystal structure of copper, viewed along a diagonal with opposite corners held vertical to the viewer. The resultant SAED pattern is shown at right.*

This example highlights the fact that a combination of views from different angles is needed to determine the full structure. Most minerals are far more complicated, and SAED patterns are correspondingly complex, but this is the gist of why multiple SAED images are required to identify a mineral.

By way of example, the patterns in **Figure 15** are the three SAED patterns for tremolite looking down the three zone axes. Note that each image is different. Each image taken in isolation can correspond to other minerals,[50] but together these three uniquely identify tremolite.

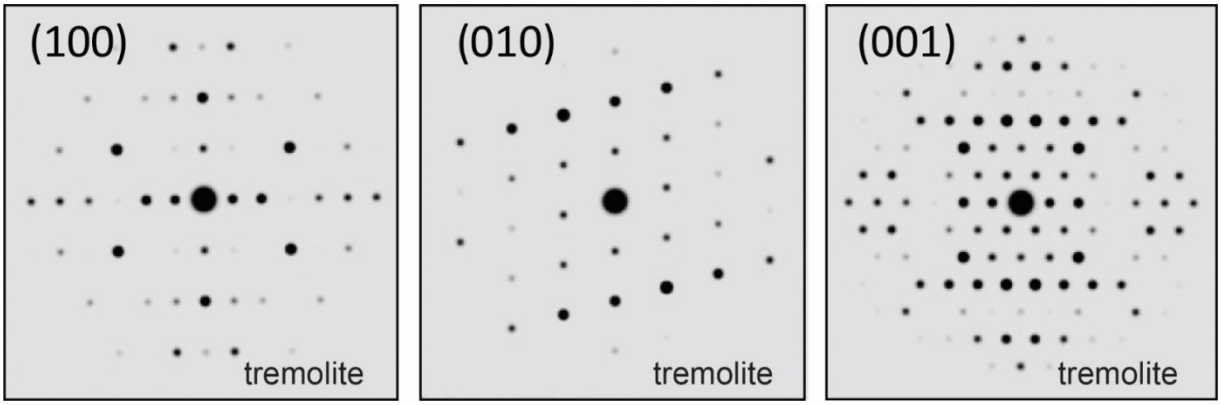

Figure 15. *Simulated SAED patterns for tremolite projected onto different crystallographic orientations, indicated by the numbers in parentheses in each pattern. Adapted from Figure 15.2 in Dyar and Gunter (2008).*

[50] Yamate, EPA, 1984.

The difference between a real SAED pattern (**Figure 11**) and a simulated one (**Figure 15**) demonstrates the importance of operator skill in acquiring these patterns.

It is not a simple process to align a sample on a zone axis parallel to the electron beam. The ISO 22262-1 document, page 65, explains it like this:

> "Rotate the sample until the fibre image indicates that the fibre is oriented with its length coincident with the tilt axis of the goniometer, and adjust the sample height until the fibre is at the eucentric position. Tilt the fibre until an ED pattern appears which is a symmetrical, two dimensional array of spots. The recognition of zone-axis alignment conditions requires some experience on the part of the operator. During tilting of the fibre to obtain zone-axis conditions, the manner in which the intensities of the spots vary should be observed. If weak reflections occur at some points on a matrix of strong reflections, the possibility of twinning or multiple diffraction exists, and some caution should be exercised in the selection of diffraction spots for measurement and interpretation. It is important to recognize that not all zone-axis patterns that can be obtained are definitive."

C. SAED Images In The Longo/Rigler MDL Reports Are Of Very Low Quality And Are Poorly Documented

Summary: The Longo/Rigler MDL Reports use visual inspection of low-quality and poorly documented images, which cannot uniquely identify minerals unless one has already concluded one is looking at asbestos *prior* to the SAED analysis.

As can be seen in examples from one of the Longo/Rigler MDL Reports (2018.1.16) in **Figure 16**, not all of the SAED patterns in the Longo/Rigler MDL Reports look like anything close to those in **Figure 15**. Most of these patterns are inconclusive and inconsistent, depending on the orientation of each crystal and its likely mineralogy.

[**Figure 16** on next page.]

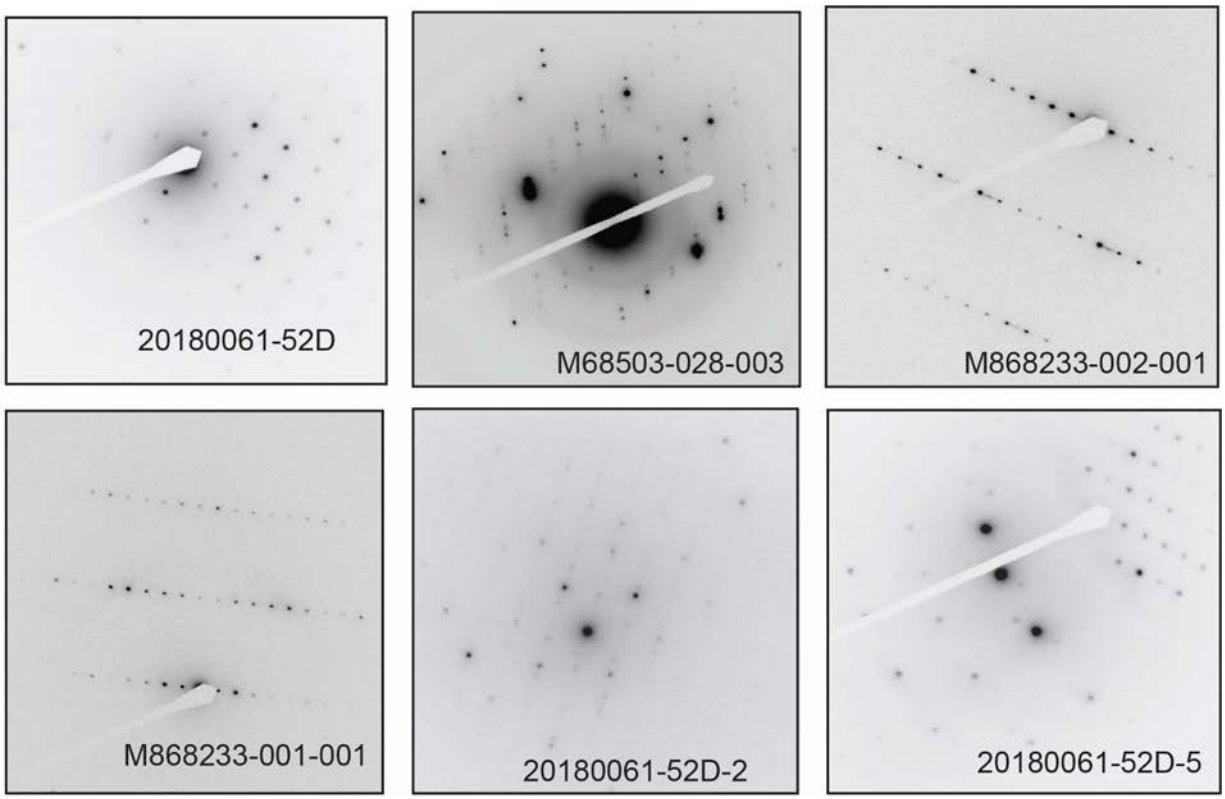

Figure 16. *SAED patterns for "anthophyllite" from the 2019.1.16 Longo/Rigler MDL Report.*

Most of these images are of such low quality that they can only be used to indicate that this is a crystalline material. With only a few exceptions,[51] the reports do not indicate at what orientation each image was taken. Finally, spacings and angles between the dots are given only for a handful of samples given in the *Diffraction Verification* documents (see below). The SAED patterns are labeled with mineral species names using only visual inspection based on operator experience,[52] a methodology for which the Longo/Rigler MDL Reports cite no support. This practice may be able to distinguish among species for materials that are already known to contain asbestos, but it may fail in the applications where the spectrum of possible mineralogy is broad. The use of only visual inspection shows a lack of understanding of the complexity of identification of these minerals using electron diffraction.

[51] In the *Diffraction Verification* documents, some zone axes are indicated, but only for a subset of particles examined. In the main reports, no information on orientation is given.

[52] *See* 2/5/19 Longo Depo. 246:22-47:4.

D. The SAED Patterns In The Longo/Rigler MDL Reports Do Not Uniquely Identify Tremolite Or Anthophyllite

Summary: The *d*-spacing information given for the SAED patterns in the Longo/Rigler MDL Reports does not uniquely identify tremolite and anthophyllite because their methodology is flawed and inadequate.

It is not clear that Drs. Longo and Rigler's analysts even used the *d*-spacing values for their SAED images. Drs. Longo and Rigler testified that the *d*-spacing numbers that they produced (in their *Diffraction Verification* documents) were only used **after** the mineral identification as a way of "verifying" results.[53] If true, Drs. Longo and Rigler did not interpret the SAED patterns in a manner consistent with generally acceptable scientific principles, and indeed, Drs. Longo and Rigler do not cite any publication for interpreting a SAED report without using the *d*-spacing. Dr. Rigler testified that these numbers were generated after the initial expert reports were served,[54] but then changed his testimony when confronted with the implications of this (that conclusions were made without consulting *d*-spacings).[55]

Either way, the *d*-spacing values in the Longo/Rigler MDL Reports do not allow identification of tremolite and anthophyllite. Specifically, in the *Diffraction Verification* documents provided by Drs. Longo and Rigler, SAED patterns are "read" from 219 patterns from six samples by measuring and calculating the spacings between rows of dots. In those patterns, the space between the lines was measured and then converted to units of angstrom (Å)[56] using an **unspecified constant.** Lacking knowledge of that constant, *d*-spacings cannot be easily verified for the patterns in the Longo/Rigler MDL Reports.[57]

Take the following **Figure 17** as a specific example of a Longo/Rigler SAED pattern, to exemplify one of the many problems with their SAED analysis:

[**Figure 17** on next page.]

[53] 2/6/19 Rigler Depo. 116:22-118:17; 2/5/19 Longo Depo. 182:16-183:11.

[54] 2/6/19 Rigler Depo. 118:6-14.

[55] 2/6/19 Rigler Depo. 127:2-129:3.

[56] The diffraction camera constant is unique to each particular TEM instrument, as well as the magnification and focal length used to obtain the pattern, and is expressed in units of mm × Å. It is divided by the distance between two adjacent dots to arrive at the *d*-spacing values. According to Dr. Rigler, the lab uses calculations based on lattice parameters of gold to calibrate their SAED patterns. 2/6/19 Rigler Depo. 114:20-115:3.

[57] In the *Diffraction Verification* documents, the camera constant is given, but it is specified in units of pixels. Because the images have been scanned, it is impossible to apply that constant to the images, and thus the spacings cannot be verified.

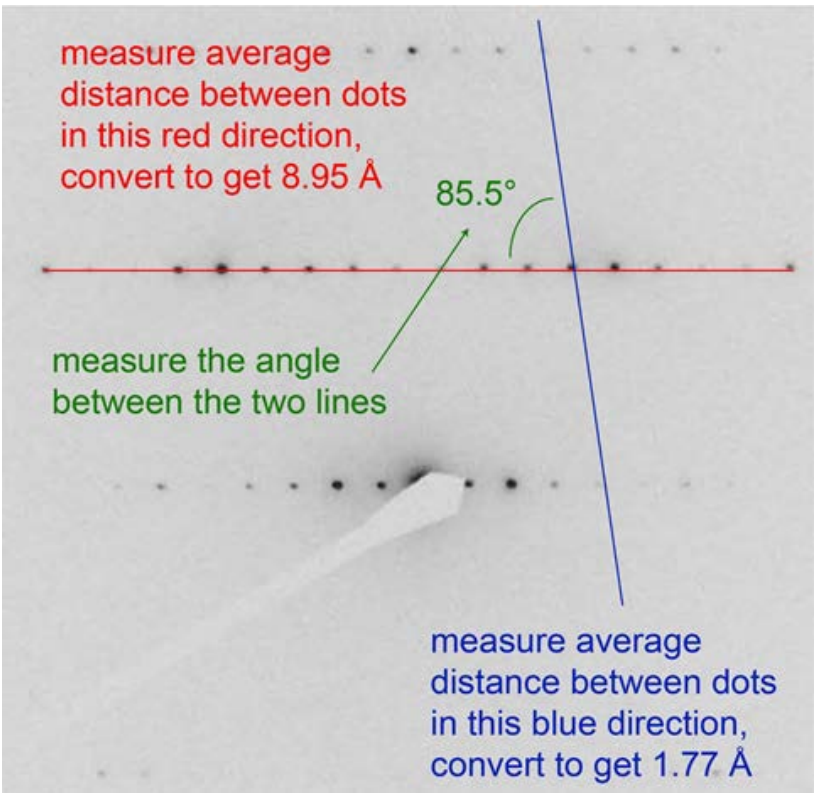

Figure 17*. SAED pattern of M68233-001-001 from p. 693 of the 2019.1.16 Longo/Rigler MDL Report (colored annotation added).*

For the example shown in **Figure 17**, the relevant values are *d*(hk0) = 8.95 Å, *d*(hkl) = 1.77 Å, and θ = 85.5°. Next, it is necessary to find those three values in "look-up tables." Below is the only look-up table that Drs. Longo and Rigler used (found on each "Diffraction Verification" page):

Amphibole Type	Pg. #	Card #	Calculated Spancing	Range +/- 5%
Grunerite	449	31-631	5.2	4.94 - 5.46
Actinolite	4	25-157	5.13	4.87 - 5.39
Tremolite	1192	13-437	5.09	4.84 - 5.34
Crocidolite	993	19-1061	5.19	4.93 - 5.45
Anthophyllite	48	9-455	5.28	5.02 - 5.54

This means that **Drs. Longo and Rigler used tables only for the five recognized asbestos amphibole species and therefore did not check to see if their values corresponded to non-asbestiform minerals**.[58] To the extent Drs. Longo and Rigler already concluded they were looking at asbestos prior to the SAED analysis, as strongly implied by the table, their analysis was predetermined and conclusion-oriented, not scientific.

[58] 2/6/19 Rigler Depo. 101:2-17.

E. Drs. Longo And Rigler Use Incomplete *d*-Spacing Data

Summary: Use of only one *d*-spacing value, as reported by Drs. Longo and Rigler and their analysts, is almost never diagnostic of any mineral. Indeed, their *d*-spacing calculation can correspond to ~25% of all common rock-forming minerals, not one specific mineral.

As explained with the analogy using a cube, above, **finding only one *d*-spacing is only rarely diagnostic of any mineral** because minerals are three-dimensional. In the *Diffraction Verification* documents from Drs. Longo and Rigler, each page has a listing at the top that shows **one** of the calculated *d*-spacings for each of the five amphiboles:

Amphibole Type	Pg. #	Card #	Calculated Spancing	Range +/- 5%
Grunerite	449	31-631	5.2	4.94 - 5.46
Actinolite	4	25-157	5.13	4.87 - 5.39
Tremolite	1192	13-437	5.09	4.84 - 5.34
Crocidolite	993	19-1061	5.19	4.93 - 5.45
Anthophyllite	48	9-455	5.28	5.02 - 5.54

These pages then go on to provide a single "Calculated Spacing Å." For example, there are 31 pages of patterns for sample M69757, for which only **one** *d*-spacing has been calculated. No zone axis information is presented.

The problem here is that providing a single *d*-spacing is not diagnostic of any specific mineral species, or even mineral group. A search of the mineral database[59] from Dyar and Gunter (2008) shows **that 93 out of 369 (25%) mineral species have at least one *d*-spacing of 4.94 to 5.46** Å. A more comprehensive analysis using the American Mineralogist Crystal Structure database shows **more than one thousand** crystal structures that have at least one *d*-spacing in the range above.[60] Finally, a search was made of the Inorganic Crystal Structure Database,[61] which contains 203,830 inorganic crystal structures (minerals and chemical compounds). In that database, 8%, 7%, and 6% of the structures had *a*, *b*, or *c*, respectively in the range of 4.94 to 5.46 Å. Some of these are shown below in **Table 2**, where it is apparent that many different minerals, many of which are not amphiboles, have a unit cell dimension of 5.3 Å in some direction. Therefore, deriving a 5.3 Å spacing from an SAED pattern would be completely inconclusive. **A single unit cell dimension (*d*-spacing) is almost never diagnostic enough to uniquely identify a mineral species.**

---

[59] The Mineral Database search engine and database, which is sold on the Apple web site at https://itunes.apple.com/us/app/mineral-database/id815681529?mt=12, was designed to allow searches on a database consisting only of common rock-forming minerals. The list of minerals with at least one *d*-spacing of 4.94 to 5.46 Å includes (in addition to the minerals listed in **Table 2**) such common minerals as aragonite, calcite, hematite, ilmenite, biotite and phlogopite mica, pyrite and quartz.

[60] The database is found at http://rruff.geo.arizona.edu/AMS/amcsd.php, for minerals under Cell Parameter and Symmetry. Searching each of the *a*, *b* and *c* axes for *d*-spacing between 4.94 and 5.46 Å produces 1897 records, 1227 records, and 2245 records, respectively. Note that these are individual crystal structure refinements, and multiple examples of different mineral species are included.

[61] https://ucsd.libguides.com/crystallography/icsd

Table 2. Unit Cell Dimensions for Selected Relevant Mineral Species

Mineral	Formula	a (Å)	b (Å)	c (Å)
enstatite	$MgSiO_3$	18.2	8.8	5.2
anthophyllite	$Mg_7Si_8O_{22}(OH)_2$	18.5	18.0	5.3
magnesiocummingtonite	$Mg_7Si_8O_{22}(OH)_2$	9.5	18.2	5.3
sepiolite	$Mg_4Si_6O_{15}(OH)_2.6H_20$	13.5	26.7	5.2
antigorite	$Mg_3Si_2O_5(OH)_4$	5.3	9.5	14.9
talc	$Mg_3Si_4O_{10}(OH)_2$	5.3	9.5	18.9
tremolite	$Ca_2Mg_5Si_8O_{22}(OH)_2$	9.8	18.1	5.3
actinolite	$Ca_2(Mg,Fe)_5Si_8O_{22}(OH)_2$	9.8	18.1	5.3
ferrowinchite	$CaNaFe^{2+}{}_4(Al,Fe^{3+})Si_8O_{22}(OH)_2$	9.8	18.1	5.3
richterite	$Na(CaNa)Mg_5Si_8O_{22}(OH)_2$	10.3	18.4	5.2
ferrorichterite	$Na(CaNa)Fe^{2+}{}_5Si_8O_{22}(OH)_2$	10.0	18.2	5.3
riebeckite	$Na_2Fe^{2+}{}_3Fe^{3+}{}_2Si_8O_{22}(OH)_2$	9.8	18.0	5.3
magnesioriebeckite	$Na_2Mg_3Fe^{3+}{}_2Si_8O_{22}(OH)_2$	9.8	18.0	5.2

In his deposition on February 6, 2019, Dr. Rigler acknowledged this problem. When asked, "Can you distinguish anthophyllite from cummingtonite with SAED alone?", Dr. Rigler acknowledged that "you'd have to do zone axis in a couple of different zones to tell."[62] In his deposition, Dr. Longo confirmed this statement, saying that identification of anthophyllite requires measuring both "*d*-spacing and a second pattern from a different crystalline orientation."[63] Despite this acknowledgment, Drs. Longo and Rigler only report two zone axes for a single anthophyllite grain,[64] and give a single zone axis measurement for only two other samples (M69042-008 and M68503-001).

The testimony of Drs. Longo and Rigler confirms that their methodology does not identify specific minerals.[65]

---

[62] 2/6/19 Rigler Depo. 108:23-109:18.

[63] 2/5/19 Longo Depo. 133:3-9.

[64] These zone axes are provided in the *Diffraction Verification* documents. Several values of *d*(hk0), *d*(hkl), and θ are given for sample M69757-007, but no zone axis is derived. For sample M69042-002, several values are given for sample *d*(hk0) only. For sample M68233, four different zone axes are presented; this is the only sample for which more than one zone axis is given.

[65] 2/5/19 Longo Depo. 157:3-8 ("Q. Okay. What other amphibole in the Mineral Powder Diffraction File have *d*-spacing ranges that span 5.23? A. Most of your amphibole minerals, both monoclinic and orthorhombic, will have *d*-spacings in this range."); 2/6/19 Rigler Depo. 119:3-8 ("Q. Now, for this verification page, you calculated a *d*-spacing of 5.23; correct? A. Correct. Q. And that falls within the range of every single amphibole on that list; right? A. Correct."); *see also id.* 119:22-120:8.

F. Unfeasible *d*-Spacings In Longo/Rigler *Diffraction Verification* Documents

Summary: Some of the Longo/Rigler *d*-spacing interpretations have impossible values.

Lack of understanding of *d*-spacings is also shown by reports of indefensible *d*-spacings. Page 14 of the M69757 *Diffraction Verification* document demonstrates particularly poor methodology:

VERIFICATION OF AMPHIBOLE DIFFRACTION PATTERN AT ZERO TILT

Camera K (pixelÅ)	Meas. Distance (pixels)	Calculate Spacing (Å)
810.7	411.6	1.97

Streaking Observed: _____ **Closely spaced dots:** _____

Type of amphibole diffraction verified: Anthophyllite

MAS Job #: M69757-007-001 **Film #:** NA

Analyst: JC **Date of Photo:** 12/15/2018

Date Verified: 12/18/2018 **EDS Verified:** YES

Zone Axis Information

d(hk0) = 10.1
d(hkl) = 1.97
Angle = 83
ZA =

Under the heading "Zone Axis Information," the *d*(hk0) value is indicated to be 10.1 Å. A user would then look for this value in the look-up tables. But as seen on the first page of the anthophyllite reference sheet shown below, **there are no (hk0) values higher than 9.25 Å**.

ANTHOPHYLLITE ***d*-Spacing (Å) and Interfacial Angle *θ* (°)** Page 1 of 32

(**JCPDS 9-455**: *a* 18.5Å *b* 17.9Å *c* 5.28Å *α* 90° *β* 90° *γ* 90°, Orthorhombic)

[Space Group **Pnma** permits only **h=2n** diffractions for (hk0) and **(k+l)=2n** for (0kl)]

Zone Axis	(h k 0)	(h k l)	*d*(hk0)	*d*(hkl)	(hk0)/(hkl)	*θ*	To C-Axis(°)
[0 1 0]	(2 0 0)	(1 0 1)	9.25	5.08	1.82	74.1	90.0
[0 1 1]	(2 0 0)	(0 1 1)	9.25	5.06	1.83	90.0	73.6
[0 1 1]	(2 0 0)	(1 1 1)	9.25	4.88	1.89	74.7	73.6
[0 1 0]	(2 0 0)	(2 0 1)	9.25	4.59	2.02	60.3	90.0
[0 1 1]	(2 0 0)	(2 1 1)	9.25	4.44	2.08	61.3	73.6
[0 1 2]	(2 0 0)	(1 2 1)	9.25	4.42	2.09	76.2	59.5
[0 1 2]	(2 0 0)	(2 2 1)	9.25	4.08	2.27	63.8	59.5
[0 1 0]	(2 0 0)	(3 0 1)	9.25	4.01	2.31	49.4	90.0
[0 1 1]	(2 0 0)	(3 1 1)	9.25	3.91	2.36	50.6	73.6
[0 1 2]	(2 0 0)	(3 2 1)	9.25	3.66	2.53	53.6	59.5
[0 1 0]	(2 0 0)	(4 0 1)	9.25	3.48	2.66	41.2	90.0
[0 1 1]	(2 0 0)	(4 1 1)	9.25	3.42	2.71	42.4	73.6
[0 1 2]	(2 0 0)	(4 2 1)	9.25	3.24	2.85	45.5	59.5
[0 1 0]	(2 0 0)	(1 0 2)	9.25	2.61	3.54	81.9	90.0

A second sample, M69042-008 particle 37, lists a *d*-spacing of 13.46. In these cases, **either the measurement itself is bad or these cannot be anthophyllite, or both.**

In addition, many of the other *d*-spacings calculated in the *Diffraction Verification* documents lie outside their own stated ranges for amphiboles: M69757-005 particle 23; M69757-007 particles 30 and 31, M6942-002 particles 12, 15, 16, 19, 20, 22; M68503-001 particle 7, M68503-002 particle 10, M68503-026 particles 35, 57, and 58. In some cases, the values are likely for (hkl), which also has a wide range of values at 1.7±5% Å. But in most of these examples, the stated *d*-spacings are just anomalous and likely incorrect for any of the asbestiform amphiboles.

G. The *d*-Spacing For What Drs. Longo And Rigler Identify As Anthophyllite Actually Corresponds To One Of Two Other Minerals

Summary: The *d*-spacing for "anthophyllite" identified by the Longo/Rigler MDL Reports actually corresponds to cummingtonite or grunerite.

In a small number of instances,[66] the Longo/Rigler MDL Reports identify the zone axis. For example, because the M68233-001-001 pattern in **Figure 17** was assumed to be anthophyllite (as indicated by the label on the image on page 693), the anthophyllite look-up table[67] was employed. Part of the relevant page from that look-up table is given below.

[66] Zone axes are identified in 41 particles from only 6 of the 70 samples in the Longo/Rigler MDL reports.

[67] Look-up tables were created by Su (2003) *How to Use the d-Spacing/Interfacial Angle Tables to Index Zone-Axis Patterns of Amphibole Asbestos Minerals Obtained by Selected Area Electron Diffraction in Transmission Electron Microscope*, 2008 report, Asbestos Analysis Consulting.

ANTHOPHYLLITE ***d*-Spacing (Å) and Interfacial Angle *θ* (°)** Page 3 of 32

(**JCPDS 9-455**: ***a*** 18.5Å ***b*** 17.9Å ***c*** 5.28Å ***α*** 90° ***β*** 90° ***γ*** 90°, Orthorhombic)

[Space Group **Pnma** permits only **h=2n** diffractions for (hk0) and **(k+l)=2n** for (0kl)]

Zone Axis	(h k 0)	(h k l)	*d*(hk0)	*d*(hkl)	(hk0)/(hkl)	*θ*	To C-Axis(°)
[1 0 2]	(0 2 0)	(4 5 2)	8.95	1.93	4.64	57.4	60.3
[2 0 3]	(0 2 0)	(3 6 2)	8.95	1.88	4.75	50.9	66.8
[2 0 1]	(0 2 0)	(1 7 2)	8.95	1.83	4.90	44.4	81.9
[1 0 1]	(0 2 0)	(2 7 2)	8.95	1.80	4.97	45.2	74.1
[2 0 3]	(0 2 0)	(3 7 2)	8.95	1.76	5.08	46.5	66.8
[3 0 1]	(0 2 0)	(1 0 3)	8.95	1.75	5.11	90.0	84.6
[1 0 0]	(0 2 0)	(0 1 3)	8.95	1.75	5.11	84.4	90.0
[3 0 1]	(0 2 0)	(1 1 3)	8.95	1.74	5.13	84.4	84.6
[3 0 2]	(0 2 0)	(2 0 3)	8.95	1.73	5.18	90.0	79.2
[3 0 2]	(0 2 0)	(2 1 3)	8.95	1.72	5.20	84.5	79.2

There is no listing specifically for *d*(hk0) = 8.95, *d*(hkl) = 1.77, (hk0)/(hkl) = 5.07, and θ = 85.5°. Therefore, the analyst chooses something close, as highlighted in yellow. Importantly, the **85.5° is not the same as 90°**, as can be plainly seen in **Figure 17**. This **indicates that the SAED pattern is NOT a match to anthophyllite, but likely from a different amphibole**. Either the analyst mis-read the table or she/he used the angle relative to the *c*-axis instead of to θ. In either case, the methodology and the science are incorrect.

There are many amphibole minerals with similar compositions (**Table 1**). If a SAED pattern is not consistent with anthophyllite, then another amphibole file can be tried, such as that for the grunerite[68] mineral series, as given below. The yellow highlights in this table represent a good match to the M68233-001-001 SAED pattern. The *d*(hkl) and the angle are exact matches, suggesting that this mineral is from the cummingtonite-grunerite series. A different amphibole might give an even better match, but **there are no other look-up tables**.

This reliance on look-up tables that only exist for asbestiform mineral species virtually guarantees that an asbestos mineral will be identified. This is a serious flaw in methodology.

[68] Minerals in the cummingtonite-grunerite series all have very nearly the same crystal structure (with slight variations due to the size difference between Mg^{2+} and Fe^{2+}), and thus share the same look-up table. These minerals have a very different structure from anthophyllite even though the formulas are similar. So the failure by Drs. Longo and Rigler's analysts to use the proper look-up table is an egregious error.

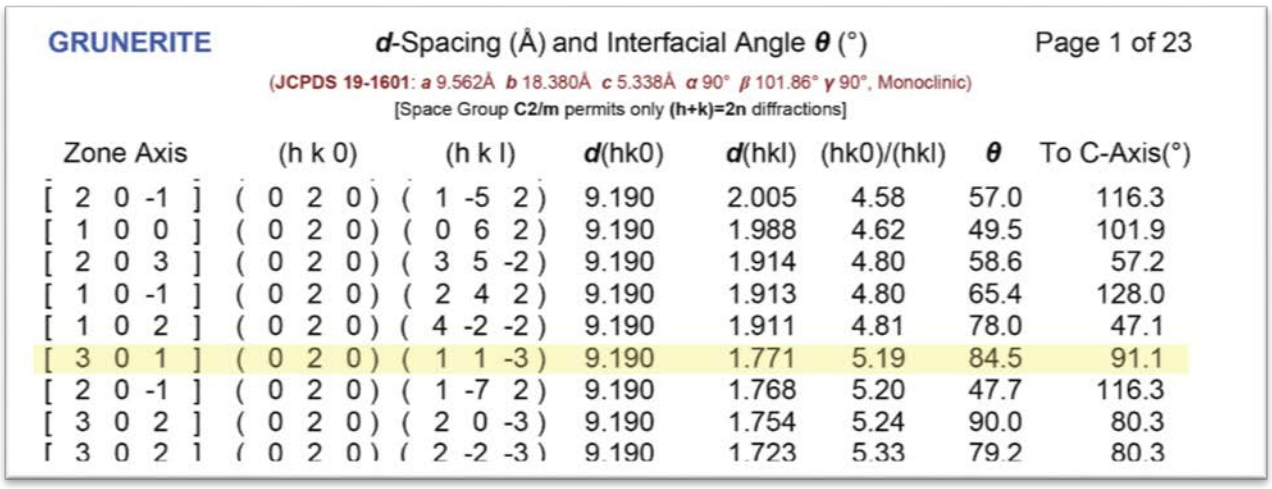

GRUNERITE ***d*-Spacing (Å) and Interfacial Angle *θ* (°)** Page 1 of 23

(JCPDS 19-1601: *a* 9.562Å *b* 18.380Å *c* 5.338Å *α* 90° *β* 101.86° *γ* 90°, Monoclinic)

[Space Group **C2/m** permits only **(h+k)=2n** diffractions]

Zone Axis	(h k 0)	(h k l)	*d*(hk0)	*d*(hkl)	(hk0)/(hkl)	*θ*	To C-Axis(°)
[2 0 -1]	(0 2 0)	(1 -5 2)	9.190	2.005	4.58	57.0	116.3
[1 0 0]	(0 2 0)	(0 6 2)	9.190	1.988	4.62	49.5	101.9
[2 0 3]	(0 2 0)	(3 5 -2)	9.190	1.914	4.80	58.6	57.2
[1 0 -1]	(0 2 0)	(2 4 2)	9.190	1.913	4.80	65.4	128.0
[1 0 2]	(0 2 0)	(4 -2 -2)	9.190	1.911	4.81	78.0	47.1
[3 0 1]	(0 2 0)	(1 1 -3)	9.190	1.771	5.19	84.5	91.1
[2 0 -1]	(0 2 0)	(1 -7 2)	9.190	1.768	5.20	47.7	116.3
[3 0 2]	(0 2 0)	(2 0 -3)	9.190	1.754	5.24	90.0	80.3
[3 0 2]	(0 2 0)	(2 -2 -3)	9.190	1.723	5.33	79.2	80.3

This analysis shows that the analysists used by Drs. Longo and Rigler and their analysts incorrectly used the anthophyllite table to identify the zone axis in a particle that was likely from the cummingtonite/grunerite series. The same mismatch can be observed for all the values of *d*(hk0), *d*(hkl), and the interfacial angle θ compiled for anthophyllite in the report on sample M68233 entitled *Diffraction Verification*.

H. Drs. Longo And Rigler And Their Analysts Do Not Follow EPA Methodology, Including Confirmation On At Least Two Zone Axes

Summary: The EPA "Yamate III" methodology for confirming the presence of asbestos in talc requires *two* SAED zone axis determinations and an EDS analysis, which the Longo/Rigler MDL Reports do not provide.

The protocol for "Methodology for the Measurement of Airborne Asbestos by Electron Microscopy" (Yamate, EPA, 1984) states in Section 2, "Conclusions and Recommendations" (p. 3) that there are three necessary levels of effort:

> The EM methodology for measuring the concentration of airborne asbestos fibers has been refined and specified, and is recommended for field evaluation. The methodology is based on a TEM analytical protocol that is divided into three levels of effort: Level I, for screening many samples; Level II, for regulatory action; and Level III, for confirmatory analysis of controversial samples. The three-level analytical methodology is cost-effective, and will provide the required results for proper assessment of asbestos.

Level III is used in these cases (Section 6, Level III Asbestos Analysis, Discussion of Protocol, from p. 44):

> The Level III protocol is an extension of the Level II analysis procedures described in Section 5. This extension may be necessitated by the need for positive identification of the specific amphibole species in situations where (1) fundamental disagreements between parties involved in a litigation require further clarification;

> (2) for identification purposes, e.g., as causative agents in medical diagnosis or studies; (3) for quality control of Level II analysis in special situations, and/or; (4) for source samples, whether as bulk material or bulk-air type where a legal judgment is anticipated.

The protocol states that identification requires **two** SAED zone axis determinations and an EDS analysis. Dr. Rigler stated in his deposition that anthophyllite particles were double-verified by *d*-spacing analysis (2/6/19 Rigler Depo. 125:18-20). But out of **hundreds of particles** studied by Drs. Longo and Rigler (or their analysts), zone axis determinations are provided for only 41 particles in **six** samples. In fact, zone axis information is provided for only **one** "anthophyllite," M68233.[69] **As such, Drs. Longo and Rigler and their analysts do not follow EPA protocol**.

Indeed, both Dr. Rigler and Dr. Longo admit to problems inherent in using too few zone axis, despite doing it themselves.

I. Conclusions Relating to SAED Analysis

- **SAED images in the Longo/Rigler MDL Reports are often of very low quality with poor documentation.** Some of them are uninterpretable. The reports do not provide the calibration constant needed to convert dot spacings into atom spacings.

- **Indexing of diffraction patterns using look-up tables is done incorrectly.** The use of asbestos mineral species' look-up tables to determine zone axes presumes that the mineral species of the sample has already been identified. Even lacking such information, Drs. Longo and Rigler and their analysts consistently use the anthophyllite look-up table, and do not consider whether another mineral species might give a better match. "Anthophyllite" diffraction patterns indexed by Drs. Longo and Rigler do not match those in look-up tables for that mineral.

- **Unfeasible *d*-spacings exist in the Longo/Rigler *Diffraction Verification* documents.** In two of the 41 cases for which zone axis information is provided, the calculated *d*-spacing is impossible. In several other cases, the single *d*-spacing lies outside the stated range for amphibole minerals.

- **Drs. Longo and Rigler and their analysts do not follow EPA methodology for "confirmatory analysis of controversial samples."** Although Drs. Longo and Rigler both admitted in deposition that two zone axis determinations are necessary to confirm the identity of anthophyllite, zone axis data are provided for only 41 particles in six samples, and the requisite two zone axes on the same sample aliquot are given for only three samples.

[69] Although Drs. Longo and Rigler (or their analysts) believe this particle to be anthophyllite, it is actually a mineral in the cummingtonite-grunerite series.

- **Even when patterns are correctly acquired, the same mineral will have very different SAED patterns depending on its orientation.**

- **SAED patterns alone cannot determine the morphology of a mineral particle.** Even if an SAED pattern can be matched with a specific mineral and orientation, this only identifies which mineral species is present. Such analysis cannot determine whether or not the mineral is asbestiform.

VI. MINERAL IDENTIFICATION USING PLM

The Longo/Rigler MDL Reports purport to use polarizing light microscopy ("PLM") to identify asbestos in talc. This section discusses the proper use of PLM, as compared to how it was used in plaintiffs' experts' reports.

A. How PLM Works

Summary: PLM, when properly used, can identify asbestos mineral content by observing the morphology and refractive indices of the particles in the sample.

PLM is a technique that uses a specially-equipped microscope to polarize the beams of light that pass through a sample (**Figure 18**). This "polarization" causes all the waves of light to vibrate in the same direction, creating a set of near-parallel light waves. When a sample is rotated on the microscope stage, the parallel waves of light interact with the sample differently depending on the angle between the layers of atoms in the sample and their spacings.

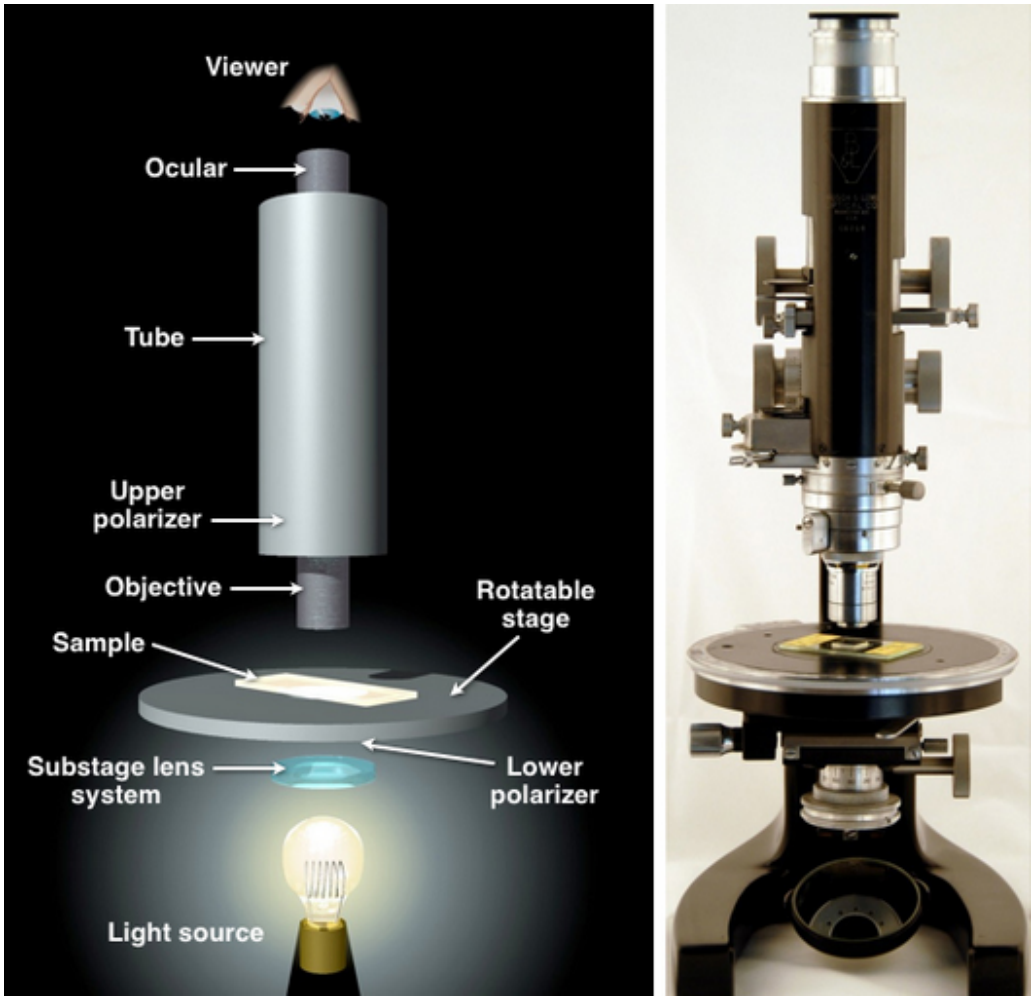

Figure 18. *Photograph and sketch of a simple polarizing light microscope, from Dyar and Gunter (2008), Figure 17.2.*

The polarizers above and below the microscope stage allow a user to study how parallel waves of light interact with rows of atoms in a crystal structure. Changes in appearance upon rotation can be diagnostic of specific mineral groups and, sometimes, mineral species.

The PLM method is, by Longo's own admission, "primarily used today for the analysis of asbestos-added products where the asbestos contents of these products are typically over 1% by weight."[70] PLM allows mineral species to be identified using inherent properties of each mineral: the shape of the grains, the way they break and their densities.

Drs. Longo and Rigler and analysts examined 61 samples using PLM (ISO 22262-1 method), which requires that asbestos be idenitfied using six types of observations:

- Morphology
- Color and pleochroism
- Birefringence
- Extinction charactertistics
- Sign of elongation
- Refractive index

The last property, refractive index (R.I.), is a ratio between the speed of light traveling through a vacuum and how fast it travels through (in this case) a mineral. The value of *n* is different in varying directions of a mineral, and so the change in refractive index with orientation can be diagnostic of a mineral group or species.

To measure the value of *n* in an unknown grain, it is surrounded by an oil with a known *n*, and the crystal is examined. For example, in the protocol used by Drs. Longo and Rigler, "three mounts of the talcum powder samples are placed on two glass slides, a drop of the 1.605 refractive index fluid was placed on each of the three . . . mounts, stirred with the point of a scalpel blade, and then covered with . . . [a] glass cover slip."[71] This procedure is shown in **Figure 19**. In this method, grains with exactly the same *n* will be invisible, while grains with higher or lower values of *n* will appear to have positive or negative relief.

[**Figure 19** on next page.]

[70] 2/1/19 MDL Report, page 5.

[71] 2/1/19 Longo/Rigler MDL Report, page 10.

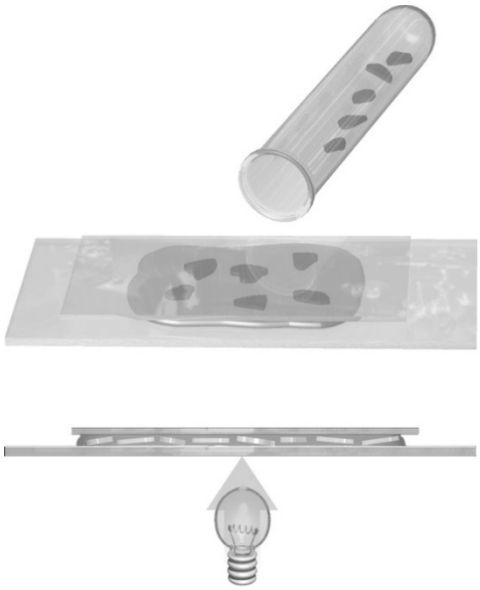

Figure 19. *For microscopy using refractive index oils, grains of mineral are placed on a microscope slide surrounded by a liquid with a refractive index matching the mineral. From Dyar and Gunter (2008), Figure 17.6.*

In the technique called "dispersion staining" used by Drs. Longo and Rigler, a special 10× objective is used on the microscope to cause dispersion of light waves and create certain specific colors. The colors become more red, orange and yellow when $n_{mineral} > n_{oil}$, and more like indigo, purple and turquoise when $n_{mineral} < n_{oil}$. The color will change when the microscope stage is rotated because the densities of atoms are different along different planes in each crystal's structure.

The problems that arise from the optical images and their interpretation are similar to those of SAED. It is difficult to distinguish minerals with very similar structures (e.g., tremolite and actinolite) because the spacings of layers of atoms and the compositions are identical or very similar. As a result, many of the minerals from **Table 1**, as well as many other amphibole group minerals, will have overlapping optical characteristics that can make them difficult to distinguish from one another, rendering any optical analyses (even PLM, even using dispersion staining) inconclusive.

Consider, for example, the list of mineral refractive indices at this url: https://nature.berkeley.edu/classes/eps2/wisc/ri.html, or the extensive list of Shannon et al. (2017).[72] A survey of the Berkeley list shows that 87 of the 204 mineral species (43%) listed there have at least one refractive index that falls in the range of n = 1.55-1.65. Careful PLM work requires that refractive indices be obtained at different orientations (preferably using a range of oils to pinpoint the value of n at each orientation) to refine the identification. It may be necessary in geological studies to corroborate microscope mineral identifications using chemical data obtained by a high-accuracy method.

[72] Shannon et al. (2017) Refractive indices of minerals and synthetic compounds. *Amer. Mineral.*, **102**, 1906-1914. The refractive index table is available under the listing for page 1906 on this url: http://www.minsocam.org/MSA/AmMin/TOC/2017/Sep2017_data/Sep2017_data.html.

B. All Of The ISO PLM Tests Returned Results Consistent With A Finding Of No Asbestos

There are three sources of ISO PLM data: (1) results from the analysts working for Drs. Longo and Rigler; (2) results from the J3 laboratory that are reported in the Longo/Rigler MDL Reports; and (3) results from the J3 laboratory that (for some unknown reason) are not reported in the Longo/Rigler MDL Reports. The Longo/Rigler MDL Reports do not synthesize these data in one place. Notwithstanding that issue, the results appear to be as follows:

- All the reported ISO PLM test results – whether from Drs. Longo and Rigler's laboratory or the J3 laboratory – were either "no asbestos detected" or less than 0.1% by weight asbestos detected, which is consistent with detecting no asbestos.

- Of the at least 39 bottles tested by J3 using ISO PLM, the result of each was "no asbestos detected." [73]

- There are at least eight instances of, for a single bottle, J3 finding "no asbestos detected," while Drs. Longo and Rigler's analysts found "< 0.1% by weight" of asbestos by ISO PLM,[74] as follows:

MDL SAMPLE	LONGO/RIGLER ISO PLM RESULT (wt%)	J3 RESOURCES ISO PLM RESULT (wt%)
M68503-004	< 0.1 Trem/Act	No asbestos detected
M68503-026	< 0.1 Trem/Act	No asbestos detected
M68503-023	< 0.1 Anth	No asbestos detected
M68503-042	< 0.1 Trem/Act, < 0.1 Anth	No asbestos detected
M68503-057	< 0.1 Trem/Act, < 0.1 Anth	No asbestos detected
M68503-020	< 0.1 Anth	No asbestos detected
M68503-059	< 0.1 Trem/Act, < 0.1 Anth	No asbestos detected

Thus, in summary, **all** the ISO PLM testing was consistent with the **absence of asbestos** in the samples.

Moreover, there are also 10 instances where the Longo/Rigler reports identify concentrations of asbestos by the "Blount PLM" method that, if correct, are well above the sensitivity limits of ISO PLM. Thus, **all** such "positives" should have registered as positives on the ISO PLM. Yet here are the results, comparing these 10 instances to the results from the PLM testing at J3:

---

[73] These are Nos. M68503-010, M68503-009, M68503-024, M68503-004, M68503-014, M68503-011, M68503-027, M68503-019, M68503-038, M68503-026, M68503-005, M68503-029, M68503-021, M68503-023, M68503-028, 02D, M68503-046, M68503-042, M68503-057, M68503-020, 07D, 15D, 50D, M68503-059, 10D, 38D, 63D, 52D, 65D, 37D, 45D, 51D, 66D, 21D, M68503-001, 31F, 31G, M68503-016 and M68503-01.

[74] These are Nos. M68503-004, M68503-026, M68503-023, M68503-042, M68503-057, M68503-020, M68503-059 and M68503-001.

LONGO/RIGLER SAMPLE	LONGO/RIGLER BLOUNT PLM RESULT (wt%)	J3 RESOURCES ISO PLM RESULT (wt%)
O7D STS	0.2 Trem/Act, 0.5 Anth	No asbestos detected
15D STS	0.3 Trem	No asbestos detected
10D STS	0.2 Trem/Act	No asbestos detected
38D STS	0.2 Trem/Act	No asbestos detected
63D STS	0.2 Trem/Act	No asbestos detected
52D STS	0.2 Trem/Act, 0.5 Anth	No asbestos detected
65D STS	0.2 Trem/Act, 0.2 Anth	No asbestos detected
66 D STS	0.1 Trem/Act	No asbestos detected
31F STS	0.3 Trem/Act, <0.1 Anth	No asbestos detected
31G STS	0.7 Tre/Act	No asbestos detected

Thus, even where the Longo/Rigler Blount PLM testing result purportedly was seven times the sensitivity reported for the ISO PLM testing, it did not register on the latter. This represents a gross inconsistency, and suggests issues with the PLM work at either or both of Longo/Rigler's laboratory and J3. These results show that the PLM work in the Longo/Rigler MDL Reports does not appear to be reproducible.

C. Dispersion Staining Was Not Used Correctly

The Longo/Rigler MDL Reports purport to find asbestos using dispersion staining, but generally accepted scientific methodologies were not followed. The goal of this methodology is to "meet the requirements set forth by EPA (1993) and NIST (1994) […in which] analysts must measure and record two principle refractive indices, n_α and n_γ, of every type of asbestos mineral found in bulk samples"[75]

The protocol described by the Su article, which Dr. Longo testified that his analysts followed,[76] sets forth a particular methodology to do the dispersion staining characterization described above. It recommends employing a statistical observation method to determine the refractive index. This involves the following:

> "To estimate n_α, analysts randomly select a fiber, rotate it to the extinction position when the fiber elongation axis is nearly parallel (tremolite or actinolite) or exactly parallel (anthophyllite) to the N-S cross hair (assuming the vibration direction of polarizer is E-W) and observe its CSDS color. After 10 to 20 fibers are examined in this way, the fiber with the longest l0 is assumed to exhibit the RI value closest to n_α. To estimate n_γ, 10 to 20 fibers are examined at the extinction position when the fiber elongation axis is nearly parallel (tremolite or actinolite) or exactly parallel (anthophyllite) to

[75] Su (2003).

[76] 2/5/19 Longo Depo. 285:9-14.

> the E-W cross hair; the fiber with the shortest l0 is then assumed to exhibit the RI value closest to n_γ."

There is no indication on any of the PLM outputs in the Longo/Rigler MDL Reports that multiple grains were measured, as recommended in the protocol.

Moreover, **Figure 20** shows an image from the Longo/Rigler MDL Report of a field of talc particles with one amphibole crystal that is a slightly different color than the surrounding talc.

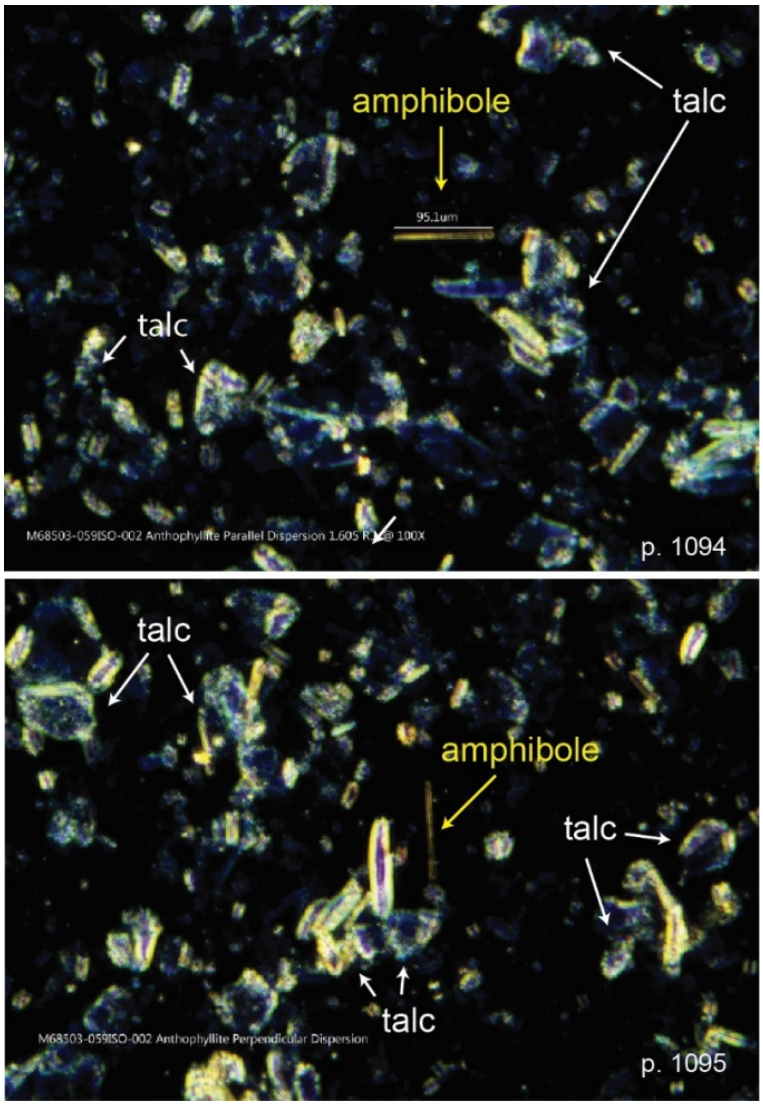

***Figure 20**. Dispersion staining PLM images showing the same field of view rotated 90°. The change in color of the amphibole grain is diagnostic. Images from pages 1094 and 1095 of the January 2019 Longo/Rigler MDL Report.*

Here, the surrounding talc crystals are scattered across the field of view. Some of them appear to have slightly different colors at the edges, but these are likely to be places where the sheets of talc curl up (like chocolate curls). Note that the color variations in these images are very subtle, and it is quite difficult to unequivocally determine if the crystal labelled "amphibole" is

truly a different color than the surrounding grains. This is why the Su (2003) paper recommends looking at many different grains to calculate refractive index correctly.[77]

Another issue is that the dispersion staining images should have used an immersion oil with a refractive index of 1.625 to identify anthophyllite, according to Su (2003) **Table 1**. Instead, the samples were analyzed using a "drop of the 1.605 refractive index fluid."[78] The report cites ISO 22262-1 as the source of the choice of 1.605, when in fact, the report states "For identification of tremolite, actinolite, anthophyllite, and richterite/winchite, RI liquids in the range 1.605 to 1.660 are required, at intervals of 0.005."[79] There is no evidence in the Longo/Rigler MDL Reports to indicate that such a progression of oils was used.

A second example of a confusing PLM image is given in **Figure 21**.

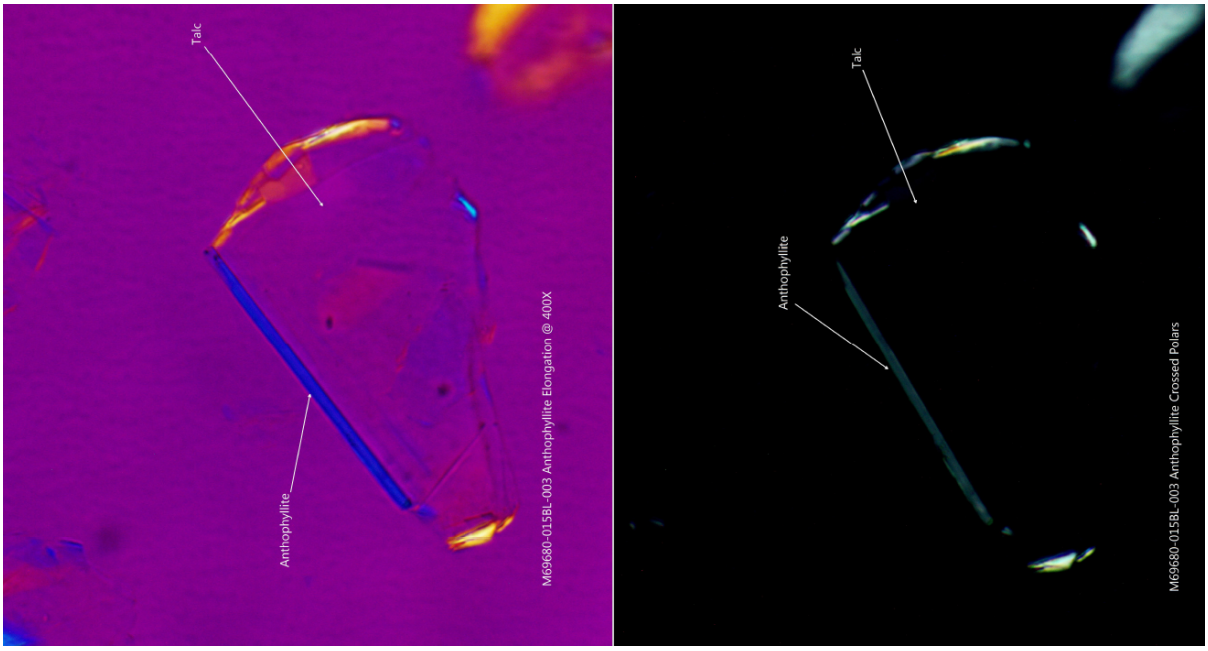

***Figure 21**. Images of a talc grain with the leftmost edge curled up out of the page.*

The curled edge is erroneously identified in the Longo/Rigler MDL Reports as a separate crystal of anthophyllite, but this is highly unlikely. The "anthophyllite" grain would not just "happen" to lie exactly along the edge of the talc grain.

The view at left is pink because it is a dispersion staining image, in which a special wave plate is inserted in the microscope to make the colors more intense (and more diagnostic). These are images of a grain of talc. The straight edge of the talc grain is labeled as "anthophyllite," but in fact, this is a curled-up edge of the talc grain. Because of the curl, the grain is showing a different orientation within the crystal structure, which has different optical properties, and therefore shows

---

[77] Su (2003) at 1980 ("After 10-20 fibers are examined in this way. …10-20 fibers are examined at the extinction position…").

[78] 1/16/19 Longo/Rigler MDL Report, page 9.

[79] 1/16/19 Longo/Rigler MDL Report, page 15.

up as blue. Very few of the PLM images in the Longo/Rigler MDL Reports have labels. There is little discussion of PLM results in any of the reports.

There is also no mention of utilizing proper protocol for distinguishing between talc and anthophyllite with dispersion staining. As noted in ISO 22262-1:

> "Some sources of talc contain fibres that can be mistaken for anthophyllite. These fibres have intergrowths of both the anthophyllite and talc crystal structures. The fibres exhibit refractive indices that are lower than those of anthophyllite and intermediate between those of talc and anthophyllite. If this type of fibre is present, examine the sample in a liquid of RI 1,615. If no γ indices are observed that are higher than 1,615, classify the fibres as talc. Classify any fibres with γ indices equal to or exceeding 1,615 as anthophyllite."

It does not appear that this protocol was followed.

D. The "Point Counting" Method Was Not Used, Yet It Is The Only Way To Estimate Concentration By PLM, As Recognized By ISO 22262

Summary: The ISO 22262-1 protocol provides a methodology for estimating concentration by PLM using "point counting." Drs. Longo and Rigler and their analysts did not do this. Instead, their estimates were based on purported charts generated by Drs. Longo and Rigler's lab's own methodology that are not accepted by the scientific community and that were not produced.

The standard method for estimating concentrations of minerals in geological materials by PLM is called "point counting."[80] In this technique, a sliver of rock or loose particles is placed on an *x-y* stage on a microscope so it can be moved in different directions. The operator then looks down the microscope and uses the technique of choice (usually the optical properties of the minerals as they interact with plane polarized light) to identify the grain at the center of the field of view. Then the stage is moved slightly and the process is repeated. Typically, 100-400 locations on a rock are thus analyzed, from which a quantitative estimate of the abundance of minerals in the rock can be obtained. It is well-recognized that the accuracy of a point count depends on the number of grains counted. This is acknowledged in ISO 22262-1, which says:

> "The statistical reliability of a point count for determination of asbestos depends on the number of asbestos points, not on the total non-empty points examined. Accordingly for comparison against a regulatory standard of 0.1 % asbestos by weight, continue point

[80] An excellent summary of this method is given at http://geologylearn.blogspot.com/2015/08/point-counting-technique-used-in.html. *See also* Neilson and Brockman (1977) *Amer. Mineral.*, **62**, 1238-1244.

> counting until either a minimum of 20 asbestos points, or the equivalent of 13,000 non-empty points have been accumulated."[81]

At his deposition, Dr. Longo confirmed that the Longo/Rigler MDL Reports did not use point counting.[82] Rather, the Longo/Rigler MDL Reports state that "a visual estimation of the quantity of asbestos observed was based on eye calibration through review of lab generated weight percent standards."[83] First off, Drs. Longo and Rigler did not produce those "lab generated weight percent standards," so there is no evidence that the standards are reliable or based in accepted science. Moreover, given the similarities in color of talc and amphibole in these images, these visual estimates are unreliable and unreproducible. The estimates of abundances are orders of magnitude different from the estimates produced by the TEM measurements due to analytical sensitivity issues, also noted by Drs. Longo and Rigler. Probably for this reason, little attention is paid to the amounts of amphibole observed by the PLM method. Instead, PLM is used in the Longo/Rigler MDL Reports mostly to determine presence/absence of amphibole in asbestos. For example, the January 2019 report notes that 20 of the 61 samples tested "were positive for regulated amphibole asbestos."[84]

Moreover, it is not clear what these "weight percentage standards" are, as Drs. Longo and Rigler did not produce them. In that sense, their results are unverifiable and unreproducible.

E. Conclusions Relating To PLM Analysis

- **Dispersion staining was not used correctly.** In contrast to the recommended protocol, the Longo/Rigler MDL Reports use only a single refractive index liquid and do not count the requisite number of particles.

- **The Longo/Rigler MDL Reports purport to find asbestos using dispersion staining, but generally accepted scientific methodologies were not followed.** Indeed, it does not appear that the protocol cited was followed.

- **The reported quantities of asbestos based on PLM used "visual estimation" rather than point counting.** Apparently, the estimates were produced by comparisons against unspecified and unregulated "weight percentage standards." The results are very different from those obtained by TEM, and are mostly ambiguous.

- **Drs. Longo and Rigler and their analysts did not follow the methodology for estimating concentration by PLM using "point counting."** Instead, their estimates were based on purported charts generated by Drs. Longo and Rigler's lab's own methodology that are not accepted by the scientific community and that were not produced.

---

81 ISO 22262-1, page 29.

82 2/5/19 Longo Depo. 269: 20-23, 272:15-17.

83 1/16/19 Longo/Rigler MDL Report, page 9.

84 1/16/19 Longo/Rigler MDL Report, page 7.

VII. MORPHOLOGY IDENTIFICATION USING VISUAL INSPECTION BY TEM

The primary method used in the Longo/Rigler MDL Reports to establish having found asbestiform habit minerals is visual inspection using TEM images. Yet, the methods that they purport to follow expressly state that TEM "cannot be used to discriminate between individual fibers of the asbestos and non-asbestos analogs of the same amphibole material."[85]

Evaluation of whether a particle is a bundle, fiber or cleavage fragment by visual inspection is highly subjective and subject to personal biases, as will be shown below. This section addresses how the methodologies in the Longo/Rigler MDL Reports for identifying talc are scientifically unacceptable, and that the conclusions reached thereby are unsupportable.

A. Differences Among Fibers, Bundles And Fragments

Summary: There are important morphological differences between asbestiform fibers, asbestiform bundles and non-asbestiform cleavage fragments.

Fibers are described as very thin fibrils, usually less than 0.5 mm in width (*cf.* **Figure 1**), rather than the chunky particles identified in the Longo/Rigler MDL Reports. Fibers are identified on the basis of their curvature, flexibility and high tensile strength. **Figure 22** below shows the visual difference between asbestiform and non-asbestiform versions of the same minerals:

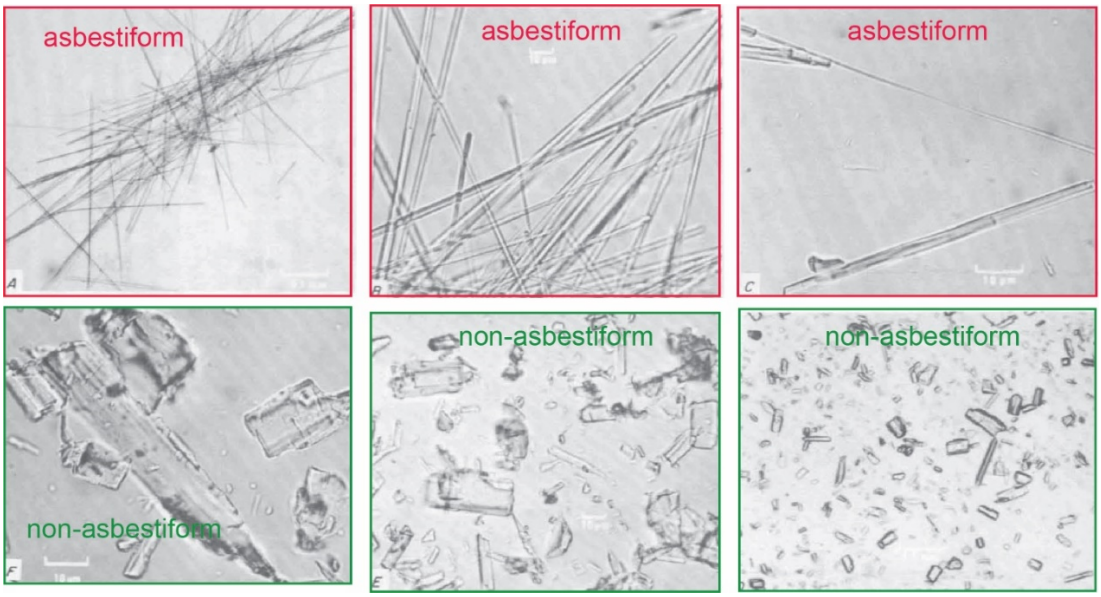

Figure 22. *Examples of asbestiform vs. non-asbestiform particles from Figure 39 of the classic paper by Campbell et al. (1977).*

The differences between asbestiform and non-asbestiform minerals go back to the first definitions given in this report. Recall that the ISO 22262-1, 2, 3 documents define asbestiform as a "specific type of mineral fibrosity in which the fibres and fibrils possess high tensile strength

[85] ISO 10312 (1995), at 1; *see* ISO 13794 (1999) (same), at 1; ISO 22262-1 (2012) at 31 ("Full details relating to identification of asbestos fibers using TEM are given in ISO 10312 and ISO 13794.").

and flexibility." The particles in the top row of **Figure 22** all seem to comply with this definition. A non-asbestiform particle is often called a cleavage fragment, which means it is a small particle that has broken off a larger crystal. These will appear to be chunkier, as seen in the bottom row of **Figure 22**.

Even if a particle of a mineral that can have an asbestiform habit is long and thin, it may not be an asbestos fiber. Again, that term relates as much to physical properties such as tensile strength and flexibility as it does to aspect ratio. **Figure 23a** shows three examples of fibers that are not "asbestos," but rather cleavage fragments of non-asbestiform amphibole.

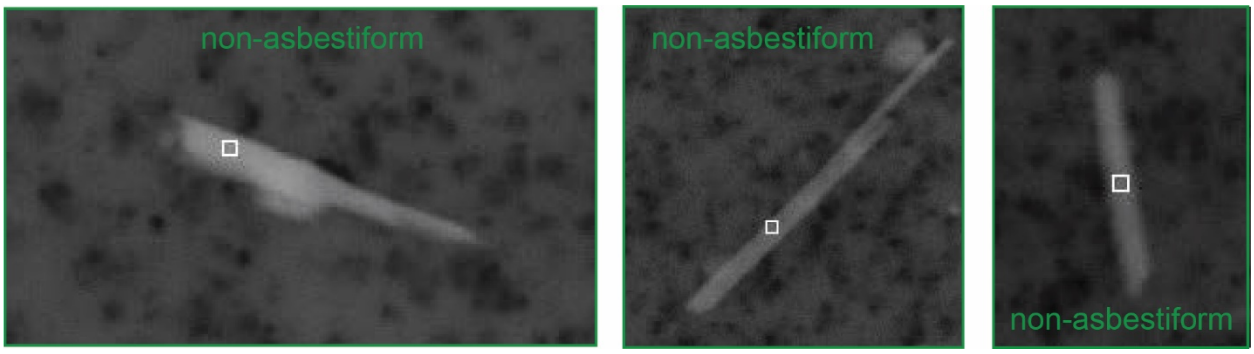

Figure 23a. *Images of non-asbestiform particles from Gunter (2010).*

Asbestos particles can come in fibers or bundles. Bundles occur as separable groups of parallel fibers with **splayed** ends and matted masses as seen in **Figure 23b**. They are defined in ISO 22262-1 as structures "composed of parallel, smaller diameter fibers attached along their lengths."

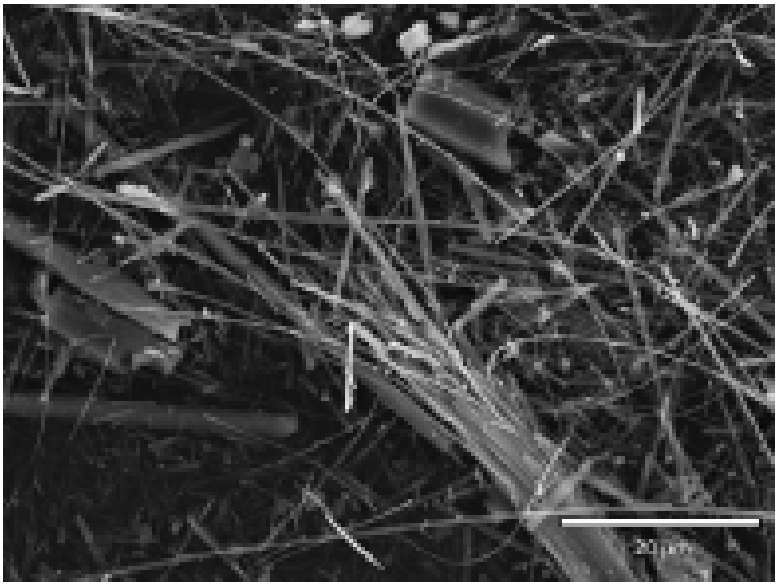

Figure 23b. *Image of tremolite bundle of asbestiform particles from Harper et al. (2010).*[86]

[86] Harper et al. (2014) Characterization of Lone Pine, California tremolite asbestos and preparation of research material. *Ann. Occp. Hyg.*, **2014**, 1-13.

The assessment of whether a particle is an asbestiform fiber or bundle versus a cleavage fragment is fairly straightforward. Asbestiform fibers are greatly elongated with high aspect ratios. At the end of a bundle, the fibers generally bend out like the straws at the end of a broom. Note in **Figure 23b** that the particles do splay out at the end, and it is obvious that the bundle at lower right is indeed "composed of parallel, smaller diameter fibers attached along their lengths."

Alternatively, cleavage fragments tend to be short and fat particles that cannot maintain the thinness and long aspect-ratios associated with asbestiform minerals because they are generally brittle. Non-asbestiform cleavage fragments are blocky, and may show stair-step cleavage fractures on the ends of the grains.

B. Drs. Longo And Rigler Misidentify Cleavage Fragments As Bundles And Fibers

Summary: Drs. Longo and Rigler and their analysts did not apply objective criteria for distinguishing between cleavage fragments, bundles and fibers, as demonstrated by the inconsistent results of their analysts.

The Longo/Rigler MDL Reports consistently demonstrate confusion over the identification of non-asbestiform cleavage fragments vs. the asbestiform habit. For example, the particles shown in **Figure 23c**, which are explicitly identified as fibers and bundles, are effectively identical to the non-asbestiform cleavage fragments in the Longo/Rigler MDL Reports shown in **Figure 23d**.

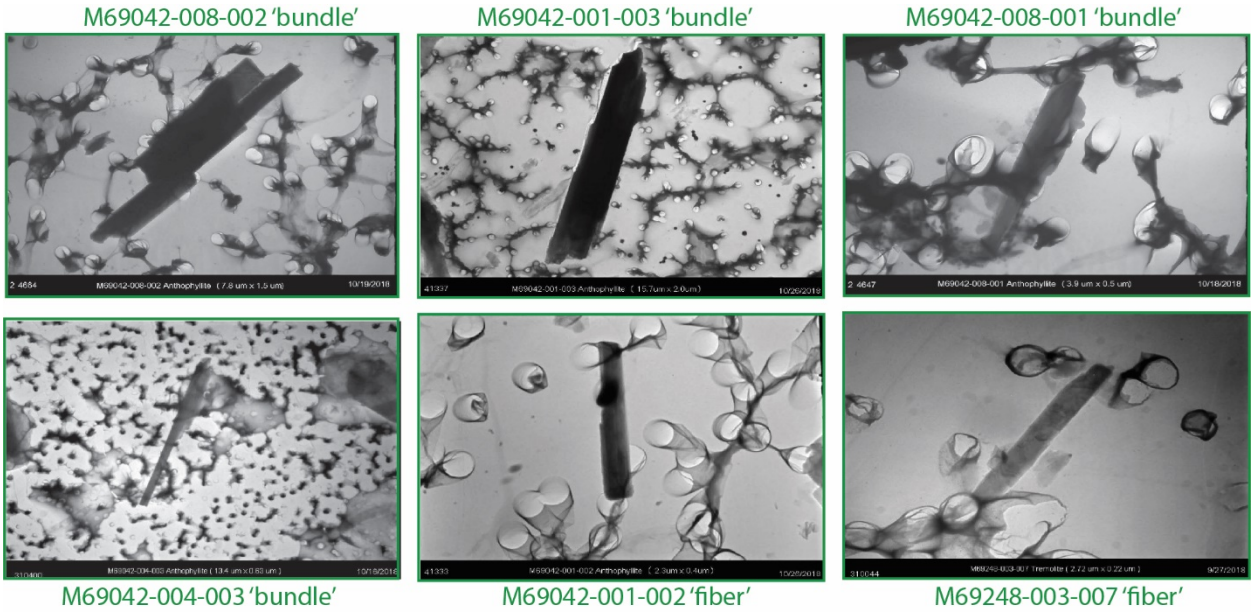

Figure 23c. *Particles from the 1/16/19 Longo/Rigler MDL Report and assignments. Compare to* ***Figures 23a, b*** *and* ***c****. This comparison shows visually that the bundles and fibers identified in the Longo/Rigler MDL Report are NOT fibers and bundles, but rather, non-asbestiform particles.*

Figure 23d. *Dispersion staining photomicrographs from the January 2019 Longo/Rigler MDL report with ambiguous annotations. For sample M69503-010, the PLM ANALYSIS report states the presence of "actinolite/tremolite cleavage fragments" (p. 120).*

For sample M69503-026, the PLM ANALYSIS report states the presence of "tremolite/actinolite asbestos observed. Actinolite/Tremolite cleavage fragments observed."

Compare these images to **Figure 23e**, which shows PLM dispersion staining images of tremolite cleavage fragments from the peer-reviewed paper by Pierce et al. (2017). These dispersion photomicrographs were imaged by RJ Lee Group and Forensic Analytical, Hayward, CA. Particles in **Figures 23e** and **23f** are effectively identical, and here, the analysts employed by Drs. Longo and Rigler correctly identify these particles as cleavage fragments.

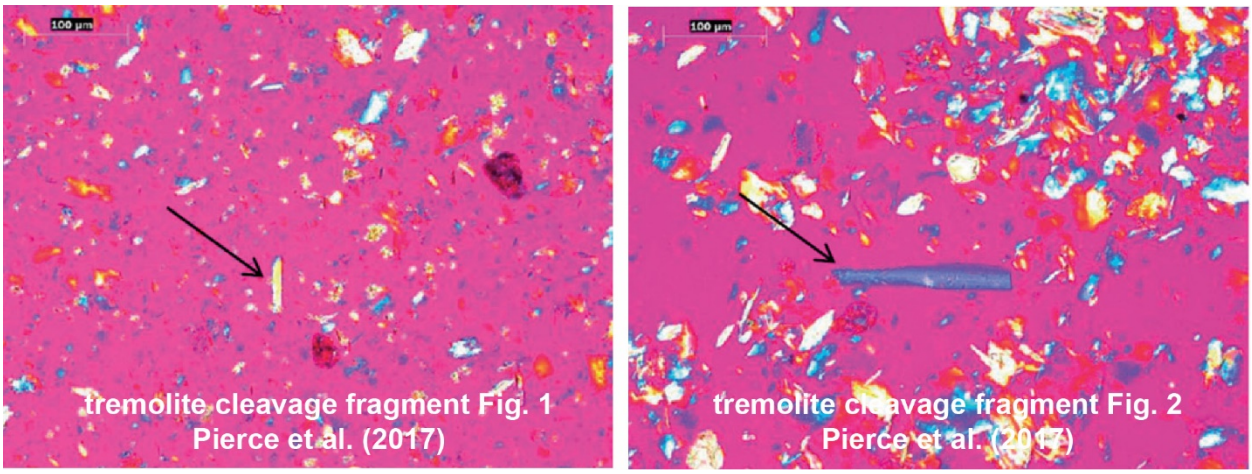

Figure 23e. *PLM dispersion staining images of tremolite* ***non-asbestiform cleavage fragments*** *from the peer-reviewed paper by Pierce et al. (2017).*

But the particles seen in **Figure 23f**, which are strikingly similar, are indicated in the Longo/Rigler MDL Reports to be **asbestiform bundles**, even though they demonstrate none of the objective criteria for such bundles. **They look nothing like the bundle shown in Figure 23c.**

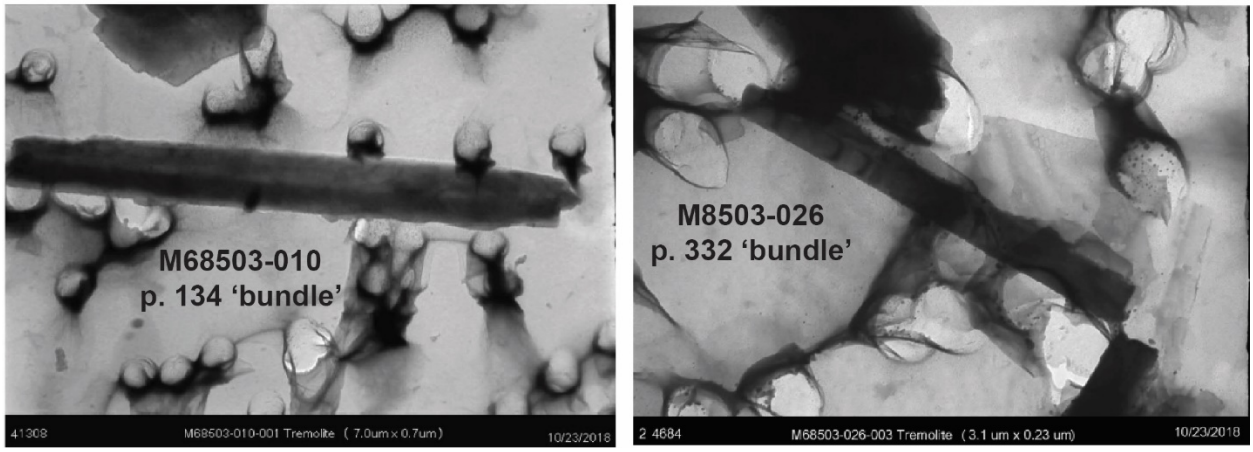

Figure 23f *(left) The TEM report for sample M69503-010 (p. 131) identified 4 bundles of tremolite. No mention is made of cleavage fragments (right).*

The TEM report for sample M69503-026 (p. 321) identified 31 bundles of tremolite. Note that the shape of the "bundles" identified in the Longo/Rigler TEM images is the same as the shape of the cleavage fragments in Pierce et al. (2017).

There is obvious confusion in the Longo/Rigler MDL Reports over these identifications. Nearly all of the amphiboles referred to as "fibers" and "bundles" in the Longo/Rigler MDL Reports are likely to be either non-asbestiform amphibole cleavage fragments, or in some cases, talc particles viewed on edge.

C. Results Of Analysts Working For Drs. Longo And Rigler Are Inconsistent

Summary: The results reported in the Longo/Rigler MDL Reports are inconsistent from analyst to analyst, highlighting the unreliability of their method of visual identification using TEM.

The inconsistent results of the analysts working for Drs. Longo and Rigler in characterizing fibers and bundles is further proof of the lack of repeatability of the analysis in the Longo/Rigler MDL Reports. Because criteria for describing particle morphology are so ambiguous, it comes as no surprise that different analysts would produce wildly variable results (**Figure 24**). Some analysts, such as Mehrdad Motamedi, are far more likely to classify a particle as a fiber, and Anthony Keaton, for example, finds far more fibers than either Jayme Callan or Lee Poye.

[**Figure 24** on next page.]

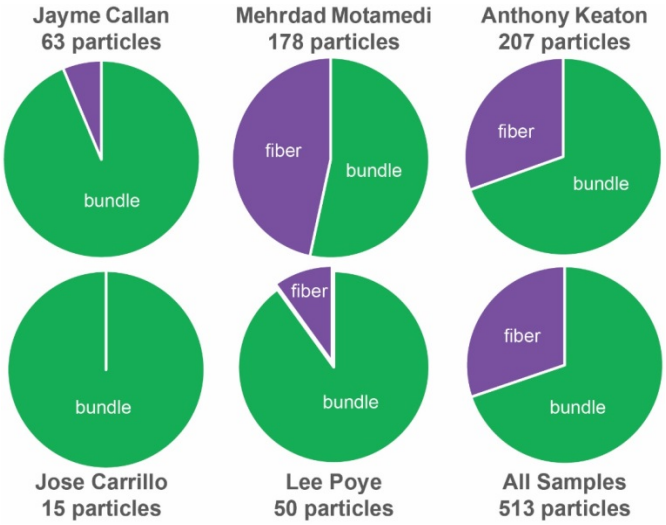

Figure 24. Comparison of fiber vs. bundle identifications made by different analysts. Note that totals are different from those in the mineral identification figures because morphologies were not reported for some particles. Data sources as in Figure 8.

Figure 25 shows that the percentage of observed bundles vs. fibers also increases over time. Because the talc samples studied were randomly selected from various collections, such a conclusion is highly unlikely, and simply shows operator bias. This renders the distinctions made in the Longo/Rigler MDL Reports between fibers and bundles arbitrary.

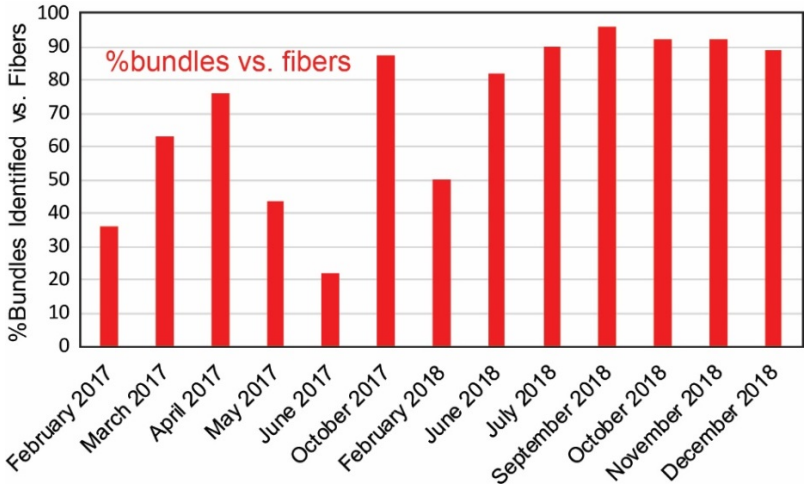

Figure 25. Identifications of bundles vs. fibers over time by analysts working for Drs. Longo and Rigler. Data sources as in Figure 8.

Finally, **Figure 26** shows results from a test undertaken to supposedly demonstrate the "Coefficient of Variation" of their analysts.[87] The stated goal of this document is "to determine the MAS [Longo/Rigler] TEM analysis coefficient of variation (CV or relative standard deviation RSD)" of measurements made on cosmetic talc spiked with asbestos standard reference material. In other words, this testing sought to confirm consistency of results from the company's testing.

87 TEM Coefficient of Variation for Tremolite and Anthophyllite in Talc: A Quality Control Study.

Two TEM grids were studied. Supposed "asbestos" particles were searched for in each of 100 squares in each grid. Then four of the analysts working for Drs. Longo and Rigler were asked to measure the particles and judge if they are fibers or bundles. Each analyst looked at exactly the same particles. The document does calculate the mean and standard deviation of the **number** of particles observed on each sample. Standard deviation in this instance indicates how reproducible the measurement is, but says nothing about accuracy – i.e., how close it is to the true value.

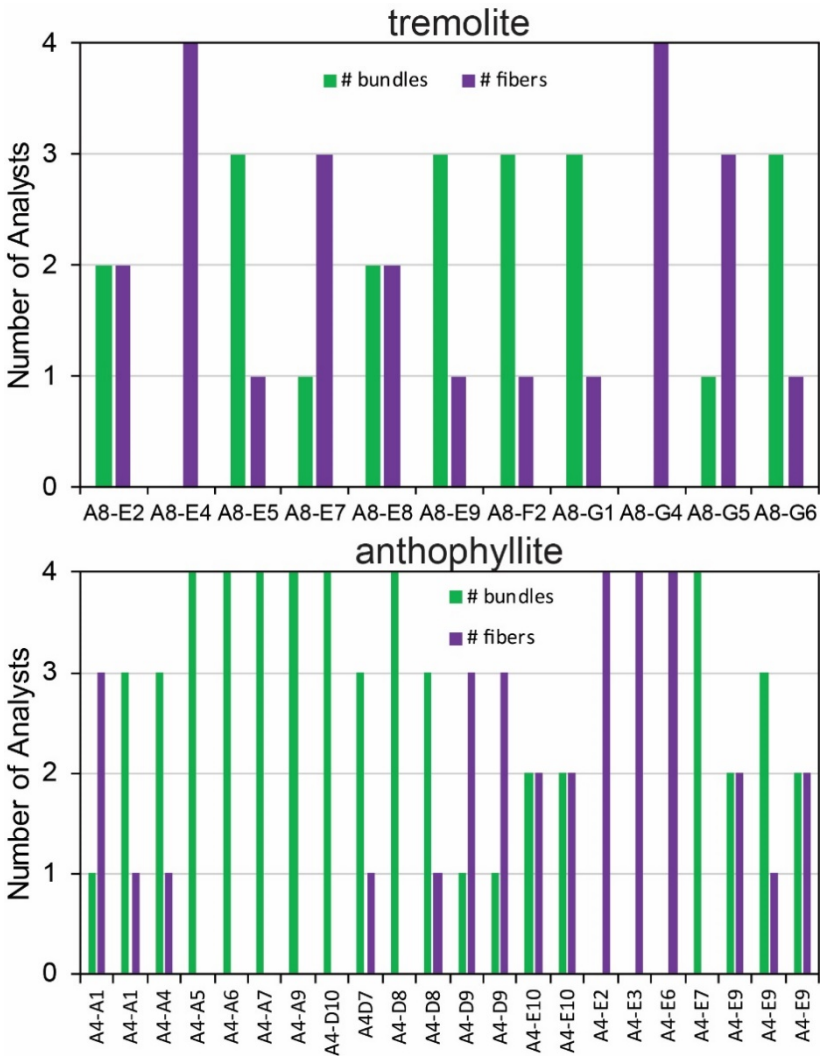

Figure 26*. The Longo/Rigler MDL report entitled TEM Coefficient of Variation for Tremolite and Anthophyllite in Talc: A Quality Control Study shows results from four different analysts who identified the same particles in the same set of two TEM grids, one for tremolite (top) and one for anthophyllite (bottom). Out of 44 particles, there are only 9 cases in which all four analysts agree on whether a particle is a fiber or a bundle. In other words, they disagree 80% of the time. This represents an unacceptable inconsistency and reveals the arbitrary nature of these judgments.*

But the document also shows the alarming inconsistency of analysts working for Drs. Longo and Rigler with respect to identification of bundles vs. fragments. **Figure 26** shows that the four analysts all agreed on fiber vs. bundle identification for only 9 of the 44 particles. In other words, only 20% of the time did the four analysts concur on their judgments. This result, when

coupled with the results presented in **Figures 24** and **25**, firmly establishes that the visual distinctions made between particles and bundles by Drs. Longo and Rigler's analysts are scientifically invalid and unacceptable.

D. Statistical Distinctions Between Fibers And Fragments

As noted above, visual distinctions between fibers, bundles of fibers and non-asbestiform cleavage fragments are quite subjective – and in the case of the analysts employed by Drs. Longo and Rigler, done unreliably and in a way that is not reproducible. There is a scientifically accepted methodology, however, for determining whether a population of amphibole is asbestiform or non-asbestiform, based on their **statistical** distinction between their distributions of sizes.

Specifically, a population of amphiboles will have different, characteristic distributions of aspect ratio, depending on whether they are asbestiform or non-asbestiform.[88] These can be analyzed accurately and in a way that is reproducible using statistics.

1. Background on statistical tests of population differences

Summary: A *t* test assesses whether two populations have the same or different means. We can use this test to determine whether the data from the Longo/Rigler MDL Reports show a population of non-asbestiform cleavage fragments or asbestiform fibers.

As noted in my geostatistics textbook, "today's earth scientists need to be able to critically evaluate sampling designs, to understand the concept of statistical analysis, and be able to evaluate and interpret the results of statistical tests applied in a wide range of fields."[89] In considering the problem of particle size distributions in talcum powder impurities, only the most basic of such statistical methods is necessary – the need to distinguish among the average particle dimensions based on the ratio of length to width (aspect ratio). Comparisons between the mean (≈average) are so basic that even Microsoft Excel can calculate them. Here, the need for statistics is based on the problem of discriminating among known populations of non-asbestiform tremolite, asbestiform tremolite and the particle measurements in the Longo/Rigler MDL reports. For simplicity, these populations can be compared two at a time.

The appropriate test here is called a **two-tailed *t* test**. It allows for testing of the hypothesis that "the two samples are drawn from populations with different means."[90] In conducting this analysis, the underlying assumption is that the two populations (here, asbestiform vs. non-

---

[88] 2/5/19 Longo Depo. 290:11-21 ("Q. Okay. And the nonasbestiform version of the same amphibole has a different characteristic distribution? A. Yes, it does. Q. And you did not generate a particle size distribution chart like the one in Blount's paper -- the ones in Blount's paper in your report? A. Not for the MDL samples, no."); 2/6/19 Rigler Depo. 190:10-25 ("Q. That there's a characteristic -- there is a characteristic particle size distribution for asbestos; is that correct? A. Well, depending on how that sample's been processed, you're going to have different fiber sizes, different – they're going to be different. You're going to have different aspect ratios and different sizes. Q. For any given sample that everyone agrees is asbestos, it's going to have a characteristic particle size distribution; right? A. It can."); *id.* 191:10-13 ("Q. Do cleavage fragments have a different particle size distribution than asbestos? A. They can.").

[89] McKibbin and Dyar (201) *Geostatistics Explained*. Cambridge University Press.

[90] *ibid*.

asbestiform) have comparable variation – this is called "equal variance" in statistics-speak. Then a critical value for the *t* test is selected to specify the desired level of confidence for the answer. It is conventional to use a 95% confidence limit, which means that conclusions can be drawn with a 95% chance that they are correct.

Thus, **Figure 27a** shows a normal distribution for a hypothetical population.

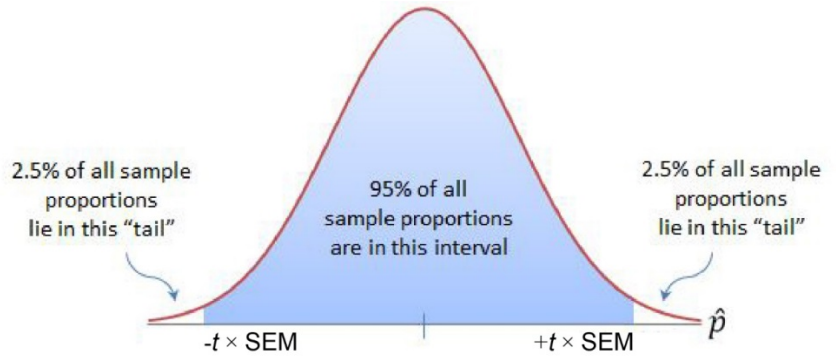

Figure 27a. *Schematic of a normal population distribution illustrating the concept of confidence interval.*

Here, the 95% confidence interval, which is estimated from a sample by using the *t* statistic, is indicated in blue, where SEM is the standard error of the mean of the population.[91] Therefore, 5% of the means of this sample will lie outside this range, but if the mean lies within the 95 interval, then it will be considered to have come from a population with a mean the same as this one.

The *t* test is used to assess whether the mean of a sample lies within or outside the 95% confidence limit of a population, implying that the two samples come from the same population. **Figure 27b** shows two populations that are being compared:

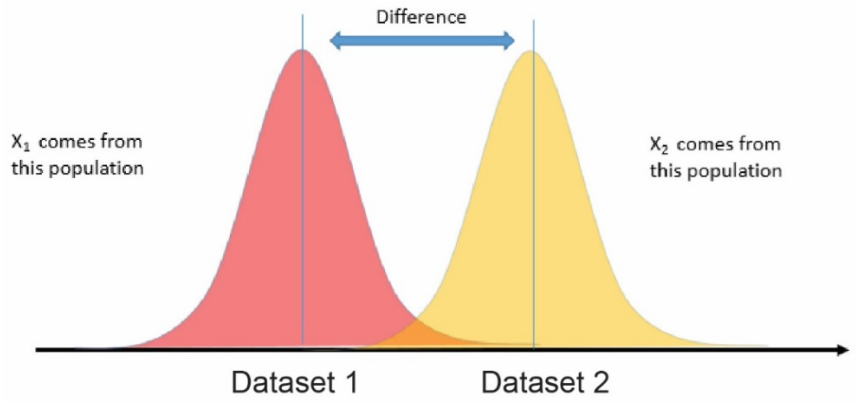

Figure 27b. *Adapted from https://rexplorations.wordpress.com/2015/08/13/hypothesis-tests-2-sample-tests-ab-tests/.*

[91] McKillip and Dyar (2010) *Geostatistics Explained*. Cambridge University Press.

In the figure, the two populations barely overlap, and only within the 2.5% confidence limit on the extreme edges of the curves. As illustrated, these two populations can be said to derive from different sources.

A *t* test assesses whether two populations have the same or different means, which can be employed to assess if the data from the Longo/Rigler MDL Reports come from a population of non-asbestiform cleavage fragments or asbestiform fibers.

2. Statistically significant differences are seen between asbestiform tremolite and non-asbestiform tremolite cleavage fragments

Summary: Use of the *t* test applied to peer-reviewed data shows two distinct populations of shapes: asbestiform and non-asbestiform.

Now, consider the application of the two-tailed *t* test to making distinctions between asbestiform and non-asbestiform particle morphologies. Here, the hypothesis is whether the aspect ratio (particle length divided by width) is statistically different for non-asbestiform tremolite than for asbestiform tremolite. To understand this problem, comparisons among pairs of datasets can be made using three available populations of data:

1. Non-asbestiform amphiboles from the compilation of **Wylie and Virta (2016)**, who provide data on the lengths and widths of amosite, crocidolite, chrysotile and nonfibrous tremolite;[92]

2. Asbestiform tremolite data from **Harper et al. (2014)**;[93] and

3. Particles in the **Longo/Rigler MDL Report**.

Using these data, the first test is whether asbestiform and non-asbestiform particle populations are different. These are shown here, in **Figure 28a**:

[**Figure 28a** on next page.]

[92] Wylie and Virta (2016) Size distribution measurements of amosite, crocidolite, chrysotile, and nonfibrous tremolite. *Digital Repository at the University of Maryland*, http://dx.doi.org/10.13016/M2798Z.

[93] Harper et al. (2014) Characterization of Lone Pine, California tremolite asbestos and preparation of research material. *Ann. of Occp. Hyg.*, **2014**, 1-13, https://academic.oup.com/annweh/article/59/1/91/2464346#supplementary-data.

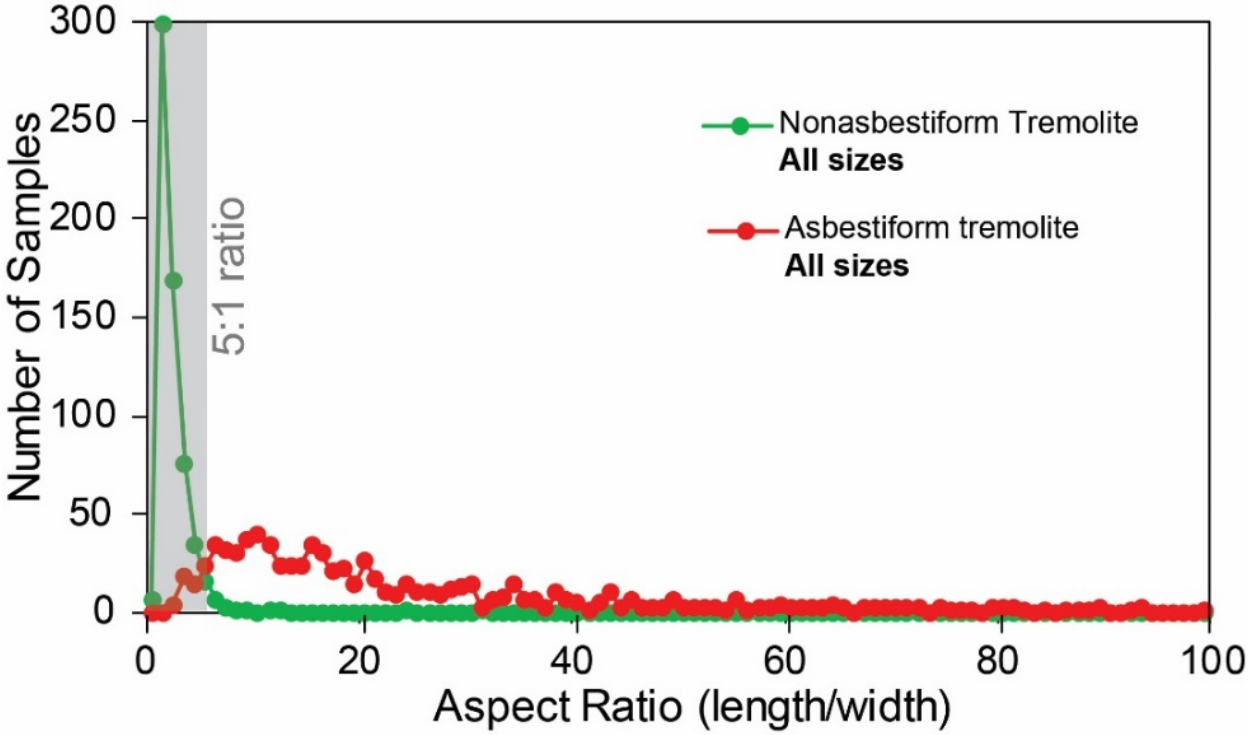

Figure 28a*. Distribution of aspect ratios for non-asbestiform vs. asbestiform particles of amphibole, the dominant impurity found in talcum powder. This graph shows all the data in the two repositories, Wylie and Virta (2016) and Harper et al. (2014).*

Using the available peer-reviewed data, cleavage fragments (non-asbestiform tremolite) are indicated in green and asbestiform tremolite in red. Note that asbestiform fibers can have extremely large aspect ratios – the longest particle in the asbestos suite is 55 μm × 0.15 μm – it is so large that it has been cropped out of the figure for clarity. In fact, there are 13 samples in the asbestiform data set with aspect ratios over 100. By contrast, of the 615 non-asbestiform tremolite cleavage fragments, only one has an aspect ratio greater than 32 (it has a value of 115.38). In other words, the two types of particles have very different characteristics. Note also the shaded bar, which indicates the region with an aspect ratio of 5:1 or less. Most of the non-asbestiform tremolite is within that region, most of the asbestiform tremolite is outside.

Figure 28b is the exact same graph as **Figure 28a**, just with the "less than 5:1" region deleted, which becomes interesting when discussing the population distributions. Again notice that there are many particles even at very high aspect ratios above 10 – this is a characteristic of asbestiform fibers. In comparison, almost none of the non-asbestiform particles has an aspect ratio above 10.

[**Figure 28b** on next page.]

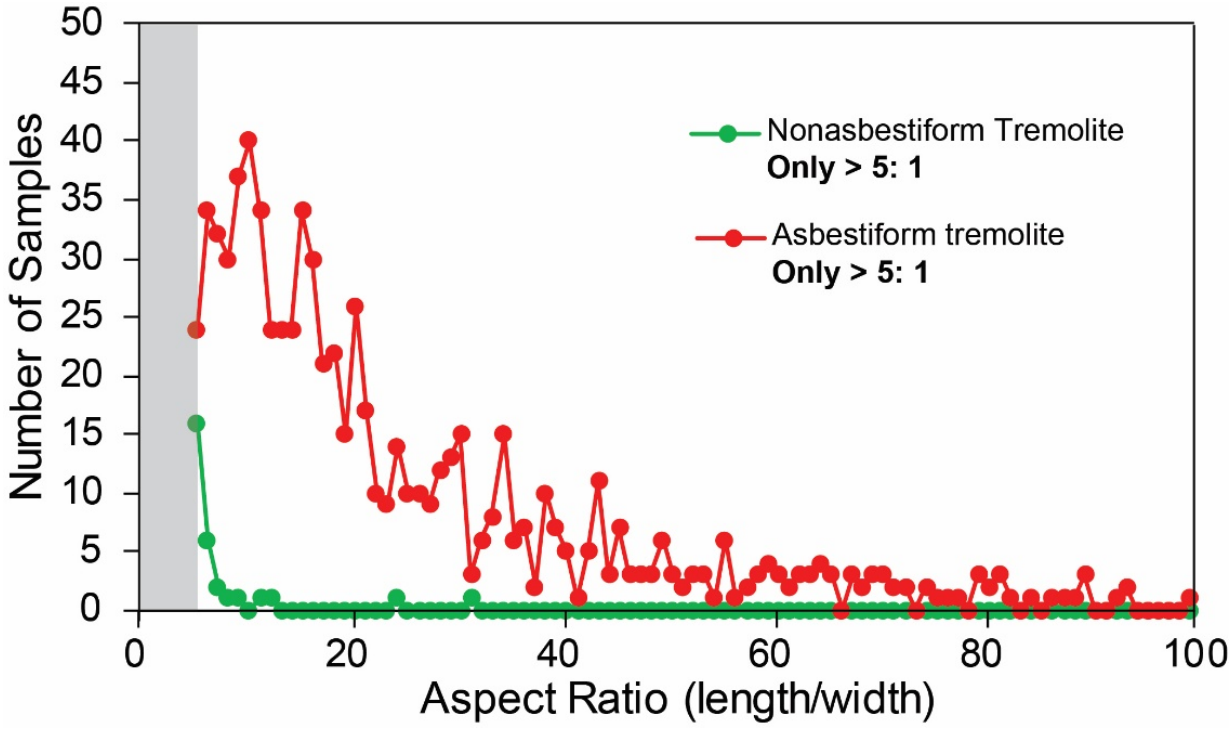

Figure 28b. *The same data as* ***Figure 28a****, except with the "5:1 and less" region deleted.*

Visual examination of these plots suggests that non-asbestiform tremolite has different shapes than asbestiform tremolite. This can be proven using the statistical *t* test described above to see if these samples come from the same population. **Figure 27a** showed the distribution curve for ONE population – but now the test asks if the asbestiform population is the same as the non-asbestiform population. In other words, do the two population distribution curves overlap?

To make this comparison rigorously, the *t* test described above is used to compare the means of these two populations. **The results shown below in Table 3 demonstrate that these two populations are statistically different.** The top half of the table compares all the population data for asbestiform vs. non-asbestiform tremolite – some 615 and 817 samples, respectively. There, the value of the *t* statistic is -21.44, a value that is far outside the 95% confidence limit. This means that the **non-asbestiform and asbestiform tremolite particles really are drawn from samples with different means**.

[**Table 3** on next page.]

Table 3. Results of *t*-Tests Assuming Equal Variance

ALL Non-asbestiform tremolite (NAT) compared to asbestiform tremolite (AT)

	NAT	AT
Mean	2.70	25.73
# Observations	615	817
t Stat	-21.44	
t Critical two-tail	1.96	

-21.44 lies outside the 95% confidence interval, so the means are different and these samples are not drawn from the same population.

Non-asbestiform tremolite (NAT) compared to asbestiform tremolite (AT) with aspect ratios >5:1

	NAT	AT
Mean	10.76	26.77
# Observations	35	780
t Stat	-3.54	
t Critical two-tail	1.96	

-3.54 lies outside the 95% confidence interval, so the means are different and these samples are not drawn from the same population.

3. Comparison to results in the Longo/Rigler MDL Reports

Summary: Use of the *t* test applied to data from the Longo/Rigler MDL Reports vs. published population data shows that the particles in talcum powder belong to the population of non-asbestiform amphibole.

Returning to the visual evidence presented in **Figures 28a and b**, now consider **Figure 28c**, which is **Figure 28b** with results from the Longo/Rigler MDL Report added in black:

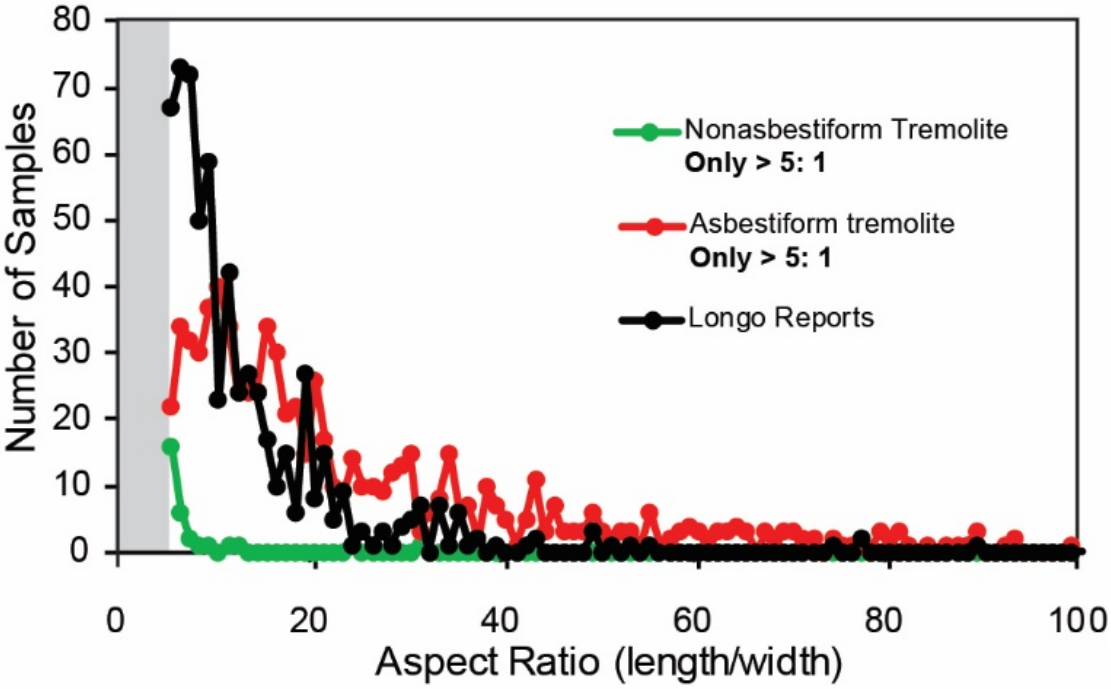

Figure 28c. *Data from* ***Figure 28b*** *with Longo/Rigler MDL Report results added in black.*

Significantly, the data from the Longo/Rigler MDL Reports appears to be trending toward a peak aspect ratio below 5:1, which is characteristic of non-asbestiform tremolite.

Unfortunately, the data collected by the analysts working for Drs. Longo and Rigler do not represent the population of non-asbestiform particles because **they only counted particles with aspect ratios of greater than 5:1.**[94] Their experimental design neglected to count the vast majority of particles in the typical size range for cleavage fragments, as seen in **Figure 28b**. This omission renders their analysis completely invalid. Indeed, this is a rejection of ISO 22262 methodologies, in particular as found on page 23 of ISO 22262-1, which makes certain observations about whether a population can be considered asbestiform based on observations of the **entire** population, but certainly not the population cut off at a 5:1 aspect ratio.

[94] The methodologically recognized dimensions for fibers are 3:1 for polarizing light microscopes (PLM) and 5:1 for TEM measurements. Although the Longo/Rigler MDL Reports utilize PLM for evaluating optical properties, the reports do not give aspect ratios for studied particles, either on the photomicrographs themselves or in any tables.

Table 4. Results of *t*-Tests Assuming Equal Variance

Particles measured in the Longo/Rigler MDL Reports compared to asbestiform tremolite (AT) with aspect rations >5:1

	AT	LONGO/RIGLER
Mean	26.77	13.34
# Observations	780	632
t Stat	12.09	
t Critical two-tail	1.96	

12.09 lies outside the 95% confidence interval, so the means are different and these samples are not drawn from the same population.

Particles measured in the Longo/Rigler MDL Reports compared to non-asbestiform tremolite (NAT) with aspect ratios >5:1

	NAT	LONGO/RIGLER
Mean	10.76	13.34
# Observations	35	632
t Stat	-1.41	
t Critical two-tail	1.96	

-1.41 lies inside the 95% confidence interval, so the means are the same; samples are drawn from the same population.

Fortunately, the Wylie and Virta (2016) data set is large enough to include a significant number of samples with aspect ratios >5:1, so comparisons with that limited size range can still be made.[95] To make this conclusion using statistics, **Table 4** shows results from *t* tests comparing data from the Drs. Longo and Rigler's MDL Reports for particles with aspect ratios >5:1 against data from Wylie and Virta (2016)[96] and Harper et al. (2014).[97] The top set of data compares asbestiform particle aspect ratios against data from Drs. Longo and Rigler's MDL Reports. Here, the *t* statistic of 10.68 lies outside the value of 1.96 for the 95% confidence limit. This establishes that particles measured by Drs. Longo and Rigler do not belong to the same populations as those of asbestiform tremolite on the basis of their shapes. In other words, the **asbestiform and non-asbestiform populations are so different** that they can be distinguished even when a flawed experimental design provides data on particles with aspect ratios greater than 5:1. **In summary, the data from the Longo/Rigler MDL Reports show that even though counts and measurements are only reported for particles with aspect ratios >5:1, statistical tests show that they have identified a population of *non*-asbestiform cleavage fragments in the talcum powder tested.**

---

[95] Note that the available morphology data for asbestiform and non-asbestiform particles come from analyses of the mineral tremolite, which is the dominant species identified by Drs. Longo and Rigler in their November 2018 MDL Report (67%). Most, if not all, of the anthophyllite particles identified by Drs. Longo and Rigler are likely to be talc, and there is no relevant data set for talc.

[96] Wylie and Virta (2016) Size distribution measurements of amosite, crocidolite, chrysotile, and nonfibrous tremolite. *Digital Repository at the University of Maryland*, http://dx.doi.org/10.13016/M2798Z.

[97] Harper et al. (2014) Characterization of Lone Pine, California tremolite asbestos and preparation of research material. *Ann. of Occp. Hyg.*, **2014**, 1-13, https://academic.oup.com/annweh/article/59/1/91/2464346#supplementary-data.

E. Summary Of Particle Morphology Conclusions

In summary, the following flaws in evaluating particle morphology render the Longo/Rigler MDL Reports conclusions invalid:

- **Using TEM to visually distinguish non-asbestiform amphiboles and asbestiform amphiboles is scientifically invalid, as stated in the very protocols upon which Drs. Longo and Rigler purport to rely.**

- **Drs. Longo and Rigler and analysts only counted particles with aspect ratios >5:1 in their TEM studies, which improperly biases their results toward finding an asbestiform particle population.**

- **Particles in the Longo/Rigler MDL Reports belong to the non-asbestiform tremolite population.**

- **There is no evidence to suggest that the particles measured by Drs. Longo and Rigler and analysts are asbestos.**

VIII. CONCLUSIONS

The core problem with the Longo/Rigler MDL Reports is that the methods utilized in the testing and analyses produce completely inconsistent results, rendering them unscientific and subjective. Indeed, **the analysis by Drs. Longo and Rigler presented in the Long/Rigler MDL Reports applied a methodology that was inherently designed to achieve the results they desired for purposes of this litigation, and not scientific**.

Despite producing lengthy, descriptive reports and undertaking extensive measurements according to government protocols, Drs. Longo and Rigler did not properly train their personnel for the task of characterizing impurities in talc, where the possible mineralogy is unconstrained. Thus, they lack the background to understand or interpret their results, especially where, as here, the impurities are tiny, and many possible minerals can be present. Personnel employed by Drs. Longo and Rigler lack sufficient knowledge of proper mineralogical terminology beyond the six defined asbestos mineral species, have **no** understanding of the limitations and errors associated with the techniques used, and fail to compare their results to foundation studies in this discipline.

The Longo/Rigler MDL Reports fail to demonstrate an understanding of the accuracy of the Energy Dispersive Spectroscopy (EDS) technique, which is only semi-quantitative with large error bars. The technique is rarely used to determine the chemical composition of minerals in unbounded studies where the possible minerals present cover a large range of possibilities. Within generally accepted error bars on this technique (ignored and unstated by Drs. Longo and Rigler), asbestos minerals are indistinguishable from many of their non-asbestiform counterparts. In particular, EDS cannot differentiate between talc and anthophyllite. It is simply incorrect for Drs. Longo and Rigler to assert that individual amphibole mineral species can be identified by EDS alone.

The Longo/Rigler MDL Reports also use single crystal selected area electron diffraction (SAED) to confirm the EDS mineral identifications based on crystal structure. But the vast majority of the patterns collected by Drs. Longo and Rigler are not indexed, making them very difficult to interpret. **Moreover, 25% of all common rock-forming minerals have overlapping similar or identical *d*-spacings to what Drs. Longo and Rigler report**. There is no SAED evidence to prove definitively that any specific asbestiform minerals are present.

Polarizing light microscope (PLM) images of various types are used in the Longo/Rigler MDL Reports to prove presence of asbestos in the samples. Again, the PLM images themselves do not uniquely identify “asbestos” mineral species. Rather, some of them can be interpreted to suggest the presence of amphibole group minerals (there are 76 end-members, and many more intermediates) or something else. The latter might be talc, which appears to have very close to the same color as amphibole in the dispersion staining images. The PLM images alone do not categorically prove the presence of any specific mineral species.

The experimental design used by Drs. Longo and Rigler for interpreting the number of non-talc particles present in talcum powder ignores well-known databases on particle dimensions, which indicate that non-asbestiform particles occur with aspect ratios (particle length divided by width) averaging 2.7. They ignore all particles with aspect ratios less than 5:1, rendering the particle dimension analyses nearly useless for distinguishing cleavage fragments from fibers.

Because the distribution of non-asbestiform particles has some samples in the range above 5:1, **it is possible** to compare that truncated (aspect ratio greater than 5:1) dataset for cleavage fragments (average aspect ratio of 10.8) to that of asbestiform tremolite with ratios above 5 (average ~26.8). The average aspect ratio for all particles measured by Drs. Longo and Rigler is 13.3, suggesting that they are a population of cleavage fragments. **Statistical analyses of these aspect ratio populations establish that the particles measured by Drs. Longo and Rigler belong to the population represented by *non-asbestiform* amphibole.**

There is no evidence (EDS, SAED, or otherwise) to confirm that any of the "fibers" identified as anthophyllite by Drs. Longo and Rigler are really anthophyllite.

In summary, the Longo/Rigler MDL Reports contain only subjective analyses with inconsistent results that do not stand up to scientific scrutiny. It appears that Drs. Longo and Rigler and their analysts are just using the equipment and methodology with which they are familiar from their work in bulk asbestos sampling to undertake analyses in a totally different application for which they are inappropriate. The Longo/Rigler MDL Reports are far from the type of quantitative study that would withstand scientific review or be accepted for publication in a peer-reviewed scientific journal. **The Longo/Rigler MDL Reports completely fail to demonstrate that *any* recognized asbestos minerals are present in talcum powder in *any* concentration with *any* asbestiform shapes.**

Finally, given the compounding nature of all of the individual methodological errors in the Longo/Rigler MDL Reports, any resultant conclusions drawn from testing by Drs. Longo and Rigler and associates are scientifically invalid. Every methodological error in their testing results in false positive findings of asbestos, but not false negatives. The testing described in the reports can only be described as a series of errors, each of which acts to amplify the errors preceding it. **The results reported in the Longo/Rigler MDL Reports cannot be considered scientifically valid, calling into question the competence of Drs. Longo and Rigler and their analysts to undertake such work.**

MATERIALS REVIEWED AND CONSIDERED

Longo and Rigler Analyses

Analysis of Historical Johnson's Baby Powder M69042 (Oct. 2018)
Longo, Rigler, and Egeland, MAS Project 14-1852 - Below the Waist Application of Johnson & Johnson Baby Powder (Sept. 2017)
Longo and Rigler, Supplemental Expert Report & Analysis of Johnson and Johnson Baby Powder and Valeant Shower to Shower Talc Products for Amphibole Asbestos (Mar. 11, 2018)
Rigler, MAS TEM Coefficient of Variation for Tremolite and Anthophyllite in Talc - A Quality Control Study (Sept. 6, 2018)
Longo and Rigler, Analysis of Johnson's Baby Powder Historical Samples - Asian - M69248 (7 Samples) (Nov. 2, 2018)
Longo and Rigler, The Analysis of Johnson & Johnson's Historical Baby Powder & Shower to Shower Products from the 1960's to the Early 1990's for Amphibole Asbestos (Nov. 14, 2018)
Longo and Rigler, The Analysis of Johnson & Johnson's Historical Product Containers and Imerys's Historical Railroad Car Samples from the 1960's to the Early 2000's for Amphibole Asbestos (Jan. 15, 2019)
Longo and Rigler, Quality Assurance Report - Johnson and Johnson's JBP and STS, Imerys Railcar and Asian Talc for Amphibole Asbestos (Jan. 31, 2019)
Diffraction Verifications-M68233
Diffraction Verifications-M68503
Diffraction Verifications-M69042
Diffraction Verifications-M69248
Diffraction Verifications-M69751
Diffraction Verifications-M69757
Global particle table M65205-001
Global particle table M65208-001
Global particle table M65228-001
Global particle table M65329-018
Global particle table M65329-041
Global particle table M65329-043
Global particle table M66173-002
Global particle table M66173-003
Global particle table M66203-001
Global particle table M66203-006
Global particle table M66203-007
Global particle table M66352-002
Global particle table M66405-001
Global particle table M66510-001
Global particle table M66512-001
Global particle table M66514-001

Global particle table M66515-001
Global particle table M66516-001

Depositions and Exhibits

Deposition of William Longo, Nov. 6, 2018
Deposition of William Longo, Nov. 27, 2018
Deposition of William Longo, Dec. 5, 2018
Deposition of William Longo, Feb. 5, 2019, and Exhibits
Deposition of Rigler, Feb. 6, 2019, and Exhibits
Deposition of William Longo, Oct. 24, 2018
Deposition of William Longo, Oct. 31, 2018
Deposition of William Longo, Jan. 7, 2019

Scientific Literature

Bloss (1999) *Optical Crystallography*, MSA Monograph Series
Campbell et al. (1997) Information Circular 8751, U.S. Bureau of Mines.
Dyar and Gunter (2008) *Mineralogy and Optical Mineralogy*, Mineralogical Society of America
Gary, McAfee, and Wolf, Eds. (1974) *Glossary of Geology*
Gunter (2010) *Defining Asbestos: Differences between the Built and Natural Environments*, 60 CHIMIA No. 10, 747, 748
Harper et al. (2014) Characterization of Lone Pine, California tremolite asbestos and preparation of research material. *Ann. Occp. Hyg.*, **2014,** 1-13.
McCrone (1980) *Asbestos Particle Atlas*. Ann Arbor Science
McKillup and Dyar (2010) *Geostatistics Explained*, Cambridge University Press.
Miller and Mirtič (2013) Accuracy and precision of EDS analysis for identification of metal-bearing minerals in polished and rough particle samples, *Geologija*, **56**, 5-17.
Neilson and Brockman (1977) The error associated with point-counting, *Amer. Mineral.*, **62**, 1238-1244
Newbury and Rotchie (2015) Performing elemental microanalysis with high accuracy and high precision by scanning electron microscopy/silicon drift detector energy-dispersive X-ray spectrometry (SEM/SDD-EDS), *Journal of Material Sciences*, **50**, 493-518
Newbury (1995) “Standardless” quantitative electronic probe microanalysis with energy-dispersive x-ray spectrometry: Is it worth it? *Anal. Chem.*, **67**, 1866-1871.
Pierce et al. (2017) Evaluation of the presence of asbestos in cosmetic talcum products, *Inhalation Toxicology*, **29**, 443-456
Rhoades (1976) XIDENT – A computer technique for the direct indexing of electron diffraction spot patterns. Research Report 70/76, Dept. of Mechanical Engineering, Univ. of Canterbury, Christchurch, New Zealand
Severin (2004) *Energy Dispersive Spectrometry of Common Rock Forming Minerals*, Springer, Kluwer.
Severin (1984) *Energy Dispersive Spectrometry of Common Rock-Forming Minerals*, Kluwer

Shannon et al. (2017) Refractive indices of minerals and synthetic compounds, *Amer. Mineral.*, **102**, 1906-1914
Su (2003) How to Use the *d*-Spacing/Interfacial Angle Tables to Index Zone-Axis Patterns of Amphibole Asbestos Minerals Obtained by Selected Area Electron Diffraction in Transmission Electron Microscope, 2008 report, Asbestos Analysis Consulting, Newark, DE
Su (2003) A rapid and accurate procedure for the determination of refractive indices of regulated asbestos minerals, *American Mineralogist*, **88**, 1979-1982
Veblen and Wylie (1993) Mineralogy of amphiboles and 1:1 layer silicates, *Reviews in Mineralogy*, **28**, 61-138
Walitzi et al. (1989) Verfeinerung der Kristallstruktur von Anthophyllite vom Ochsenkogel/Gleinalpe, Oesterreich, *Zeitschrift für Kristallographie - Crystalline Materials*, **188**, 327
Wyckoff (1963) Cubic closest packed structure, *Crystal Structures* 1, 7 - 83
Wylie and Virta (2016) Size distribution measurements of amosite, crocidolite, chrysotile, and nonfibrous tremolite, Digital Repository at the University of Maryland, http://dx.doi.org/10.13016/M2798Z.
Zoltai (1981) Amphibole Asbestos Mineralogy, *Reviews in Mineralogy & Geochemistry*, **9**, 237-278

Standards and Regulations

40 C.F.R. 1 (7-1-03 Edition).
40 C.F.R. 763
ASTM D5755 – 09 (2014)
ASTM D5756 – 02 (2008)
Asbestos Hazard Emergency Response Act, AHERA
International Agency for Research on Cancer (2012) *Arsenic, Metals, Fibres, and Dusts*, IARC Monographs on the Evaluation of Carcinogenic Risks to Humans
International Agency for Research on Cancer (2012), *Monographs on the Evaluation of Carcinogenic Risks to Humans Vol. 100C: Asbestos (Chrysotile, Amosite, Crocidolite, Tremolite, Actinolite and Anthophyllite),*
ISO 10312 (1995)
ISO 13794 (1999)
ISO 22262-1 (2012)
ISO 22262-2 (2014)
ISO 22262-3 (2016)
National Institute for Occupational Safety and Health (2011) *Asbestos Fibers and Other Elongate Mineral Particles: State of the Science and Roadmap for Research*, Current Intelligence Bulletin 62
National Research Council (1984) *Asbestiform Fibers: Nonoccupational Health Risks*
Perkins and Harvey (1993) *Test Method: Method for the Determination of Asbestos in Bulk Building Materials*, EPA/600/R-93/116
Yamate et al. (1984) Methodology for the measurement of airborne asbestos by electron microscopy, U.S. Environmental Protection Agency Report

Web Sources

http://geologylearn.blogspot.com/2015/08/point-counting-technique-used-in.html
http://nrmima.nrm.se/
http://rruff.geo.arizona.edu/AMS/amcsd.php
http://webmineral.com/
http://www.charfac.umn.edu/instruments/eds_on_sem_primer.pdf
https://cstl.nist.gov/div837/837.02/epq/dtsa2/
https://nature.berkeley.edu/classes/eps2/wisc/ri.html
https://rexplorations.wordpress.com/2015/08/13/hypothesis-tests-2-sample-tests-ab-tests/
https://www.geologicalsocietyct.org/geoconnections-articles/recent-analyses-of-connecticut-amphiboles

EXHIBIT A

CURRICULUM VITAE
MELINDA DARBY DYAR

Department of Astronomy
Mount Holyoke College
South Hadley, MA 01075
(413) 538-3073

Planetary Science Institute
1700 East Fort Lowell, Suite 106
Tucson, AZ 85719-2395
520-622-6300

161 Chestnut St.
Amherst, MA 01002
(413) 348-9424
mdyar@mtholyoke.edu

Education:

Ph.D., Geochemistry, Massachusetts Institute of Technology, Cambridge, Mass. Thesis topic: Crystal chemistry and statistical analysis of iron in mineral standards, micas, and glasses. Advisor: Roger G. Burns.

B.A., Geology and Art History[1], Wellesley College, Wellesley, Mass. Thesis topic: Geology of the Broadmoor Wildlife Sanctuary, South Natick, MA: Structural and petrographic analysis. Advisor: Margaret Thompson. Summer Field Camp, Indiana University, Cardwell, Montana.

Employment:

Senior Scientist, Planetary Science Institute, 2015-present.

Kennedy-Schelkunoff Professor and Chair, Department of Astronomy, Mount Holyoke College and Five College Astronomy Department, 2011-present.

Associate Professor and Chair, Department of Astronomy, Mount Holyoke College and Five College Astronomy Department, 2002-2011.

Associate Professor Department of Earth and Environment, Mount Holyoke College and Five College Astronomy Department, 2002-2008.

Five College Graduate Faculty in Astronomy, University of Massachusetts, 2002-present.

Visiting Associate Professor, Department of Astronomy and Department of Earth and Environment, Mount Holyoke College and Five College Astronomy Department, 2001-2002.

Visiting Associate Professor, Department of Astronomy, University of Massachusetts (Amherst), 2001-2002.

Affiliated Staff, Department of Geological Sciences, University of Idaho, 2000-2018.

Visiting Assistant Professor, Department of Astronomy and Department of Earth and Environment, Mount Holyoke, 1998-2001.

Assistant Professor, Department of Geology and Astronomy, West Chester University, 1993-1998.

Visiting Assistant Professor, Department of Geology, Smith College, 1995-1996.

Assistant Professor, Department of Geological Sciences, University of Oregon, 1986-1993.
Member, Materials Science Institute, 1987-1993.

Research Fellow, Division of Geological and Planetary Sciences, California Institute of Technology, 1985-1986 (G.R. Rossman, supervisor).

Post-Doctoral Fellow, Department of Earth, Atmospheric, and Planetary Sciences, Massachusetts Institute of Technology, 1985 (R.G. Burns, supervisor).

Research Assistant, Department of Earth, Atmospheric, and Planetary Sciences, Massachusetts Institute of Technology, 1980-1985.

Research Staff, Chevron Oil Field Research Company, La Habra, CA, summer, 1982.

Assistant Instructor, Indiana University Geologic Field Station, Cardwell, MO, summer, 1980.

Professional Societies:

Association for Women Geoscientists
Geological Society of America (Fellow)
Mineralogical Society of America (Fellow)
American Geophysical Union
North American Society for LIBS
Geochemical Society (Fellow)

[1] Course requirements for the art history major were completed while a graduate student at MIT.

Honors:

Sigma Xi, 1980
1984 Mineralogical Society of America (M.S.A.) Grant for Research in Crystallography
1990-1991 National Lecturer, Mineralogical Society of America
Outstanding Service Award, Mineralogical Society of America, 1991
Fellow, Mineralogical Society of America, 1995
Girls' Incorporated, Holyoke, Massachusetts, Honoree, 1 April, 2004
Meribeth E. Cameron Faculty Award for Scholarship, Mount Holyoke College, 2010
Participating Scientist, Mars Science Laboratory Science Team, 2012-2014
J.K. Gilbert Award for outstanding contributions to planetary science, Geological Society of America, 2016
Fellow, Geological Society of America, 2017
Hawley Medal, 2017, Mineralogical Association of Canada
Eugene Shoemaker Distinguished Scientist Medal, NASA Solar System Exploration Research Virtual Institutes, 2018
Helmholtz International Fellow, 2018-2021
Fellow, Geochemical Society, 2019.

Professional Service:

M.S.A. Research Grants Committee, 1991
M.S.A. Science Grants Committee, 1991
The Geochemical Society Program Committee, 1991-1994
National Science Foundation Instrumentation and Laboratory Instruction Panel, 1988 and 1992
National Science Foundation Undergraduate Curriculum and Course Development Panel, 1991
National Science Foundation Workshop: The Role of Faculty in the Disciplines in the Undergraduate Education of Future Teachers, invited participant, contributor to working paper, 1992
Program Committee, Geological Society of America National Meetings, 1992-1994
American Geophysical Union Workshop: Shaping the Future of Undergraduate Earth Science Education, invited participant and contributor to working paper, 1996
M.S.A. Lecture Program Committee, 1998-2000; Chair 1999-2000
M.S.A. Crystallography Research Grant Committee 1998-1999
Council for Undergraduate Research (C.U.R.), Councillor, 1999-2000
American Geological Institute (A.G.I.) Outreach Committee, 2000-2003
Associate Editor, *American Mineralogist*, 2000-present
Review Panel, NASA Cosmochemistry Program, 2001
Review Panel, NSF/NATO Postdoctoral Fellowship Program, 2002-2003
Judges Panel, Name the Rovers contest, 2003
Review Panel, NSF, CCLI Program, 2003
Instrument Selection Review Panel, Mars Science Lander 2009, NASA, 2004
Review Panel, NSF, CCLI Program, 2004
International Program Committee, Goldschmidt Conference, 2005
Executive Committee, AWIS National Meeting, 2005
Review Panel, NASA, 2006
Review Panel, NASA, 2007
Review Panel, NASA, 2008
Review Panel, NASA, 2008
Review Panel, NSF, 2008
Review Panel, NASA, 2009
Review Panel, NSF, 2009
Review Panel, NASA, 2009

Review Panel, NASA, 2010
Review Panel, NASA, 2011
Review Panel, NASA, 2012
Review Panel, NASA, 2013
Review Panel, NASA, 2015
Review Panel, NASA, 2016
Review Panel, NSF, 2017 (×2)
Review Panel, NASA, 2018

Invited Talks and Professional Presentations:

University of California at Riverside, 1986 and 1991[2]
University of Maine at Orono, 1987 and 1991[1]
Oregon State University, 1986 and 1991
Massachusetts Institute of Technology, 1987
Wellesley College, 1987
Smith College, 1988
State University of New York at Albany, 1989
Southern Methodist University, 1989
University of Washington, 1990
University of Saskatchewan, 1991[1]
San Diego State University, 1991[1]
University of California at Davis, 1991[1]
Sonoma State University, 1991[1]
University of Calgary, 1991[1]
University of New Mexico, 1991[1]
University of Houston, 1991[1]
Louisiana State University, 1991[1]
Texas Tech, 1991[1]
University of Chicago, 1992
Penn State University, 1992
University of Kentucky, 1992
University of Colorado at Boulder, 1993
European Research Conference, Hydrogen-Containing Defects in Minerals and Ceramics, 1993
Deep Continental Studies Workshop, Microknowledge and Megathinking, 1993
Portland State University, 1993
Hopi Buttes Workshop, invited participant, 1993
Rutgers University, 1994
University of North Carolina, 1994
Southern Methodist University, 1994
University of Massachusetts at Amherst, 1996
Mount Holyoke College, 1997
University of Western Ontario, 2000
University of Idaho, 2001
Eastern Washington University, 2001
Wellesley College, 2001
State University of New York at Stony Brook, 2003
Lunar and Planetary Institute, 2003
Brearley School, 2004

---

[2]talk sponsored by Mineralogical Society of America Lecture Program.

Massachusetts Institute of Technology, 2004
University of Massachusetts, 2004
Wellesley College, 2004
Rhode Island College, 2006
SUNY Binghamton, 2007
University of New Mexico, 2007
Colby College, 2008
Rutgers University, 2009
NASA Summer Science Institute, Goddard Space Flight Center, 2009
Hartwick College, 2010
M.I.T., 2011
Wellesley College, 2011
Brown University, 2011
Indiana University, 2011
TED talk, 2012
Texas Tech University, 2013
Skidmore College, 2014
University of Massachusetts Amherst, 2014
Rutgers University, 2014
Planetary Science Institute, 2015
TED-X, Springfield, MA 2015
University of Massachusetts, Amherst, 2015
Brown University, 2015
Amherst College, 2016
Rensselaer Polytechnical Institute, 2017
M.I.T., 2017
Williams College, 2018
Keynote Plenary Speaker, AAAS, January 2018
Colby College, 2018
University of Vermont (Burlington), 2018
Goddard Space Flight Center, 2019
Applied Physics Laboratory, 2019

College and University Service:

Structural Geologist Search Committee, University of Oregon (UO) 1987-1988
Chair, Affirmative Action Search Committee, UO, 1988
Chair, X-ray and Thin Section Committee, Dept. of Geological Sciences, UO, 1986-1987
Faculty Advisor, Condon Undergraduate Society, UO, 1986-1988
Affirmative Action Liaison, Dept. of Geological Sciences, UO, 1986-1989
Materials Science Institute Budget Committee, UO, 1987-1992
Treasurer, Materials Science Institute, UO, 1988-1992
Director, Materials Science Institute Research for Undergraduates Program, UO, 1988 & 1989
Physics Department Condensed Matter Search Committee, UO, 1988 and 1989
Graduate Teaching Fellow Coordinator, Dept. of Geological Sciences, UO, 1988-1989
Seismology Search Committee, Dept. of Geological Sciences, UO, 1988-1989
Volcanologist Search Committee, Dept. of Geological Sciences, UO, 1989-1990, 1990-1991
Telephone Counselor, Dept. of Geological Sciences, UO, 1990-1991
Chair, Displays Committee for Cascade Hall, UO, 1990-1993
Computer Coordinator, Dept. of Geological Sciences, UO, 1989-1993
Member, President's Task Force on Campus Infrastructure and Technology, UO, 1990-1992
Member, Committee on Campus Hazardous Waste Remediation, UO, 1988-1993

Member, University Library Committee, UO, 1987-1989
Member, Faculty Advisory to the Museum of Art, UO, 1989-1993
Chair, Faculty Advisory to the Museum of Art, UO, 1990-1993
Member, Departmental Computer Lab Managers, UO, 1989-1993
Board Member, Faculty Club of the University of Oregon, 1988-1993
Secretary-Treasurer, Faculty Club of the University of Oregon, 1989-1990
Member, Docent Council, University of Oregon Museum of Art, 1988-1993
Member, Board of Governors, University of Oregon Museum of Art, 1988-1993
Member, Curriculum Committee, Dept. of Geology and Astronomy, WCU, 1993-1996
Member, College of Arts and Sciences Recruitment Committee, WCU, 1994-1995Internship Coordinator, Dept. of Geology & Astronomy, WCU, 1993-1997[3]
Member, Undergraduate Review Committee, Dept. of Geology & Astronomy, WCU, 1993-1998[2]
Member, Graduate Review Committee, Dept. of Geology & Astronomy, WCU, 1994-1998[2]
Member, Fellowship Committee, Mount Holyoke College, 2002-2006
Member, Planning and Budget Committee, 2003-2004
Chair, Fellowship Committee, Mount Holyoke College, 2003-2006
Coordinator of Universal Application Funding, 2003-2012
Member, Search Committee for Fellowships and Pre-Graduate Advising, 2009-2010
Task Force on Curriculum to Career, 2011
Member, Curriculum Committee, Five College Astronomy Department, 1999-present
Member, Radiation Safety Committee, Mount Holyoke College, 1999-present
Chair, Astronomy Department, 1999-present
Senate member, Five College Astronomy Department, 1999-present
Advisory Committee, 2017-2018

Miscellaneous Presentations to the College Community and Beyond:

Mathematics Department, MHC, 2000
Five College Geology Symposium, February 2001
Mount Holyoke Club of Bridgeport, CT, 2003
Lyon Lecture series, Denver, 25 Oct. 2003
Family Weekend, 31 Oct. 2003
Mathematics Department, MHC, February 2004
Five College Geology Symposium, February 2004
Mars lecture, AST 11, Amherst College, 5 March 2004
Fascinating Professor program, Francis Perkins scholars, 9 March, 2004
South Hadley Lions Club, 6 April 2004
East Longmeadow Library, 1 May, 2004
Dedication of Kendade Hall, 8 May, 2004
Class of 1959 reunion dinner, 28 May 2004
Mount Holyoke Club of South Hadley, 9 June, 2004
NOVA/WGBY fundraiser, Mount Holyoke College, 14 June, 2004
Summer math for high school students, summer Mars project, July, 2004
MHC Office of Admissions, summer staff training seminar, August, 2004
Family Weekend, 30 Oct. 2004
Hughes Symposium on Integrating Undergraduates into Research Programs, January 2005
Mount Holyoke Club of Houston, March, 2005
Springfield Star Club, April, 2005

---

[3]Maternity leave from West Chester University was taken during the academic years 1995-1996 and 1997-1998.

Mount Holyoke Reunion, June 2005
Century Club, Springfield, MA, March 2006
Mount Holyoke Reunion, June 2006
Mid-Coast Maine Mount Holyoke Club, June, 2006
MacDuffie School, January 2007
Mount Holyoke Club of New York City, March, 2007
Stargazers Club, North Scituate, RI, April 2007
Mount Holyoke Gala, Washington D.C., April 2009
Mount Holyoke Club of Bridgeport, December 2011
Development Office function in New York City, May 2012
Development Office function in San Francisco, October 2012
Development Office function in Los Angeles, October 2012
Development Office function in Boston, November 2012
Mount Holyoke Club of Cape Cod, May 2013
Mount Holyoke Club of New Hampshire, June 2013
Albany Area Amateur Astroomers, October, 2014
New England Society of Economic Geologists, January, 2015
Mount Holyoke Club of New Hampshire, October, 2015
Mount Holyoke Club of Fairfield County, October, 2015
Talk for 6th grade class at Common School, Amherst MA, May, 2017
Talk for the Development Office, October 2017
Reunion talk, class of 1967, May 2018

Courses Taught:

Mineralogy I and II (advanced undergraduate)
Igneous and Metamorphic Petrology (advanced undergraduate)
Introduction to Earth History (introductory historical geology)
Introduction to Geology (introductory physical geology)
Planet Earth (introductory geology/planetary science)
Geochemistry (graduate and undergraduate)
Spectroscopy (graduate and undergraduate)
Geometrics (applications of statistical methods) (graduate and undergraduate)
Planetary Science (introductory and advanced undergraduate)
Planetary Science seminar on Mars (advanced undergraduate)
Spectroscopy of the Planets (advanced undergraduate)
Meteorites (advanced undergraduate)

Books and Electronic Media:

Dyar, M.D., and Gunter, M.E. (2013) *Mineral Database*. App for I-pad, Mac, I-Phone.

McKillip, S. and Dyar, M.D. (2010) *Geostatistics Explained, An Introductory Guide for Earth Scientists.* Textbook. Cambridge University Press.

Dyar, M.D., and Gunter, M.E. (2008) *Mineralogy and Optical Mineralogy: A Three-Dimensional Approach*. Textbook. Mineralogical Society of America.

Dyar, M.D. (1999) *Hands-On Mineral Identification*. CD-ROM. Tasa Graphic Arts, Inc., Albuquerque, N.M.

Dyar, M.D., Busch, R.M., and Wiswall, G. (1997, 1998) *The Study of Minerals*. CD-ROM. Tasa Graphic Arts, Inc., Albuquerque, N.M.

Dyar, M.D., McCammon, C.A., and Schaefer, M.W., Eds. (1996) *Mineral Spectroscopy: A Tribute to Roger G. Burns*. Special Publication #5, The Geochemical Society, Washington, D.C., 400 pp.

Papers:

1. Dyar, M.D., and Burns, R.G. (1981) Coordination chemistry of iron in glasses contributing to remote-sensed spectra of the moon. *Proc. Lunar and Planet. Sci. Conf.*, **12B**, 695-702.
2. Burns, R.G., and Dyar, M.D. (1983) Spectral chemistry of green glass-bearing 15426 regolith. Proc. Lunar and Planet. Sci. Conf., 14, *J. Geophys. Res.*, **88**, B221-B228.
3. Dyar, M.D., and Birnie, D.P. (1984) The effects of quench media on iron partitioning and ordering in a lunar glass. Proc. 1st Intl. Conf. on Glass in Planet. and Geolog. Phenomena, *J. Non-Cryst. Sol.*, **67**, 397-412.
4. Stone, A.J., Parkin, K.M., and Dyar, M.D. (1984) STONE: a program for resolving Mössbauer spectra. DEC Users Soc. 11-720, Marlboro, Mass.
5. Dyar, M.D. (1984) Precision and interlaboratory reproducibility of measurements of the Mössbauer effect in minerals. *Amer. Mineral.*, **69**, 1127-1144.
6. Dyar, M.D. (1984) Experimental methods for quenching structures in lunar-analog silicate melts: variations as a function of quench media and composition. Proc. Lunar and Planet. Sci. Conf., 15, *J. Geophys. Res.*, **84**, supplement, C233-C239.
7. Dyar, M.D. (1985) A review of Mössbauer data on inorganic glasses: the effects of composition on iron valency and coordination. *Amer. Mineral.*, **70**, 304-316.
8. Birnie, D.P., and Dyar, M.D. (1986) Cooling rate calculations for silicate glasses. Proc. Lunar and Planet. Sci. Conf., 16, *J. Geophys. Res.*, **91(B4)**, D509-D513.
9. DeGuire, M.R., Dyar, M.D., O'Handley, R.C., and Kalongi, G. (1986) Magnetic ordering in splat-quenched ferrite-silica compositions. *J. Magn. Magn. Mater.*, **54-57**, 1337-1338.
10. Dyar, M.D., and Burns, R.G. (1986) Mössbauer spectral study of ferruginous one-layer trioctahedral micas. *Amer. Mineral.*, **71**, 955-964.
11. Dyar, M.D. (1986) Practical application of Mössbauer goodness-of-fit parameters for evaluation of real experimental results: a reply. *Amer. Mineral.*, **71**, 1266-1267.
12. DeGuire, M.R., O'Handley, R.C., Kalongi, G., and Dyar, M.D. (1986) Spinel ferrite-silica glass obtained by splat quenching. *J. Non-Cryst. Sol.*, **81**, 351-364.
13. Dyar, M.D. (1986) Comment on ferrous/ferric Mössbauer analysis of simulated nuclear waste glass with and without computer fitting. *Commun., Am. Cer. Soc.*, **69(7)**, C-160-C-162.
14. Dyar, M.D. (1987) A review of Mössbauer data on trioctahedral micas: evidence for tetrahedral Fe^{3+} and cation ordering. *Amer. Mineral.*, **72**, 102-112.
15. Dyar, M.D., Naney, M.T., and Swanson, S.E. (1987) Effects of quench methods on Fe^{3+}/Fe^{2+} ratios: a Mössbauer and wet chemical study. *Amer. Mineral.*, **72**, 792-800.
16. Fudali, R.F., Dyar, M.D., Griscom, D.L., and Schreiber, H.D. (1987) The oxidation state of iron in tektite glass. *Geochim. Cosmochim. Acta.*, **51(10)**, 2749-2756.
17. Dyar, M.D., and Naney, M.T. (1988) Effects of quench methods on Fe^{3+}/Fe^{2+} ratios: Reply. *Amer. Mineral.*, **73**, 1479.
18. Dyar, M.D. (1989) Application of Mössbauer goodness-of-fit parameters to experimental spectra: Further discussion. *Amer. Mineral.*, **74**, 688.
19. McGuire, A.V., Dyar, M.D., and Ward, K.W. [4] (1989) Neglected Fe^{3+}/Fe^{2+} ratios: a study of Fe^{3+} contents of megacrysts from alkali basalts. *Geology*, **17**, 687-689.
20. Dyar, M.D., McGuire, A.V., and Ziegler, R.D. (1989) Redox equilibria and crystal chemistry of coexisting minerals from spinel lherzolite mantle xenoliths. *Amer. Mineral.*, **74**, 969-980.
21. Dyar, M.D. (1990) Mössbauer spectra of biotite from metapelites. *Amer. Mineral.*, **75**, 656-666.
22. Guidotti, C.V., and Dyar, M.D. (1991) Ferric iron in metamorphic biotite and its petrologic and crystallochemical implications. *Amer. Mineral.*, **76**, 161-175.
23. Dyar, M.D., Perry, C.P., Rebbert, C.R., Dutrow, B., Holdaway, M.J., and Lang, H. (1991) Mössbauer spectroscopy of synthetic and naturally occurring staurolites. *Amer. Mineral.*, **76**, 27-41.
24. Burns, R.G., and Dyar, M.D. (1991) Crystal chemistry and Mössbauer spectra of babingtonite. *Amer. Mineral.*, **76**, 892-899.
25. Dyar, M.D., Colucci, M.T., and Guidotti, C.V. (1991) Forgotten major elements: Hydrogen and oxygen variation in biotite from metapelite. *Geology*, **19**, 1029-1032.

[4]Names of undergraduate coauthors are underlined.

26. Holdaway, M.J., Mukhopadhyay, B., Dyar, M.D., Dutrow, B.L., Rumble, D. III., and Grambling, J. (1991) A new perspective on staurolite crystal chemistry: Use of stoichiometric and chemical end-members for a mole fraction model. *Amer. Mineral.*, **76**, 1910-1919.
27. McGuire, A.V., Dyar, M.D., and Nielson, J.E. (1991) Metasomatic oxidation of upper mantle peridotite. *Contrib. Min. Petrol.*, **109**, 252-264.
28. Dyar, M.D., McGuire, A.V., and Mackwell, S.M. (1992) Fe^{3+}/H^{+} and D/H in mantle kaersutites - Misleading indicators of mantle source fugacities. *Geology*, **20**, 565-568.
29. Dyar, M.D., McGuire, A.V., and Harrell, M.D. (1992) Crystal chemistry of iron in two styles of metasomatism in the upper mantle. *Geochim. Cosmochim. Acta*, **56**, 2579-2586.
30. Banfield, J.M., Dyar, M.D., and McGuire, A.V. (1992) The defect microstructure of oxidized mantle olivine from Dish Hill, California. *Amer. Mineral.*, **77**, 959-975.
31. McGuire, A.V., Francis, C.A., and Dyar, M.D. (1992) Mineral standards for electron microprobe analysis of oxygen. *Amer. Mineral.*, **77**, 1087-1091.
32. Holdaway, M.J., Gunst, R.F., Mukhopadhyay, B., and Dyar, M.D. (1993) Staurolite end member molar volumes determined from unit-cell measurements of natural specimens. *Amer. Mineral.*, **78**, 56-67.
33. O'Hanley, D.S., and Dyar, M.D. (1993) The crystal chemistry of lizardite 1T and the formation of magnetite in serpentines. *Amer. Mineral.*, **78**, 391-404.
34. Dyar, M.D. (1993) Mössbauer spectroscopy of tetrahedral Fe^{3+} in trioctahedral micas - Discussion. *Amer. Mineral.*, **78**, 665-668.
35. Dyar, M.D., Guidotti, C.V., Holdaway, M.J., and Colucci, M. (1993) Nonstoichiometric hydrogen contents in common rock-forming hydroxyl silicates. *Geochim. Cosmochim. Acta.*, **57**, 2913-2918.
36. Dyar, M.D., Mackwell, S.M., McGuire, A.V., Cross, L.R., and Robertson, J.D. (1993) Crystal chemistry of Fe^{3+} and H^{+} in mantle kaersutites: Implications for mantle metasomatism. *Amer. Mineral.*, **78**, 968-979.
37. Dyar, M.D. (1993) Instructional innovation. In The role of geosciences faculty in the undergraduate education of science and mathematics teachers. In *Proceedings, National Science Foundation Workshop, Role of Faculty from the Science Disciplines in the Undergraduate Education of Future Sciences and Mathematics Teachers,* 208-210.
38. Guidotti, C.V., Yates, M.G., Dyar, M.D., and Taylor, M. (1994) Petrogenetic implications of Fe^{3+} content of muscovite in pelitic schists. *Amer. Mineral.*, **79**, 793-795.
39. Earley, D., Dyar, M.D., Ilton, E.S., and Granthem, A.A. (1995) The influence of structural fluorine on biotite oxidation in copper-bearing, aqueous solutions at low temperatures and pressures. *Geochim. Cosmochim. Acta.*, **59**, 2423-2433.
40. Hower, J.C., Graham, U.M., Dyar, M. D., Taylor, M.E., and Rathbone, R.F. (1995) Approaches to the study of iron distribution among phases in high- and low-sulfur coal fly ash. In *Coal - Energy and the Environment*, S.-H. Chiang, ed., Proceedings 12th Ann. Pittsburg Coal Conference, 1138-1143.
41. Dyar, M.D., Treiman, A.H., Beauchamp, P.M., Blaney, D.L., Kim, S.S., Klingelhoefer, G., Mehall, G., Morris, R.V., Ninkov, Z., Sprague, A.L., Zolensky, M., and Pieters, C. (1995) Mineralogy. In Morris, C. and Treiman, A. H., eds., *Planetary Surface Instrumentation Workshop, Lunar and Planetary Institute, Tech. Rep.* 95-05, 65-84.
42. Dyar, M.D., Martin, S.V., Mackwell, S.J., Carpenter, S., Grant, C.A., and McGuire, A.V. (1996) Crystal chemistry of Fe^{3+}, H^{+}, and D/H in mantle-derived augite from Dish Hill: Implications for alteration during transport. In: M.D. Dyar, C.A. McCammon, and M. Schaefer, eds., *Mineral Spectroscopy: A Tribute to Roger G. Burns*, Special Publication #5, The Geochemical Society, 273-289.
43. Delaney, J.S., Bajt, S., Sutton, S.R., and Dyar, M.D. (1996) *In situ* microanalysis of $Fe^{3+}/\Sigma Fe$ ratios in amphibole by X-ray Absorption Near Edge Structure (XANES) spectroscopy. In: M.D. Dyar, C.A. McCammon, and M. Schaefer, eds., *Mineral Spectroscopy: A Tribute to Roger G. Burns*, Special Publication #5, The Geochemical Society, 170-177.
44. Robertson, J.D., and Dyar, M.D. (1996) Nuclear methods for analysis of boron in minerals. In: E.S. Grew and L.M. Anovitz, eds., *Boron: Mineralogy, Petrology, and Geochemistry in the Earth's Crust. Reviews in Mineralogy*, vol. 32, Mineralogical Society of America, 805-820.
45. Holdaway, M.J., Mukhopadhyay, B., Dyar, M.D., Guidotti, C.V., and Dutrow, B.L. (1997) Garnet-biotite geothermometry revised: New Margules parameters and a natural specimen data set from Maine. *Amer. Mineral.*, **82**, 582-595.
46. Bettison-Varga, L., Burger, R., Creasy, J., Dyar, D., Knight, P., Shapiro Ledley, T., and McManus, D. (1996) How should we integrate research and education? In: M.F.W. Ireton, C.A. Manduca, and D.A. Mogk,

Eds., *Shaping the Future of Undergraduate Earth Science Education*, American Geophysical Union, 29-32.

47. Dyar, M.D. (1997) Color in minerals. In: J.B. Brady, Mogk, D.W., and Perkins, D., eds., *Teaching Mineralogy*, Mineralogical Society of America, 323-348.
48. Smyth, J.R., Dyar, M.D., May, H.M., Bricker, O.P., and Acker, J.G. (1997) Crystal structure refinement and Mössbauer spectroscopy of an ordered, triclinic clinochlore. *Clays Clay Mins*., **45**, 544-550.
49. Delaney, J.S., Dyar, M.D., Sutton, S.R., and Bajt, S. (1998) Redox ratios with relevant resolution: Solving an old problem using the Synchrotron microXANES probe. *Geology*, **26**, 139-142.
50. Dyar, M.D., Taylor, M.E., Lutz, T.M., Francis, C.A., Robertson, J.D., Cross, L.M., Guidotti, C.V., and Wise, M. (1998) Inclusive chemical characterization of tourmaline: Mössbauer study of Fe valence and site occupancy. *Amer. Mineral.*, **83**, 848-864.
51. O'Hanley, D.S., and Dyar, M.D. (1998) The composition of chrysotile: integration of Mössbauer and electron microprobe data and the relationship between chrysotile and lizardite. *Canad. Mineral.*, **36**, 727-739.
52. Dyar, M.D., Delaney, J.S., Sutton, S.R., and Schaefer, M.W. (1998) Fe^{3+} distribution in oxidized olivine: A synchrotron micro-XANES study. *Amer. Mineral.*, **83**, 1361-1365.
53. Dyar, M.D., Guidotti, C.V., Core, D.P., Wearn, K.M., Wise, M.A., Francis, C.A., Johnson, K., and Brady, J.B. (1999) Stable isotope and crystal chemistry of tourmaline across pegmatite - country rock boundaries at Black Mountain and Mount Mica, southwestern Maine, U.S.A. *Euro. J. Mineral.*, **11**, 281-294.
54. Bloodaxe, E.S., Hughes, J.M., Dyar, M.D., Grew, E.S., and Guidotti, C.V. (1999) Linking structure and chemistry in the schorl-dravite series. *Amer. Mineral.,* **84**, 922-928.
55. Tagg, S.L., Cho, H., Dyar, M.D., and Grew, E.S. (1999) Tetrahedral boron in naturally-occurring tourmaline. *Amer. Mineral*., **84**, 1451-1455.
56. Francis, C.A., Dyar, M.D., Williams, M., and Hughes, J.M. (1999) The occurrence and crystal structure of foitite from a tungsten-bearing vein at Copper Mountain, Taos County, New Mexico. *Canad. Mineral.*, **37**(6), 1431-1438.
57. Woods, S., Mackwell, S.J., and Dyar, M.D. (2000) Hydrogen in diopside: Diffusion profiles. *Amer. Mineral.*, **85**, 480-487.
58. King, P.L., Hervig, R.L., Holloway, J.R., Delaney, J.S., and Dyar, M.D. (2000) Partitioning of Fe^{3+}/Fe_{total} between amphibole and basanitic melt as a function of oxygen fugacity. *Earth Planet. Sci. Lets.*, 178, 97-112.
59. Hughes, J.M., Ertl, A., Dyar, M.D., Grew, E.S., Shearer, C.K., Yates, M.G., and Guidotti, C.V. (2000) Tetrahedrally coordinated boron in a tourmaline: Boron-rich olenite from Stoffhütte, Koralpe, Austria. *Canad. Mineral.*, 38, 861-868.
60. Hughes, K.-A., Hughes, J.M., and Dyar, M.D. (2001) Chemical and structural evidence for $^{[4]}B \leftrightarrow {}^{[4]}Si$ substitution in natural tourmalines. *Eur. J. Mineral.*, 13, 743-747.
61. Dyar, M.D. Delaney, J.S., and Sutton, S.R. (2001) Fe XANES spectra of iron-rich micas. *Eur. J. Mineral.*, 13, 1079-1098.
62. Righter, K., Dyar, M.D., Delaney, J.S., Vennemann, T.W., and Hervig, R.L. (2002) Correlations of octahedral cations with OH^-, O^{2-}, Cl^-, and F^- in biotite from volcanic rocks and xenoliths. *Amer. Mineral*., 142-153.
63. Dyar, M.D., Wiedenbeck, M., Robertson, J.D., Cross, L.R., Delaney, J.S., Ferguson, K., Francis, C.A., Grew, E.S., Guidotti, C.V., Hervig, R.L., Hughes, J.M., Husler, J., Leeman, W., McGuire, A.V., Rhede, D., Rothe, H., Paul., R.L., Richards, I., and Yates, M. (2002) Reference minerals for microanalysis of light elements. *Geostand. Newslet.*, **25**, 441-463.
64. Dyar, M.D. (2002) Optical and Mössbauer spectroscopy of iron in micas. In Mottana, A., and Sassi, F., Advances in Micas, Mineralogical Society of America and The Geochemical Society, *Reviews in Mineralogy and Geochemistry*, **46**, 313-349.
65. Mottana, A., Marcelli, A., Cibin, G., and Dyar, M.D. (2002) X-ray absorption spectroscopy of the micas. In Mottana, A., and Sassi, F., Advances in Micas, Mineralogical Society of America and The Geochemical Society, *Reviews in Mineralogy and Chemistry*, **46**, 371-412.
66. Dyar, M.D., Lowe, E.W., Guidotti, C.V., and Delaney, J.S. (2002) Fe^{3+} and Fe^{2+} partitioning among silicates in metapelites: A synchrotron micro-XANES study. *Amer. Mineral*., **87**, 514-522.
67. Johnson, E.R., Rossman, G.R., Dyar, M.D., and Valley, J.W. (2002) Correlation between OH concentration and oxygen isotope diffusion rate in diopsides from the Adirondack Mountains, New York. *Amer. Mineral.*, **87**, 899-908.

68. Aja, S.U., and Dyar, M.D. (2002) The stability of Fe-Mg chlorites in aqueous hydrothermal solutions: I. Results of experimental investigations between 25 and 200 °C and $P_v = P_{H20}$. *Appl. Geochem*., **17**, 1219-1239.
69. Dyar, M.D., Gunter, M.E., Delaney, J.S., Lanzarotti, A., and Sutton, S.R. (2002) Use of the spindle stage for orientation of single crystals for microXAS: Isotropy and anisotropy in Fe-XANES spectra. *Amer. Mineral.,* **87**, 1500-1504.
70. Dyar, M.D., Gunter, M.E., Delaney, J.S., Lanzarotti, A., and Sutton, S.R. (2002) Systematics in the structure and XANES spectra of pyroxenes, amphiboles, and micas. *Canad. Mineral*., **40**, 1375-1393.
71. Bishop, J., Murad, E., and Dyar, M.D. (2002) The influence of octahedral and tetrahedral cation substitution on the structure of smectites and serpentines as observed through infrared spectroscopy. *Clay Mins.,* **37**, 617-628.
72. Petersen, O.V., Francis, C.A., Dyar, M.D., and Rosing, M.T. (2002) Dravite from Qârusulik, Ameralik Fjord, southern West Greenland: a forgotten classic tourmaline occurrence. *extraLapis English*, **3**, 42-46.
73. Gunter, M.E., Dyar, M.D., Twamley, B., Foit, F.F. Jr., and Cornelius, S.B. (2003) Composition, $Fe^{3+}/\Sigma Fe$, and crystal structure of non-asbestiform and asbestiform amphiboles from Libby, Montana, U.S.A. *Amer. Mineral.*, **88**, 1944-1952.
74. Dyar, M.D. (2003) Ferric iron in SNC meteorites as determined by Mössbauer spectroscopy: Implications for martian landers and martian oxygen fugacity. *Meteor. Planet. Sci.,* 38, 1733-1752.
75. Ertl, A., Hughes, J.M., Brandstätter, F., Dyar, M.D., and Prasad, P.S.R. (2003) Disordered Mg-bearing olenite from a granitic pegmatite at Goslarn, Austria: A chemical, structural, and infrared spectroscopic study. *Canad. Mineral.*, **41**, 1363-1370.
76. Dyar, M.D., and Schaefer, M.W. (2004) Mössbauer spectroscopy on the surface of Mars: constraints and expectations. *EPSL,* **218**, 243-259.
77. Dyar, M.D., Gunter, M.E., Davis, J.D., and Odell, M.R.L. (2004) Integration of new methods into teaching mineralogy. *J. Geosci. Educ.,* **52**, 23-31.
78. Dyar, M.D., McEnroe, S.A., Murad, E., Brown, L., and Schiellerup, H. (2004) The relationship between exsolution and magnetic behavior in hemo-ilmenite: Insights from Mössbauer spectroscopy with implications for planetary magnetic anomalies. *Geophy. Res. Letts.,* **31**, L04608, doi : 10.1029/2003GL019076.
79. Hughes, J.M., Ertl, A., Dyar, M.D., Grew, E.S., Wiedenbeck, M., and Brandstätter, F. (2004) Structural and chemical response to varying $^{[4]}B$ content in zoned Fe-bearing olenite from Koralpe, Austria. *Amer. Mineral*., **89**, 447-454.
80. Ertl, A., Pertlik, F., Dyar, M.D., Prowatke, S., Hughes, J.M., Ludwig, T., and Bernhardt, H.J. (2004) Fe-rich olenite with tetrahedrally coordinated Fe^{3+} from Austria: Structural, chemical, and Mössbauer data. *Canad. Mineral.*, **42**, 1057-1063.
81. Lane, M.D., Dyar, M.D., and Bishop, J.L. (2004) Spectroscopic evidence for hydrous iron sulfate in the martian soil. *Geophy. Res. Letts*., **31**, L19702, doi: 10.1029/2004GL021231.
82. McCanta, M.C., Dyar, M.D., Rutherford, M.J., and Delaney, J.S. (2004) Iron partitioning between basaltic melts and clinopyroxene as a function of oxygen fugacity. *Amer. Mineral*., **89**, 1685-1693.
83. Bishop, J.B., Dyar, M.D., Lane, M.L., and Banfield, J. (2004) Spectral identification of hydrated sulfates on Mars and comparison with acidic environments on Earth. *Internat. J. Astrobio*., **3**, 275-285.
84. Losey, A., Rakovan, J.F., Hughes, J.M., Francis, C.A., and Dyar, M.D. (2004) Structural variation with composition in the lithiophilite-triphylite series. *Canad. Mineral.,* **42**, 1105-1115.
85. Sutton, S.R., Delaney, J.S., Karner, J., Papike, J., Newville, M., Eng, P., Rovers, M., and Dyar, M.D. (2005) Vanadium K-edge XANES of synthetic and natural basaltic glasses and application to microscale oxybarometry. *Geochim. Cosmochim. Acta*., **69**, 2333-2348.
86. Driscall, J., Jenkins, D.M., Dyar, M.D., and Bozhilov, K.N. (2005) Cation ordering in synthetic Fe-Mg-actinolite. *Amer. Mineral.*, **90**, 900-911.
87. Dyar, M.D., Treiman, A.H., Pieters, C.M., Hiroi, T., and Lane, M.D. (2005) MIL03346, the most oxidized martian meteorite: A first look at petrography, mineral chemistry, and spectroscopy. *JGR, Planets,* **110**, E09005.
88. Seaman, S.J., Dyar, M.D., and Marinkovic, N., and Dunbar, N. (2006) An FTIR Study of Hydrogen in Anorthoclase and Associated Melt Inclusions. *Amer. Mineral*, **91**, 12-20.
89. Dyar, M.D. Agresti, D.G., Schaefer, M., Grant, C.A., and Sklute, E.C. (2006) Mössbauer spectroscopy of earth and planetary materials. *Ann. Revs. Earth Planet. Sci.*, **34**, 83-125.

90. Cempírek, J., Novák, M., Ertl, A., Hughes, J.M., Rossman, G.R., and Dyar, M.D. (2006) Fe-bearing olenite with tetrahedrally coordinated Al from an abyssal pegmatite at Kutná Hora, Czech Repubic: Structure, crystal chemistry, and XANES spectra. *Canad. Mineral.*, **44**, 23-30.
91. Schiffman, P., Zierenberg, R., Marks, N., Bishop, J.L., and Dyar, M.D. (2006) Acid fog deposition at Kilauea Volcano: A possible mechanism for the formation of siliceous-sulfate rock coatings on Mars. *Geology*, **34**(11), 921-924.
92. Agresti, D., Dyar, M.D., and Schaefer, M.W. (2006) Velocity calibration for *in-situ* Mössbauer data from Mars. *Hyperfine Interactions*, **167**(1-3), 845-850, 10.1007/s10751-006-9370-x.
93. Ertl, A., Kolitsch, U., Prowayke, S., Dyar, M.D., and Henry, D.J. (2006) The F-analogue of schorl from Grasstein, Trentino – South Tyrol, Italy: Crystal structure and chemistry. *Euro. J. Mineral.*, **18**, 583-588.
94. Agresti, D.G., Dyar, M.D., and Schaefer, M.W. (2007) Velocity scales for Mars Mossbauer data. *Hyperfine Interactions*, **170**(1-3), 67-74, DOI 10.1007/s10751-006-9472-5.
95. Dyar, M.D., Klima, R.L., Lindsley, D., and Pieters, C.M. (2007) Effects of differential recoil-free fraction on ordering and site occupancies in Mössbauer spectroscopy of orthopyroxenes. *Amer. Mineral.*, **92**, 424-428.
96. Klima, R.A., Dyar, M.D., and Pieters, C.M. (2007) Spectroscopy of synthetic Mg-Fe pyroxenes I: Spin-allowed and spin-forbidden crystal field bands in the visible and near-infrared. *Meteor. Planet. Sci.*, 42(2), 235-254.
97. Bishop, J.L., Schmifman, P., Murad, E., Dyar, M.D., Drief, A., and Lane, M.D. (2007) Characterization of Alteration Products in Tephra from Haleakala, Maui: A Visible-Infrared Spectroscopy, Mössbauer Spectroscopy, XRD, EMPA and TEM Study. *Clays Clay Mins.*, **55**(1), 1-17.
98. Treiman, A.H., Dyar, M.D., McCanta, M., Noble, S.K., and Pieters, C.M. (2007) Martian dunite NWA 2737: Petrographic constraints on geological history, shock events, and olivine color. *JGR (Planets)*, **112**, E04002, doi:10.1029/2006JE002777.
99. Lee, S.S., Guggenheim, S., Dyar, M.D., and Guidotti, C.V. (2007) Chemical composition, statistical analysis of the unit cell, and electrostatic modeling of the structure of Al-saturated chlorite. *Amer. Mineral.*, **92**, 954-965.
100. Taran, M.N., Dyar, M.D., and Matsyuk, S.S. (2007) Optical absorption study of natural garnets of almandine-skiagite composition showing intervalence $Fe^{2+}+Fe^{3+} \rightarrow Fe^{3+}+Fe^{2+}$ charge-transfer transition. *Amer. Mineral.*, **92**, 753-760.
101. Oyman, T., and Dyar, M.D. (2007) Chemical substitutions in oxidized tourmaline in granite-related hydrothermal systems, Western Turkey. *Canad. Mineral.*, **45**, 1397-1413.
102. Ertl, A., Hughes, J.M., Prowatke, S., Ludwig, T., Brandstätter, F., Körner, W., and Dyar, M.D. (2007) Tetrahedrally-coordinated boron in Li-bearing olenite from "mushroom". tourmaline from Momeik, Burma: Structure and chemistry. *Canad. Mineral.* , **45**, 891-899.
103. Minitti, M.E., Rutherford, M.J., Taylor, B.E., Dyar, M.D., and Schultz, P.H. (2008) Assessment of shock effects on amphibole water contents and hydrogen isotopic compositions: 1. Amphibolite experiments. *EPSL*, **266**, 46-40.
104. Mazeina, L., Navrotsky, A., and Dyar, M.D. (2008) Enthalpy of formation of Sulfate Green Rusts, $Fe^{II}_{1-x}Fe^{III}_{x}(OH)_{2+x-2y}(SO_4)_y \cdot nH_2O$. *Geochim. Cosmochim. Acta.,* **72**, 1143-1153.
105. Minitti, M.E., Leshin, L.A., Dyar, M.D., Ahrens, T.J., Guan, Y., and Luo, S. (2008) Assessment of shock effects on amphibole water contents and H isotopic compositions: 2. Kaersutitic amphibole experiments. *EPSL*, **266**, 288-302.
106. Bishop, J.L., Dyar, M. D., Sklute, E.C., and Drief, A. (2008) Physical alteration of antigorite: a Mössbauer spectroscopy, reflectance spectroscopy and TEM study with applications to Mars. *Clay Mins.*, 43, 55-67.
107. Burbine, T.H., Rivkin, A.S., Noble, S.K., Mothé-Diniz, T., Bottke, W.F., McCoy, T.J., and Dyar, M.D. (2008) Oxygen and asteroids. *Revs. Mineral. Geochem.,* **68**, 273-343.
108. Pieters, C. M., R. Klima, T. Hiroi, M. D. Dyar, M. D. Lane, A. H. Treiman, S. Noble, J. Sunshine, and J. Bishop (2008) The origin of brown olivine in Martian dunite NWA 2737: Integrated spectroscopic analyses of brown olivine. *J.Geophys. Res.*, doi:10.1029/2007JE002939.
109. Dyar, M.D., Grew, E.S., and Henry, D.J. (2008) Petrologic mineralogy – the study of minerals in context: A memorial in honor of Charles V. Guidotti. *Amer. Mineral.*, **93**, 261-262.
110. Dyar, M.D., Schaefer, M.W., Sklute, E.C., and Bishop, J.L. (2008) Mössbauer spectroscopy of phyllosilicates: Effects of fitting models on recoil-free fractions and redox ratios. *Clay Mins.*, **43**, 3-33.
111. Bishop, J.L., Lane, M.D., Dyar, M.D., and Brown, A.J. (2008) Reflectance and emissivity spectroscopy study of phyllosilicates: Smectites, kaolin-serpentines, chlorites and micas. *Clay Mins.,* **43**, 35-54.

112. Lane, M.D., Bishop, J.L., Dyar, M.D., King, P.L., Parente, M., and Hyde, B.C. (2008) Mineralogy of the Paso Robles soils on Mars. *Amer. Mineral.*, **93**, 728-739.
113. Tosca, N.J., McLennan, S.M., Dyar, M.D., Sklute, E.C., and Michel, F.M. (2008) Fe-oxidation processes at Meridiani Planum and implications for secondary Fe-mineralogy on Mars. *J. Geophys. Res. Planets*, **113** (E5), E05005.
114. Ertl, A., Dyar, M.D., Hughes, J.M., Brandstätter, F., Gunter, M., Prem, M., and Peterson, R.C. (2008) Pertlikite, a new netragonal Mg-rich member of the voltaite group from Madeni Zakh, Iran. *Canad. J. Mineral.*, **46**, 661-669.
115. Dyar, M.D. (2008) Mössbauer spectroscopy of environmental materials and their industrial utilization (book review). *Amer. Mineral.*, **93**, 1195.
116. Sanchez, M.S., Gunter, M.E., and Dyar, M.D. (2008) Characterization of historic amphibole samples from the former vermiculite mine near Libby, Montana U.S.A. *Euro. J. Mineral.*, **20**, 1043-1053.
117. Klima, R. L., Pieters, C. M. and M. D. Dyar (2008) Characterization of the 1.2 µm M1 pyroxene band: Extracting cooling history from near-IR spectra of pyroxenes and pyroxene-dominated rocks, *Meteor. Planet. Sci.*, **43**, 1591-1604.
118. Clegg, S.A., Wiens, R.C., Barefield, J., Sklute, E.C., and Dyar, M.D. (2009) Multivariate analysis of remote laser-induced breakdown spectroscopy spectra using partial least squares, principal component analysis, and related techniques. *Spectrochim. Acta Part B: Atom. Spectr.,* **64**, 79-88.
119. Li, Y.-L., Pfiffner, S.M., Dyar, M.D., Vali, H., Konhauser, K., Cole, D.R., and Phelps, T.J. (2009) Degeneration of superparamagnetic magnetite produced by *Shewanella algae* BrY. *Geobiology,* **7**, 25-34.
120. Hurowitz, J.A., Tosca, N.J., and Dyar, M.D. (2009) Acid production by $FeSO_4{\cdot}nH_2O$ Dissolution and implications for terrestrial and martian aquatic systems. *Amer. Mineral.*, **94**, 409-414.
121. Seaman, S.J., Dyar, M.D., and Marinkovic, N. (2009) The effects of heterogeneity in magma water concentration on the development of flow banding and spherulites in rhyolitic lava. *J. Volc. Geotherm Res.*, **183**, 157-169.
122. McCanta, M.C., Treiman, A.H., Dyar, M.D., Alexander, C.M.O'D., Rumble, D. III., and Essene, E.J. (2009) The LaPaz Icefield 04840 meteorite: Mineralogy, metamorphism, and origin of an amphibole- and biotite-bearing R chondrite. *Geochim. Cosmochim. Acta*, **72**, 5757-5780.
123. Dyar, M.D., Sklute, E.C., Menzies, O.N., Bland, P.A., Lindsley, D., Glotch, T., Lane, M.D., Wopenka, B., Klima, R., Bishop,. J.L., Hiroi, T., Pieters, C.M., and Sunshine, J. (2009) Spectroscopic characteristics of synthetic olivines, with an emphasis on fayalite: An integrated multi-wavelength approach. *Amer. Mineral.*, **94**, 883-898.
124. Lupulescu, M.V., Rakovan, J., Dyar, M.D., Robinson, G.W., and Hughes, J.M. (2009) Fluoro-potassichastingsite from the Greenwood Mine, Orange County, New York: a new end-member calcic amphibole. *Canad. Mineral.*, **47**, 909-916.
125. Dufresne, C.D.M., King, P.L., Dyar, M.D., and Dalby, K.N. (2009) Effect of SiO_2, total FeO, Fe^{3+}/Fe^{2+}, and alkali elements in basaltic glasses on mid-infrared spectra. *Amer. Mineral.*, **84**, 1580-1590.
126. Pieters, C.M., Goswami, J. N., Clark, R. N., Annadurai, M., Boardman, J., Buratti, B., Combe, J-P., Dyar, M.D., Green, R., Head, J. W., Hibbitts, C., Hicks, M., Isaacson, P., Klima, R., Kramer, G., Kumar, S., Livo, E., Lundeen, S., Malaret, E. T., McCord, T., Mustard, J., Nettles, J., Petro, N., Runyon, C., Staid, M., Sunshine, J., Taylor, L. A., Tompkins, S., Varanasi, P. (2009) Character and Spatial Distribution of OH/H_2O on the Surface of the Moon seen by M^3 on Chandrayaan-1. *Science*, **326**, 568-572.
127. Belley, F., Ferre, E.C., Martin-Hernandez, F., Jackson, M.J., Dyar, M.D., and Catlos, E. (2009) The magnetic properties of natural and synthetic $(Fe_x,Mg_{1-x})_2SiO_4$ olivines. Earth. Planet. Sci. Letts., 284, 516-526.
128. Ertl, A., Hughes, J.M., Dyar, M. D., Rossman, G.R., and Prowatke, S. (2010) Tourmaline of the elbaite-schorl series from the Himalaya Mine, Mesa Grande, California, U.SA.: A detailed investigation. *Amer. Mineral.*, **95**, 24-40.
129. Dyar, M. D., Hibbitts, C.A., and Orlando, T.M. (2010) Mechanisms for incorporation of hydrogen in and on terrestrial planetary surfaces. *Icarus,* **208**, 425–437, doi:10.1016/j.icarus.2010.02.014.
130. Groat, L.A., Rossman, G.R., Dyar, M.D., Turner, D., Piccoli, P.M.B., Schultz, A.J., and Ottolini, L. (2010) Crystal chemistry of aquamarine from the True Blue showing, Yukon Territory. *Canad. Mineral.*, **48**, 597-613.
131. Dyar, M.D., Glotch, T.D., Lane, M.D., Wopenka, B., Tucker, J.M., Seaman, S.J., Marchand, G.K., Klima, R., Hiroi, T., Bishop, J.L., Pieters, C., and Sunshine, J. (2011) Spectroscopy of Yamato 984028. *Polar Res.*, **4**, 530-540.

132. Grew, E.S., Marsh, J.H., Yates, M.G., Lazic, B., Armbruster, T., Locock, A., Bell, S., Dyar, M.D., Bernhardt, H.-J., and Medenbach, O. (2010) Menzerite-(Y), a new garnet species, {(Y, REE)(Ca, Fe^{2+})$_2$}[(Mg,Fe^{2+})(Fe^{3+},Al)](Si_3)O_{12}, end-member, {Y_2Ca}[Mg_2](Si_3)O_{12}, from a pyroxene granulite, Parry Sound, Ontario. *Canad. Mineral.*, **48**, 1171-1193.
133. Tucker, J.M., Dyar, M.D., Schaefer, M.W., Clegg, S.M., and Wiens, R.C. (2010) Optimization of laser-induced breakdown spectroscopy for rapid geochemical analysis. *Chem. Geol.,* **277**, 137-148.
134. Klima, R.L., Dyar, M. D., and Pieters, C. M. (2010) Near-infrared spectra of clinopyroxenes: effects of calcium content and crystal structure. *Meteor. Planet. Sci.,* doi: 10.1111/j.1945-5100.2010.01158.x.
135. Scordari, F., Dyar, M.D., Schingaro, E., Matarrese, S., and Ottolini, L. (2010) XRD, micro-XANES, EMPA and SIMS investigation on phlogopite single crystals from Mt. Vulture (Italy). *Amer. Mineral*., **95**, 1657-1670.
136. Dyar, M.D., Tucker, J.M., Humphries, S., Clegg, S.M., Wiens, R.C., and Lane, M. (2011) Strategies for Mars remote laser-induced breakdown spectroscopy analysis of sulfur in geological samples. *Spectrochimica Acta B.*, 66, 39-56.
137. Lane, M.D., Glotch, T.D., Dyar, M. D., Pieters, C.M., Klima, R., Hiroi, T., Bishop, J.L., and Sunshine, J. (2011) Mid-infrared spectroscopy of synthetic olivines: Thermal emission, attenuated total reflectance, and spectral and diffuse reflectance studies of forsterite to fayalite. *J. Geophys. Res. Planets.*, **116**, E08010, DOI: 10.1029/2010JE003588.
138. Hibbitts, C.A., Grieves, G.A., Poston, M.J., Dyar, M.D., Alexandrov, A.B., Johnson, M.A.,and Orlando, T. (2011) Thermal stability of water and hydroxyl on the surface of the Moon from temperature-programmed desorption measurements of lunar analog materials. *Icarus,* **213**, *64-72,* 10.1016/j.icarus.2011.02.015.
139. Gunter, M.E., Dyar, M.D., Lanzirotti, A., Tucker, J.M., and Speicher, E.A. (2011) Differences in Fe-redox for asbestiform and nonasbestiform amphiboles from the former vermiculite mine, near Libby, Montana USA. *Amer. Mineral.*, **96**, 1414-1417.
140. Potter, S.L., Chan, M.A., Petersen, E.U., Dyar, M.D., and Sklute, E.C. (2011) Characterization of Navajo sandstone concretions: Mars comparison and criteria for distinguishing diagenetic origins. *EPSL*, **301**, 444-456.
141. Hyde, B.C., King, P.L., Dyar, M.D., Spilde, M.N., Ali, A.-M.S., and Kinkel, T. (2011) Methods to analyze metastable and microparticulate hydrated and hydrous iron sulfate minerals. *Amer. Mineral.*, **96**, 1856-1869.
142. Dutcher, B., Fan, M., Leonard, B., Dyar, M.D., Tang, J., Speicher, E.A., Pan, L. (2011) Use of nanoporous FeOOH as a catalytic support for $NaHCO_3$ decomposition aimed at reduction of energy requirement of Na_2CO_3/$NaHCO_3$ based CO_2 separation technology. *J. Phys. Chem. C*., **115**, 15532-15544. DOI: 10.1021/jp204899r.
143. Dyar, M.D., Carmosino, M.L.,Tucker, J.M., Brown, E.A., Clegg, S.M., Wiens, R.C., Barefield, J.E., Delaney, J.S., Ashley, G.M., and Driese, S.G. (2012) Remote laser-induced breakdown spectroscopy analysis of East African Rift sedimentary samples under Mars conditions. *Chem. Geol.*, **294-295**, 135-151.
144. Schoonen, M., Sklute, E., Dyar, M.D., and Strongin, D. (2012) Reactivity of sandstones under conditions relevant to geosequestration: 1. Hematite-bearing sandstone exposed to supercritical carbon dioxide. *Chem. Geol.,* **296–297**, 96–102.
145. Evans, B.W., Dyar, M.D., and Kuehner, S.M. (2012) Implications of ferrous and ferric iron in antigorite. *Amer. Mineral*., **97**, 184-196.
146. Dyar, M.D. (2012) Gender and geoscience specialization as a function of object and spatial visualization skills. In *Earth and Mind II: A Synthesis of Research on Thinking and Learning in the Geosciences*. GSA Special Paper **486**, 79-83, doi: 10.1130/2012.2486(13).
147. Dyar, M.D., Carmosino, M.L., Speicher, EA., Ozanne, M.V., Clegg, S.M., and Wiens, R.C. (2012) Comparison of partial least squares and lasso regression techniques for laser-induced breakdown spectroscopy of geological samples. *Spectrochim. Acta B*, **70**, 51-67.
148. Wiens, R.C., Maurice, S., Barraclough, B., Saccoccio, M., Barkley, W.C., Bell, J.F. III, Bender, S. Bernardin, J., Blaney, D., Blank, J., Bouyé, M., Bridges, N., Bultman, N., Caïs, P., Clanton, R.C., Clark, B., Clegg, S., Cousin, A., Cremers, D., Cros, A., DeFlores, L., Delapp, D., Dingler, R., D'Uston, C., Dyar, M.D., Elliott, T., Enemark, D., Fabre, C., Flores, M., Forni, O., Gasnault, O., Hale, T., Hays, C., Herkenhoff, K., Holm, R., Kan, E., Kirkland, L., Kouach, D., Landis, D., Langevin, Y., Lanza, N., LaRocca, F., Lasue, J., Latino, J., Limonadi, D., Lindensmith, C., Little, C., Mangold, N., Manhes, G., Mauchien, P., McKay, C., Miller, E., Mooney, J., Morris, R.V., Morrison, L., Nelson, T., Newsom, H., Ollila, A., Ott,

M., Pares, L., Perez, R., Provost, C., Reiter, J.W., Roberts, T., Romero, F., Sautter, V., Salazar, S., Simmonds, J.J., Stiglich, R., Storms, S., Striebig, N., Thocaven, J.-J., Trujillo, T., Ulibarri, M., Vaniman, D., Warner, N., Waterbury, R., Whitaker, R., Witt, J., and Wong-Swanson, B. (2012) The ChemCam instruments on the Mars Science Laboratory (MSL) rover: Body unit and combined system performance. *Space Sci. Revs.* DOI 10.1007/s11214-012-9902-4.

149. Ertl., A., Schuster, R., Hughes, J.M., Ludwig, T., Meyer, H.-P., Finger, F., Dyar, M.D., Ruschel, K., Rossman, G.R., Klötzi, U., Brandstätter, F., Lengauer, C.L., and Tillmans, E. (2012) Li-bearing tourmalines in Variscan pegmatites from the Moldanubic nappes, Lower Austria. *Euro. J. Mineral.*, **24**, 695–715.
150. Bishop, J.L., Franz, H.B., Goetz, W., Blake, D.F., Freissinet, C., Steininger, H., Goesmann, F., Brinckerhoff, W.B., Getty, S., Pinnick, V.T., Mahaffy, P.R., and Dyar, M.D. (2012) Coordinated analyses of Antarctic sediments as Mars analog materials using reflectance spectroscopy and current flight-like instruments for CheMin, SAM, and MOMA. *Icarus.* doi: 10.1016/j.icarus.2012.05.014.
151. Segeler, C.G., Moore, P.B., Dyar, M.D., Leans, F., and Ferraiolo, J.A. (2012) Ferrolaueite, a new mineral from Monmouth County, New Jersey, USA. *Australian J. Mineral.*, **16**, 69-76.
152. Fernández-Remolar, D.C., Preston, L.J., Sánchez-Román, M., Izawa, M.R.W., Huang, L., Southam, G., Banerjee, N.R., Osinki, G.R., Flemming, R., Gómez-Ortiz, Ballesteros, O.P., Rodriguez, M., Amils, R., and Dyar, M.D. (2012) Carbonate precipitation under bulk acidic conditions as a potential biosignature for searching life on Mars. *EPSL*, **351-352**, 13-26.
153. Vaniman, D., Dyar, M.D., Wiens, R., Ollila, A., Lanza, N., Lasue, J., Rhodes, M., Clegg, S., and Newsom, H. (2012) Ceramic ChemCam calibration targets on Mars Science Laboratory. *Space Sci. Revs.*, DOI 10.1007/s11214-012-9886-0.
154. Dyar, M.D., Breves, E.A., Emerson, E., Bell, S.M., Nelms, M., Ozanne, M.V., Peel, S.E., Carmosino, M.L., Tucker, J.M., Gunter, M.E., Delaney, J.S.., Lanzirotti, A., and Woodland, A.B. (2012) Accurate determination of ferric iron in garnets in bulk Mössbauer spectroscopy and synchrotron micro-XANES. *Amer. Mineral.*, **97**, 1726-1740.
155. Bell, S.W., Thomson, B.J., Dyar, M.D., Neish, C.D., Cahill, J.T.S., and Bussey, D.B.J. (2012) Dating fresh lunar craters with Mini-RF. *J. Geophys. Res. Planets*, **117**, E00H30, doi:10.1029/2011JE004007.
156. Greenberger, R.N., Mustard, J.F., Kuma, P.S., Dyar, M.D., Breves, E.A., and Sklute, E.C. (2012) Low temperature aqueous alteration of basalt: mineral assemblages of Deccan basalts and implications for Mars. *J. Geophys. Res.,* **117**, E00J12 , DOI: 10.1029/2012JE004127.
157. Ertl, A., Kolitsch, U., Dyar, M.D., Hughes, J.M., Rossman, G.R., Pieczka, A., Henry, D.J., Pezzotta, F., Prowatke, S., Lengauer, C.L., Korner, W., Brandstatter, F., Francis, C.A., Prem, M., and Tillmanns, E. (2012) Limitations of Fe^{2+} and Mn^{2+} site occupancy in tourmaline: Evidence from Fe2+- and Mn2+-rich tourmaline. *Amer. Mineral.*, **97**, 1402-1416.
158. King, P.L., Sham , T.-K., Gordon, R.A., and Dyar, M.D. (2013) Microbeam X-ray analysis of Ce^{3+}/Ce^{4+} in Ti-rich minerals: A case study with titanite (sphene) with implications for multivalent trace element substitution in minerals. *Amer. Mineral.*, **98**, 110-119.
159. Bishop, J.L., Perry, K.A., Dyar, M.D., Bristow, T.F., Blake, D.F., Brown, A J. and Peel, S.E. (2013) Coordinated spectral and XRD analyses of magnesite-nontronite-forsterite mixtures and implications for carbonates on Mars. *J. Geophys. Res.*, **118**, doi:10.1002/jgre.20066.
160. Bishop, J.L., Loizeau, D., McKeown, N.K., Saper, L., Dyar, M.D., Des Marais, D., Parente, M., and Murchie, S.L. (2013) What the ancient phyllosilicates at Mawrth Vallis can tell us about possible habitability on early Mars. *Planet. Space Sci.*, DOI: 10.1016/j.pss.2013.05.006.
161. Bishop, J.L., Franz, H.B., Goetz, W., Blake, D.F., Freissinet, C., Steininger, H., Goesmann, F., Brinckerhoff, W.B., Getty, S., Pinnick, V.T., Mahaffy, P.R., and Dyar, M.D. (2013) Coordinated analyses of Antarctic sediments as Mars analog materials using reflectance spectroscopy and current flight-like instruments for CheMin, SAM, and MOMA. *Icarus*, **224**, 309-325.
162. Poston, M.J., Grieves, G.A., Aleksandrov, A.B., Hibbitts, C.A., Dyar, M.D., and Orlando, T.M. (2013) Water interactions with micronized lunar surrogates JSC-1A and albite under ultra-high vacuum with application to lunar observations. *J. Geophys. Res.,* **118**, 105–115, doi:10.1029/2012JE004283.
163. Osaky, M., Geramian, M., Dyar, M.D., Sklute, E.C., Valter, M., Ivey, D.G., Liu, Q., and Etsell, T.H. (2013) Characterization of petrological end members of oil sands from the Athabasca Region, Alberta, Canada. *Canad. J. Chem. Engineer*., **91**, 1402-1415.
164. Popa, T., Fan, M., Argyle, M.D., Dyar, M.D., Gao, Y., Tang, J., Speicher, E.A., and Kammen, D.M. (2013) H_2 and CO_x generation from coal gasification catalyzed by a cost-effective iron catalyst. *Applied Catalysis*, **464-465**, 207-217.

165. McCanta, M., Dobosh, P.A., and Dyar, M.D. (2013) Testing the veracity of LIBS analyses on Mars using the LIBSSIM program. *Space Science Reviews*, 81, 48-54.
166. Dyar, M.D., Klima, R.E., Fleagle, A., and Peel, S.E. (2013) Fundamental Mössbauer parameters of synthetic Ca-Fe-Mg pyroxenes. *Amer. Mineral.,* **98**, 1172-1186.
167. Osacky, M., Geramian, M., Dyar, M.D., Sklute, E.C., Valter, M., Ivey, D.G., Liu, Q., and Etsell, T.H. (2013) Characterization of petrologic end members of oil sands from the Athabasca region, Alberta, Canada. Canda. *J. Chem. Engineer.*, **9999**, 1-14.
168. Wiens, R.C., Maurice, S., Lasue, J., Forni, O., Anderson, R.B., Clegg, S., Bender, S., Blaney, D., Barraclought, B.L., Cousin, A., Deflores, L., Delapp, D., Dyar, M.D., Fabre, C., Gasnault, O., Lanza, N., Mazoyer, J., Melikechi, N., Meslin, P.-Y., Newsom, H., Ollila, A., Perez, R., Tokar, R.L., Vaniman, D., and the ChemCam team (2013) Pre-Flight calibration and initial data processing for the ChemCam laser-induced breakdown spectroscopy (LIBS) instrument on the Mars Science Laboratory (MSL) rover. *Spectrochimica Acta B.,* **B82**, 1-27.
169. Meslin, P.-Y., Anderson, R., Berger, G., Bish, D., Blake, D., Blaney, D., Bridges, N., Clark, B., Clegg, S., Cousin, A., D-'Uston, L., de la Torre, M., Dromart, G., Dyar, M.D., Ehlmann, B., Fabre, C., Fisk, M.R., Forni, O., Gasnault, O., Goetz, W., Herkenhoff, K., Lacour, J.L., Langevin, Y., Lanza, N., Lasue, J., Le Mouélic, S., Leshin, L., Leveille, R., Lewin, E., Madsen, M., Mangold, N., Maurice, S., McConnochie, T., Moores, J., Newson, H.E., Ollila, A., Perez, R., Rampe, E., Renno, N.O., Sautter, V., Schroder, S., Sirven, J.B., Vaniman, D., Wiens, R., Archer, D., Barraclough, B., Bender, S., Blank, J., DeFlores, L., Delapp, D., Gondet, B., Grotzinger, J., Harri, A.-M., Johnson, J., Melikechi, N., Mezzacappa, A., Mischna, M., Tokar, R., Yingst, R. (2013) Soil diversity and hydration as observed by ChemCam at Gale crater, Mars. *Science*, **341**, DOI: 10/1126/science.1238670.
170. Stolper, E.M., Baker, M.B., Newcombe, M.E., Schmidt, M.E., Treiman, A.H., Cousin, A., Dyar, M.D., Fisk, M.R., Gellert, R., King, P.L., Leshin, L., Maurice, S., McLennan, S.M., Minitti, M.E., Perrett, G., Rowland, S., Sautter, V., Wiens, R.C., and the MSL Scienec tean. (2013) The petrochemistry of Jake_M: a martian mugearite. *Science*, **341**, DOI: 10.1126/science.1239463.
171. McLennan, S.M., Anderson, R.B., Bell, J.F. III, Bridges, J.C., Calef, F. III, Campbell, J.L., Clark, B.C., Clegg, S., Conrad, P., Cousin, A., Des Marais, D.J., Dromart, G., Dyar, M.D., Edgar, L.., Ehlmann, B.L., Fabre, C., Forni, O., Gasnault, O., Gellert, R., Gordon, S., Grant, J.A., Grotzinger, J.P., Gupta, S., Herkenhoff, K.E., Huroqitz, J.A., King, P.L., Le Mouelic, S., Leshin, L.A., Leveille, R., Lweis, K.W., Mangold, N., Maurice, S., Ming, D.W., Morris, R.V., Nachon, M., Newson, H.E., Ollila, A.M., Perrett, G.M., Rice, M.S., Schmidy, M.E., Schwenzer, S.P., Stack, K., Stolper, E.M., Sumner, D.Y., Treiman, A.H., VanBommel, S., Vaniman, D.T., Vasavada, A., Wiens, R.C., and Yingst, R.A. (2013) Elemental geochemistry of sedimentary rocks in Yellowknife Bay, Gale Crater, Mars. *Science*, DOI: 10.1126/science.1244734
172. Dyar, M.D., Breves, E.A., Jawin, E., Marchand, G., Nelms, M., O'Connor, V., Peel, S., Rothstein, Y., Sklute, E.C., Lane, M.D., Bishop, J.L., and Mertzman, S.A. (2013) Mössbauer parameters of iron in sulfate minerals. *Amer. Mineral.*, **98**, 1943-1965.
173. Cuadros, J., Michalski, J.R., Dekov, V., Bishop, J., Fiore, S., and Dyar, M.D. (2013) Crystal-chemistry of interstratified clay minerals from seafloor hydrothermal sites. *Chem. Geol.*, **360**, 142-158.
174. Ollila, A.M., Newsom, H.E., Clark, B., III, Wiens, R.C., Cousin, A., Blank, J.G., Mangold, N., Sautter, V., Maurice, S., Clegg, S.M., Gasnault, O., Forni, O., Tokar, R., Lewin, E., Dyar, M.D., Lasue, J., Anderson, R., McLennan, S.M., Bridges, J., Vaniman, D., Lanza, N., Fabre, C., Melikechi, N., Perrett, G.M., Campbell, J.L., King, P.L., Barraclough, B., Celapp, D., Johnstone, S., Meslin, P.-E., Rosen-Gooding, A., Williams, J., and the MSl Science Team (2013) Trace element geochemistry (Li, Ba, Sr, and Rb) using Curiosity's ChemCam: Early Results for Gale Crater from Bradbury Landing Site to Rocknest. *JGR Planets*, DOI: 10.1002/2013JE004517.
175. Izenberg, N.R., Klima, R.L., Murchie, S.L., Blewet, D.T., Holsclaw, G.M., McClintock, W.E., Malaret, E., Mauceri, C., Vilas, F., Sprague, A.L., Helbert, J., Domingue, D.L., Head, J.W. III, Goudge, T.A., Solomon, S.C., Hibbitts, C.A., and Dyar, M.D. (2014) The low-iron, reduced surface of Mercury as seen in spectral reflectance by MESSENGER. *Icarus,* **226**, 364-374.
176. Harding, S.C., Nash, B.P., Petersen, E.U., Ekdale, A.A., Bradbury, C.D., and Dyar, M.D. (2014) Mineralogy and geochemistry of the Main Glauconite Bed in the Middle Eocene of Texas: Paleoenvironmental implications for the Verdine Facies. *Plos One*, **9**, e87656, doi:10.1371/journal.pone.0087656.

177. Monterroso, R., Fan, M., Argyle, M.D., Varga, K., Dyar, D., Tang, J., Sun, Q., Towler, B., Elliot, K.W., and Kammen, D. (2014) Characterization of the mechanism of gasification of a powder riverbasin coal with a composite catalyst for producing desired syngasesand liquids. *Appl. Catalysis A*, **475**, 116-126.
178. McCanta, M.C., Dyar, M.D., and Treiman, A.H. (2014) Alteration of Hawaiian basalts under sulfur-rich conditions: Applications to understanding surface-atmosphere interactions on Mars and Venus. *Amer. Mineral.,* **99**, 291-302, doi:10.2138/am.2014.4584.
179. Melikechi, N., Mezzacappa, A., Cousin, A., Lanza, N.L., Lasue, J., Clegg, S.M., Berger, G., Wiens, R.C., Maurice, S., Tokar, R.L., Bender, S., Forni, O., Breves, E.A., Dyar, M.D., Frydenvang, J., Delapp, D., Gasnault, O., Newsom, H., Ollila, A.M., Lewin, E., Clark, B.C., Ehlmann, B.L., Blaney, D., and Fabre, C. (2014) Correcting for variable laser-target distances of laser-induced breakdown spectroscopy measurements with ChemCam using emission lines of Martian dust spectra. *Spectrochim. Acta B*., **96**, 51-60.
180. Evans, K.A., Dyar, M.D., Reddy, S.M., Lanzirotti, A., Adams, D.T., and Tailby, N. (2014) Variation in XANES in biotite as a function of orientation, crystal composition, and metamorphic history. *Amer. Mineral.*, **99**, 443-457.
181. Isaacson, P.J., Klima, R.L., Sunshine, J.M., Pieters, C.M., Hiroi, T., and Dyar, M.D. (2014) Visible to near-infrared reflectance spectroscopy of pure synthetic olivine across the olivine solid solution. *Amer. Mineral.*, **99**, 467-478.
182. Lin, T.J., Breves, E.A., Dyar, M.D., Ver Eecke, H.C., Jamieson, J.W., and Holden, J.F. (2014) Magnetite formation from ferrihydrite by hyperthermophilic archaea from Endeavour Segment, Juan de Fuca Ridge hydrothermal vent chimneys. *Geobiology*, **12**, 200-211.
183. Dyar, M.D., Jawin, E., Breves, E.A., Marchand, G.J., Nelms, M., Lane, M.D., Mertzman, S.A., Bish, D.L., and Bishop, J.L. (2014) Mössbauer parameters of iron in phosphate minerals: Implications for interpretation of Martian data. *Amer. Mineral.,* **99**, 914-942.
184. McLennan, S.M., Anderson, R.B., Bell, J.F., Bridges, J.C., Calef, F., Campbell, J.L., Clark, B.C., Clegg, S., Conrad, P., Cousin, D., Des Marais, D.J., Dormart, G., Dyar, M.D., Edgar, L.A., Ehlmann, B.L., Fabre, C. Forni, O., Gasnault, O., Gellert, R., Gordon, S., Grant, J.A., Grotzinger, J.P., Gupta, S., Herkenhoff., K.E., Hurowitz, J.A., King, P.L., Le Mouélic, S., Leshin, L.A., Léveillé, R., Lewis, K.W., Mangold, N., Maurise, S., Ming, D.W., Morris, R.V., Nachon, M., Newsom, H.E., Ollila, A.M., Perrett, G.M., Rice, M.S., Schmidt, M.E., Schwenzer, S.P., Stack, K., Stolper, E.M., Sumner, D.Y., Treiman, A.H., VanBommel, S., Vaniman, D.T., Vasavada, A., Wiens, R.C., Yingst, R.A., MSL Sience Team. (2014) Elemental Geochemistry of Sedimentary Rocks at Yellowknife Bay, Gale Crater, Mars. *Science,* **24**, 343 (6169).
185. Clegg, S., Wiens, R., Misra, A., Sharma, S., Lambert, J., Bender, S., Newell, R., Nowak-Lovato, K., Smrekar, S., Dyar, M.D., and Maurice, S. (2014) Planetary geochemical investigations by Raman-LIBS spectroscopy. *Spectrochim. Acta B.,* **68**, 925-936, DOI: 10.1366/13-07386.
186. Bishop, J.L., Quinn, R., and Dyar, M.D. (2014) Spectral and thermal properties of perchlorate salts and implications for Mars. *Amer. Mineral*., **99**, 1580-1592.
187. Jawin, E.R., Kiefer, W.S., Fassett, C.F., Bussey, D.B.J., Cahill, J.T.S. Dyar, M.D., Lawrence, S.J., and Spudis, P.D. (2014) The relationship between radar scattering and surface roughness of lunar volcanic features. *J. Geophys. Res.*, **119**, 2331-2348.
188. Blaney, D.L., Wiens, R.C., Maurice, S., Clegg, S.M., Anderson, R.B., Kah, L.C., Le Mouelic, S., Ollila, A., Bridges, N., Tokar, R., Berger, G., Bridges, J.C., Cousin, A., Clark, B., Dyarm M.D., King, P.L., Lanza, N., Mangold, N., Meslin, P.-Y., Newsom, H., Schröder, S., Rowland, S., Johnson, J., Edgar, L., Gasnault, O., Forni, O., Schmidt, M., Goetz, W., Stack, K., Sumner, D., Fisk, M., Maden, M.B., and the MSL Science Team. (2014) Chemistry and texture of the rocks at Rocknest, Gale Crater: Evidence for sedimentary origin and diagenetic alteration. *J. Geophys. Res., Planets*, **119**, 2109-2131.
189. Schröder, S. Meslin, P.-Y., Gasnault, O., Maurice, S., Cousin, A., Wiens, R.C., Rapin, W., Dyar, M.D., Mangold, N., Forni, O., Nachon, M., Clegg, S., Johnson, J.R., Lasue, J., Le Mouélic, S., Ollila, A., Pinet, P., Sautter, V., and Vaniman, D. (2015) Hydrogen detection with ChemCam at Gale crater. *Icarus*, **249**, 43-61.
190. Bishop, J.L., Lane, M.D., Dyar, M.D., King, S.J., Brown, A.J., and Swayze, G. (2014) Spectral properties of Ca-sulfates: Gypsum, bassanite, and anhydrite. *Amer. Mineral*., **99**, 2105-2115.
191. Jackson, C.R.M., Cheek, L.C., Williams, K.B., Donaldson Hanna, Kerri, Pieters, C.M., Parman, S.W., Cooper, R.F., Dyar, M.D., Nelms, M., and Salvatore, M.R. (2014) Visible-infrared spectral properties of iron-bearing aluminate spinel under lunar-like redox conditions. *Amer. Mineral.*, **99**, 1821-1833.

192. Nachon, M., Clegg, S.M., Mangold, N., Schröder, S., Kah, L.C., Dromart, G., Ollila, A., Johnson, J.R., Oehler, D.Z., Bridges, J.C.., Le Mouelic, S., Forni, O., Wiens, R.C., Anderrson, R.B., Blaney, D.L., Bell, J.F., Clark, B., Cousin, A., Dyar, M.D., Ehlmann, B., Fabre, C., gasnault, O., Grotzinger, J., Lasue, J., Lewin, E., Leveille, R., MeLennan, S., Maurice, S., Meslin, P.-Y., Rapin, W., Rice, M., Sqyres, S., Stack, K., Sumner, D.Y., Vaniman, D., and Wellington, D. (2014) Calcium sulfate veins characterized by ChemCam/Curiosity at Gale crater, Mars. *J. Geophys. Res.*, **119**, 1991-2016.
193. Boucher, T.F., Carey, C., Mahadevan, S., and Dyar, M.D. (2015) Aligning mixed manifolds. *AAAI Conference Proceedings*, paper 1951.
194. Lane, M.D., Bishop, J.L., Dyar, M.D., Hiroi, T., Mertzman, S.A., Bish, D.L., King, P.L., and Rogers, A.D. (2015) Mid-infrared emission spectroscopy and visible/near-infrared reflectance spectroscopy of Fe-sulfate minerals. *Amer. Mineral*., **100**, 66-82.
195. Boucher, T.F., Ozanne, M.V., Carmosino, M.L., Dyar, M.D., Mahadevan, S., Breves, E.A., Lepore, K.H., and Clegg, S.M. (2015) Nine machine learning regression methods for major elemental analysis of rocks using laser-induced breakdown spectroscopy. *Spectrochim. Acta B*, **107**, 1-10.
196. Carey, C., Dyar, M.D., Boucher, T., and Mahadevan, S. (2015) Machine learning tools for mineral recognition and classification from Raman spectroscopy. *J. Raman Spectros*., **46**, 894-903.
197. Bartholomew, P.R., Dyar, M.D., and Brady, J.B. (2015) The role of intensity and instrument sensitivity in Raman mineral identification. *J. Raman Spectrosc*., **46**, 889-893.
198. Carey, C., Boucher, T., Giguere, S., Mahadevan, S.., and Dyar, M.D. (2015) Automatic whole-spectrum matching AI in Space Workshop, Intl. Joint Conf. Artificial Intelligence, Buenos Aires, July 2015.
199. Greenberger, R.N., Mustard, J.F., Cloutis, E.A., Pratt, L.M., Sauer, P.E., Mann, P., Turner, K., Dyar, M.D., and Bish, D.L. (2015) Serpentinization, iron oxidation, and aqueous conditions in an ophiolite: Implications for hydrogen production and habitability on Mars. *Earth Planet. Sci. Letts.*, **416**, 21-34.
200. Bishop, J.L., Murad, E., and Dyar, M.D. (2015) Akaganéite and schwertmannite: Spectral properties and geochemical implications of their possible presence on Mars. *Amer. Mineral.*, **100**, 738-746.
201. Forni, O., Gaft, M., Toplis, M.J., Clegg, S.M., Maurice, S., Wiens, R.C., Mangold, N., Gasnault, O., Sautter, V., LeMouelic, S., Meslin, P.-Y., Nachon, M., McInroy, R.E., Ollila, A.M., Cousin, A., Bridges, J.C., Lanza, N.L., and Dyar, M.D. (2015) First detection of fluorine on Mars: Implications for Gale Crater's geochemistry. *Geophys. Res. Letts.*, **42**, 1020-1028.
202. Schröder, S., Meslin, P.Y., Gasnault, O., Maurice, S., Cousin, A., Wiens, R.C., Rapin, W., Dyar, M.D., Mangold, N., Forni, O., Nachon, M., Clegg, S., Johnson, J.R., Lasue, J., Le Mouelic, S., Ollila, A., Sautter, V., and Vaniman, D. (2015) *Icarus*, **249**, 43-61.
203. Poston, M.J., Grieves, G.A., Aleksandrov, A.B., Hibbitts, C.A., Dyar, M.D., and Orlando, T.M. (2015) Temperature programmed desorption studies of water interactions with Apollo lunar samples 12001 and 72501. *Icarus*, **255**, 24-29.
204. Boucher, T., Dyar, M.D., Mahadevan, S., and Clegg, S.M. (2015) Comparison of linear and non-linear approaches to manifold learning predictions of chemical compositions in geological samples using laser-induced breakdown spectroscopy under Mars conditions. *J. Chemometrics*, doi: 10.1002/cem.2727.
205. Friedlander, L.R., Glotch, T.D., Bish, D.L., Dyar, M.D., Sharp, T.G., Sklute, E.C., and Michalski, J.R. (2015) Structural and spectroscopic changes to natural nontronite induced by experimental impacts between 10 and 40GPa. *J. Geophys. Res. Planets,* **120**, 888-912.
206. Boucher, T., Carey, C., Giguere, S., Mahadevan, S., Dyar, M.D., Clegg, S., Wiens, R. (2015) Manifold learning for regression of Mars spectra. AI in Space Workshop, Intl. Joint Conf. Artificial Intelligence, Buenos Aires, July 2015.
207. Michalski, J.R., Cuadros, J., Bishop, J.L., Dyar, M.D., Dekov, V., and Fiore, S. (2015) Constraints on the crystal-chemistry of Fe/Mg-rich smectitic clays on Mars and links to global alteration trends. *Earth Planet. Sci. Letts.,* **427**, 215-225.
208. Giguere, S., Carey, C., Boucher, T., Mahadevan, S., and Dyar, M.D. (2015) An optimization perspective on baseline removal for spectroscopy. AI in Space Workshop, Intl. Joint Conf. Artificial Intelligence, Buenos Aires, July 2015.
209. Ody, A., Poulet, F., Quantin, C., Bibring, J.P., Bishop, J.L., and Dyar, M.D. (2015) Candidates source regions of martian meteorites as identified by OMEGA/Mex. *Icarus*, **258**, 366-383.
210. Corona, J.C., Jenkins, D.M., and Dyar, M.D. (2015) The experimental incorporation of Fe into talc: a study using X-ray diffraction, Fourier transform infrared spectroscopy, and Mössbauer spectroscopy. *Contrib. Mineral. Petrol.*, 170, 29, 10.1007/s00410-015-1180-1.

211. Taran, M.N., Dyar, M.D., Naumenko, E.V., and Vyshnevsky, O.A. (2015) Spectroscopy of red dravite from Northern Tanzania. *Phys. Chem. Mineral.*, **42**, 559-568.
212. Dyar, M.D., McCanta, M., Breves, E., Carey, C.J., and Lanzirotti, A. (2016) Accurate predictions of iron redox state in silicate glasses: A multivariate approach using x-ray absorption spectroscopy. *Amer. Mineral.*, **101**, 744-748.
213. Dyar, M.D., Speicher, E.A., Gunter, M.E., Lanzirotti, A., Tucker, J.M., Carey, CJ, Peel, S.A., Brown, E.B., Oberti, R., and Delaney, J.S. (2016) Use of multivariate analysis for synchrotron micro-XANES analysis of iron valence state in amphiboles. *Amer. Mineral.,* **101**, 1171-1189.
214. Ertl, A., Kolitsch, U., Dyar, M.D., Meyer, H.-P., Henry, D.J., Rossman, G.R., Prem, M., Ludwig, T., Nasdala, L., Lengauer, C.L., Tillmanns E., and Niedermayr, G. (2016) Fluor-schorl, a new member of the tourmaline supergroup, and new data on schorl from the cotype localities. *Eur. J. Mineral.*, **28**, 163-177.
215. Lin, T.J., Ver Eecke, H.C., Breves, E.A., Dyar, M.D., Jamieson, J.W., Hannington, M.D., Dahle, H., Bishop, J.L., Lane, M.D., Butterfield, D.A., Kelley, D.S., Lilley, M.D., Baross, J.A., and Holden, J.F. (2016) Linkages between mineralogy, fluid chemistry, and microbial communities within hydrothermal chimneys from the Endeavour Segment, Juan de Fuca Ridge. *Geochem., Geophysi., Geosystems*, **17**, 300-323.
216. Maurice, S., Clegg, S.M., Wiens, R.C., Gasnault, O., Rapin, W., Forni, O., Cousin, A., Sauter, V., Mangold, N., Le Deit, L., Nachon, M., Anderson, R.B., Lanza, N.L., Fabre, C., Payre, V., Lasue, J., Maeslin, P.Y., Leveille, R.J., Barraclough, G., Beck, P., Bender, S.C., Berger, G., Bridges, J.C., Bridges, N.T., Dromart, G., Dyar, M.D., Francis, R., Frydenvang, J., Gondet, B., Ehlmann, B.L., Herkenhoff, K.E., Johnson, J.R., Langevin, Y., Madsen, M.B., Melikechi, N., Lacour, J.L., Le Mouelic, S., Lewin, E., Newsom, H., Olilla, A.M., Pinet, P., Schröder, S., Sirven, J.B., Tokar, R.L., Toplis, M.J., d'Uston, C., Vaniman, D.T., Vasavada, A.R. (2016) ChemCam activities and discoveries during the nominal mission of the Mars Science Laboratory in Gale crater, Mars. *J. Anal. Spectrosc.*, **31**, 863-889.
217. Mezzacappa, A., Melikechi, N., Cousin, A., Wiens, R.C., Lasue, J., Clegg, S., Tokar, S., Bender, S., Lanza, N.L., Maurice, S., Berger, G., Forni, O., Gasnault, O., Dyar, M.D., Boucher, T., Lewin, E., and Fabre, C. (2016) Application of distance correction to ChemCam LIBS measurements. *Spectroch. Acta.* B, **120**, 19-29, doi:10.1016/j.sab.2016.03.009.
218. Dyar, M.D., Fassett, C.I., Giguere, S., Lepore, K., Byrne, S., Boucher, T., Carey, CJ, and Mahadevan, S. (2016) Comparison of univariate and multivariate models for prediction of major and minor elements from laser-induced breakdown spectra with and without masking. *Spectroch. Acta B.*, **123**, 93-104.
219. Dyar, M.D., Giguere, S., Carey, CJ, and Boucher, T. S. (2016) Comparison of baseline removal methods for laser-induced breakdown spectroscopy of geological samples. *Spectroch. Acta B.*, **126**, 53-64.
220. Williams, K.B., Jackson, C.R.M., Cheek, L.C., Donaldson Hanna, K.L., Parman, S.W., Pieters, C.M., Dyar, M.D., and Prissel, T.C. (2016) Reflectance spectroscopy of chromium-bearing spinel with application to recent orbital data from the Moon. *Amer. Mineral.*, **101**, 726-734.
221. Berlanga, G., Hibbitts, C.A., Takir, D., Dyar, M.D., and Sklute, E.C. (2016) Spectral nature of CO_2 adsorption onto meteorites. *Icarus*, **280**, 366-377.
222. Chan, A., Jenkins, D.M., and Dyar, M.D. (2016) Partitioning of chlorine between NaCl brines and ferro-pargasite: Implications for the formation of chlorine-rich amphiboles in mafic rocks. *Canad. Mineral.*, **54**, 337-351.
223. McEnroe, S.A., Robinson, P., Miyajama, N., Fabian, K., Dyar, M.D., and Sklute, E. (2016) Lamellar magnetism and exchange bias in billion-year-old titanohematite with nanoscale ilmenite exsolution lamellae: I. Mineral and magnetic characterization. *Geophys. J. International*., **206**, 470-486.
224. Clegg, S.M., Wiens, R.C., Anderson, R., Forni, O., Frydenvang, J., Lasue, J., Cousin, A., Payre, C., Boucher, T., Dyar, M.D., McLennan, S.M., Morris, R.V., Graff, T.G., Mertzman, S.A., Ehlmann, B.L., Belgacem, I., Newsom, H., Clark, B.C., Melikechi, N., Mezzacappa, A., McInroy, R.E., Martinez, R., Gasda, P., Gasnault, O., and Maurice, S. (2016) Recalibration of the Mars Science Laboratory ChemCam instrument with an expanded geochemical database. *Spectrochim. Acta B*, **129**, 64-85.
225. Burgess, K.D., Stround, R. M., Dyar, M.D., and McCanta, M.C. (2016) Sub-micron scale spatial heterogeneity in silicate glasses using abberation-corrected scanning transmision electron microscopy. *Amer. Miner.*, **101**, 2677-2688.
226. Lepore, K.H., Fassett, C.I., Breves, E.A., Byrne, S., Giguere, S., Boucher, T., Rhodes, J.M., Vollinger, M., Anderson, C.H., Murray, R.W., and Dyar, M.D. (2017) Matrix effects in quantitative analysis of laser-induced breakdown spectroscopy of rock powders doped with Cr, Mn, Ni, Zn, and Co. *Appl. Spectros.,* **71**, 600-626.

227. Giguere, S., Boucher, T., Carey, CJ, Mahadevan, S., and Dyar, M.D. (2017) A fully-customized baseline removal framework for spectroscopic applications. *Appl. Spectros.*, **71**, 1457-1470.
228. Edwards, P.H., Bridges, J.C., Wiens, R., Anderson, R., Dyar, M.D., Fisk, M., Thompson, L., Gasda, P., Filiberto, J., Schwenzer, S.P., Blaney, D., and Hutchinson, I. (2017) Basalt-trachybasalt samples in Gale Crater, Mars *Meteor. Planet. Sci.,* **52**, 2931-2410.
229. Anderson, D.E., Ehlmann, B.L., Forni, O., Clegg, S.M., Cousin, A., Thomas, N.H., Lasue, J., Delapp, D.M., McInroy, R.E., Gasnault, O., Dyar, M.D., Schröder, S., Maurice, S., and Wiens, R.C. (2017) Characterization of laser-induced breakdown spectroscopy (LIBS) emission lines for the identification of chlorides, carbonates, and sulfates in salt/basalt mixtures for the application to MSL ChemCam data. *J. Geophys. Res. Planets.*, **122**, 744-770, DOI: 10.1002/2016JE005164.
230. McCanta, M. and Dyar, M.D. (2017) Impact-related thermal effects on the redox state of Ca-pyroxene. *Meteor. Planet. Sci.*, **52**, 320-332.
231. Mueller, B.L., Jenkins, D.M., and Dyar, M.D. (2017) Chlorine incorporation in amphiboles synthesized along the magnesio-hastingsite–hastingsite compositional join. *Eur. J. Mineral.*, **29**, 167-180.
232. Boucher, T., Dyar, M.D., and Mahadevan, S. (2017) Proximal methods for calibration transfer. *J. Chemometrics*, **31**, e2877.
233. Sklute, E.C., Kashyap, S., Dyar, M.D., Holden, J.F., Tague, T., Wang, P., and Jaret, S.J. (2017) Spectral and morphological characteristics of synthetic nanophase iron (oxyhydr)oxides. *Phys. Chem. Minerals,* **45**, 1-26*,* DOI 10.1007/s00269-017-0897-y.
234. Fassett, C.I., Crowley, M.C., Leight, C., Dyar, M.D., Minton, D.A., Hirabayashi, M., Thomson, B.J., and Watters, W. (2017) Evidence for rapid topographic evolution and crater degradation on Mercury from simple crater morphometry. *Geophys. Res. Letts.*, **44**, 5326-5335.
235. McCanta, M., Dyar, M.D., and Dobosh, P. (2017) Extracting bulk rock properties from microscale measurements: Subsampling and analytical guidelines. *GSA Today*, **27**, doi: 10.1130/GSATG290A.1.
236. Michalski, J., Glotch, T., Friedlander, L., Dyar, M., Bish, D., Sharp, T., and Cater, J. (2017) Shock metamorphism of clay minerals on Mars by meteor impact. *Geophys. Res. Letts*., **44**, 6562-6569. 10.1002/2017GL073423.
237. Farrand, W., Wright, S., Glotch, T., Schröder, C., Sklute, E., and Dyar, M.D. (2018) Spectroscopic examinations of hydro- and glaciovolcanic basaltic tuffs: Modes of alteration and relevance for Mars. *Icarus*, **309**, 241-259.
238. Taran, M.N., Dyar, M.D., Knomenko, V.M., and Boesenberg, J.S. (2017) Optical absorption, Mössbauer, and FTIR spectroscopic studies of two blue bazzites. *Phys. Chem. Mins.*, **44**, 497-507.
239. Ytsma, C. and Dyar, M.D. (2018) Effects of univariate and multivariate regression the accuracy of hydrogen quantification with laser-induced breakdown spectroscopy. *Spectrochim. Acta B*., 139, 27-37.
240. Breves, E.A., Lepore, K., Dyar, M.D., Bender, S.C., Tokar, R.L., and Boucher, T. (2017) Laser-induced breakdown spectra of rock powders at variable ablation and collection angles under Mars-analog conditions. *Spectrochim. Acta B*, **137**, 46-58.
241. McCanta, M., Dyar, M., Rutherford, M.J., Lanzirotti, A., Sutton, S., Thomson, B. (2017) In situ measurement of ferric iron in lunar glass beads using Fe-XAS. *Icarus*, **285**, 95-102, 10.1016/j.icarus.2016.12.029.
242. Sklute, E.C., Rogers, D., Gregerson, J.C., Jensen, H.B., Reeder, R.J., and Dyar, M.D. (2018) Amorphous salts formed from rapid dehydration of multicomponent chloride and ferric sulfate brines: Implications for Mars. *Icarus*, **302**, 285-295.
243. Taran, M.N., Dyar, M.D., and Khomenko, V.M. (2018) Spectroscopic study of synthetic hydrothermal Fe^{3+}-bearing beryl. *Phys. Chem. Minerals.*, **45**, 489-496.
244. Swayze, G.A., Lowers, H.A., Benzel W.M., Clark, R.N., Driscoll, R.L., Perlman, Z.S., Hoerfen, T.M., and Dyar, M. D. (2018) Characterizing the source of potentially asbestos-bearing commercial vermiculite insulation using in situ IR spectroscopy. *Amer. Mineral.*, **103**, 517-549.
245. Levy, J.S., Fassett, C.I., Rader, L.X., King, I.R., Chaffey, P.M., Wagoner, C.M., Hanlon, A.E., Watters, J.L., Kreslavsky, M.A., Holt, J.W., Russell, A.T., and Dyar, M.D. (2018) Distribution and characteristics of boulder halos at high latitudes on Mars: Ground ice and surface processes drive surface reworking. *J. Geophys. Res.*, **123**, 322-334.
246. Sun, Z., Chen, S.Y., Hu, J., Chen, A.M., Rony, A.H., Russell, C.K., Xiang, W.G., Fan, M.H., Dyar, M.D., and Sklute, E.C. (2018) $Ca_2Fe_2O_5$: A promising oxygen carrier for CO/CH_4 conversion and almost-pure H_2 production with inherent CO_2 capture over a two-step chemical looping hydrogen generation process. *Applied Energy*, **211**, 431-442.

247. Sklute, E.C., Kashyap, S., Dyar, M.D., Holden, J.F., Tague, T., Wang, P., and Jaret, S.J. (2018) Spectral and morphological characteristics of synthetic nanophase iron (oxyhydr)oxides. *Phys. Chem. Minerals.*, **45**, 1-26.
248. Dyar, M.D., Smrekar, S.E., and Glaze, L.S. (2018) The case for Venus. *Physics Today*, DOI:10.1063/PT.6.3.20180323a. https://physicstoday.scitation.org/action/showDoPubSecure?doi=10.1063%2FPT.6.3.20180323a&format=full
249. Thomas, N.H., Ehlmann, B.L., Anderson, D.E., Clegg, S.M., Forni, O., Schröder, S., Rapin, W., Meslin, P.-Y., Lasue, J., Delapp, D.M., Dyar, M.D. Gasnault, O., Wiens, R., and Maurice, S. (2018) Characterization of hydrogen in basaltic materials with laser-induced breakdown spectroscopy (LIBS) for application to MSL ChemCam. *J. Geophys. Research,* 10.1029/2017JE005467.
250. Breitenfeld, L.B., Dyar, M.D., Carey, CJ, Tague, T.J. Jr., Wang, P. (2018) Predicting olivine composition using Raman spectroscopy through band shift and multivariate analyses. *Amer. Mineral.*, **103**, 1827-1836.
251. Chrysochoou, M., Oakes, J., and Dyar, M.D. (2018) Investigation of iron reduction by green tea polyphenols. *Appl. Geochem.*, **97**, 263-269.
252. Lanzirotti, A., Dyar, M.D., Sutton, S., Newville, M., Head, E., Carey, CJ, McCanta, M., Lee, L., King, P.L., and Jones, J. (2018) Accurate predictions of microscale oxygen barometry in basaltic glasses using vanadium K-edge x-ray absorption spectroscopy: A multivariate approach. *Amer. Mineral.*, **103**, 1282-1297.
253. Jones, B.M., Aleksandrov, A., Hibbitts, K., Dyar, M.D., and Orlando, T.M. (2018) Solar wind-induced water cycle on the Moon. *Geophys. Res. Letts.*, **45**, 10959-10967.
254. Rucks, M., Whitaker, M., Glotch, T.D., Parise, J.B., Jaret, S.J., Catalano, T., and Dyar, M.D. (2018) Making tissintite: Mimicking meteorites in the multi-anvil. *Amer. Mineral.*, **103**, 1516-1519.
255. Kashyap, S., Sklute, E.C., Dyar, M.D., and Holden, J.F. (2018) Reduction and morphological transformation of synthetic nanophase iron oxide minerals by hyperthermophilic archaea. *Frontiers in Microbio.*, **9**, 1550, 10.3389/fmicb.2018.01550.
256. Dyar, M.D., Smrekar, S., and Kane, S. (2019) Venus: The Exoplanet Next Door. *Scientific American*, **320**, 56-63.
257. Knafelc, J., Filiberto, J., Ferre,E.C., Conder, J.A., Costello, L., Crandall, J.R., Dyar, M.D., Friedman, S.A., Hummer, D.R., and Schwenzer, S.P. (2019) The effect of oxidation on the miernalogy and magnetic properties of olivine. *Amer. Mineral.*, in press.
258. Loiselle, L., King, P.L., McCraig, M.A., Dyar, M.D., Leveille, R., Shieh, S.R., and Southam, G. (submitted) A spectral comparison of Meridiani-type jarosites using techniques relevant to the robotic exploration of biosignatures on Mars. *Life*.
259. Di Guiseppe, D., Harper, M., Bailey, M., Erskine, B., Della Ventura, G., Ardit, M., Pasquali, L., Tomaino, G., Ray, R., Mason, H., Dyar, M.D., Hanuskove, M., Giacobbe, C., Zoboli, A., and Gualitieri, A.F. (submitted) Characterization and assessment of the potential toxicity/pathogenicity potential of fibrous glaucophane. *Toxicology and Applied Pharmacology*.

Abstracts and Presentations:

1. Dyar, M.D., and Burns, R.G. (1981) Temperature-induced spectral variations of lunar-simulated Fe-Ti silicate glasses. In *Lunar and Planetary Science XII*, The Lunar and Planetary Science Institute, 243-245.
2. Burns, R.G., and Dyar, M.D. (1981) Coordination chemistry of iron in silicate glasses. Abstract to G.S.A. Annual Meeting, Cincinnati, OH, 420.
3. Dyar, M.D., and Consolomagno, G.J. (1982) Ferric iron in lunar glasses and the interpretation of lunar spectra. In *Lunar and Planetary Science XIII*, The Lunar and Planetary Science Institute, 193-194.
4. Consolomagno, G.J., and Dyar, M.D. (1982) Unsampled mare basalts and the evolution of the moon. In *Lunar and Planetary Science XIII*, The Lunar and Planetary Science Institute, 129-130.
5. Dyar, M.D., and Burns, R.G. (1982) Cation disorder and variable ferrous-ferric ratios in babingtonites. Abstract to G.S.A. Annual Meeting, New Orleans, LA, 480.
6. Dyar, M.D., and Burns, R.G. (1982) Optimization of experimental technique for measuring the Mössbauer effect in minerals. *Eos*, **63**, 1139.
7. Burns, R.G., and Dyar, M.D. (1983) Spectral chemistry of green glass-bearing 15426 regolith. In *Lunar and Planetary Science XIV*, The Lunar and Planetary Science Institute, 82-83.

8. Dyar, M.D., and Birnie, D.P. (1983) Crystallization processes in lunar green glass-type compositions as viewed by the Mössbauer effect. Abstract to the Glass in Planetary and Geological Phenomena Conf., August, 1983, Alfred, NY.
9. Dyar, M.D. (1983) Effects of quench media on iron-bearing glasses quenched from melts. Abstract to G.S.A. Annual Meeting, Indianapolis, IN, 564.
10. Dyar, M.D., and Birnie, D.P. (1984) Cooling rate dependence of 57-Fe coordination in quenched glasses. Abstract to Am. Ceram. Soc. Meeting, Pittsburg, PA, *Bull. Am. Ceram. Soc.*, 452.
11. Dyar, M.D. (1984) Quenching effects on iron site partitioning in the Apollo 17 orange glass composition. In *Lunar and Planetary Science XV*, The Lunar and Planetary Science Institute, 236-237.
12. Burns, R.G., and Dyar, M.D. (1984) Crystal chemistry of ferric micas. Abstract to G.S.A. Annual Meeting, Reno, NV, 459-460.
13. Dyar, M.D., Naney, M.T., and Swanson, S.E. (1984) The quench: a Mössbauer study of the influence of melt quenching on iron site occupancy in silicate glasses. Abstract to G.S.A. Annual Meeting, Reno, NV, 497.
14. Burns, R.G., Burns, V.M., Dyar, M.D., and Ryan, V.L. (1984) Stabilization of transition metal cations in meteoritic hibonites: evidence from Mössbauer spectroscopy. *EOS*, **65**, 1144.
15. Burns, R.G., and Dyar, M.D. (1984) Spectral chemistry of green glass-bearing 15426 regolith. *EOS*, Feb 21, 1984.
16. Dyar, M.D., Ryan, V.L., and Burns, R.G. (1985) Crystal chemistry and origin of blue color in meteoritic hibonite: evidence from Mössbauer spectra of 57-Fe-doped analogues. In *Lunar and Planetary Science XVI*, The Lunar and Planetary Science Institute, 202-203.
17. Dyar, M.D., Birnie, D.P., Naney, M.T., and Swanson, S.E. (1985) The theoretical determination and experimental effects of cooling history on silicate glasses. In *Lunar and Planetary Science XVI*, The Lunar and Planetary Science Institute, 200-201.
18. DeGuire, M.R., Dyar, M.D., O'Handley, R.C., and Kalongi, G. (1985) Iron environments in rapidly-solidified spinel ferrite-silica compositions. Abstract to Int'l. Conf. on Magnetism, San Francisco.
19. Burns, R.G., Burns, V.M., Dyar, M.D., Ryan, V.L., and Solberg, T. (1985) Iron coordination symmetries in silicates: correlations from Mössbauer parameters of ferrous and ferric iron in identical sites. Abstract to G.S.A. Annual Meeting, Orlando, FL, 535.
20. Dyar, M.D., Burns, R.G., and Rossman, G.R. (1985) Is there tetrahedral ferric iron in biotite? Abstract to G.S.A. Annual Meeting, Orlando, Fl., 571.
21. Phillips, W.S., and Dyar, M.D. (1986) Program SEARCH: A method for extracting exchange vectors from mineral compositional data. Abstract to Int'l Mineral. Assoc. Annual Meeting, Stanford, CA.
22. Dyar, M.D., Hickmott, D., Guidotti, C.V., and Cheney, J.T. (1986) M2/M1 ordering of iron in biotites from northwestern Maine. Abstract to Int'l Mineral. Assoc. Annual Meeting, Stanford, CA.
23. Dyar, M.D., Grover, T.W., Rice, J., and Guidotti, C.V. (1987) Presence of ferric iron and octahedral ferrous ordering in biotites from pelitic schists: implications for garnet-biotite geothermometry. Abstract to G.S.A. Annual Meeting, Phoenix, AZ, 650.
24. Dyar, M.D. (1988) Direct evidence of hydronium substitution in biotite. Abstract to G.S.A. Annual Meeting, Denver, CO, A102.
25. Perry, C.P., and Dyar, M.D. (1988) Increased resolution Mössbauer spectroscopy of natural and synthetic staurolites. *Eos*, **69**, 1483.
26. Ward, K.A., McGuire, A.V., and Dyar, M.D. (1988) Ferric iron content of megacrysts in alkali basalts. *Eos*, **69**, 1483.
27. Dyar, M.D., and McGuire, A.V. (1989) Crystal chemistry of clinopyroxene from mantle xenoliths. Abstract to G.S.A. Annual Meeting, St. Louis, MO, A241.
28. McGuire, A.V., and Dyar, M.D. (1989) Redox effects of mantle metasomatism. Abstract to G.S.A. Annual Meeting, St. Louis, MO, A105.
29. Mukhopadhyay, B., Holdaway, M.J., Gunst, R., and Dyar, M.D. (1990) End member thermochemical parameters and mixing parameters of 3-hydrogen Fe-staurolite. Abstract to G.S.A. Annual Meeting, Dallas, TX, A349.
30. Dyar, M.D. (1990) H, O, and Fe^{3+} in biotite and muscovite. Abstract to G.S.A. Annual Meeting, Dallas, TX, A215.
31. Dyar, M.D. (1991) Hydrogen and oxygen variation in micas from metapelites. Abstract to A.G.U./M.S.A. Spring Meeting, Supplement to *EOS*, April 23, 1991, 142.
32. McGuire, A.V., Francis, C.A., and Dyar, M.D. (1991) Characterization of standards for quantitative EPMA of oxygen. *Microbeam Analysis-1991*, 54-56.

33. Colucci, M.T., Gregory, R.L., Dyar, M.D., and Guidotti, C.V. (1991) Hydrogen isotope partitioning between biotite and muscovite. Abstract to G.S.A. Annual Meeting, San Diego, CA, A394.
34. Dyar, M.D., and O'Hanley, D.S. (1991) The crystal chemistry of lizardite and the formation of magnetite. Abstract to G.S.A. Annual Meeting, San Diego, CA, A157.
35. Harrell, M.T., Dyar, M.D., and McGuire, A.V. (1991) Redox behavior of metasomatism in a composite xenolith. Abstract to G.S.A. Annual Meeting, San Diego, CA, A272.
36. Mukhopadhyay, B., Holdaway, M.J., and Dyar, M.D. (1991) Crystal chemistry of Fe and Mg-end member cordierite. Abstract to G.S.A. Annual Meeting, San Diego, CA, A391.
37. Banfield, J.F., Dyar, M.D., and McGuire, A.V. (1991) The defect microstructure of oxidized mantle olivine. Abstract to A.G.U. Fall Meeting, Supplement to *EOS*, October 29, 1991, 478.
38. Zhou, F., Lindsley, D., and Dyar, M.D. (1992) Experimental study and thermodynamic properties of Mg-Fe biotites at 800□C. Abstract to Third Goldschmidt Conference, 1992, Reston, VA.
39. Dyar, M.D., McGuire, A.V., and Mackwell, S.J. (1992) Fe^{3+}/H^{+} and D/H in kaersutites - Misleading indicators of mantle source fugacities. Abstract to A.G.U. Spring Meeting, Montreal (invited).
40. McGuire, A.V., and Dyar, M.D. (1992) Characterization of cation oxidation states in geologic materials. Abstract to M.A.S. Annual Meeting, Boston (invited).
41. Dyar, M.D., Guidotti, C.V., Harper, G.D., McKibben, M.A., and Saccocia, P.J. (1992) Controls on ferric iron in chlorite. Abstract to G.S.A. National Meeting, Cincinnati, A130.
42. Colucci, M.T., Dyar, M.D., Gregory, R.T., Guidotti, C.V. and Holdaway, M.J. (1992) Stable isotope systematics of coexisting biotite and muscovite in high-grade pelitic rocks of southwestern Maine. Abstract to G.S.A. National Meeting, Cincinnati, A250.
43. Earley, D., III, Ilton, E.S., Dyar, M.D., and Veblen, D.R. (1992) Solid state redox chemistry of biotite during chemisorption of Cu^{2+} and 25□C and 1 bar. Agronomy Abstracts, 368.
44. Dyar, M.D., Guidotti, C.V., Meadows, E., and Robertson, J.D. (1992) PIGE analyses of F and Li in muscovite and biotite from metapelites and associated granites of W. Maine. Abstract to A.G.U. Fall Meeting, Supplement to *Eos*, October 27, 1992, 618.
45. Robertson, J.D., Meadows, E., Cross, L., and Dyar, M.D. (1993) PIGE analysis of Li and F in mineral separates. *Bull. Amer. Physical Soc.*, **38**, 928-929 (invited).
46. Robertson, J.D., Cross, L.R., Grant, C., Dyar, M.D., and Guidotti, C.V. (1993) Determination of fluorine in minerals by proton-induced gamma-ray emission analysis. Abstract to G.S.A. Annual Meeting, Boston, MA, A371-A372.
47. Swope, J.R., Munoz, J.L., Smyth, J.R., and Dyar, M.D. (1993) Single-crystal x-ray study of halogen-rich 1M biotites with implications for octahedral Fe-Mg ordering. Abstract to G.S.A. Annual Meeting, Boston, MA, A371.
48. Dyar, M.D., Francis, C.A., Wise, M.A., Guidotti, C.V., McGuire, A.V., and Robertson, J.D. (1994) Complete chemical characterization of tourmaline. Abstract to A.G.U. Spring Meeting, Baltimore, MD, 187.
49. Francis, C.A., Dyar, M.D., McGuire, A.V., and Robertson, J.D. (1994) Mineral standards for geochemistry. Abstract to 16th Meeting of the International Mineralogical Association, Pisa, Italy, 124-125.
50. McGuire, A.V., and Dyar, M.D. (1994) Ferric iron in upper mantle minerals. Abstract to 16th Meeting of the International Mineralogical Association, Pisa, Italy, 272-273.
51. Dyar, M.D. and Guidotti, C.V. (1994) Ferric iron, H, and light elements in silicates from metapelites in western Maine, U.S.A. Abstract to 16th Meeting of the International Mineralogical Association, Pisa, Italy, 108-109.
52. Mukhopadhyay, B., Holdaway, M.J., Guidotti, C.V., Dyar, M.D., and Dutrow, B.L. (1994) Garnet-biotite geothermometer: a recalibration. Abstract to 16th Meeting of the International Mineralogical Association, Pisa, Italy, 290.
53. Holdaway, M.J., Mukhopadhyay, B., Dyar, M.D., Guidotti, C.V., and Dutrow, B.L. (1994) A re-examination of the muscovite-almandine-biotite-sillimanite geobarometer. Abstract to 16th Meeting of the International Mineralogical Association, Pisa, Italy, 177.
54. Swope, R.J., Munoz, J.L., Smyth, J.R., Zanetti, K.S., Dyar, M.D., and Guidotti, C.V. (1994) Crystal chemistry of 1M ferromagnesian micas: a single crystal X-ray study. Abstract to G.S.A. Annual Meeting, Seattle, WA, A166.
55. Earley, D., Dyar, M.D., Ilton, E.S., and Granthem, A.A. (1994) The influence of structural F on biotite oxidation in Cu-bearing, aqueous solutions at low temperatures and pressures. Abstract to G.S.A. Annual Meeting, Seattle, WA, A223.

56. Robertson, J.D., Dyar, M.D., Paul, R.L., Nabalek, P.I., and Glascock, M.D. (1994) Nuclear methods for analysis of boron in minerals. Abstract to G.S.A. Annual Meeting, Seattle, WA, A-516.
57. Grant, C.A., and Dyar, M.D. (1994) Sources of experimental and analytical error in measurements of the Mössbauer effect in minerals. Abstract to G.S.A. Annual Meeting, Seattle, WA, A-166.
58. Dyar, M.D., Guidotti, C.V., and Robertson, J.D. (1994) Complete chemical characterization of silicates from metapelites in western Maine: A spectroscopic and analytical challenge. Abstract to A.G.U. Fall Meeting, San Francisco, 624.
59. Grant, C.A., and Dyar, M.D. (1995) Fe site populations in cummingtonite-grunerite. Abstract to A.G.U. Spring Meeting, Baltimore, S157.
60. Taylor, M.E., and Dyar, M.D. (1995) Distribution and valence state of iron in tourmaline. Abstract to A.G.U. Spring Meeting, Baltimore, S157.
61. Hower, J.C., Graham, U.M., Dyar, M.D., and Taylor, M.E. (1995) Iron distribution among phases in high- and low-sulfur coal fly ash. Abstract to the Pittsburgh Coal Conf., Pittsburg.
62. May, H.M., Acker, J.G., Smyth, J.R., Bricker, O.P., and Dyar, M.D. (1995) Aqueous dissolution of low-iron chlorite in dilute acid solutions at 25°C. Abstract to Clay Minerals Society Annual Meeting, Baltimore, MD.
63. Hower, J.C., Graham, U.M., Dyar, M. D., Taylor, M.E., and Rathbone, R.F. (1995) Approaches to the study of iron distribution among phases in high- and low-sulfur coal fly ash. 1995 Ash Utilization Symposium, Lexington, KY.
64. Dyar, M.D., Martin, S.V., Mackwell, S.M., Carpenter, S, Grant, C.A., and McGuire, A.V. (1995) Fe(III), H, and D/H in mantle-derived augite megacrysts from Dish Hill: Implications for alteration during transport. Abstract to G.S.A. Annual Meeting, New Orleans, A48.
65. McGuire, A.V., Begay, S., Lameman, T.L., and Dyar, M.D. (1995) Comparison of ferric iron in pyroxenites and associated composite xenoliths from Kilbourne Hole and Potrillo Maar, NM. Abstract to G.S.A. Annual Meeting, New Orleans, A48.
66. Delaney, J.S., Bajt, S., Sutton, S., and Dyar, M.D. (1995) Quantitative *in situ* measurement of ferric/ferrous ratios in amphibole and implications for volatile fugacity variations. Abstract to A.G.U. Fall Meeting, San Francisco, F705-F706.
67. Delaney, J.S., Bajt, S., Dyar, M.D., Sutton, S.R., McKay, G., Roeder, P. (1996) Comparison of quantitative synchrotron microXANES (SMX) $Fe^{3+}/(Fe^{3+}+Fe^{2+})$ results for amphibole and silicate glass with independent measurements. Lunar and Planetary Science XXVII, pages 299-300 (extended abstract) Lunar and Planetary Institute, Houston TX.
68. Dyar, M.D., Kahlenberg, V., Langer, K., and Terzenbach, H. (1996) Polarized single crystal spectra of natural and reheated olivines in the near ultraviolet spectral region and the problem of Fe^{3+} -bearing structural defects. *Phys. Chem. Minerals*., 23, 285.
69. Dyar, M.D., Delaney, J.S., Sutton, S.R., and Bajt, S. (1996) *In situ* microanalysis of ferric/ferrous in geophysically important mineral groups. Abstract to G.S.A. Annual Meeting, Denver, A102.
70. Delaney, J.S., Sutton, S.R., Dyar, M.D., Bajt, S., Moore, G., Carmichael, I.S.E., and Roeder, P. (1996) *In situ* microanalysis of ferric/ferrous in geologically significant glasses. Abstract to G.S.A. Annual Meeting, Denver, A419.
71. Delaney, J.S., Bajt, S., Newville, M., Sutton, S.R., and Dyar, M.D. (1996) Measurement of Fe oxidation state and coordination in geological glasses by synchrotron microXANES spectroscopy. Abstract to AGU Fall Meeting, San Francisco, *Eos*, 77, 835.
72. Carmichael, S., Acosta, R., Dyar, M.D., and Wise, M.A. (1997) Contrasts in crystal chemistry of tourmaline in simple and complex pegmatites, S.W. Maine. Abstract to N.E. G.S.A., King of Prussia, PA, 35-36.
73. Dyar, M.D., Guidotti, C.V., Core, D., Wearn, K., Wise, M.A., Francis, C.A., Johnson, K., and Brady, J.B. (1997) Chemistry of tourmaline across pegmatite-country rock boundaries at Black Mountain and Mount Mica, southwestern Maine, U.S.A. Abstract to Tourmaline '97 conference, Brno, Czech Republic, 14-17.
74. Guidotti, C.V., Yates, M.G., Grew, E.S., Dyar, M.D., Wiedenbeck, M., and Fowler, G. (1997) Stoichiometry of natural tourmaline from western Maine. Abstract to G.S.A. Annual Meeting, Salt Lake City, A-401.
75. Dyar, M.D., Delaney, J.S., Sutton, S.R., and Guidotti, C.V. (1997) In situ microanalysis and partitioning of ferric/ferrous in metapelite from western Maine. Abstract to G.S.A. Annual Meeting, Salt Lake City, A-399.
76. Delaney, J.S., Sutton, S.R., Dyar, M.D., and Bajt, S. (1997) Chemical state microanalysis using synchrotron micro-XANES spectroscopy: progress and prospects. Abstract to Fall AGU Meeting, San Francisco, *Eos*, **78**(46) F789.

77. Dyar, M.D., Crowley, P.D., Harrington, D., Stamski, E., Nevle, R., Delaney, J.S., Sutton, S.R., Morrison, H., Chervasia, M.B., Brown, Z., Gutmann, E., Guetschau, H., and Monders, A. (1997) Coordination effects on Fe pre-edge SmX spectra of garnet. Abstract to Fall AGU Meeting, San Francisco, *Eos*, **78**(46) F769.
78. Francis, C.A., Dyar, M.D., and DeMark, R.S. (1997) A fourth world occurrence of foitite at Copper Mountain, Taos Co., New Mexico. *New Mexico Geology*, **20**(2), 64.
79. Delaney, J.S., Sutton, S.R., and Dyar, M.D. (1998) Variable oxidation states of iron in martian meteorites. 29th Lunar and Planetary Science Conference, Houston, #1241.
80. Crowley, P.D., Stamski, R.E., Dyar, M.D., Nevle, R.J., Delaney, J.S., Monders, A.G., Jin Young, S., Guetschow, H.A., Gutmann, E.D., Harrington, D.F., Graham, R., Cheversia, M.B., Sutton, S.R., and Shea-McCarthy, G. (1998) Partitioning of ferric and ferrous iron between coexisting mafic silicates from Adirondack Metamorphic Rocks. National Synchrotron Light Source Activity Report 1997, B-228.
81. Crowley, P.D., Stamski, R.E., Dyar, M.D., Nevle, R.J., Delaney, J.S., Morrison, H.R., Cheversia, M.B., Brown, Z.M., Monders, A.G., Harrington, D.F., Guetschow, H.A., Gutmann, E.D., Graham, R., Sutton, S.R., and Shea-McCarthy, G. (1998) Coordination effect on Fe pre-edge SmX spectra of garnet. National Synchrotron Light Source Activity Report 1997, B-228.
82. Delaney, J.S., Bajt, S., Sutton, S.R., and Dyar, M.D. (1998) Ferric/ferrous microanalysis of geological glasses by synchrotron micro-XANES (SmX). National Synchrotron Light Source Activity Report 1997, B-229.
83. Delaney, J.S., Dyar, M.D., Sutton S.R., Bajt, S. (1998) Redox ratios with outrageous resolution: Solving an old geological problems with the synchrotron microXANES probe. National Synchrotron Light Source Activity Report 1997, B-229.
84. Dyar, M.D., Guidotti, C.V., Grew, E.S., Yates, M., Delaney, J.S., McGee, J.J., McGuire, A.V., Paul, R.L., Robertson, J.D., Cross, L.R., Sisson, V.M., Wiedenbeck, M.W., and Fowler, G. (1998) Interlaboratory comparison of tourmaline analyses: major elements including B, Li, and Fe. Abstract to 17th International Mineralogical Association meeting, Toronto, paper #494.
85. Dyar, M.D., Delaney, J.S., Sutton, S.R., Graham, C., and Kinny, P. (1998) Comparison of microanalysis and bulk analysis of ferric iron, water, and D/H in mantle kaersutite. Abstract, Geological Society of America, Annual Meeting, Toronto, A-186.
86. Bloodaxe, E.S., Hughes, J.M., Dyar, M.D., Grew, E.S., and Guidotti, C.V. (1998) Linking structure and chemistry in tourmalines. Abstract, Geological Society of America, Annual Meeting, Toronto, A-382.
87. Delaney, J.S., Dyar, MD., and Sutton, S.R. (1999) Mineralogical $Fe^{3+}/\Sigma Fe$ measurements as proxies of volatile budgets: I. Preamble. 30th Annual Lunar and Planetary Science Conference, #1704.
88. Dyar, M.D., Delaney, J.S., and Sutton, S.R. (1999) Mineralogical $Fe^{3+}/\Sigma Fe$ measurements as proxies of volatile budgets: II. Comparison of micro- and macro-scale data, and applications such as K_D derivation. 30th Annual Lunar and Planetary Science Conference, #1445.
89. Delaney, J.S., Dyar, M.D., Sutton, S.R., Polyak, D., and Stefanis, M. (1999) Mineralogical $Fe^{3+}/\Sigma Fe$ measurements as proxies of volatile budgets: III. Oxidation state zoning in martian basalt. 30th Annual Lunar and Planetary Science Conference, #1861.
90. Dyar, M.D., Delaney, J.S., McGuire, A.V., Stefanis, M.S., and Polyak, D.E. (1999) Mineralogical $Fe^{3+}/\Sigma Fe$ measurements as proxies of volatile budgets: IV. Crystal chemistry of iron in extraterrestrial pyroxene. 30th Annual Lunar and Planetary Science Conference, #1712.
91. Polyak, D.E., Dyar, M.D., Delaney, J.S., and Tegnar, C. (1999) Mineralogical $Fe^{3+}/\Sigma Fe$ measurements as proxies of volatile budgets: V. Crystal Chemistry of Fe in plagioclase from four heavenly bodies. 30th Annual Lunar and Planetary Science Conference, #1911.
92. Hughes, J.M., Ertl, A., Dyar, M.D., Grew, E.S., Shearer, C.K., Yates, M.G. (1999) Boron in the tourmaline tetrahedral site: Chemistry and structure of a boron-rich olenite. 2nd European Workshop on Tourmaline and Borosilicates. Paris.
93. Dyar, M.D., Grew, E.S., Guidotti, C.V., Hughes, J.M., Bloodaxe, E., Tagg, S.L., Cho, H., Shearer, C.K., Robertson, J.D., Paul, R.L., and Yates, M.G. (1999) The search for tetrahedral boron in tourmaline: an analytical challenge. 2nd European Workshop on Tourmaline and Borosilicates. Paris.
94. Delaney, J.S., Sutton, S.R., and Dyar, M.D. (1999) Iron in martian meteorites: Microanalysis of $Fe^{3+}/\Sigma Fe$ by synchrotron microXANES (SmX) as indicators of variable oxygen fugacity. Science Highlights, Activity Report 1998, National Synchrotron Light Source, 2-53-2-56.
95. King, P.L., Delaney, J.S., Dyar, M.D., Hervig, R.L., Holloway, J.R., and Righter, K. (1999) Micro-analysis of Fe^{3+}/Fe_{total} in natural and synthetic amphiboles. Activity Report 1999, National Synchrotron Light Source, 7-305.

96. Dyar, M.D., Polyak, D.E., Delaney, J.S., Sutton, S.R., McEnroe, S.A., and Tegner, C. (1999) Feldspar with and without micro-inclusions: Ferric iron determination by SmX. Abstract, Geological Society of America, Annual Meeting, Denver, A-358.
97. Dyar, M.D., Delaney, J.S., and Sutton, S.R. (2000) Advances in interpretation of Fe XANES pre-edge spectra, and resultant improvements in microanalysis of ferric/ferrous ratios on thin sections. 31st Annual Lunar and Planetary Science Conference, Houston.
98. Dyar, M.D., Delaney, J.S., Kinny, P.D., and Graham, C.M. (2000) Implications of dehydrogenation processes in amphibole for planetary hydrogen and oxygen budgets. 31st Annual Lunar and Planetary Science Conference #1768.
99. Delaney, J.S., Sutton, S.R, Newville, M., Jones, J.H., Hanson, B., Dyar, M.D., and Schreiber, H. (2000) Synchrotron micro-XANES measurements of Vanadium oxidation state in Glasses as a function of oxygen fugacity: experimental calibration of data relevant to partition coefficient determination. 31st Annual Lunar and Planetary Science Conference #1806.
100. Delaney, J.S., and Dyar, M.D. (2000) Correction of the calibration of ferric/ferrous determinations in pyroxene from Martian samples and achondritic meteorites by synchrotron microXANES spectroscopy. 31st Annual Lunar and Planetary Science Conference, #1981.
101. Dyar, M.D., Wiedenbeck, M., Cross, L., Delaney, J.S., Francis, C.A., Grew, E.S., Guidotti, C.V., Hervig, R.L., Hughes, J.M., Leeman, W., McGuire, A.V., Paul, R.L., Robertson, J.D., and Yates, M. (2000) Mineral standards for microanalysis of light elements (invited). Geoanalysis 2000, Pont à Mousson, Lorraine France.
102. Dyar, M.D. (2000) Spectroscopy of Iron in Mica (invited). Micas 2000 Conference, Italian National Academy, Rome.
103. Mottana, A., Marcelli, A., Cibin, G., and Dyar, M.D. (2000) X-ray absorption spectroscopy of the micas. Micas 2000 Conference, Italian National Academy, Rome.
104. Dyar, M.D., Lowe, E.W., Delaney, J.S., and Sutton, S.R. (2000) Microanalysis of Fe^{3+} and Fe^{2+} partitioning among minerals in metapelites (invited). Geological Soc. Amer., Reno, NV, A-53.
105. Guidotti, C.V., Grew, E.S., Yates, M.G., Dyar, M.D., Francis, C.A., Fowler, G., Husler, J., Shearer, C.K., and Wiedenbeck, M. (2000) Lithium in coexisting micas and tourmaline from western Maine. Geological Soc. Amer., Reno, NV, (invited), A-53.
106. Cartwright, B., Dyar, M.D., Seaman, S.J., and Delaney, J.S. (2000) Plagioclase ferrous/ferric correlation with magma oxygen fugacity in a volcanic succession. Geological Soc. Amer., Reno, NV, A-434.
107. Dyar, M.D., Rossman, G.R., Delaney, J.S., Sutton, S.R., and Newville, M. (2001) Interpretation of Fe- Xanes pre-edge spectra: Predictions based on Co and Fe optical spectra. 32nd Annual Lunar Planet. Sci. Conf., #1816.
108. Dyar, M.D., Delaney, J.S., and Tegner, C. (2001) Ferric iron in feldspar as an indicator of evolution of planetary oxygen fugacity. 32nd Annual Lunar Planet. Sci. Conf., #1065.
109. Gunter, M.E., Brown, B.M., Bandli, B.R., and Dyar, M.D. (2001) Amphibole asbestos, vermiculite mining, and Libby, Montana: What's in a name? Eleventh Annual Goldschmidt Conference, #3435.
110. Consolmagno, G.J., and Dyar, M.D. (2001) Rethinking the magma ocean. Geological Soc. Amer. Boston, MA, #19689.
111. Dyar, M.D., and Gunter, M.E. (2001) Mössbauer spectroscopy of amphibole-asbestos from Libby, Montana: Implications for asbestos classification. Geological Soc. Amer. Boston, MA, #26963.
112. Driscall, J.I., Jenkins, D.M., and Dyar, M.D. (2001) Iron-magnesium intersite partitioning in amphiboles synthesized near the tremolite-ferro-actinolite join. Geological Soc. Amer. Boston, MA, #25521.
113. Delaney, J.S., and Dyar, M.D. (2001) Magmatic magnetite in martian meteorite melt inclusions from Chassigny. *Meteor. Planet. Sci.*, 36, Suppl., A48.
114. Tegner, C., Delaney, J.S., and Dyar, M.D. (2001) Ferric/ferrous iron in plagioclase of the Skaergaard intrusion. *Eos, Trans. AGU*, 82(47), Fall Mtng. Suppl., V32E-1037.
115. Delaney, J.S., Mollel, G., Ashley, G.M., Dyar, M.D., and Sutton, S.R. (2001) Micrometer scale ferric/ferrous zoning quantified by synchrotron micro-XANES spectroscopy of pyroxene phenocrysts in phonolitic eruptives from Plio-Pleistocene volcano, Satiman, Tanzania. *Eos, Trans. AGU*, 82(47), Fall Mtng. Suppl., V32D-0996.
116. Bishop, J.L., Pieters, C.M., Dyar, M.D., Hamilton, V.E., and Harloff, J. (2002) A spectral, chemical, and mineralogical study of Mars analog rocks. 33rd Ann. Lunar Planet. Sci. Conf., #1161.
117. McEnroe, S.A., Dyar, M. D., and Brown, L.B. (2002) Magnetic signatures on planets without magnetic fields. 33rd Ann. Lunar Planet. Sci. Conf., #1287.

118. Gunter, M.E., Dyar, M.D., Delaney, J.S., Sutton, S.R., and Lanzirotti, A. (2002) Effects of preferred orientation on microscale XANES measurements of $Fe^{3+}/\Sigma Fe$ in biopyriboles. 33rd Ann. Lunar Planet. Sci. Conf., #1654.
119. Therkelsen, J.P., Dyar, M. D., and Morgan, P. (2002) Geologic and temporal constraints on the martian dichotomy using outflow channels. 33rd Ann. Lunar Planet. Sci. Conf., #1691.
120. Therkelsen, J.P., Dyar, M. D., Delaney, J.S., Johnson, J., and Horz, F. (2002) Effects of shock on ferric iron and major elements in plagioclase, pyroxene, and olivine: First reconnaisance. 33rd Ann. Lunar Planet. Sci. Conf., #1696.
121. Delaney, J.S., and Dyar, M.D. (2002) Compositional and oxidation state zoning in martian pyroxene: Paradox or process indicator. 33rd Ann. Lunar Planet. Sci. Conf., #1659.
122. Dyar, M.D., Housely, R.M., and Stiltner, S.A. (2002) Mössbauer study of ^{57}Fe-doped synthetic anorthite: Implications for interpretation of lunar anorthite spectra. 33rd Ann. Lunar Planet. Sci. Conf., #1725.
123. Seaman, S., Dyar, M.D., and Marinkovic, N. (2002) Fourier transform infrared spectroscopy (FTIR) studies of volcanic materials. N.E. G.S.A. Mtng., #32249.
124. Therkelsen, J.P., Dyar, M. D., Delaney, J.S., Johnson, J., and Hörz, F. (2002) Effects of shock on ferric iron and major elements in plagioclase, pyroxene, and olivine. N.E. G.S.A. Mtng., #31944.
125. Law, A.D. and Dyar, M.D. (2002) Studies of the Orthamphiboles. V. – Reconsideration of Doublet Assignments in Mössbauer Spectra. 18th IMA Meeting Edinburgh, Scotland, p 92, A-4-12.
126. Dyar, M.D. (2002) Mössbauer spectroscopy of SNC meteorites. Unmixing the SNC's. LPI Conf., Houston, #6011.
127. Delaney, J.S., and Dyar, M.D. (2002) What should we be looking for in Martian meteorites? Is evidence of crustal process or mantle process more important… and to whom? Unmixing the SNCs. LPI Conf., #6021.
128. Delaney, J.S., Dyar, M.D., Hörz, F., and Johnson, J.R. (2003) Evidence for coordination and redox changes of iron in shocked feldspar from synchrotron micro-XANES. 34th Ann. Lunar Planet. Sci. Conf., #1417.
129. Schaefer, M.W., Dyar, M.D., and Benison, K.C. (2003) Mössbauer spectroscopy of Mars-analog rocks from an acid saline sedimentary environment. 34th Ann. Lunar Planet. Sci. Conf., #1690.
130. Bishop, J.L., Drief, A., and Dyar, M.D. (2003) The influence of abrasion on martian dust grains: evidence from a study of antigorite grains. 34th Ann. Lunar Planet. Sci. Conf., #1512.
131. Dyar, M.D., and Schaefer, M.W. (2003) Mössbauer spectroscopy on the martian surface: Constraints on Interpretation of MER data. 34th Ann. Lunar Planet. Sci. Conf., #1329.
132. Schaefer, M.W., and Dyar, M.D. (2003) Mössbauer spectroscopy on the martian surface: Predictions. 34th Ann. Lunar Planet. Sci. Conf., #1381.
133. McCanta, M.C., Rutherford, M.J., Dyar, M.D., and Delaney, J.S. (2003) $Fe^{3+}/\Sigma Fe$ ratios in pigeonite as a function of f_{O2}: A preliminary investigation. 34th Ann. Lunar Planet. Sci. Conf., #1361.
134. Dyar, M.D. (2003) Mössbauer spectroscopy of mineral separates from SNC meteorites. 34th Ann. Lunar Planet. Sci. Conf., #1701.
135. Delaney, J.S. and Dyar, M.D. (2003) Comparison of synchrotron microXANES determination of $Fe^{3+}/\Sigma Fe$ with Mössbauer values for clean mineral separates of pyroxene from Martian meteorites. 34th Ann. Lunar Planet. Sci. Conf., #1979.
136. Tegner, C., Delaney, J.S., Dyar, M.D., and Lundgaard, K.L. (2003) Iron in plagioclase as a monitor of oxygen fugacity in Skaergaard, Bushveld, and Bjerkreim-Sokndal layered intrusions, and anorthosite of the Rogaland Igneous Province. EGS/AGU/EUG, EAE03-A-08789.
137. Seaman, S.J., Dyar, M.D., and Marinkovic, N. (2003) Aspects of the behavior of water during feldspar crystallization in rhyolitic magmas. EGS/AGU/EUG, EAE03-A-14375.
138. Bishop, J.L., Drief, A., and Dyar, M.D. (2003) The influence of abrasion on martian dust grains: evidence from a study of antigorite. 6th Intl. Mars. Conf., Pasadena, July 2003, #3008.
139. Seaman, S.J., Dyar, M. D., and Marinkovic, N. (2003) FTIR study of the effects of heterogeneity in water concentration on the origin of flow banded rhyolites. G.S.A. Annual Mtng., #67831.
140. Sutton, S.R., Karner, J.M., Papike, J.J., Delaney, J.S., and Dyar, M.D. (2004) Oxygen barometry of basaltic glasses based on vanadium valence determinations using synchrotron microXANES. 35th Ann. Lunar Planet. Sci. Conf., #1725.
141. Karer, J.M., Sutton, S.R., Papike, J.J., Delaney, J.S., Shearer, C.K., Newville, M., Eng, P., Rivers, M., and Dyar, M.D. (2004) A new oxygen barometer for solar system basaltic glasses based on vanadium valence. 35th Ann. Lunar Planet. Sci. Conf., #1269.

142. Pieters, C.M., Dyar, M.D., Hiroi, T., Bishop, J., Sunshine, J., Klima, R. (2004) Pigeonite masquerading as olivine at Mars: First results from the Mars Spectroscopy Consortium. 35th Ann. Lunar Planet. Sci. Conf., #1171.
143. McCanta, M.M., Rutherford, M.J., and Dyar, M.D. (2004) The relationship between clinopyroxenite Fe^{3+} and oxygen fugacity. 35th Ann. Lunar Planet. Sci. Conf., #1198.
144. Sunshine, J.M., Bishop, J. ,Dyar, M.D., Hiroi, T., Klima, R., and Pieters, C.M. (2004) Near-infrared spectra of martian pyroxene separates: first results from the Mars Spectroscopy Consortium. 35th Ann. Lunar Planet. Sci. Conf., #1636.
145. Dyar, M.D., Mackwell, S.J., Seaman, S.J., and Marchand, G.J. (2004) Evidence for a wet, reduced martian interior. 35th Ann. Lunar Planet. Sci. Conf., #1348.
146. Dyar, M.D., Schaefer, M.W., Griswold, J.L., Hanify, K.M., and Rothstein, Y. (2004) Mars mineral spectroscopy web site: A resource for remote planetary spectroscopy. 35th Ann. Lunar Planet. Sci. Conf., #1356.
147. Sheffer, A.A., and Dyar, M.D. (2004) ^{57}Fe Mossbauer spectroscopy of fulgurites : Implications for chemical reduction. 35th Ann. Lunar Planet. Sci. Conf., #1372.
148. Schaefer, M.W., Dyar, M.D., Rothstein, Y., Hanify, K.M., and Griswold, J.L. (2004) Temperature dependence of the Mössbauer fraction in Mars-analog minerals. 35th Ann. Lunar Planet. Sci. Conf., #1768.
149. Berlin, J., Spilde, M., Brearley, A.J., Draper, D.S., and Dyar, M.D. (2004) *In situ* determination of $Fe^{3+}/\Sigma Fe$ of spinels by electron microprobe: an evaluation of the Flank method. Oxygen Workshop, #3033.
150. Sheffer, A.A., and Dyar, M.D. (2004) ^{57}Fe Mossbauer spectroscopy of fulgurites : Implications for chemical reduction. Goldschmidt Conference 2004, Copenhagen, #472.
151. Bishop, J.L., Dyar, M.D., Parente, M., Drief, A., and Mancinelli, R.L. What iron oxides/hydroxides can tell us about surface alteration, aqueous processes, and life on Mars. 2nd Conference on Early Mars, #8046.
152. Keskula-Snyder, A.J., Seaman, S.J., ,and Dyar, M.D. (2005) Water in glass and feldspar in icelandic rhyolites. N.E.G.S.A. meeting, Abstract #34-4.
153. Delaney, J.S., Dyar, M.D., Gunter, M.E., Sutton, S.R., and Lanzirotti, A. (2005) Broad spectrum characterization of returned samples: Orientation constraints of small samples on X-ray and other spectroscopies. 36th Ann. Lunar Planet. Sci. Conf., #1130.
154. Dyar, M.D., Pieters, C.M., Hiroi, T., Lane, M.D., and Marchand, G.J. (2005) Integrated spectroscopic studies of MIL 03346. 36th Ann. Lunar Planet. Sci. Conf., #1261.
155. Lane, M.D., Bishop, J.L., Dyar, M.D., Forray, F.L., and Hiroi, T. (2005) Integrated spectroscopic studies of anhydrous sulfate minerals. 36th Ann. Lunar Planet. Sci. Conf., #1442.
156. Bishop, J.L., Schiffman, P., Lane, M.D., and Dyar, M.D. (2005) Solfataric alteration in Hawaii as a mechanism for formation of the sulfates observed on Mars by OMEGA amd the MER instruments. 36th Ann. Lunar Planet. Sci. Conf., #1456.
157. Klima, R.L., Pieters, C.M., and Dyar, M.D. (2005) Pyroxene spectroscopy: Effects of major element composition on near, mid, and far-infrared spectra. 36th Ann. Lunar Planet. Sci. Conf., #1462.
158. Dyar, M.D., Lane, M.D., Bishop, J.L., O'Connor, V., Cluotis, E., and Hiroi, T. (2005) Integrated spectroscopic studies of hydrous sulfate minerals. 36th Ann. Lunar Planet. Sci. Conf., #1622.
159. Sklute, E.C., Rothstein, Y., Schaefer, M.W., Menzies, O.N., Bland, P.A., and Berry, F.J. (2005) Temperature dependence and recoil-free fraction effects in olivines across the Mg-Fe solid solution. 36th Ann. Lunar Planet. Sci. Conf., #1888.
160. Agresti, D.G., Dyar, M.D., and Schaefer, M.W. (2005) MERVIEW: A new computer program for easy display of MER-acquired Mössbauer data. 36th Ann. Lunar Planet. Sci. Conf., #1941.
161. Sklute, E.C., Dyar, M.D., Minitti, M.E., Leshin, L.A., Guan, Y., Luo, S., and Ahrens, T.J. (2005) Mössbauer spectroscopy of shocked amphiboles. 36th Ann. Lunar Planet. Sci. Conf., #2040.
162. Schaefer, M.W., Dyar, M.D., Agresti, D.G., and Schaefer, B.E. (2005) Error analysis of remotely-acquired Mössbauer spectra. 36th Ann. Lunar Planet. Sci. Conf., #2047.
163. Rothstein, Y., Dyar, M.D., Schaefer, M.W., Lane, M.D., and Bishop, J.L. (2005) Fundamental Mössbauer parameters of hydrous iron sulfates. 36th Ann. Lunar Planet. Sci. Conf., #2108.
164. Rothstein, Y., Sklute, E.C., Dyar, M.D., and Schaefer, M.W. (2005) Effects of variable temperature on Mössbauer data acquisition: laboratory-based and MER A results. 36th Ann. Lunar Planet. Sci. Conf., #2216.
165. Bentley, M.S., Ball, A.J., Dyar, M.D., Pieters, C.M., Wright, I.P., and Zarnecki, J.C. (2005) Space weathering: laboratory analyses and in-situ instrumentation. 36th Ann. Lunar Planet. Sci. Conf., #2255.

166. Delaney, J.S., Dyar, M.D., Gunter, M.E., Sutton, S.R. and Lanzirotti, A. (2005) Geometric constraints of *in situ* synchrotron micro-XANES determinations of oxidation state. 15th Goldschmidt Conf.
167. Dyar, M.D., Delaney, J.S., Gunter, M.E., Sutton, S.R., and Lanzirotti, A. (2005) Transmission and fluorescence mode microXAS analysis of oriented mineral grains. 15th Goldschmidt Conf.
168. Bishop, J.L., Lane, M.D., and Dyar, M.D. (2005) Spectral identification of hydrated sulfates on Mars and comparison with sulfate-rich terrestrial sites. EGU05-A-05737.
169. O'Connor, V.A., Brady, J.B., Dyar, M.D., Lane, M.D., and Bishop, J.L. (2005) Chemistry, crystallography, and spectroscopy of hydrous sulfates. *GSA Annual Mtng.*, Salt Lake, Abstr. 126-10.
170. Schaefer, M.W., and Dyar, M.D. (2005) Comparison of several methods of Mössbauer spectroscopic analysis. *GSA Annual Mtng*., Salt Lake, #126-5.
171. Bishop, J.L., Bibring, J.-P., Dyar, M.D., Gendrin, A., Lane, M.D., Mustard, J., Parente, M. (2005) Searching for aqueous activity on Mars through analyses of OMEGA spectra, *AAS-DPS 37th Annual Meeting*, Cambridge, U.K., abs.#21.08.
172. Agresti, D.G., Dyar, M.D., and Schaefer, M.W. (2005). Velocity calibration for in-situ Mössbauer data from Mars. *Internat. Conf. Appl. Mössbauer Effect* (Sept. 5-9, 2005, Montpelier), T6-P1.
173. Bishop, J.L., Rothstein, Y., Dyar, M.D., Lane, M.D., Klima, R., Brophy, G. (2005) Distinguishing Na, K, and H_3O^+ Jarosite and Alunite on Mars using VNIR, Emittance and Mössbauer Spectroscopy on the MER and Mars Express/OMEGA Missions. Eos Trans. AGU, 86(52), Fall Meet. Suppl., Abstract P21A-0126.
174. Low, P.C., Dyar, M.D., and Seaman, S.J. (2005) Oxidation state of iron in feldspars from felsic to intermediate volcanic rocks as an indicator of magma oxygen. *EOS*, Transactions of the American Geophysical Union, Fall, 2005 Annual Meeting, V23B-04.
175. Lane, M.D., Dyar, M.D., and Bishop, J.L. (2005) The use of the thermal infrared region for studying the chemistry and hydration state of sulfates on Mars. *EOS*, Transactions of the American Geophysical Union, Fall, 2005 Annual Meeting, P21C-0164.
176. Seaman, S.J., Dyar, M. D., and Marinkovic, N. (2005) Flow Banding in Rhyolites: A Manifestation of Water Concentration Heterogeneity in the Melt? *EOS*, Transactions of the American Geophysical Union, Fall, 2005 Annual Meeting, V41I-05.
177. Keskula-Snyder, A.J., Seaman, S.J., ,and Dyar, M.D. (2005) Water concentrations and distribution in evolving melts as suggested by melt inclusions and matrix glasses. *EOS*, Transactions of the American Geophysical Union, Fall, 2005 Annual Meeting, V13B-0538.
178. Agresti, D.G., Dyar, M.D., and Schaefer, M.W. (2006). Velocity calibration for Mars Mössbauer data. *Nassau Conference on Application of the Mossbauer Effect.* New York.
179. Lupulescu, M., Rakovan, J., Dyar, M.D., and Pyle, J.M. (2006) F-, Cl- and K-rich amphiboles of the Hudson Highlands, New York. *GSA Abstracts with Programs,* 38(2), Abstr. 100433.
180. Dopfel, E.C., Dyar, M. D., and Sorensen, S.S. (2006) Crystal chemistry and spectroscopy of jadeite. *GSA Abstracts with Programs*, 38(2), Abstr. 100772.
181. Agresti, D.G., Dyar, M.D., and Schaefer, M.W. (2006) Derivation of velocity scales for Mars Mössbauer data. . *Lunar Planet. Sci. XXXVII.*, Lunar Planet. Inst., Houston, CD-ROM #1517 (abstr.).
182. Bishop, J.L., Schiffman, P., Dyar, M.D., Lane, M.D., Murad, E., and Drief, A. (2006) Soil-Forming Processes on Mars as Determined by Mineralogy: Analysis of Recent Martian Spectral, Chemical And Magnetic Data and Comparison with Altered Tephra From Haleakala, Maui. *Lunar Planet. Sci. XXXVII.*, Lunar Planet. Inst., Houston, CD-ROM #1423 (abstr.).
183. Bishop, J.L., Dyar, M.D., Parente, M., Drief, A., Mancinelli, R. L., Lane, M.D., and Murad, E. (2006) Understanding Surface Processes on Mars Through Study of Iron Oxides/Oxyhydroxides: Clues to Surface Alteration and Aqueous Processes. *Lunar Planet. Sci. XXXVII.*, Lunar Planet. Inst., Houston, CD-ROM #1438 (abstr.).
184. Burbine, T.H., Dyar, M.D., Seaman, S.J., and McCoy, T.J. (2006) Water content of nominally anhydrous minerals in the Ibitira eucrite. *Lunar Planet. Sci. XXXVII.*, Lunar Planet. Inst., Houston, CD-ROM #2220 (abstr.).
185. Dyar, M.D., Rothstein, Y., Schaefer, M.W., and Agresti, D.G. (2006) Mössbauer Spectroscopy of outcrop at the Meridiani Planum Site. *Lunar Planet. Sci. XXXVII.*, Lunar Planet. Inst., Houston, CD-ROM #2382 (abstr.).
186. Greenwood, J.P., Gilmore, M.S., Blake, R.E., Martini, A.M., Gomes, M., Tracy, S., Dyar, M.D., Gilmore, J.A., and Varekamp, J. (2006) Nascent jarosite mineralization of sulphur springs, St. Lucia, W.I.: Implications for Meridiani jarosite formation. *Lunar Planet. Sci. XXXVII.*, Lunar Planet. Inst., Houston, CD-ROM #2230 (abstr.).

187. Lane, M.D., Dyar, M.D., Bishop, J.L., King, P.L., and Cloutis, E. (2006) Laboratory emission, visible-near infrared, and Mössbauer spectroscopy of iron sulfates: application to the bright Paso Robles soils in Gusev crater. *Lunar Planet. Sci. XXXVII.*, Lunar Planet. Inst., Houston, CD-ROM #1799 (abstr.).
188. McCanta, M.C., Dyar, M.D., and Hörz, F.P. (2006) Shock oxidation of pyroxene: effects on redox ratio. *Lunar Planet. Sci. XXXVII.*, Lunar Planet. Inst., Houston, CD-ROM #1903 (abstr.).
189. McCanta, M.C., Dyar, M.D., Treiman, A.H., Pieters, C.M., Hiroi, T., Lane, M.D., and Bishop, J.L. (2006) Mössbauer and synchrotron microXANES analysis of NWA2737. *Lunar Planet. Sci. XXXVII.*, Lunar Planet. Inst., Houston, CD-ROM #1751 (abstr.).
190. Pieters, C.M., Dyar, M.D., Hiroi, T., Lane, M.D., Treiman, A.H., McCanta, M., Bishop, J.L., and Sunshine, J. (2006) Optical properties of martian dunite NWA 2737: a record of martian processes. *Lunar Planet. Sci. XXXVII.*, Lunar Planet. Inst., Houston, CD-ROM #1634 (abstr.).
191. Klima, R.L. Pieters, C.M., and Dyar, M.D. (2006) Pyroxene spectroscopy at visible wavelengths: effect of iron content on spin-forbidden absorption features. *Lunar Planet. Sci. XXXVII.*, Lunar Planet. Inst., Houston, CD-ROM #1637 (abstr.).
192. Rothstein, Y., Dyar, M.D., and Bishop, J.L. (2006) Mössbauer spectroscopy of synthetic jarosite with variable compositions and temperatures. *Lunar Planet. Sci. XXXVII.*, Lunar Planet. Inst., Houston, CD-ROM #1727 (abstr.).
193. Schaefer, M.W., Dyar, M.D., and Agresti, D.G. (2006) Comparison of Mössbauer spectra of soils from Gusev crater and Meridiani Planum. *Lunar Planet. Sci. XXXVII.*, Lunar Planet. Inst., Houston, CD-ROM #2111 (abstr.).
194. Sheffer, A.A., Dyar, M.., and Sklute, E.C. (2006) Lightning strike glasses as an analog for impact glasses: ^{57}Fe Mössbauer spectroscopy of fulgurites. *Lunar Planet. Sci. XXXVII.*, Lunar Planet. Inst., Houston, CD-ROM #2009 (abstr.).
195. Sklute, E.C., Dyar, M.D., and Schaefer, M.W. (2006) Mössbauer spectroscopy of olivines across the Mg-Fe solid solution. *Lunar Planet. Sci. XXXVII.*, Lunar Planet. Inst., Houston, CD-ROM #2109 (abstr.).
196. Treiman, A.H., McCanta, M., Dyar, M.D., Pieters, C.M., Hiroi, T., Lane, M.D., and Bishop, J.L. (2006) Brown and clear olivine in Chassignite NWA 2737: water and deformation. *Lunar Planet. Inst.*, Houston, CD-ROM #1314 (abstr.).
197. Bishop J. L., Lane M. D., Dyar M. D., Brown A. J., and Parente M. (2006) Sulfates on Mars as markers of aqueous processes: An integrated multi-disciplinary study of minerals, Mars analog sites and recent mission data. *Mars Water Workshop*, NASA-Ames Research Center, Moffett Field, CA, February 23-24, 2006.
198. Bishop J. L., Lane M. D., Dyar M. D., and Brown A. J. (2006) Sulfates on Mars: Indicators of aqueous processes on Mars. *Astrobiology Science Conference*, Washington, DC, March 26-30, 2006.
199. Bishop, J.L., Brown, A.J., Cloutis, E., Dyar, M.D., Hiroi, T., Lane, M.D., Milliken, R.E., Murad, E., and Mustard, J.F. (2006) A Multispectral Study of Clay Minerals: Mössbauer, Reflectance, Transmittance, and Emission Spectroscopy. 3rd Mid-European Clay Conference, Opatija, Croatia.
200. Dyar, M.D., Bishop, J.L., and Drief, A. (2006) The Influence of Physical Alteration on the Mössbauer and Reflectance Spectra of Antigorite and Applications to Soil Alteration Processes on Mars. 3rd Mid-European Clay Conference, Opatija, Croatia.
201. Sanchez, M.S., Gunter, M. E., Dyar, M.D., Badger, S.R., Hobbs, G.C., Van Orden, D.R., and Potter, M.S. (2006) Characterization of historical amphibole samples from the former vermiculite mine near Libby, Montana U.S.A. Abstract to G.S.A. Annual Meeting, Philadelphia, #118-6.
202. Dyar, M.D., and Guidotti, C.V. (2006) Iron site occupancy and valence state in metapelitic chlorite from western Maine. Abstract to G.S.A. Annual Meeting, Philadelphia, #16-3.
203. Low, P.C., Seaman, S.J., Williams, M., Jercinovic, M., Dyar, M.D., and Karlstrom, K.E. (2006) Compositional and textural evidence of an igneous origin for olivine coronas in lherzolite from mile 91 canyon. Abstract to G.S.A. Annual Meeting, Philadelphia, #118-22.
204. Seaman, S.J., Helfrich, E., and Dyar, M.D. (2006) The role of water in the growth of spherulites in rhyolitic lava flows. Abstract to G.S.A. Annual Meeting, Philadelphia, #107-7.
205. Lane, M.D., Bishop, J.L., Parente, M., Dyar, M.D., King, P.L., and Cloutis, E. (2006) Determining the chemistry of the bright Paso Robles soils on Mars using multispectral data sets. *Workshop on Martian Sulfates as Recorders of Atmospheric-Fluid-Rock Interactions.*
206. Bishop, J.L., Brown, A., Parente, M., Lane, M. D., Dyar, M.D., Schiffman, P., Murad, E., and Cloutis, E. (2006) VNIR spectra of sulfates formed in solfataric and aqueous acid sulfate environments and

applications to Mars. *Workshop on Martian Sulfates as Recorders of Atmospheric-Fluid-Rock Interactions,* #7037.

207. Clegg, S.M., Wiens, R.C., Dyar, M.D., Vaniman, D.T., Thompson, J.R. Sklute, E.C., and Barefield, J.E., and Maurice, S. (2006) Laser Induced Breakdown Spectroscopy (LIBS) remote detection of sulfates on Mars Science Laboratory Rover. *Workshop on Martian Sulfates as Recorders of Atmospheric-Fluid-Rock Interactions.*
208. Dyar, M.D., Podratz, L., Sklute, E.C., Rusu, C., Rothstein, Y., Tosca, N., Bishop, J.L., and Lane, M.D. (2006). Mössbauer spectroscopy of synthetic alunite group minerals. *Workshop on Martian Sulfates as Recorders of Atmospheric-Fluid-Rock Interactions,* #7053.
209. Sklute, E.C., Dyar, M.D., Bishop, J.L., Lane, M.D., King, P.L., and Cloutis, E. (2006) Mössbauer spectra of sulfates and applications to Mars. *Workshop on Martian Sulfates as Recorders of Atmospheric-Fluid-Rock Interactions,* #7057.
210. Greenwood, J.P., Gilmore, M.S., Martini, A.M., Blake, R.E., Dyar, M.D., Gilmore, J.A., and Varekamp, J. (2006) Martian and St. Lucian jarosite: What we can learn about Meridiani from an Earth analog. *Workshop on Martian Sulfates as Recorders of Atmospheric-Fluid-Rock Interactions*, #7050.
211. Dyar, M.D., Sklute, E.C., Schaefer, M.W., and Bishop, J.L. (2007) Mössbauer spectroscopy of clay minerals at variable temperatures. *Lunar Planet. Sci. XXXVIII.*, Lunar Planet. Inst., Houston, CD-ROM #2282 (abstr.).
212. Weins, R.C., Maurice, S., Clegg, S., Vaniman, D., Thompson, J., Dyar, M.D., Sklute, E.C., Newsom, H., Lanza, N., Sautter, V., Dubessy, J., Lacour, J.-L., Sallé, B., Mauchien, P., Blaney, D., Langevin, Y., Herkenhoff, K., Bridges, N., Manhes, G., and the ChemCam team. (2007) Preparation of onboard calibration targets for the ChemCam instruments on the Mars Science Laboratory rover. *Lunar Planet. Sci. XXXVIII.*, Lunar Planet. Inst., Houston, CD-ROM #1180 (abstr.).
213. Podratz, L.A., Gunter, M.E., Williams, T.J., Tosca, N., and Dyar, M.D. (2007) Refinement of the jarosite-alunite cell parameters as a function of compositional variance. *Lunar Planet. Sci. XXXVIII.*, Lunar Planet. Inst., Houston, CD-ROM #2274 (abstr.).
214. Lane, M.D., Dyar, M.D., and Bishop, J.L. (2007) Spectra of phosphate minerals as obtained by visible-near infrared reflectance, thermal infrared emission, and Mössbauer lab analyses. *Lunar Planet. Sci. XXXVIII.*, Lunar Planet. Inst., Houston, CD-ROM #2210 (abstr.).
215. Dyar, M.D., McCanta, M.C., Treiman, A.H., Sklute, E.C., and Marchand, G.J. (2007) Mössbauer spectroscopy and oxygen fugacity of amphibole-bearing R-chondrite LAP04840. *Lunar Planet. Sci. XXXVIII.*, Lunar Planet. Inst., Houston, CD-ROM #2047 (abstr.).
216. Bishop, J.L., Lane, M.D., Dyar, M.D., and Brown, A.J. (2007) Multi-spectral study of phyllosilicates and applications to Mars. *Lunar Planet. Sci. XXXVIII.*, Lunar Planet. Inst., Houston, CD-ROM #1815 (abstr.).
217. Klima, R.L., Pieters, C.M., and Dyar, M.D. (2007) VIS-NIR spectroscopy of synthetic pyroxenes: calcium-bearing pyroxenes and application to the HED meteorites. *Lunar Planet. Sci. XXXVIII.*, Lunar Planet. Inst., Houston, CD-ROM #1733 (abstr.).
218. Lane, M.D., Bishop, J.L., Dyar, M.D., Parente, M., King, P.L., and Hyde, B.C. (2007) Identifying the phosphate and ferric sulfate minerals in the Paso Robles soils (Gusev crater) using an integrated spectral approach. *Lunar Planet. Sci. XXXVIII.*, Lunar Planet. Inst., Houston, CD-ROM #2176 (abstr.).
219. Klima, R., Pieters, C.M., Sunshine, J., Hiroi, T., Bishop, J., Lane, M., Dyar, M.D., and Treiman, A.H. (2007) Coordinated spectroscopic and petrologic investigation of LAP04840: First results of infrared, thermal, and Raman spectroscopy. *Lunar Planet. Sci. XXXVIII.*, Lunar Planet. Inst., Houston, CD-ROM #1710 (abstr.).
220. Clegg, S.M., Weins, R.C., Dyar, M.D., Vaniman, D.T., Thompson, J.R., Sklute, E.C., Barefield, J.E., Sallé, B.,Sirven, J.-B., Mauchien, P., Lacour, J.-L., and Maurice, S. (2007) Sulfur geochemical analysis with remote laser-induced breakdown spectroscopy on the 2009 Mars Science Laboratory rover. *Lunar Planet. Sci. XXXVIII.*, Lunar Planet. Inst., Houston, CD-ROM #1960 (abstr.).
221. McCanta, M.C., Treiman, A.H., Alexander, C.M.O'D, and Dyar, M.D. (2007) Mineralogy and petrology of the amphibole-bearing R-Chondrite LAP04848. *Lunar Planet. Sci. XXXVIII.*, Lunar Planet. Inst., Houston, CD-ROM #2149 (abstr.).
222. Sklute, E.C., Dyar, M.D., Clegg, S.M., Wiens, R.C., and Barefield, J.E. (2007) Laser-induced breakdown spectroscopy of samples with variable composition. *Lunar Planet. Sci. XXXVIII.*, Lunar Planet. Inst., Houston, CD-ROM #1949 (abstr.).

223. Nzokwe, G.Y., Ferré, E.C., Fifarek, R., Banerjee, S.K., Dyar, M. D., Hamilton, V.E., Maurizot, P. and Tessarolo, C. (2007) Laterites developed on a peridotitic bedrock and magnetic similitudes with Martian regoliths.
224. Dyar, M.D., Sklute, E.C., Schaefer, M.W., and Bishop, J.L. (2007) Mössbauer spectroscopy of phyllosilicates: dependence of recoil-free fractions and %Fe^{3+} on lineshape models. *Clay Mins. Soc., 44th Ann. Mtng.*, Sante Fe, NM.
225. Clegg, S.M., Sklute, E.C., Dyar, M.D., Barefield, J.E., and Wiens, R.C. (2007) Quantitative analysis of samples with variable composition by remote laser-induced breakdown spectroscopy. *7th Mars Conference*, Pasadena, CA.
226. Lane, M.D., Bishop, J.L., Dyar, M.D., Parente, M., King, P.L., and Hyde, B.C. (2007) The ferric sulfate and ferric phosphate minerals in the light-toned Paso Robles rover track soils: A multi-instrument analysis. *7th Mars Conference*, Pasadena, CA.
227. Belley, F., Ferré, E.C., Martín-Hernández, F., Jackson, M.J., Dyar, M.D., and Catlos, E.J. (2007) Compositional, thermal, and orientation dependency of olivine magnetic properties. *EOS Trans. AGU*, 88(23) Jt. Assem. Suppl. Abstract GP21A-13.
228. Pieters, C.M., Klima, R.L., Hiroi, T., Dyar, M.D., Lane, M.D., Treiman, A.H., Noble, S.K., Sunshine, J.M., and Bishop, J.L. (2007) The origin of brown olivine in Martian dunite NWA 2737. *Met. Soc*.
229. Lane, M.D., and Dyar, M.D. (2007) Thermal emission spectroscopy of synthetic olivines: Fayalite to forsterite. *Met. Soc.*, abst. #5136.
230. Váczi, T., Nasdala, L., Kronz, A., Götze, J., Dyar, M.D., Hanchar, J.M., and Wildner, M. (2007) The location and valence of Fe in iron-doped zircon. *Austrian Mineralogical Society.*
231. Wiens, R.C., Clegg, S., Barefield, J. II., Vaniman, D., Lanza, N., Newsom, H., Herkenhoff, K., Bridges, N., Blaney, D., Maurice, S., Gasnault, O., Blank, J., Dyar, M.D., Milliken, R., Grotzinger, J., Crisp, J., and the ChemCam and MSL teams (2008) ChemCam remote analyses and imaging on the Mars Science Laboratory 2007 slow motion field test. *Lunar Planet. Sci. XXXIX,* Lunar Planet. Inst., Houston, CD-ROM #1500 (abstr.).
232. Dyar, M.D., Klima, R.L., and Pieters, C.M. (2008) Reflectance and Mössbauer spectroscopy of synthetic pyroxenes: I. Implications for interpreting cooling rates of remote-sense surfaces. *Lunar Planet. Sci. XXXIX,* Lunar Planet. Inst., Houston, CD-ROM #22248 (abstr.).
233. Klima, R.L., Dyar, M.D., and Pieters, C.M. (2008) Reflectance and Mössbauer spectroscopy of synthetic pyroxenes: II. Characterizing the cooling histories of HEDs using reflectance spectroscopy. *Lunar Planet. Sci. XXXIX,* Lunar Planet. Inst., Houston, CD-ROM #2289 (abstr.).
234. Elkinton, H., Jones, J.H., and Dyar, M.D. (2008) Differentiation of the HED parent body and an evaluation of the MELTS computational program. *Lunar Planet. Sci. XXXIX,* Lunar Planet. Inst., Houston, CD-ROM #2093 (abstr.).
235. Dyar, M.D., Clegg, S.M., Barefield, J.E. II, Wiens, R.C., Sklute, E.C., and Schaefer, M.W. (2008) Approaches to matrix-effect corrections in laser-induced breakdown spectroscopy of geologic samples. *Lunar Planet. Sci. XXXIX,* Lunar Planet. Inst., Houston, CD-ROM #2146 (abstr.).
236. Schaefer, M.W., Dyar, M.D., Clegg, S.M., and Wiens, R.C. (2008) An IDL routine for preprocessing and analysis of LIBS data. *Lunar Planet. Sci. XXXIX,* Lunar Planet. Inst., Houston, CD-ROM #2171 (abstr.).
237. Clegg, S.M., Wiens, R.C., Barefield, J.E. II., Dyar, M.D., Delaney, J.S., Ashley, G.M., and Driese, S.G. (2008) Simulated ChemCam laboratory investigations of East African Rift sedimentary samples. *Lunar Planet. Sci. XXXIX*, Lunar Planet. Inst., Houston, CD-ROM #2107 (abstr.).
238. Burbine, T.H., Dyar, M.D., and Hamilton, C.M. (2008) Integrating a planetary science curriculum into geology and astronomy curricula. *Lunar Planet. Sci. XXXIX*, Lunar Planet. Inst., Houston, CD-ROM #2274 (abstr.).
239. Bishop, J.L., Garcia, N., Dyar, M.D., Parente, M., Murad, E., Mancinelli, R.L., Drief, A., Lane, M.D. (2008) Maghemite as an astrobiology indicator on the Martian surface: Reduction of iron oxides by early organic compounds to generate magnetic phases. *Geophysical Research Abstracts*, 10.
240. Bishop, J.L., Alpers, C.N., Coleman, M.L., Sobron, P., Lane, M.D., Dyar, M.D., and Schiffman, P. (2008) Sulfates on Mars: Comparisons with spectra properties of analog sites. 17th Goldschmidt Conf.
241. Bishop, J.L., Lane, M.D., Dyar, M.D., Parente, M., Roach, L.H., Murchie, S., and Mustard, J.F.(2008) Sulfates on Mars: How Recent discoveries from CRSM, OMEGA and the MERs are changing our view of the planet. 17th Goldschmidt Conf., #18D-1678.

242. Alpers, C.N., Majzlan, J., Bender Koch, C., Bishop, J.L., Coleman, M.L., Dyar, M.D., Mcclesky, R.B. , Myneni, S.C.B. , Nordstrom, D.K., and Sobron, P. (2008) Chemistry and spectroscopy of iron-sulfate minerals from Iron Mountain, California, U.S.A. 17th Goldschmidt Conf., p. A17.
243. King P.L., Lane M.D., Hyde B.C., Dyar M.D., Bishop J.L. (2008) Fe-Sulfates on Mars: Considerations for Martian Environmental Conditions, Mars Sample Return and Hazards. Ground Truth From Mars: Science Payoff from a Sample Return Mission, LPI, #4017.
244. Van Alboom, A., De Resende, V.G., De Grave, E., Dyar, M.D., and Gómez, J.A. (2008) Low temperature Mössbauer spectra of rozenite and szomolnokite. EUCMOS 2008.
245. Gunter, M.E., and Dyar, M.D. (2008) Teaching Mineralogy to Earth Scientists Using Spiral Learning and Computer Animations. GSA National Meeting, Denver, Abstr. #221-13.
246. Klima, R., Pieters, C.M., and Dyar, M.D. (2008) Integrated spectroscopy of pyroxenes: pushing Remote Geochemical Analyses Further. GSA National Meeting, Denver, Abstr. #293-5.
247. Keskula, A., Seaman, S., and Dyar, M.D. (2008) Volatile Evolution in Silicic Magmas of Torfajökull Volcano, as Determined by FTIR Micro-Spectroscopy. GSA National Meeting, Denver, Abstr. #331-11.
248. Dyar, M.D., Schaefer, M.W., Clegg, S., Wiens, R., Tucker, J., and Barefield, J.E.II. (2008) Comparisons among calibration strategies for LIBS spectroscopy on Mars. Abstr. #08-RC-67-AAS-DPS. *Workshop on Martian Phyllosilicates: Recorders of Aqueous Processes?*
249. Tucker, J.M., Dyar, M.D., Clegg, S.M., Wiens, R.C., Barefield, J.E.II., Schaefer, M.W., and Bishop, J.L. (2008) Quantitative chemistry of phyllosilicate minerals using laser-induced breakdown spectroscopy. *Workshop on Martian Phyllosilicates: Recorders of Aqueous Processes?* Abstr. 7028.
250. Dyar, M.D., Schaefer, M.W., Clegg, S., Wiens, R., Tucker, J., and Barefield, J.E. II. (2008) Comparisons among calibration strategies for LIBS Spectroscopy on Mars, *DPS*, abstr. #32.14.
251. Belley, F., Ferre, E.C., Martin-Hernandez, F., Jackson, M.J., Dyar, M.D., Catlos, E J. (2008) Fe-Ti oxide inclusions in natural and synthetic $(Fe_x, Mg_{1-x})_2 SiO_4$ olivines. *EOS Trans. AGU*, 89(23) Jt. Assem. Suppl. Abstract GP31B-0080.
252. Bishop, J.L., Parente, M., Lane, M.D., Dyar, M.D., Bish, D.L., Sarrazin, P., King,P.L., McKeown, N., Milliken, R., Roach, L., Swayze, G., Weitz, C., Murchie, S., and Mustard, J.F. (2008) Coordinating CRISM observations of sulfates near Valles Marineris with the subsurface bright salty soils exposed in Gusev Crater via lab experiments. *EOS Trans. AGU*, 89(23) Jt. Assem. Suppl. Abstract P43B-1397.
253. Lane, M.D., Bishop, J.L., Dyar, M.D., King, P.L., and Hyde, B.C. (2008) Iron sulfate and sulfide spectroscopy at thermal infrared wavelengths for application to Mars. *EOS Trans. AGU*, 89(23) Jt. Assem. Suppl. Abstract P43B-1398.
254. Dyar, M.D., Tucker, J.M., Clegg, S.M., Barefield, J.E., and Wiens, R.C. (2008) Quantitative sulfur analysis using stand-off Laser-Induced Breakdown Spectroscopy. *EOS Trans. AGU*, 89(23) Jt. Assem. Suppl. Abstract P43B-1399.
255. Knutson, J., Dyar, M.D., Sklute, E.C., Lane, M.D., Bishop, J.L. (2008) Using crystal structure groups to understand Mössbauer parameters of ferric sulfates. *EOS Trans. AGU*, 89(23) Jt. Assem. Suppl. Abstract P43B-1403.
256. Tucker, J.M., Dyar, M.D., Schaefer, M.W., Clegg, S.M., Barefield, J.E., Wiens, R.C., and Bishop, J.L. (2008) Laser-induced breakdown spectroscopy of phyllosilicates for ChemCam calibration. *EOS Trans. AGU*, 89(23) Jt. Assem. Suppl. Abstract P53A-1429.
257. Dyar, M.D., Henry, D., and Guidotti, C.V. (2009) Systematics of major element partitioning among graphitic metapelites from western Maine. GSA Abstracts with Programs, Vol. 41, No. 3.
258. Lane, M.D., Glotch, T.D., Dyar, M.D., Bishop, J.L., Pieters, C.M., Klima, R., Hiroi, T., and Sunshine, J.M. (2009) Thermal infrared spectroscopy of a synthetic olivine series (forsterite-fayalite) and interpretation of the Nili Fossae, Syrtis Major, and Isidis regions. *Lunar Planet. Sci. XXXX*, Lunar Planet. Inst., Houston, CD-ROM #2469 (abstr.).
259. Hibbits, C.A., Dyar, M.D., Orlando, T.M., Grieves, G., and Szanyi, J. (2009) Cold trapping of volatiles in the lunar regolith. *Lunar Planet. Sci. XXXX*, Lunar Planet. Inst., Houston, CD-ROM #1926 (abstr.).
260. Bishop, J.L., Dyar, M.D., Majzlan, J., and Lane, M.D. (2009) Spectral properties of copiapites with variable cation compositions and implications for characterization of copiapite on Mars. *Lunar Planet. Sci. XXXX*, Lunar Planet. Inst., Houston, CD-ROM #2073 (abstr.).
261. Dyar, M.D., Holden, J.F., Bishop, J.L., and Lane, M.D. (2009) Spectroscopic characterization of hydrothermal sulfide chimneys at the Juan de Fuca ridge. *Lunar Planet. Sci. XXXX*, Lunar Planet. Inst., Houston, CD-ROM #2221 (abstr.).

262. Dyar, M.D., Sklute, E.C., Bishop, J.L., Murad, E., and Muirhead, A.C. (2009) Mössbauer and reflectance spectroscopy of iron oxide mixtures. *Lunar Planet. Sci. XXXX*, Lunar Planet. Inst., Houston, CD-ROM #2209 (abstr.).
263. Klima, R.L., Pieters, C.M., and Dyar, M.D. (2009) Pyroxene spectroscopy: Probing composition and thermal history of the lunar surface. *Lunar Planet. Sci. XXXX*, Lunar Planet. Inst., Houston, CD-ROM #2155 (abstr.).
264. Cheek, L.C., Pieters, C.M., Dyar, M.D., and Milam, K.A. (2009) Revisiting plagioclase optical properties for lunar exploration. *Lunar Planet. Sci. XXXX*, Lunar Planet. Inst., Houston, CD-ROM #1928 (abstr.).
265. Sharma, S.K., Misra, A.K., Clegg, S.M., Barefield, J.E. II., Wiens, R.C., Quick, C.R., Dyar, M.D., McCanta, M.C., and Elkins-Tanton, L. (2009) Venus Geochemical Analysis by Remote Raman — Laser Induced Breakdown Spectroscopy (Raman-LIBS*) Lunar Planet. Sci. XXXX*, Lunar Planet. Inst., Houston, CD-ROM #2548 (abstr.).
266. Wiens, R.C., Clegg, S., Bender, S., Lanza, N., Barrachough, B., Perez, R., Maurice, S., Dyar, M.D., Newsom, H., and the Chemcam Team (2009) Initial calibration of the ChemCam LIBS instrument for the Mars Science Laboratory (MSL) rover. *Lunar Planet. Sci. XXXX*, Lunar Planet. Inst., Houston, CD-ROM #1461 (abstr.).
267. Tucker, J.M., Dyar, M.D., Clegg, S.M., Schaefer, M.W., Wiens, R.C., and Barefield, J.E. II. (2009) LIBS analysis of minor elements in geologic samples. *Lunar Planet. Sci. XXXX*, Lunar Planet. Inst., Houston, CD-ROM #2024 (abstr.).
268. Clegg, S.M., Barefield, J.E. II., Wiens, R.C., Quick, C.R., Sharma, S.K., Misra, A.K., Dyar, M.D., McCanta, M.C., and Elkins-Tanton, L. (2009) Venus Geochemical Analysis by Remote Raman — Laser Induced Breakdown Spectroscopy (Raman-LIBS*) Venus Geochemistry: Progress, Prospects, and New Missions*, Houston, CD-ROM #2013 (abstr.).
269. Van Alboom, A., de Resende, V.G., De Grave, E., and Dyar, M.D. (2009) Hyperfine interactions in rozenite. *ICAME* 2009.
270. Dyar M. D., Hiroi T., Glotch T., Lane M. D., Wopenka B., Klima R., Bishop J. L., Pieters C., Sunshine J., Marchand G. J. and Seaman S. J. (2009) Reflectance, Transmission, Emission, Raman, and Mössbauer Spectroscopy of Yamato 984028. *32nd Symposium on Antarctic Meteorites*.
271. Dyar, M.D., Tucker, J.M., Clegg, S.M., Schaefer, M.W., Wiens, R.C., and Barefield, J.E. II (2009) Probing Martian surface chemistry with LIBS: Major and minor element analyses with Laser-Induced Breakdown Spectroscopy. *New Martian Chemistry Workshop*, Abstract #8019.
272. McCord, T.B., Taylor, L.A., Orlando, T.M., Clark, R.N., Pieters, C.M., Combe, J.P., Kramer, G.Y., Sunshine, J.M., Dyar, M.D., and Hibbitts, C. (2009) Interpretations of OH/HOH IR absorptions on the Moon from Chandrayaan-1 Moon Mineralogy Mapper. *EOS Trans. AGU*, P34A-04, Jt. Assem. Suppl. Abstract.
273. Green, R.O., Pieters, C.M., Goswami, J., Clark, R.N., Annadurai, M., Boardman, J.W., Buratti, B.J., Combe, J.P., Dyar, M.D., Head, J.W., Hibbitts, C., Hicks, M., Isaacson, P., Klima, R.L., Kramer, G.Y., Kumar, S., Livo, K.E., Lundeen, S., Malaret, E., McCord, T.B., Mustard, J.F., Nettles, J.W., Petro, N.E., Runyon, C.J., Staid, M., Sunshine, J.M., Taylor, L.A., Tompkins, S., and Varanasi, P. (2009) Spectroscopic character and spatial distribution of hydroxyl and water absorption features measured on the lunar surface by the Moon Mineralogy Mapper imaging spectrometer on Chandrayaan-1. *EOS Trans. AGU*, P34A-02, Jt. Assem. Suppl. Abstract.
274. Lane, M.D., Glotch, T.D., Dyar, M.D., Pieters, C.M., Klima, R., Hiroi, T., Bishop, J.L., and Sunshine, J.M. (2009) Midinfrared multi-technique spectroscopy of synthetic olivines (forsterite to fayalite). *EOS Trans. AGU*, P23A-1232, Jt. Assem. Suppl. Abstract.
275. Clegg, S.M., Barefield, J.E., Humphries, S., Wiens, R.C., Vaniman, D., Dyar, M.D., Tucker, J.M., Sharma, S.K., and Misra, A.K. (2009) Remote Laser Induced Breakdown Spectroscopy (LIBS) geochemical investigation under Venus atmospheric conditions. *EOS Trans. AGU*, P31D-07, Jt. Assem. Suppl. Abstract.
276. Dyar, M.D., Hibbitts, C., Liu, Y., Taylor, L.A., Rossman, G.R., Orlando, T.M., Seaman, S.J., Tucker, J.M., and Pieters, C.M. (2009) Mechanisms for incorporation of hydrogen in and on the lunar surface. *EOS Trans. AGU*, P33D-07, Jt. Assem. Suppl. Abstract.
277. Tucker, J.M., Dyar, M.D., Gunter, M., Delaney, J.S., and Lanzirotti, A. (2009) High-resolution Fe XANES pre-edge spectroscopy of micas. *EOS Trans. AGU,* MR13A-1654, Jt. Assem. Suppl. Abstract.
278. Lambert, J., Morookian, J., Roberts, T. Polk, J., Smerkar, S., Clegg, S.M., Wiens, R.C., Dyar, M.D., and Treiman, A. (2010) Standoff LIBS and Raman spectroscopy under Venus conditions. *Lunar Planet. Sci. XXXXI*, Lunar Planet. Inst., Houston, CD-ROM #2608 (abstr.).

279. Wiens, R.C., Clegg, S. M., Bender, S., Lanza, N., Barraclough, B., Perez, R., Forni, O., Maurice, S., Dyar, M.D., Newson, H. and the ChemCam team. Progress on calibration of the ChemCam instrument for the Mars Science Laboratory (MSL) rover. *Lunar Planet. Sci. XXXXI*, Lunar Planet. Inst., Houston, CD-ROM #2205 (abstr.).
280. Moriarity, D., Hibbitts, C.A., Dyar, M.D., Harlow, G., Ebel, D., and Lisse, C. (2010) near-Far IR spectra of sulfide minerals relevant to comets. *Lunar Planet. Sci. XXXXI*, Lunar Planet. Inst., Houston, CD-ROM #2447 (abstr.).
281. Hibbitts, C.A., Dyar, M.D., Orlando, T.M., Grieves, G., Moriarity, D., Poston, M., and Johnson, A. (2010) Thermal stability of water and hydroxyl on airless bodies. *Lunar Planet. Sci. XXXXI*, Lunar Planet. Inst., Houston, CD-ROM #2417 (abstr.).
282. Tucker, J.M., Dyar, M.D., Schaefer, M.W., Clegg, S. M., and Wiens, R.C. (2010) Multivariate LIBS analysis of geologic materials. *Lunar Planet. Sci. XXXX*, Lunar Planet. Inst., Houston, CD-ROM #1970 (abstr.).
283. Grieves, G. Hibbitts, C.A., Dyar, M.D., Orlando, T.M., Poston, M., and Johnson, A. (2010) Mobility and subsurface redistribution of volatiles through regolith dust. *Lunar Planet. Sci. XXXXI*, Lunar Planet. Inst., Houston, CD-ROM # (abstr.).
284. Dyar, M.D., Hibbitts, C.A., and Orlando, T.M. (2010) Mechanisms for incorporation of hydrogen in or on terrestrial planetary surfaces. *Lunar Planet. Sci. XXXXI*, Lunar Planet. Inst., Houston, CD-ROM #2116 (abstr.).
285. Dyar, M.D., Lane, M.D., Glotch, T., Hiroi, T., Wopenka, B., Klima, R., Bishop, J.L., Pieters, C., Sunshine, J., Marchand, G.J., and Seaman, S.J. (2010) Spectroscopy of Yamato 984028. *Lunar Planet. Sci. XXXXI*, Lunar Planet. Inst., Houston, CD-ROM #1831 (abstr.).
286. Clegg, S.M., Barefield, J.E., Wiens, R.C., Sharma, S.K., Misra, A.K., Tucker, J., Dyar, M.D., Lambert, J., Smrekar, S., and Treiman, A. (2010) Venus geochemical analysis by remote Laser-Induced Breakdown Spectroscopy (LIBS). *Lunar Planet. Sci. XXXXI*, Lunar Planet. Inst., Houston, CD-ROM #1631 (abstr.).
287. Barbieri, L., Dickson, J.L., Head, J.W., and Dyar, M.D. (2010) Deciphering Late-Amazonian climate change on Mars: Evidence for episodic gully activity preserved in gully fan stratigraphy. *Lunar Planet. Sci. XXXXI*, Lunar Planet. Inst., Houston, CD-ROM #2745 (abstr.).
288. Dyar, M.D., Tucker, J.M., Gunter, M.E., and Lanzirotti, A. (2010) Iron redox in fibers and fragments of Libby, Montana asbestos. *45th Ann. GSA NE Section Mtng.*, Abstr. #169670.
289. Reynolds, V.S., Crapster-Pregont, E.J., Dyar, M.D., Jawin, E., McDonough, W.F., Qui, L., and Rumble, D. (2010) Lithium and oyxgen isotopes and oxidation state of lower oceanic crust: Atlantic Massif, 30° N. *Goldschmidt Conf. 2010*, Abstract #3044.
290. Hyde, B.C., King, P.L., Dyar, M.D., Splide, M.N., Ali, A.-M., and Atudorei, N.V. (2010) Hydrated and hydrous iron sulfate synthesis and analysis on the bulk and micro-scales. *GSA Ann. Mtng.,* Abstract #262-4.
291. Schoonen, M.A.A., DeCesare, M.R., Murphy, R.T., Strongin, D.R., and Dyar, M.D. (2010) Influence of H_2S and SO_2 in CO_2 fluid reactivity of sandstone under near-field and far-field conditions. *GSA Ann. Mtng.*, Abstract #137-10.
292. Dyar, M.D., Peel, S.E., and Klima, R.L. (2010) Relationships between crystal structure and NIR spectroscopy of synthetic pyroxenes. *GSA Ann. Mtng.*, Abstract #213-15.
293. Clegg, S.M., Barefield, J.E., Humphires, S.D., Wiens, R.C., Vaniman, D.T., Sharma, S.K., Misra, A.K., Dyar, M.D., and Smerkar, S.E. (2010) Remote Raman – laser-induced breakdown spectroscopy (LIBS) geochemical investigation under Venus atmospheric conditions. *EOS Trans. AGU*, P44A-07.
294. Orlando, T.M., McLain, J., Poston, M., Grieves, G., Alexandrov, A., Dyar, M.D., and Hibbittts, C.(2010) Probing adsorbed water on lunar regolith materials using thermal and non-thermal desorption. *EOS Trans. AGU*, P13E-02.
295. Holden, J.F., Ver Eecke, H.C., Lin, T.J., Butterfield, D.A., Olson, E.J., Jamieson, J., Knutson, J.K., and Dyar, M.D. (2010) Modeling the growth and constraints of thermophiles and biogeochemical processes in deep-sea hydrothermal environments. *EOS Trans. AGU*, OS14A-01.
296. Dyar, M.D., Tucker, J.M., Humphries, S., Clegg, S.M., Wiens, R.C., and Carmosino, M.L. (2010) Geochemical predictions of elemental compositions using remote LIBS under Mars conditions. *EOS Trans. AGU*, P54A-07.
297. Tucker, J.M., Dyar, M.D., Humphries, S., Clegg, S.M., Wiens, R.C., and Lane, M.D. (2010) Strategies for Mars remote laser-induced breakdown spectroscopy analysis of sulfur in geological samples. *EOS Trans. AGU*, P11C-1349.

298. Sharma, S.K., Misra, A.K., Acosta, T.E., Dyar, M.D., Speicher, E.A., Clegg, S.M., Wiens, R.C., and Treiman, A.H. (2011) Raman spectroscopy of low concentration of minerals in basaltic glass analog matric applicable to planetary exploration. *Lunar Planet. Sci. XLII*, Lunar Planet. Inst., Houston, CD-ROM #1250 (abstr.).
299. Dyar, M.D., Carmosino, M.L., Tucker, J.M., Speicher, E.A., Brown, E.B., Clegg, S.M., Wiens, R.C., Barefield, J.E., Delaney, J.S., Ashley, G.M., and Driese, S.G. (2011) Error analysis for remote laser-induced breakdown spectroscopy analysis using combinations of igneous, sedimentary, and phyllosilicate samples. *Lunar Planet. Sci. XLII*, Lunar Planet. Inst., Houston, CD-ROM #1258 (abstr.).
300. Jawin, E.R., Dyar, M.D., Lane, M.D., Bishop, J.L., and Marchand, G.J. (2011) Inter-relationships among Mössbauer parameters of phosphate minerals and crystal structures. *Lunar Planet. Sci. XLII*, Lunar Planet. Inst., Houston, CD-ROM #1259 (abstr.).
301. Lane, M.D., Mertzman, S.A., Dyar, M.D., and Bishop, J.L. (2011) Phosphate minerals measured in the visible-near infrared and thermal infrared: spectra and XRD analyses. *Lunar Planet. Sci. XLII*, Lunar Planet. Inst., Houston, CD-ROM #1013 (abstr.).
302. Bell, S.W., Thomson, B. J., Dyar, M.D., and Bussey, D.B.J. (2011) Dating fresh lunar craters with Mini-RF. *Lunar Planet. Sci. XLII*, Lunar Planet. Inst., Houston, CD-ROM #1342 (abstr.).
303. Carmosino, M.L., Bender, S., Speicher, E.A., Dyar, M.D., Clegg, S.M., and Wiens, R.C. (2011) End-to-end models for effects of system noise on LIBS analyses of igneous rocks. *Lunar Planet. Sci. XLII*, Lunar Planet. Inst., Houston, CD-ROM #1739 (abstr.).
304. Dyar, M.D., Sklute, E.C., Knutson, J.K., Glotch, T.D., Che, C., Zelin, S.L., Lin, J., and Holden, J.F. (2011) Spectroscopy of mineral reaction products form bioreduction by hyperthermophiles: Potential for remote sensing biomarkers. *Lunar Planet. Sci. XLII*, Lunar Planet. Inst., Houston, CD-ROM #1375 (abstr.).
305. Cheek, L.C., Pieters, C.M., Parman, S.W., Dyar, M.D., and Speicher, E.A. (2011) First look at spectral characteristics of plagioclase with variable iron content: Applications to remote sensing of the lunar crust. *Lunar Planet. Sci. XLII*, Lunar Planet. Inst., Houston, CD-ROM #1617 (abstr.).
306. Poston, M.J. Aleksandrov, A.B., Grieves, G.A., Hibbitts, C.A., Dyar, M.D., and Orlando, T.M. (2011) Thermal desorption properties of water and hydroxyl adsorbed on micronized lunar surrogates JSC-1A and albite. *Lunar Planet. Sci. XLII*, Lunar Planet. Inst., Houston, CD-ROM #2189 (abstr.).
307. Aveline, D.C., Abbey, W.J., Choukroun, M., Treiman, A.H., Dyar, M.D., Smrekar, S.E., and Feldman, S.M. (2011) Rock and mineral weathering experiments under model Venus conditions. *Lunar Planet. Sci. XLII*, Lunar Planet. Inst., Houston, CD-ROM #2165 (abstr.).
308. McCanta, M.C., Dyar, M.D., Elkins-Tanton, L.T., and Treiman, A.H. (2011) Weathering of Hawaiian basalts under sulfur-rich conditions: applications to understanding surface-atmosphere interactions on Venus. *Lunar Planet. Sci. XLII*, Lunar Planet. Inst., Houston, CD-ROM #1396 (abstr.).
309. Clegg, S.M., Sharma, S.K., Misra, A.K., Dyar, M.D., Hecht, M., Lambert, J., Feldman, S., Dallmann, N., Wiens, R.C., Humphries, S.D., Vaniman, D.T., Speicher, E.A., Carmosino, M.L., Smrekar, S., Treiman, A., Wang, A., Maurice, S., and Esposito, L. (2011) Remote Raman-laser-induced breakdown spectroscopy (LIBS) geochemical investigation under Venus atmospheric conditions. *Lunar Planet. Sci. XLII*, Lunar Planet. Inst., Houston, CD-ROM #1568 (abstr.).
310. Klima, R.L., Dyar, M.D., and Peel, S.E. (2011) Spectral modeling and crystallographic parameters of Al and Ti-rich pyroxenes. *Lunar Planet. Sci. XLII*, Lunar Planet. Inst., Houston, CD-ROM #2181 (abstr.).
311. Peel, S.E., Dyar, M.D. Klima, R.L., and Fleagle, A.L. (2011) Crystal structure parameters as predictors of VNIR spectroscopy of synthetic pyroxenes. *Lunar Planet. Sci. XLII*, Lunar Planet. Inst., Houston, CD-ROM #1394 (abstr.).
312. Speicher, E.A., Dyar, M.D., Carmosino, M.L., Tucker, J.M., Clegg, S.M., and Wiens, R.C. (2011) Single variable and multivariate analyses of remote laser-induced breakdown spectra for predictions of Rb, Sr, Cr, Ba, S, and V in igneous rocks. *Lunar Planet. Sci. XLII*, Lunar Planet. Inst., Houston, CD-ROM #2385 (abstr.).
313. Speicher, E.A., Dyar, M.D., Gunter, M.E., Lanzirotti, A., Tucker, J.M., Peel, S.E., Brown, E.B., and Delaney, J.S. (2011) Synchrotron micro-XANES analysis of Fe^{3+} in oriented amphiboles. *Lunar Planet. Sci. XLII*, Lunar Planet. Inst., Houston, CD-ROM #2287 (abstr.).
314. Greenberger, R.N., Mustard, J.F., Kumar, P.S., Dyar, M.D., Speicher, E.A., and Sklute, E. C. (2011) Weathering products of Deccan basalts and implications for Mars. *Lunar Planet. Sci. XLII*, Lunar Planet. Inst., Houston, CD-ROM #2548 (abstr.).

315. Greenwood, J.P., Itoh, S., Sakamoto, N., Warren, P.H., Dyar, M.D., and Yurimoto, H. (2011) Origin of lunar water and evidence for a wet Moon from D/H and water in lunar apatites. *Lunar Planet. Sci. XLII*, Lunar Planet. Inst., Houston, CD-ROM #2753 (abstr.).
316. Perry, K.A., Bishop, J.L., Dyar, M.D., Blake, D.F., Peel, S., and Brown, A.J. (2011) Spectral analysis of nontronite-magnesite-olivine mixtures and implications for carbonates on Mars. . *Lunar Planet. Sci. XLII*, Lunar Planet. Inst., Houston, CD-ROM #1554 (abstr.).
317. Dyar, M.D., Carmosino, M.L., Speicher, E.A., Clegg, S.M., and Wiens, R.C. (2011) Effects of training set selection on quantitative LIBS analyses of geological samples. 3rd North American Symposium on Laser-Induced Breakdown Spectroscopy, Clearwater Beach, FL, July 2011.
318. Carmosino, M.L., Dyar, M.D., Speicher, E.A., Clegg, S.M., and Wiens, R.C. (2011) Binary classification for empirical description of quantification limits in LIBS instruments. 3rd North American Symposium on Laser-Induced Breakdown Spectroscopy, Clearwater Beach, FL, July 2011, P02.
319. Speicher, E.A., Dyar, M.D., Carmosino, M.L., Clegg, S.M., and Wiens, R.C. (2011) Univariate and multivariate analyses of remote laser-induced breakdown spectra from prediction of trace Cr, Rb, and Sr in igneous rocks under Mars atmospheric conditions. 3rd North American Symposium on Laser-Induced Breakdown Spectroscopy, Clearwater Beach, FL, July 2011.
320. Hibbitts, C.A., Dyar, M.D/., Orlando, T., Grieves, G., and Poston, M. (2011) Why there is water on the Moon but apparently none on main-belt basaltic asteroids? EPS-DPS Joint Meeting 2011, EPSC-DPS2011-1668.
321. Dyar, M.D., Carmosino, M.L., Speicher, E.A., Ozanne, M.V., Clegg, S.M., and Wiens, R.C. (2011) Approaches to calibration of quantitative elemental analysis with laser-induced breakdown spectroscopy (LIBS). *GSA Ann. Mtng.*, 43, 234.
322. Dyar, M.D., Nelms, M., Speicher, E.A., Ozanne, M.V., Gunter, M.E., and Lanzirotti, A. (2011) Multivariate analysis of XANES spectra for measurement of ferric iron in garnets, amphiboles, micas, and glasses. *GSA Ann. Mtng.*, 43, 232.
323. Greenberger, R.N., Mustard, J.T., Kumar, P.S., Dyar, M.D., Speicher, E.A., and Sklute, E.C. (2011) A vertical section of Deccan basalts as a spectroscopic and mineral assemblage analog to phyllosilicate stratigraphies on Mars. *GSA Ann. Mtng.*, 43, 267.
324. Shank, E.M., Klima, R.L., and Dyar, M.D. (2011) Characterizing pyroxene cooling rate using reflectance spectra. *EOS Trans. AGU*, P43A-1657.
325. Poston, M.J., Grieves, G.A., Aleksandrov, A.B., Hibbitts, C.A., Dyar, M.D., Johnson, M.A,m McLain, J., and Orlando, T.M. (2011) Water interactions with micronized lunar surrogates and application to behavior of water on the Moon. *EOS Trans. AGU*, P13D-1729.
326. Dyar, M.D., Hibbitts, C.A., Orlando, T.M., Poston, M.J., and Grieves, G.A. (2011) Effects of crystallinity, composition, and texture on hydrogen solubility and adsorption in lunar surface materials and their relevance to remote sensing. *EOS Trans. AGU*, P13C-06.
327. Hibbitts, C.A., Orlando, T.M., Dyar, M.D., Grieves, G.A., Poston, M.J., and McLain, J. (2011) Review of laboratory and modeling efforts to understand and predict the evolution of water and hydroxyl on the Moon. *EOS Trans. AGU*, P13H-02.
328. Lane, M.D., Bishop, J.L., and Dyar, M.D. (2011) Iron sulfates measured using thermal infrared emission and visible-near infrared reflectance spectroscopy. *EOS Trans. AGU*, P23B-1709.
329. Farrell, W.M., Bussey, B., Collier, M.R., Delory, G.T., Dyar, M.D., Elphic, R.C., Halekas, J.S., Hibbitts, C., Hodges, R.R., Hurley, D.M., Grieves, G.A., Keller, J.W., Killen, R.M., Marshall, J.R., Orlando, T.M., Saranto, M., and Stubbs, T.J. (2011) Solar wind manufacturing of water on the Moon: An ongoing NLSI discussion. *EOS Trans. AGU*, P13H-05.
330. Jawin, E.R., Kiefer, W.S., Bussey, B., Cahill, J.T., Dyar, M.D., Fassett, C.I., and Spudis, P.D. (2012) Analyzing the evolution of surface roughness of lunar mare. *Lunar Planet. Sci. XLIII*, Lunar Planet. Inst., Houston, CD-ROM #1343 (abstr.).
331. Jawin, E.R., Kiefer, W.S., Bussey, B., Cahill, J.T., Dyar, M.D., Fassett, C.I., Lawrence, S., and Spudis, P.D. (2012) The relationship between radar scattering and surface roughness of lunar volcanic domes. *Lunar Planet. Sci. XLIII*, Lunar Planet. Inst., Houston, CD-ROM #1333 (abstr.).
332. Newson, H.E., Blaney, D., Wiens, R.C., Clegg, S., Lanza, N., Vaniman, D., Maurice, S., Gasnault, O., King, P., Bridges, N., Dyar, M.D., Melikechi, N., Blank, J.G., Cousin, A., Ollila, A., Baxter, A., Vasavada, A., Mangold, N., Le Mouelic, S., and the ChemCam Team (2012) Operational strategies for the ChemCam experiment on MSL. *Lunar Planet. Sci. XLIII*, Lunar Planet. Inst., Houston, CD-ROM #2477 (abstr.).

333. Sharp, T.G., Michalski, J.R., Dyar, M.D., Bish, D.L., Friedlander, L.R., and Glotch, T. (2012) Effects of shock metamorphisms on phyllosilicate structures and spectroscopy. *Lunar Planet. Sci. XLIII*, Lunar Planet. Inst., Houston, CD-ROM #XXXX (abstr.).
334. Ozanne, M.V., Dyar, M.D., Carmosino, M.L., Breves, E.A., Clegg, S.M., and Wiens, R.C. (2012) Comparison of lasso and elastic net regression for major element analysis of rocks using laser-indeuced breakdown spectroscopy (LIBS). *Lunar Planet. Sci. XLIII*, Lunar Planet. Inst., Houston, CD-ROM #2391 (abstr.).
335. Carmosino, M.L., Breves, E.A., Dyar, M.D., Ozanne, M.V., Clegg, S.M., and Wiens, R.C. (2012) Behavior of feature selection in LIBS spectroscopy as a function of varying distance and data pre-processing. *Lunar Planet. Sci. XLIII*, Lunar Planet. Inst., Houston, CD-ROM #2285 (abstr.).
336. Dyar, M.D., Hibbitts, K.A., King, P.L., Breves, E.A., Orlando, T.M., Poston, M.J., Grieves, G.A., Tucker, J.M., and Seaman, S.J. (2012) Remote sensing of H in lunar surface materials: the effect of composition on hydrogen solubility and quantification. *Lunar Planet. Sci. XLIII*, Lunar Planet. Inst., Houston, CD-ROM #2264 (abstr.).
337. Friedlander, L.R., Glotch, T., Michalski, J.R., Sharp, T.G., Dyar, M.D., and Bish, D.L. (2012) Spectroscopic studies of nontronite after inpacts at 3 pressures. *Lunar Planet. Sci. XLIII*, Lunar Planet. Inst., Houston, CD-ROM #XXXX (abstr.).
338. Dobosh, P.A., Breves, E.A., Dyar, M.D., and McCanta, M. (2012) LIBSSIM: Simulation of LIBS sample on rock surfaces. *Lunar Planet. Sci. XLIII*, Lunar Planet. Inst., Houston, CD-ROM #1480 (abstr.).
339. Greenberger, R.N., Mustard, J.F., Kumar, P.S., Dyar, M.D., Speicher, E.A., and Sklute, E.C. (2012) Mineral assemblages of Deccan basalts and Al-phyllosilicate deposits on Mars: Implications for leaching processes on Mars. *Lunar Planet. Sci. XLIII*, Lunar Planet. Inst., Houston, CD-ROM #1907 (abstr.).
340. McCanta, M.C., Dyar, M.D., Dobosh, P.A. and Newson, H.E. (2012) Using the LIBSSIM program to calculate rock composition: Testing the potential of LIBS analyses. *Lunar Planet. Sci. XLIII*, Lunar Planet. Inst., Houston, CD-ROM #1993 (abstr.).
341. Greenspon, A.S., Hibbitts, K.A., and Dyar, M.D. (2012) Compositional dependencies in ultraviolet reflectance spectra of synthetic glasses relevant to airless bodies. *Lunar Planet. Sci. XLIII*, Lunar Planet. Inst., Houston, CD-ROM #2490 (abstr.).
342. Clegg, S/M., Sharman, S.K., Misra, A.K., Dyar, M.D., Dallman, N., Wiens, R.C., Vaniman, D.T., Speicher, E.A., Smrekar, S.E., Treiman, A. Wang, A., Maurice, S., and Esposito, L. (2012) Raman and laser-induced breakdown spectroscopy (LIBS) remote geochemical analysis under Venus atmospheric pressure. *Lunar Planet. Sci. XLIII*, Lunar Planet. Inst., Houston, CD-ROM #2105(abstr.).
343. Sklute, E.C., Glotch, T.D., and Dyar, M.D. (2012) VNIR optical constant determination of synthetic jarosites for quantitative abundance analysis of remote sensing data sets. *Lunar Planet. Sci. XLIII*, Lunar Planet. Inst., Houston, CD-ROM #XXXX (abstr.).
344. Clegg, S.M., Lasue, J., Forni, O., Bender, S., Wiens, R.C., Maurice, S., Barraclough, B., Blaney, D., Cousin, A., deFlores, L., Delapp, D., Dyar, M.D., Fabre, C., Gasnault, O., Lanza, N., Morris, R.V., Nelson, H., Newsom, H., Ollila, A., Perez, R., Sautter, V., and Vaniman, D.T. (2012) ChemCam flight model calibration. *Lunar Planet. Sci. XLIII*, Lunar Planet. Inst., Houston, CD-ROM #2076 (abstr.).
345. Poston, M.J., Grieves, G.A., Aleksandrov, A.B., McLain, J.L., Hibbitts, C.A., Dyar, M.D., and Orlando, T.M. (2012) Formation and time evolution off hydroxyl on lunar regolith by proton implantation and diffusion. *Lunar Planet. Sci. XLIII*, Lunar Planet. Inst., Houston, CD-ROM #XXXX (abstr.).
346. Bishop, J. L., Loizeau, D., McKeown, N. K., Saper, L. M., Dyar, M. D., Des Marais, D. J., Parente, M. & Murchie, S. L. (2012) Early Martian Habitability and Phyllosilicates at Mawrth Vallis. *Third Conference on Early Mars: Geologic, Hydrologic, and Climatic Evolution and the Implications for Life*, abs. #7014.
347. Gunter, M.E., and Dyar, M.D. (2012) Spiraling systematically through a mineralogy course. *GSA Ann. Mtng.*, 44, 242-1.
348. Dyar, M.D. and Gunter, M.E. (2012) use of the spindle stage for orientation of single crystals for Fe-XANES spectroscopy. *GSA Ann. Mtng.*, 44, 16-4.
349. Dyar, M.D. (2012) Multivariate analysis, chemometrics, and the future of spectroscopy: How statistics can complement spectroscopy. *GSA Ann. Mtng.*, 44, 267-13 (invited).
350. Lane, M.D., Bishop, J.L., and Dyar, M.D. (2012) Thermal Infrared Emission Measurements of Iron Sulfate and Phosphate Samples for Application to Mars. *AGU Fall Mtng.,* P11E-1871.
351. Bishop, J.L., Lane, M.D., and Dyar, M.D. (2012) Reflectance spectra of hydrated sulfates, phosphates and perchlorates. *AGU Fall Mtng*., P11E-1872.

352. Dyar, M.D., Nelms, M., and Breves, E.A. (2012) Measuring H, O, Li, B, and Be on planetary surfaces: Calibration of laser-induced breakdown spectroscopy (LIBS) under air, vacuum, and CO_2. *AGU Fall Mtng.,* P11F-02.
353. Michalski, J.R., Glotch, T.D., **Friedlander, L.**, Bish, D.L., Sharp, T.G., and Dyar, M>D. (2012) Effects of shock metamorphism on clay mineralogy: Implications for remote sensing of martian clays. *AGU Fall Mtng.,* P13A-1901.
354. Maurice, S., Wiens, R.C., Blaney, D., Bridges, J., Bridges, N., Clark, B., Clegg, S., Dromart, G., D'Uston, C., yar, D., Fabre, C., Gasnault, O., Herkenhoff, K., Langevin, Y., Mangold, N., Mauchien, P., McKay, C., Newsom, H., Vaniman, D., Anderson, R., Barraclough, B., Bender, S., Berger, G., Blank, J., Cousin, A., DeFlores, L., Delapp, D., Donny, C., Ehlmann, B., Forni, O., Gondet, B., Guillemot, P., Johnson, J., Johnstone, S., Lacour, J.-L., Lafaille, V., Lanza, N., Lasue, J., Moores, J., Le Mouelic, S., Lewin, E., Lorigny, E., Melikechi, N., Meslin, P.-Y., Mezzacappa, A., Nelson, T., Ollila, A., Pinet, P., Sautter, V., Schröder, S., Sirven, J.-B., Tokar, R., Toplis, M., Yana, C., Léveille, R., and the MSl science team. Overview of 100 sols of ChemCam operations at Gale crater. *Lunar Planet. Sci. XLIV*, Lunar Planet. Inst., Houston, CD-ROM #1979 (abstr.).
355. Wiens, R.C., Maurice, S., Sautter, V., Blaney, D. bridges, N., Clark, B., Clegg, S., Dromart, G. D'Uston, C. Fabre, C., Gasnault, O., Herkenhoff, K., Langevin, Y., Mangold, N., Mauchien, P., McKay, C., Newsom, H., Vaniman, D., Anderson, R., Baroukh, J., Barraclough, B., Bender, S., Berger, G., Blank, J., Cousin, A., Cros, A., DeFlores, L., Delapp, D., Donny, C., Forni, O., Gondet, B., Guillemot, P., Johnstone, S., Lacour, J.-L., Lafaille, V., Lanza, N., Lasue, J., Le Mouelic, S., Lewin, E., Lorigny, E., Melikechi, N., Meslin, P.-Y., Mezzacappa, A., Nelson, T., Ollila, A., Perez, R., Pinet, P., Saccoccio, M., Schröder, S., Sirven, J.-B., Tokar, R., Toplis, M., Yana, C., Dyar, M.D., Ehlmann, B., Johnson, J., Léveille, R., Moores, J., Bridges, J., Fisk, M.R., Grotzinger, J., and the MSl science team (2013) Compositions determined for ChemCam along Curiosity's traverse from Bradbury Station to Glenelg in Glae Crater, Mars. *Lunar Planet. Sci. XLIV*, Lunar Planet. Inst., Houston, CD-ROM #1363 (abstr.).
356. Tokar, R.L., Wiens, R.C., Maurice, S., Lasue, J., Johnson, J.R., Anderson, R.B., Cousin, A., Forni, O., Delapp, D.M., Lanza, N.L., Clegg, S.M., Bender, S.C., Barraclough, B.L., Dyar, M.D., and the MSL Science Team (2013) Searching for chemical variation across the surface of "Rocknest_3" using MSL ChemCam spectra. *Lunar Planet. Sci. XLIV*, Lunar Planet. Inst., Houston, CD-ROM #1283 (abstr.).
357. Blaney, D.L., Anderson, R., Berger, G., Bridges, J., Bridges, N., Clark, B., Clegg, S., Dyar, M.D., Ehlmann, B., Goetz, W., King, P.L., Lanza, N., Mangold, N., Meslin, P.-Y., Newson, H., and the MSL Science Team (2013) Assessment of potential rock coatings at Rocknest, Gale Crater, with ChemCam. *Lunar Planet. Sci. XLIV*, Lunar Planet. Inst., Houston, CD-ROM #1568 (abstr.).
358. Bridges, J.C., Schwenzer, S.P., Westall, F., and Dyar, M.D. (2013) Gale Crate's Bathurst Inlet and Rocknest_3 compositions. *Lunar Planet. Sci. XLIV*, Lunar Planet. Inst., Houston, CD-ROM #1973 (abstr.).
359. Clegg, S.M., Mangold, N., Le Mouelic, S., Olillia, A., Anderson, R., Blaney, D.L., Clark, B., Cousin, A., Dyar, M.D., Ehlmann, B., Fabre, C., Forni, O., Lasue, J., Meslin, P.-Y., Schröder, S., Sirven, J.-B., Vaniman, D., Maurice, ., and Wiens, R.C. (2013) High calcium phase observed at Rocknest with ChemCam. *Lunar Planet. Sci. XLIV*, Lunar Planet. Inst., Houston, CD-ROM #2087 (abstr.).
360. Olillia, A.M., Newsom, H,E., Wiens, R.C., Lasue, J., Clegg, S.M., Cousin, A., Gasnault, O., Forni, O., Maurice, S., Schröder, S., Meslin, P.-Y., Dyar, M.D., Blank, J.G., Clark, B., Barraclough, B., and the MSL Team. (2013) Early results from Gale Crater on ChemCam detections of carbon, lithium, and rubidium. *Lunar Planet. Sci. XLIV*, Lunar Planet. Inst., Houston, CD-ROM #2188 (abstr.).
361. Lasue, J., Forni, O., Anderson, R.B., Berger, G., Clegg, S.M., Cousin, A., Dyar, M.D., Fabre, C., Gasnault, O., Lewin, E., Meslin, P.-Y., Maurice, S., Tokar, R.L., Wiens, R.C., and the MSL team. (2013) Partial Least Squares sensitivity analysis and improvements for CHEMCAM LIBS data analysis on Mars. *Lunar Planet. Sci. XLIV*, Lunar Planet. Inst., Houston, CD-ROM #2230 (abstr.).
362. Shank, E.M., Klima, R.L., and Dyar, M.D. (2013) Charactetrizing pyroxene cooling rate using reflectance spectra (2013) *Lunar Planet. Sci. XLIV*, Lunar Planet. Inst., Houston, CD-ROM #2371 (abstr.).
363. Ehlmann, B.L., Clegg, S.M., Anderson, R.B., Forni, O., Lasue, J., Lanza, N.L., Meslin, P.-Y., Olilla, A., Dyar, M.D., Stolper, E.M., Rossman, G.R., Sautter, V., Blaney, D., Clark, B.C., Maurice, S., Wiens, R.C., and the MSL Science Team. An expanded training set for processing of MSL ChemCam LIBS data: Spectral library samples added and effects on elemental composition results from Mars. *Lunar Planet. Sci. XLIV*, Lunar Planet. Inst., Houston, CD-ROM #2600 (abstr.).

364. Poston, M.J., Aleksandrov, A.B., Grieves, G.A., Hibbitts, C.A., and Dyar, M.D. (2013) Thermal stability of adsorbed water molecules on lunar materials. *Lunar Planet. Sci. XLIV*, Lunar Planet. Inst., Houston, CD-ROM #217 (abstr.).
365. Berlanga, G., Hibbitts, C.A., Takir, D., and Dyar, M.D. (2013) Spectral nature of CO_2 adsorption on meteorites. *Lunar Planet. Sci. XLIV*, Lunar Planet. Inst., Houston, CD-ROM #2904 (abstr.).
366. Lin, T.J., Breves, E.A., Dyar, M.D., and Holden, J.F. (2013) Hyperthermophile-mienral interactions and correlating mineral transformations. *Lunar Planet. Sci. XLIV*, Lunar Planet. Inst., Houston, CD-ROM #2560 (abstr.).
367. Newsom, H.E., Berger, J., Olilla, A., Gordon, S., Wiens, R.C., Sautter, V., Maurice, S., Blaney, D., Ehlmann, B., Dyar, M.D., Bridges, N., Clark, B., Clegg, S., DeFlores, L., Dromart, G., D'Uston, C., Fabre, C., gasnault, O., Herkenhoff, K., Langevin, Y., Mangold, N., Mauchien, P., McKay, C., Vaniman, D., Anderson, R., Baroukh, J., Barraclough, B., Bender, S., Berger, G., Blank, J., Cousin, A., Cros, A., Delapp, D., Donny, C., Forni, O., Gondet, B., Guillemot, P., Johnstone, S., lacour, J.-L., Lafaille, V., Lanza, N., Lasue, J., Le Moulic, S., Lewin, E., Lorigny, E., Melikechi, N., Meslin, P.-Y., mezzacappa, A., Nelson, T., Perez, R., Pinet, P., Saccoccio, M., Schröder, S., Sirven, J.-B., Tokar, R., Toplis, M., Yana, C., Gellert, R., King, P.L., Schmidt, M., Boynton, W., Leveille, R., Bridges, J., and the MSL Science Team (2013) Regional and global context of soil and rock chemistry from Che,mCam and APXS at Gale Crater. *Lunar Planet. Sci. XLIV*, Lunar Planet. Inst., Houston, CD-ROM #1832 (abstr.).
368. Harding, S.C., Ekdale, A.A., Petersen, E.U., Nash, B.P., and Dyar, M.D. (2013) Ichnology and mineralogy of the Main Glauconite Bed, Claiborne Group, Middle Eocene, Texas: Paleoenvironmental implications. Gulf Coast Assoc. Geological Soc., 63rd Ann. Mtng.
369. Michalski, J., Cuadros, J., Dekov, V., Bishop, J.L., Fiore, S., and Dyar, D. (2013) Constraints on the crystal chemistry of Martian clays from infrared spectroscopy of analogue materials. *Euro. Planet. Sci. Conf.*
370. Dyar, M.D., Breves, E., Blau, H., Boucher, T., Clegg, S., Anderson, R., Lanza, N., Newsom, H., Treiman, A. (2013) Mineralogy at Gale Crater on Mars as measured by the ChemCam LIBS. *Sci-X* 2013, Milwaukee, Abstract #260.
371. Boucher, T., Dyar, M.D., Carmosino, M., Mahadevan, S., Clegg, S., and Wiens, R. (2013) Manifold regression of LIBS data from geological samples for application to ChemCam on Mars. *Sci-X* 2013, Milwaukee, *Sci-X* 2013, Milwaukee, Abstract #24.
372. Clegg, S., Forni, O., Lasue, J., Anderson, R., Dyar, M., Bender, S., Tokar, R., Maurice, S., Wiens, R., and the Chemcam Science Team (2013) ChemCam quantitative geochemical analysis on Mars Curiosity rover, *Sci-X* 2013, Milwaukee, Abstract #309.
373. Clegg, S., Wiens, R., Misra, A., Sharman, S., Bender, S., Newell, R., Lambert, J., Smrekar, S., Dyar,m M.D., and Maurice, S. (2013) Planetary geochemical investigations by Raman-LIBS spectroscopy (RLS). *Sci-X* 2013, Milwaukee, Abstract #663.
374. Dyar, M.D., King, P.L., Larsen, J.F., and Hibbitts, C.A. (2013) Quantifying H abundance on the Moon: The roles of composition, optical constraints, and band shape. *Geological Society of American Annual Meeting, Denver*, Abstract #67-6.
375. Dyar, M.D., Bridges, J., and Wiens, R.C. (2013) Mineralogy at Bradbury Landing and Yellowknife Bay, Gale Crater, Mars as measured by the ChemCam LIBS. *Geological Society of American Annual Meeting, Denver*, Abstract #6-5.
376. Holden, J.F., Lin, T.J., Ver Eecke, H.C., Breves, E. Dyar, M.D., Jamieson, J.W., Hannington, M.D., Butterfield, D.A., Bishop, J.L., and Lane, M.D. (2013) Microbial and mineral descriptions of the interior habitable zones of active hydrothermal chimneys from the Endeavour Segment, Juan de Fuca Ridge. *AGU Fall Mtng.*, B13C-0479.
377. Stander, A., Nelms, M., Wilkinson, K., Dyar, M.D., and Cardace, D. (2013) Potential hydrogen yields from ultramafic rocks of the Coast Range Ophiolite and Zambales Ophiolite: Inferences from Mössbauer spectroscopy. *AGU Fall Mtng.*, B13C-0482.
378. Wiens, R.C., Maurice, S., Grotzinger, J.P., Gellert, R., Mangold, N., Sautter, V., Ollila, A., Dyar, M.D., Le Mouelic, S., Ehlmann, B.L., Clegg, S.M., Lanza, N., Cousin, A., Forni, O., Gasnault, O., Lasue, J., Blaney, D.L., Newsom, H.E., Herkenhoff, K.E., Anderson, R.B., D'Uston, L., Bridges, N.T., Fabre, C., Mselin, P.-Y., Johnson, J., Vaniman, D., Bridges, J., Dromart, G., Schmidt, M.E., and the mSL Science Team. *AGU Fall Mtng.*, P21D-05.
379. Clegg, S.M., Mangold, N., Nachon, M., Le Mouelic, S., Ollila, A., Vaniman, D.T., Kah, L.C., Dromart, G., Bridges, J., Rice, M.S., Wellington, D.F., Bell, J.F., Anderson, R.B., Clark, B.C., Cousin, A., Forni, O.,

Lasue, J., Schroeder, S., Meslin, P.-Y., Dyar, M.D., Blaney, D.L., Maurice, S., Wiens, R.C., and the MSL Science Team. *AGU Fall Mtng.*, P23C-1797.

380. Schoonen, M.A., Sklute, E.C., Strongin, D.R., and Dyar, M.D. (2013) Reactivity of iron-bearing minerals in deep saline formations subjected to carbon injection. *AGU Fall Mtng.*, V41A-2738.
381. McCanta, M.C., Dyar, M.D., and Breves, E. (2013) Effects of composition on Fe-XANES redox calibrations in glasses. *AGU Fall Mtng.*,V44B-03.
382. Hibbitts, C.A., Dyar, M.D., and Greenspon, A.S. (2014) Ultraviolet reflectance spectra material relevant to airless bodies. *Lunar Planet. Sci. XLV*, Lunar Planet. Inst., Houston, CD-ROM #2611 (abstr.).
383. Ollila, A.M., Newsom, H.E., Wiens, R.C., Maurice, S., Sautter, V., Mangold, N., Clark, B., Vaniman, D., Blank, J.G., Bridges, J., Cousin, A., Tokar, R.L., Gasnault, O., Forni, O., Lasue, J., Anderson, R., Clegg, S.M., Dyar, M.D., Fabre, C., Lanza, N., RosenGooding, A., and the MSL Team. (2014) Trace element (strontium, barium, rubidium, and lithium) analyses by ChemCam for the first 360 sols in Gale Crater, Mars. *Lunar Planet. Sci. XLV*, Lunar Planet. Inst., Houston, CD-ROM #2490 (abstr.).
384. Clegg, S.M., Wiens, R.C., Maurice, S., Gasnault, O., Sharma, S.K., Misra, A.K., Newell, R., Bender, S., Forni, O., Lasue, J., Dyar, M>D., and Nowak-Lovato, K.L. (2014) Remote Raman and LIBS spectroscopy for future Mars rover missions. *Lunar Planet. Sci. XLV*, Lunar Planet. Inst., Houston, CD-ROM #2463 (abstr.).
385. Clegg, S.M., Anderson, R., Forni, O., lasue, J., Dyar, M.D., Morris, R.V., Ehlmann, B.L., McLennan, S.M., Bender, S., Cousin, A., Gasnault, O., artinez, R., McInroy, R., Delapp, D., Melikechi, N., Mesline, P.-Y., Ollila, A., Tokar, R.L., Maurice, S., and Wiens, R.C. (2014) Expansion of the ChemCam calibration batabase. *Lunar Planet. Sci. XLV*, Lunar Planet. Inst., Houston, CD-ROM #2378 (abstr.).
386. Poston, M.J., Aleksandrov, A.B., Grieces, G.A., Hibbitts, C.A., Dyar, M.D., and Orlando, T.M. (2014) Temperature program desorption measurementsof water molecules on lunar samples 12001 and 72501. *Lunar Planet. Sci. XLV*, Lunar Planet. Inst., Houston, CD-ROM #2283 (abstr.).
387. Blaney, D.L., Wiens, R.C., Maurice, S., Clegg, S.M., Anderson, R.B., Kah, L.C., Le Mouelic, S., Ollila, A., Bridges, N., Berger, G., Bridges, J.C., Cousin, A., Clark, B., Dyar, M.D., King, P.L., Lanza, N., Mangold, N., Schmidt, P., Goetz, W., Stack, K., Sumner, D., Fisk, M., Maden, M.B., Tokar, R., and the MSL Science Team (2014) Rocknest and beyond: iron-bearing cemented sediments in Gale Crater from ChemCam observations. *Lunar Planet. Sci. XLV*, Lunar Planet. Inst., Houston, CD-ROM #2122 (abstr.).
388. Nachon, M., Clegg, S.M., Mangold, N., Schroder, S., Kah, L.C., Dromart, G., Ollila, A., Johnson, J.R., Oehler, D.Z., Bridges, J.C., LeMouelis, S., Forni, O., Wiens, R.C., Anderson, R.B., Blaney, D.L., Bell, J.F. III, Clark, B., Cousin, A., Dyar, M.D., Ehlmann, B., Fabre, C., Gasnault, O., Grotzinger, J., Lasue, J., Lwein, E., Leveille, R., McLennan, S., Maurice, S., Meslin, P.-Y., Rice, M., Squyres, S.W., Stack, K., Sumner, D., Vaniman, D., and Wellington, D. (2014) Calcium sulfate characterized by ChemCam/*Curiosity* at Gale Crater, Mars. *Lunar Planet. Sci. XLV*, Lunar Planet. Inst., Houston, CD-ROM #2006 (abstr.).
389. Dyar, M.D., Dobosh, P., Bridges, J., Wiens, R., Johnson, J., and the MSL Science Team (2014) Mineralogy at Bradbury Landing site and YellowKnife Bay in Gale Crater, Mars, as measured using cation ratios, for sols 13-360. *Lunar Planet. Sci. XLV*, Lunar Planet. Inst., Houston, CD-ROM #1788 (abstr.).
390. Michalski, J.R., Cuadros, J., Dekov, V., Bishop, J.L., Fiore, S., and Dyar, M.D. (2014) Constraints on the crystal chemistry of Fe-Mg clays on mars based on infrared analyses of fe-rich seafloor clays. *Lunar Planet. Sci. XLV*, Lunar Planet. Inst., Houston, CD-ROM #1781 (abstr.).
391. Ferrari, S., Helbert, J., Maturilli, A., Muller, N., Dyar, M.D., and Elkins-Tanton, L.T. (2014) the surface of Venus after VIRTIS on Venus Express: laboratory analogs and the Venus Emissivity Mapper. *Lunar Planet. Sci. XLV*, Lunar Planet. Inst., Houston, CD-ROM #1775 (abstr.).
392. Fisk, M., Dyar, M., Cousin, A., Bridges, N., Bridges, J., Anderson, R., Johnson, J., Blaney, D., Mangold, N., Herkenhoff, K., Wiens, R., Clegg, S., Meslin, P.-Y., gasnault,O., Forni, O., Clark, B., Pinet, P., and the MSL Science Team. Silica-Fe-rich components of rocks, Gale Crater, Mars. *Lunar Planet. Sci. XLV*, Lunar Planet. Inst., Houston, CD-ROM #1674 (abstr.).
393. Jackson, C.R.M., Cheek, L.C., Williams, K.B., Donaldson hanna, K., Pieters, C.M., Parman, S., Cooper, R.F., Dyar, M.D. Nelms, M., and Salvatore, M.R. (2014) Visible to near-infrared spectra of iron-bearing spinel with application to Sinus Aestuum and lunar spinel anorthosite. *Lunar Planet. Sci. XLV*, Lunar Planet. Inst., Houston, CD-ROM #1561 (abstr.).
394. Mezzacappa, A., Melikechi, N., Cousin, A., Lasue, J., Lanza, N., Wiens, R.C., Clegg, S.M., Maurice, S., Bender, S., berger, G., Forni,O., Gasnault, O., Newsom, H., Ollila, A.M., Clark, B., Dyar, M.D., Blaney,

D., and the MSL Science Team (2014) Effects of distance correction on ChemCam LIBS measurements (sols 13-360). *Lunar Planet. Sci. XLV*, Lunar Planet. Inst., Houston, CD-ROM #1517 (abstr.).

395. Dobosh, P.A., and Dyar, M.D. (2014) Software tools for exploring and analyzing ChemCam data. *Lunar Planet. Sci. XLV*, Lunar Planet. Inst., Houston, CD-ROM #1188 (abstr.).
396. Dyar, M.D., Treiman, A.H., Clegg, S.M., Wiens, R.C., Filiberto, J., Sharma, S.K., and Misra, A.K. (2014) *Venus Exploration Targets Workshop*, LPI, CD-ROM #6010 (abstr.)
397. Clegg, S.M., Dyar, M.D., Sharman, S.K., Misra, A.K., Wiens, R.C., Smrekar, S.E., and Maurice, S. (2014) raman and laser-induced breakdown spectroscopy (LIBS) geochemical analysis under Venus atmosphereic pressure. *Venus Exploration Targets Workshop*, LPI, CD-ROM #tbd (abstr.)
398. Helbert, J., Müller, N., Ferrari, S., Dyar, D., Smrekar, S.E., Head, J.W., and Elkins-Tanton, L. (2014) Mapping the surface composition of Venus in the near-Infrared. *Venus Exploration Targets Workshop*, LPI, CD-ROM #tbd (abstr.)
399. Ferrari, S., Helbert, J., Maturilli, A., Dyar, M.D., Müller, N., and Elkins-Tanton, L. (2014) The surface of Venus after VIRTIS on Venus Express: Laboratory analogs and the Venus Emissivity Mapper.. *Venus Exploration Targets Workshop*, LPI, CD-ROM #tbd (abstr.)
400. Dyar, M.D., Bridges, J.C., Dobosh, P., Edwards, P., Wiens, R., Johnson, J., Maurice, S., and the MSL team. Mineralogy en route to Mount Sharp, Mars, as measured using cation ratios from ChemCam data. Mars 8, Pasadena, CA, Abstr. #1159.
401. Cousin, A., Mesline, P., Wiens, R., Rapin, W., Mangold, N., Fabre, C., Tokar, R., Ollila, A., Schroder, S., Lasue, J., Maurice, S., Sautter, V., Newsom, H., Vaniman, D., Le Mouelic, S., Dyar, D., Berger, G., Blaney, D., Nachon, M., Dromarrt, G., Lanza, N., Clark, B., Clegg, S., Goetz, W., Berger, J., Barrachough, B., Delapp, D., and the MSL Science Team (2014) Chemistry of coarse particles in soils and their relationship with local rocks. Mars 8, Pasadena, CA, Abstr. #1095.
402. Wiens, R.C., Maurice, S., Blaney, D.L., Gortzinger, J.P., Mangold, N., Clegg, S., Sauter, V., Bridges, J., Bridges, N., Clark, B., D'Uston, C., Dyar, M.D., Edgar, L., Ehlmann, B., Forni, O., Fabre, C., Gasnault, O., Herkenhoff, K., Johnson, J., Leveille, R., Newsom, H., Vaniman, D., Cousin, A., Deflores, L., Lanza, N., Lasue, J., Meslin, P.-Y., Pinet, P., Schroder, S., Rapin, W., Fisk, M.R., Melikechi, N., Mezzacappa, A., Le Deit, L., Le Mouelic, S., Nachon, M., Toplis, M., Jackson, R., Williams, J., and Williams, A. (2014) Geochemistry at Gale from ChemCam: Implications for martian igneous and sedimentary processes and for habitability. Mars 8, Pasadena, CA, Abstr. #1170.
403. Friedlander, L.R., Glotch, T.D., Michalski, J.R., Bish, D.L., Sharp, T., and Dyar, M.D. (2014) The impact of impacts on martian phyllosilicates. Mars 8, Pasadena, CA, Abstr. #1034.
404. Blaney, D.L., Wiens, R.C., Maurice, S., Clegg, S.M., Anderson, R.B., Kah, L.C., Le Mouelic, S., Ollila, A., Bridges, N., Berger, G., Bridges, J.C., Cousin, A., Clark, B., Dyar, M.D., King, P.L., Lanza, N., Mangold, N., Meslin, P.-Y., Newsom, H., Schroder, S. Rowland, S., Johnson, J., Edgar, L., Forni, O., Schmidt, M., Goetz, W., Stack, K., Sumner, D., Fisk, M., Maden, M.B., Tokar, R., and the MSL Science Team (2014) Rocknest, Bradbury Plateau, and Kimberly: Iron cemented sediments observed in Gale Crater with ChemCam. Mars 8, Pasadena, CA, Abstr. #1258.
405. Anderson, R.B., Clegg, S.M., Ehlmann, B.L., Morris, R.V., McLennan, S.M., Boucher, T., Dyar, M.D., McInroy, R., Delapp, D., Wiens, R.C., Frydenvang, J., Forni, O., Maurice, S., Gasnault, O., Lasue, J., and Fabre, C. (2014) Expanded compositional database for ChemCam quantitative calibration. Mars 8, Pasadena, CA, Abstr. #1275.
406. Nachon, M., Clegg, S.M., Mangold, N., Schroder, S., Kah, L.C., Dromart, G., Ollilia, A., Johnson, J.R., Oehler, D.Z., Bridges, J.C., Dyar, M.D., Ehlmann, B., Fabre, C., Gasnault, O., Grotzinger, J., Lasue, J., Lewin, E., Leveille, R., McLennan, S., Maurice, S., Meslin, P.-Y., Rice, M., Squyres, S.W., Stack, K., Sumner, D.Y., Vanima, D., and Wellington, D. (2014) Calcium sulfate characterized by ChemCam/ Curiosity at Gale Crater, Mars. Mars 8, Pasadena, CA, Abstr. #1334.
407. Lasue, J., Clegg, S.M., Forni, O., Anderson, R.B., Dyar, M.D., Fabre, C., Gasnault, O., Lewin, E., Maurice, S., Tokar, R.L., Wiens, R.C., and the MSL Science Team (2014) ChemCam LIBS multivariate regression models accuracy assessment. Mars 8, Pasadena, CA, Abstr. #1444.
408. Dyar, M.D., Dobosh, P., Bridges, J., Wiens, R., Johnson, J., and the MSL Science Team (2014) Mineralogy at Bradbury Landing site and YellowKnife Bay in Gale Crater, Mars, as measured using cation ratios, for sols 13-360. Lunar Planet. Sci. XLV, Lunar Planet. Inst., Houston, CD-ROM #1788 (abstr.).
409. Dyar, M.D., Breves, E.A., Boucher, T.F., and Mahadevan, S. (2014) Successes and challenges of laser-induced breakdown spectroscopy (LIBS) applied to chemical analyses of geological samples. *Microscopy and Microanalysis 2014*, Hartford, CT.

410. Carey, C., Boucher, T., Mahadevan, S., Dyar, M.D., and Bartholomew, P. (2014) Machine learning tools for mineral recognition and classification from Raman spectroscopy. *Geo-Raman 8*, St. Louis, MS, Abstract #5053.
411. Brady, J.B., Dyar, M.D., McGowan, E., and Bartholomew, P. (2014) Building analytical competence for geoscience students through use of Raman spectroscopy. *Geo-Raman 8*, St. Louis, MS, 5053. Abstract #5037.
412. Helbert, J., Ferrari, S., Maturilli, and Dyar, D. (2014) Obtaining 1 micron emissivity measurements of Venus analog materials at 730K. *Asia Oceania Geosciences Society*, Sappora, Japan, PS07-A028.
413. Clegg, S., Forni, O., lasue, J., Dyar, M.D., Morris, R., Ehlmann, B., McLennan, S., Bender, S., Cousin, A., Gasnault, O. (2014) Generating multivariate calibration methods from the ChemCam laboratory instrument. *Sci-X 2014*, Reno, NV, abstract #194.
414. Carey, C.J., Boucher, T.F., Mahadevan, S.,Dyar, M.D., and Bartholomew, P. (2014) Machine learning tools for mineral recognition and classification from Raman spectroscopy. *Sci-X 2014*, Reno, NV, abstract #274.
415. Boucher, T.F., Dyar, M.D., Carey, C.J., Mahadevan, S., Mezzacappa, A., Melikechi, N. (2014) Recognizing the contribution of dust to ChemCam spectra of rocks and minerals on Mars. *Sci-X 2014*, Reno, NV, abstract #377.
416. Boucher, T., Dyar, M.D., Carey, C.J., Mahadevan, S. (2014) Using manifold embedding to preprocess LIBS spectra to improve regression model performance for chemical decomposition. *Sci-X 2014*, Reno, NV, abstract #432.
417. Dyar, M.D., Shaner, A.J., Shipp, S. (2014) Exciting the public about LIBS through outreach about the ChemCam laser on Mars Science Laboratory. *Sci-X 2014*, Reno, NV, abstract #733.
418. Bishop, J., Murad, E., and Dyar, M.D. (2014) Akaganéite and schweertmannite – spectral properties and geochemical implications of their presence on Mars. *92nd Duetsche Mineralogische Gesellschaft*, 2014, abstract #ENV-T11.
419. Dyar, M.D., and McCanta, M. (2014) Ferric iron concentrations in silicate glasses: a Mössbauer and XAS study. *AGU*, Abstract #V53B-4858.
420. Dyar, M.D., McCanta, M., Lanzirotti, A., Sutton, S., Carey, C., Mahadevan, S., and Rutherford, M. (2014) Redox state of iron in lunar glasses using x-ray absorption spectroscopy and multivariate analysis. *AGU*, Abstract #P12B-01.
421. Michalski, J., Cuadros, J., Dekov, V., Dyar, M., Bishop, J., and Stephen, N. (2014) Constraints on the crystal chemistry of Fe/Mg-rich smectitic clays on Mars and links to global alteration trends. *AGU*, Abstract #P34A-01.
422. Fisk, M., Dyar, M., Bridges, J., Anderson, R., Schmidt, M., Gasnault, O., Mangoild, N., Tokar, R., Wiens, R., Gellert, R., Blake, D., Schwenzer, S., and Edwards, P. (2014) Hypotheses on the source of potassium enrichment in some Gale Crater rocks. *AGU*, Abstract #P54A-08.
423. Greenberg, R., Mustard, J., Cloutis, E., Pratt, L., Sauer, P., Mann, P., Turner, K., and Dyar, M. (2014) Aqueous conditions and habitability associated with formation of a serpentinite: Using analyses of ferric iron and stable carbon isotopes to reconstruct hydrogen production. *AGU*, Abstract #P33C-4040.
424. Edwards, P., Bridges, J., Dyar, M., Fisk, M., Schwenzer, S., Forni, O., and Wiens, R. (2014) Comparing MSL ChemCam analyses to shergottite and terrestrial rock types. *AGU*, Abstract #P43D-4010.
425. Helbert, J., Maturilli, A., Ferrari, S., Dyar, M., and Smrekar, S. (2014) First laboratory high-temperature emissivity measurements of Venus analog measurements in the near-infrared atmospheric windows. *AGU*, Abstract #P21B-3911.
426. Burgess, K.D., Stround, R. M., De Gregorio, B.T., Dyar, M.D., and McCanta, M.C. (2015) Measurement of Fe oxidation state using aberration-corrected scanning transmission electron microscopy. *Lunar Planet. Sci. XLVI*, Lunar Planet. Inst., Houston, (abstr.).
427. Boucher, T., Dyar, M.D., Carey, C., Giguere, S., Mahadevan, S., Clegg, S., Anderson, R., and Wiens, R. (2015) Calibration transfer of LIBS spectra to correct for Mars-Earth lab differences. *Lunar Planet. Sci. XLVI*, Lunar Planet. Inst., Houston, #2773 (abstr.).
428. Breves, E.A., Breitenfeld, L.B., Ketley, M.N., Roberts, A.L., Dyar, M.D., Fassett, C.I., Sklute, E.C., Lepore, K.H., Marchand, G.J., Rhodes, J.M., Vollinger, M., Byrne, S.A., Crowley, M.C., Boucher, T.F., and Mahaevan, S. (2015) Cr, Ni, Mn, Co, Zn, and S standards for use in laser-induced breakdown spectroscopy. *Lunar Planet. Sci. XLVI*, Lunar Planet. Inst., Houston, #2338 (abstr.).

429. Dyar, M.D., Dobosh, P., Bridges, J., and Wiens, R. (2015) Pure mineral phases sqamples by the ChemCam instrument in Gale crater, Mars, as measured using cation ratios for sols 13-801. *Lunar Planet. Sci. XLVI*, Lunar Planet. Inst., Houston, #1514 (abstr.).
430. Giguere, S., Carey, C., Dyar, M.D., Boucher, T.F., Parente, M., Tague, T.J. Jr., and Mahadevan, S. (2015) Baseline removal in LIBS and FTIR spectroscopy: Optimization techniques. *Lunar Planet. Sci. XLVI*, Lunar Planet. Inst., Houston, #(abstr.).
431. McCanta, M.C., Dyar, M.D., Carey, C., Mahadevan, S., Lanzirotti, A., and Sutton, S. (2015) Preliminary calibration for measuring ferric iron in silicate glasses: A Mössbauer and X-ray absorption spectroscopy study. *Lunar Planet. Sci. XLVI*, Lunar Planet. Inst., Houston, #1388 (abstr.).
432. Glotch, T.D., Dyar, M.D., Bleacher, J.E., Schoonen, M.A.A., Petro, N.E., and Jones, A. (2015) Remote, in situ, and synchrotron studies for science and expoloration (RIS^{4}E): First year of science and exploration. *Lunar Planet. Sci. XLVI*, Lunar Planet. Inst., Houston, (abstr.).
433. Breves, E.A., Lepore, K.H., and Dyar, M.D. (2015) Laser-induced breakdown spectroscopy of glasses and rocks at varying ablation and collection angles. *Lunar Planet. Sci. XLVI*, Lunar Planet. Inst., Houston, #2536 (abstr.).
434. Dyar, M.D., Breves, E.A., Lepore, K.H., Boucher, T.F., Bender, S., Tokar, R., Berlanga, G., Clegg, S.M., and Wiens, R.C. (2015) Calibration suite for Mars-analog laser-induced spectroscopy. *Lunar Planet. Sci. XLVI*, Lunar Planet. Inst., Houston, #1510 (abstr.).
435. Michalski, J.R., Sharp, T.G., Freidlander, L., Glotch, T., Bish, D., and Dyar, M.D. (2015) Effects of shock metamorphism on the structure of kaolinite. *Lunar Planet. Sci. XLVI*, Lunar Planet. Inst., Houston, #2246 (abstr.).
436. Byrne, S.A., Dyar, M.D., Bessette, E.E., Breitenfeld, L.B., Crowley, M.C., Hoff, C.M., Marchand, G.J., Ketley, M.N., Roberts, A.L., Sklute, E.C., and Parente, M. (2015) Pure mineral separates for mixing experiments to simulate planetary surfaces. *Lunar Planet. Sci. XLVI*, Lunar Planet. Inst., Houston, #1499 (abstr.).
437. McCanta, M.C., Dyar, M.D., Rutherford, M.J., Lanzirotti, A., and Sutton, S. (2015) In situ measurement of ferric iron in lunar glasses using Fe-XAS: Implications for lunar eruption mechanisms. *Lunar Planet. Sci. XLVI*, Lunar Planet. Inst., Houston, #1500 (abstr.).
438. Lepore, K.H., Boucher, T.F., Breves, E.A., Dyar, M.D., Fassett, C.I., Sklute, E.C., Marchand, G.J., Rhodes, J. M., Vollinger, M., Byrne, S.A., Breitenfeld, L.B., Ketley, M.N., Crowley, M.C., Roberts, A.L., and Mahadevan, S. (2015) Nickel calibration for use in laser-induced breakdown spectroscopy on Mars. *Lunar Planet. Sci. XLVI*, Lunar Planet. Inst., Houston, #2720 (abstr.).
439. Fassett, C.I., and Dyar, M.D. (2015) Accumulation of meteoritic nickel on Mars. *Lunar Planet. Sci. XLVI*, Lunar Planet. Inst., Houston, #1875 (abstr.).
440. Carey, C., Dyar, M.D., Boucher, T.F., Giguere, S., Hoff, C.M., Breitenfeld, L.B., Parente, M., Tague, T.J. Jr., Wang, P., and Mahadevan, S. (2015) Baseline removal in Raman spectroscopy: optimization techniques. *Lunar Planet. Sci. XLVI*, Lunar Planet. Inst., Houston, #2464 (abstr.).
441. Sklute, E.C., Dyar, M.D., Friedlander, L., Glotch, T.D., Bish, D.L., Sharp, T.G., and Michalski, J.R. (2015) Mössbauer analysis of shocked clays – What do we really know about Mars? *Lunar Planet. Sci. XLVI*, Lunar Planet. Inst., Houston, #2048 (abstr.).
442. Tokar, R.L., Wiens, R.C., Maurice, S., Pilleri, A., Gellert, R., Anderson, R.B., Bender, S.C., Clegg, S.M., Dyar, M.D., Fabre, C., Forni, O., Gasnault, O., Lasue, J., and Melikechi, N. (2015) Relationship between MSL/ChemCam laser focus, plasma temperature, and compositional calibrations. *Lunar Planet. Sci. XLVI*, Lunar Planet. Inst., #1369 Houston, (abstr.).
443. Helbert, J., Ferrarri, S., Maturilli, A., Dyar, M.D. Müller, N., and Smrekar, S. (2015) Studying the surface composition of Venus in the near-infrared. *Lunar Planet. Sci. XLVI*, Lunar Planet. Inst., Houston, (abstr.).
444. Parente, M., Saranathan, AM., and Dyar, D. (2015) An overview of the spectroscopy lab at UMass, Amherst. *Lunar Planet. Sci. XLVI*, Lunar Planet. Inst., Houston, (abstr.).
445. Treiman, A.H. and Dyar, M.D. (2015) Instrument requirements for geochemistry (elemental abundances): an approach. *Venus Science Priorities*, abstract #4020.
446. Giguere, S., Boucher, T., Carey, C., Dyar, M.D., and Mahadevan, S. (2015) A framework for fully-customized baseline removal. *Sci-X 2015*, Providence, RI, paper #288.
447. Boucher, T., Dyar, M.D., Carey, C., Guguere, S., and Mahadevan, S. (2015) A convex optimization approach to calibration transfer. *Sci-X 2015*, Providence, RI, paper #287.

448. Lepore, K., Breves, E., Dyar, M.D. (2015) Exploring matrix effects on quantitative analysis of LIBS data from rock powders doped with Cr, Ni, Mn, Co, Zn, and S. *Sci-X 2015*, Providence, RI, paper #140.
449. Breves, E., Lepore, K., Dyar, M.D. (2015) Laser-induced breakdown spectra of rocks at variable ablation and collection angles. *Sci-X 2015*, Providence, RI, paper #89.
450. Dyar, M.D., Boucher, T., Carey, C., Giguere, S., and Mahadevan, S. (2015) Choices and improvements in baseline removal in LIBS spectroscopy. *Sci-X 2015*, Providence, RI, paper #138.
451. Carey, C., Boucher, T., Giguere, S., Dyar, M.D., and Mahadevan, S. (2015) Optimal preprocessing and similarity for automatic whole-spectrum matching. *Sci-X 2015*, Providence, RI, paper #767.
452. Boucher, T.F., Dyar, M.D., Carey, CJ, Mahadevan, S. (2016) Calibration transfer for spectroscopy in space science. *Lunar Planet. Sci. XLVII*, Lunar Planet. Inst., Houston, (abstr.) #2784.
453. Carey, CJ, Breitenfeld, L.B., Dyar, M.D., Crowley, M.C., Leight, C., Watts, E. (2016) Quantifying mineral abundances in mixtures using Raman spectroscopy: Toward a method for spectral unmixing. *Lunar Planet. Sci. XLVII*, Lunar Planet. Inst., Houston, (abstr.) #2626.
454. Thomas, N.H., Ehlmann, B.L., Clegg, S.M., Forni, O., Schröder, S., Anderson, D.E., Rapin, W., Cousin, A., Meslin, P.-Y., Lasue, J., Delapp, D.M., McInroy, R.E., Dyar, M.D., Rossman, G.R., Gasnault, O., Wiens, R., Maurice, S. (2016) Characterization of hydrogen in basaltic materials with laser-induced breakdown spectroscopy (LIBS). *Lunar Planet. Sci. XLVII*, Lunar Planet. Inst., Houston, (abstr.) #2494.
455. Smrekar, S.E., Hensley, S., Dyar, M.D., Helbert, J., and the VERITAS team (2016) VERITAS (Venus Emissivity, Radio Science, InSAR, Topography and Spectroscopy): A proposed Discovery mission. *Lunar Planet. Sci. XLVII*, Lunar Planet. Inst., Houston, (abstr.) #2439.
456. Breitenfeld, L.B., Dyar, M.D., Crowley, M.C., Leight, C., and Watts, E. (2016) Quantifying mineral abundances in mixtures using Raman spectroscopy: Creating mineral mixtures. *Lunar Planet. Sci. XLVII*, Lunar Planet. Inst., Houston, (abstr.) #2430.
457. Anderson, D.E., Ehlmann, B.L., Forni, O., Clegg, S.M., Cousin, A., Thomas, N.H., Lasue, J., Delapp, D.M., McInroy, R.E., Gasnault, O., Dyar, M.D., Maurice, S., Wiens, R.C. (2016) Emission Lines Selected for the identification of chlorides, carbonates, and sulfates dispersed in basaltic rock using laser-induced breakdown spectroscopy (LIBS). *Lunar Planet. Sci. XLVII*, Lunar Planet. Inst., Houston, (abstr.) #2303.
458. Mueller, N., Tsang, C., Smrekar, S., Helbert, J., and Dyar, M.D. (2016) Venus atmosphere variability as error source for surface emissivity. *Lunar Planet. Sci. XLVII*, Lunar Planet. Inst., Houston, (abstr.) #2260.
459. Dyar M.D., Breitenfeld, L.B., Carey, CJ, Bartholomew, P., Tague, T.J., Wang, P., Mertzman, S., Byrne, S.A., Crowley, M.C., Leight, C., Watts, E., Campbell, J.C. Celestian, A., McKeeby, B., Jaret, S. Glotch, T., Berlanga, G., and Misra, A.K. (2016) Interlaboratory and cross-instrument comparison of Raman spectra of 96 minerals. *Lunar Planet. Sci. XLVII*, Lunar Planet. Inst., Houston, (abstr.) #2240.
460. Dehouck, E., McLennan, S.M., Sklute, E.C., and Dyar, M.D. (2016) Stability of 2-line ferrihydrite at Gale Crater, Mars: Experimental approach. *Lunar Planet. Sci. XLVII*, Lunar Planet. Inst., Houston, (abstr.) #2223.
461. Dyar, M.D., Breves, E.A., Sklute, E.C. (2016) Facilities for Mössbauer and laser-induced breakdown spectroscopy at Mount Holyoke College. *Lunar Planet. Sci. XLVII*, Lunar Planet. Inst., Houston, (abstr.) #2205.
462. Kashyap, S., Sklute, E.C., Holden, J.F., Dyar, M.D. (2016) Characterization of nanophase iron oxides produced through bioreduction by hyperthermophiles. *Lunar Planet. Sci. XLVII*, Lunar Planet. Inst., Houston, (abstr.) #2223.
463. Lepore, K.H., Giguere, S., Boucher, T., Byrne, S., Fassett, C.I., and Dyar, M.D. (2016) Univariate vs. multivariate models for predictions of major and trace elements from LIBS spectra with and without masking. *Lunar Planet. Sci. XLVII*, Lunar Planet. Inst., Houston, (abstr.) #2191.
464. Breitenfeld, L.B., Dyar, M.D., Tague, T.J., Wang, P., Mertzman, S., Byrne, S.A., Crowley, M.C., Leight, C., and Watts, E. (2016) Quantifying mineral abundances in mixtures using Raman spectroscopy: Calculating Raman coefficients using a diamond reference. *Lunar Planet. Sci. XLVII*, Lunar Planet. Inst., Houston, (abstr.) #2186.
465. Filiberto, J., Knafelc, J., Dyar, M.D., Ferre, E.C., Friedman, S.A., Walsh, K., and Feinberg, J.M. (2016) Olivine oxidation and implications for planetary processes. *Lunar Planet. Sci. XLVII*, Lunar Planet. Inst., Houston, (abstr.) #2171.
466. Bridges, J.C., Edwards, P.H., Anderson, R., Dyar, M.D., Fisk, M., Thompson, L., Gasda, P., Schwenzer, S.P., Goetx, W., Blaney, D., Filiberto, J., and Wiens, R.C. (2016) Igneous differentiation on Mars: Trachybasalts in Gale Crater./ *Lunar Planet. Sci. XLVII*, Lunar Planet. Inst., Houston, (abstr.) #2160.

467. Sklute, E.C., Hiroi, T., Pieters, C., Milliken, R., Glotch, T.D., and Dyar, M.D. (2016) Preliminary VNIR optical constants of bytownite using radiative transfer theory. *Lunar Planet. Sci. XLVII*, Lunar Planet. Inst., Houston, (abstr.) #2147.
468. Sklute, E.C., Dyar, M.D., Kashyap, S., Holden, J.F., and Jaret, S. (2016) Spectral characteristics of nanophase iron oxides and hydroxides. *Lunar Planet. Sci. XLVII*, Lunar Planet. Inst., Houston, (abstr.) #2112.
469. Helbert, J., Matturilli, A., Ferrari, S., Dyar, M.D., Muller, N., ands Smrekar, S. (2016) Progress on studying the surface composition of Venus in the near-infrared. *Lunar Planet. Sci. XLVII*, Lunar Planet. Inst., Houston, (abstr.) #1947.
470. Helbert, J., Wendler, D., Walter, I., Widemann, T., Marcq, E/. Maturilli, A., Ferrari, S., D'Amore, Muller, N., Dyar, M.D., Smrekar, S. (2016) The Venus Emissivity Mapper (VEM) concept. *Lunar Planet. Sci. XLVII*, Lunar Planet. Inst., Houston, (abstr.) #1913.
471. Rogers, A.D., Gregerson, J., Sklute, E.C., Rucks, M., Jensen, H.B., Reeder, R.J., and Dyar, M.D. (2016) Sequestration of mixed salts in the amorphous soil fraction on Mars. *Lunar Planet. Sci. XLVII*, Lunar Planet. Inst., Houston, (abstr.) #1736.
472. Wiens, R.C., Mangold, N., Maurice, S., Gasnault, O., Clegg, S.M., Blaney, D.L., Gasda, P., Frydenvang, J., Forni, O., Cousin, A., Lasue, J., Lanza, N., Anderson, R.B., Sautter, V., Bridges, J., Le Deit, L., Nachon, M., Rapin, W., Mesline, P.-Y., Newsom, H., Clark, B., Vaniman, D., Bridges, N., Herkenhoff, K., Ehlmann, B., Dyar, M.D., Fisk, M., Francis, R., Leveille, R., Johnson, J.R., Melikechi, N., Jackson, R., Fabre, C., Payre, V., Grotzinger, J.P., Vasavada, A.R., Crisp, J. (2016) Major-element compositions seen by ChemCam along the Curiosity rover traverse: The first 8,000 observations. *Lunar Planet. Sci. XLVII*, Lunar Planet. Inst., Houston, (abstr.) #1336.
473. Giguere, S., Dyar, M.D., Carey, C., Boucher, T., Mahadevan, S. (2016) A fully-customized baseline removal framework. *Lunar Planet. Sci. XLVII*, Lunar Planet. Inst., Houston, (abstr.) #1321.
474. Giguere, S., Dyar, M.D., Carey, C., Boucher, T., and Mahadevan, S. (2016) Fully-customized baseline removal applied to LIBS spectroscopy under Mars conditions. *Lunar Planet. Sci. XLVII*, Lunar Planet. Inst., Houston, (abstr.) #1318.
475. Breves, E.A., Lepore, K., Dyar, M.D., Bender, S.C., and Tokar, R. (2016) Laser-induced breakdown spectra of rock powders at variable ablation and collection angles under a Mars-analog atmosphere. *Lunar Planet. Sci. XLVII*, Lunar Planet. Inst., Houston, (abstr.) #1318.
476. Carey, CJ, and Dyar, M.D. (2016) Whole spectrum unmixing for Raman and FTIR applications. Sci-X 2016, Minneapolis, Abstract #162.
477. Gemp, I., Dyar, D., Parente, M., Saranath, A. (2016) Deep Semi-Supervised Generative Models for spectroscopic data. Sci-X 2016, Minneapolis, Abstract #710.
478. Boucher, T., and Dyar, D. (2016) Big data for extraterrestrial spectroscopy. Sci-X 2016, Minneapolis, Abstract #712.
479. Lepore, K., Fassett, C., Breves, E., Giguere, S., Boucher, T., Rhodes, J.M., Vollinger, M., Anderson, C., Murray, R., and Dyar, R. (2016) Quantitative analysis of rock powders doped with Cr, Mn, Ni, Zn, and Co. Sci-X 2016, Minneapolis, Abstract #861.
480. Dyar, M.D., Giguere, S., Carey, CJ, Boucher, T., and Gemp, I. (2016) Baseline removal versus feature selection in LIBS. Sci-X 2016, Minneapolis, Abstract #862.
481. Dyar, M.D. (2016) The future of spectroscopy. GSA National Meeting, Denver, paper 197-1.
482. McCanta, M., Dyar, M.D., Rutherford, M., and Lanzirotti, A. (2016) In situ measurements of ferric iron in lunar glass beads using Fe-XAS. GSA National Meeting, Denver, paper 197-7.
483. McEnroe, S., Robinson, P., Dyar, M.D., Tegner, C., and Church, N. (2016) Crystal magnetic signature of planets: Tracking the solid solution of Fe and exsolution of magnetite in plagioclases of 21.05 Ga rocks from the Bushveld Complex, South Africa, by magnetic, chemical, and Mössbauer properties. GSA National Meeting, Denver, paper 197-14.
484. Sklute, E.C., Dyar, M.D., Kashyap, S., and Holden, JH. (2016) The challenge of distinguishing iron (hydr)oxides and what It meanbs for Mars. GSA National Meeting, Denver, paper 197-10.
485. Klima, R.L., Dyar, M.D., Lane, M.D., and Glotch, T. (2016) Synthetic pyroxenes: Strengthening the foundation of remote geochemical analysis. GSA National Meeting, Denver, paper 197-5.
486. Fassett, C.I., Dyar, M.D., and Lepore, K. (2016) Attempting to quantify meteoritic contamination of Mars sediments at the MSL landing site. GSA National Meeting, Denver, paper 197-9.
487. Carey, C., Dyar, M.D., Boucher, T., and Giguere, S. (2017) Web-based software for preprocessing, matching, fitting, prediction and visualization of spectroscopic data: The data exploration, visualization, and

Analysis of Spectra (DEVAS) website. *Lunar Planet. Sci. XLVIII*, Lunar Planet. Inst., Houston, (abstr.) #1097.

488. Dyar, M.D., Helbert, J., Boucher, T., Wendler, D., Walter, I., Widemann, T., Marcq, E., Maturilli, A., Ferrari, S., D'Amore, M., Mueller, N., and Smreker, S. (2017) Probing rock type, Fe redox state, and transition metal contents with six-window VNIR spectroscopy under Venus conditions. *Lunar Planet. Sci. XLVIII*, Lunar Planet. Inst., Houston, (abstr.) #3014.
489. Ytsma, C.R., Dyar, M.D., Lepore, K.M., Waggoner, C., and Hanlon, A. (2017) Normalization and baseline removal effects on univariate and multivariate hydrogen prediction accuracy using laser-induced breakdown spectroscopy. *Lunar Planet. Sci. XLVIII*, Lunar Planet. Inst., Houston, (abstr.) #2979.
490. Leight, C., Fassett, C.I., Crowley, M.C., and Dyar, M.D. (2017) Crater morphometry and degradation on Mercury: Mercury Laser Altimeter (MLA) measurements and comparison to stereo-DTM derived results. *Lunar Planet. Sci. XLVIII*, Lunar Planet. Inst., Houston, (abstr.) #2809.
491. Wendler, D., Helbert, J., Walter, I., Widemann, T., Guignan, G., Marcq, E., Maturilli, A., Ferrari, S., D'Amore, M., Meller, N., Dyar, M., and Smrekar, S. (2017) Yhe Venus Emissivity Mapper (VEM) prototype. *Lunar Planet. Sci. XLVIII*, Lunar Planet. Inst., Houston, (abstr.) #2645.
492. Berlanga, G., Dyar, M.D., Breitenfeld, L., Wagoner, C., Hanlon, A., Bartholomew, P., Dharma, S.K., and Misra, A.K. (2017) Detection limits for silicates in Raman spectra of mixtures with volcanic glass. *Lunar Planet. Sci. XLVIII*, Lunar Planet. Inst., Houston, (abstr.) #2255.
493. Mueller, N., Tsang, C.C., Smrekar, S., Helbert, J., and Dyar, M.D. (2017) Derivation of thermal emission from VIRTIS on Venus Express 1000–1400 nm spectra. *Lunar Planet. Sci. XLVIII*, Lunar Planet. Inst., Houston, (abstr.) #2200.
494. Gregerson, J., Rogers, A.D., Sklute, E.C., Reeder, R.J., and Dyar, M.D. (2017) Phase transitions of amorphous iron(III) sulfates at an intermediate humidity. *Lunar Planet. Sci. XLVIII*, Lunar Planet. Inst., Houston, (abstr.) #2100.
495. Breitenfeld, L.B., Dyar, M.D., Carey, C., Tague, T.J., and Wang, P. (2017) Predicting olivine composition using Raman spectroscopy through band shift and multivariate analysis. *Lunar Planet. Sci. XLVIII*, Lunar Planet. Inst., Houston, (abstr.) #1898.
496. Gemp, I., Durughar, I., Parente, M., Dyar, M.D., and Mahadevan, S. (2017) Deep learning models for spectroscopic data: Semi-supervised generative models applied to laser-induced breakdown spectroscopic data. *Lunar Planet. Sci. XLVIII*, Lunar Planet. Inst., Houston, (abstr.) #1696.
497. Lanzirotti, A., Dyar, M.D., Sutton, S.R., Newville, M., Head, E., Carey, C., McCanta, M., and Jones, J. (2017) Preliminary calibration for accurate predictions of microscale oxygen barometry in silicate glasses using vanadium X-ray absorption spectroscopy: A multivariate approach. *Lunar Planet. Sci. XLVIII*, Lunar Planet. Inst., Houston, (abstr.) #1650.
498. Helbert, J., Maturilli, A., Dyar, M.D., Ferrari, S., Mueller, N., and Smrekar, S. (2017) First set of laboratory Venus analog spectra for all atmospheric windows. *Lunar Planet. Sci. XLVIII*, Lunar Planet. Inst., Houston, (abstr.) #1512.
499. McCanta, M.C., and Dyar, M.D. (2017) Visible/near-infrared spectra of Ca-pyroxene: Effects of Fe^{3+} and shock. *Lunar Planet. Sci. XLVIII*, Lunar Planet. Inst., Houston, (abstr.) #1431.
500. Rader, L.X., Fassett, C.I., Levy, J.S., King, I.R., Chaffey, P., Wagoner, C., Hanlon, Watters, J.L., Kreslavsky, M.A., Holt, J.W., and Dyar, M.D. (2017) The geographic distribution of boulder halo craters at mid-to-high latitudes on Mars. *Lunar Planet. Sci. XLVIII*, Lunar Planet. Inst., Houston, (abstr.) #1294.
501. Lepore, K.H., Mackie, J., Dyar, M.D., Ytsma, C., and Fassett, C.I. (2017) Unreported emission lines of Ce, La, Pb, Rb, Se, Sr, Y, and Zr detected using laser-induced breakdown spectroscopy. *Lunar Planet. Sci. XLVIII*, Lunar Planet. Inst., Houston, (abstr.) #1293.
502. Mackie, J., Dyar, M.D., Ytsma, C., Lepore, K., Fassett, C.I., Hanlon, A., Wagoner, C., and Treiman, A. (2017) Standards for analysis of Ce, La, Pb, Rb, Se, Sr, Y, and Zr in rock samples using laser-Induced breakdown spectroscopy and X-ray fluorescence. *Lunar Planet. Sci. XLVIII*, Lunar Planet. Inst., Houston, (abstr.) #1292.
503. Lepore, K.H., Breves, E.A., Dyar, M.D., Bender, S.C., and Tokar, R.L. (2017) Laser-induced breakdown spectroscopy of rock powders performed at variable angles of ablation and collection. *Lunar Planet. Sci. XLVIII*, Lunar Planet. Inst., Houston, (abstr.) #1122.
504. Sklute, E.C., Carey, C., Dyar, M.D., and Glotch, T.G. (2017) Web-based, open-source, visible and near-infrared optical constant determination of geological materials. *Lunar Planet. Sci. XLVIII*, Lunar Planet. Inst., Houston, (abstr.) #1071.

505. Dyar, M.D., Helbert, J., Maturilli, A., Ferrari, S., Müller, N., and Smrekar, S. (2017) Emissivity measurements for hot planetary surfaces. GSA, Seattle, Paper #54-1.
506. Lanzirotti, A., Sutton, S.R., Dyar, M.D., McCanta, M.C., and Head, E. (2017) Advances in high-resolution synchrotron micro-XANES for constraining the redox evolution of terrestrial and extraterrestrial magma. Fall AGU, Abstract #V53B-08.
507. Helbert, J., Dyar, M.D., Maturilli, A., D'Amore, M., Ferrari, S., Müller, N., and Smrekar, S. (2017) Venus surface peeking through the atmosphere - gaining a global perspective on the surface composition through near infrared observations. Fall AGU, Abstract #P13G-02.
508. Dyar, M.D., Boucher, T.F., Parente, M., Gemp, I., and Mullen, T.H. (2017) Calibration transfer in LIBS and Raman spectroscopy for planetary applications. Fall AGU, Abstract #P13G-01.
509. Mullen, T.H., Parente, M., Gemp, I., and Dyar, M.D. (2017) A deep learning approach to LIBS spectroscopy for planetary applications. Fall AGU, Abstract #P11E-2542.
510. Müller, N., Tsang, C., Nunes, D.C., Helbert, J., Dyar, M.D., and Smrekar, S.E. (2017) Near-infrared multispectral mapping of Venus supports the hypothesis that tessera plateau material was formed in the presence of surface water. Fall AGU, Abstract #P53A-2645.
511. Kashyap, S., Sklute, E., Dyar, M.D., and Holden,J.F. (2017) Biogenic iron oxide transformation by hyperthermophiles: spectral and physiological potentials. Fall AGU, Abstract #P41B-2837.
512. Fassett, C., Crowley,M.C., Leight, C., Dyar, M.D., Minton, D., Hiranayashi, M., Thomson, B.J., and Watters, W.A. (2017) Using measurements of topography to infer rates of crater degradation and surface evolution on the Moon and Mercury. Fall AGU, Abstract #P24C-01.
513. Rader, L.X., Thomson, B.J., Fassett, C.I., Beyer, R.A., and Dyar, M.D. (2018) Mapping stratigraphic layers of exposed impact craters on the edge of Valles Marineris. *Lunar Planet. Sci. XLIX*, Lunar Planet. Inst., Houston, (abstr.) #2723.
514. Ytsma, C.R., Dyar, M.D., Lepore, K., and Ostrand, C. (2018) Predicting lithium, boron, carbon, and sulfur under vacuum, Earth, and Martian atmospheres. *Lunar Planet. Sci. XLIX*, Lunar Planet. Inst., Houston, (abstr.) #2409.
515. Lane, M.D., Klima, R.L., Glotch, T.D., and Dyar, M.D. (2018) Mid-infrared spectra of synthetic pyroxenes over the entire Ca-Mg-Fe quadrilateral. *Lunar Planet. Sci. XLIX*, Lunar Planet. Inst., Houston, (abstr.) #2722.
516. Clegg, S.M., Dyar, M.D., Newell, R.T., DeCroix, D.S., Okhuysen, B.S., Sharma, S.K., Maurice, M., Wiens, R.C., and Glaze, L. (2018) Venus elemental and mineralogical camera (VEMCAM). *Lunar Planet. Sci. XLIX*, Lunar Planet. Inst., Houston, (abstr.) #2676.
517. Orlando, T.M., Jones, B., Alexandrov, A., Hibbitts, C.A., and Dyar, M.D. (2018) Diurnal variation of th solar wind-induced optical signature of water on the lunar surface. *Lunar Planet. Sci. XLIX*, Lunar Planet. Inst., Houston, (abstr.) #1660.
518. Valvur, H.T., Kashyap, S., Sklute, E., Holden, J.F., Wang, P., Tague, T.J., and Dyar, M.D. (2018) Spectroscopy of nanophase iron (oxyhydr)oxides bioreduce by *Geobacter Metallireducens*. *Lunar Planet. Sci. XLIX*, Lunar Planet. Inst., Houston, (abstr.) #1439.
519. Mikuchi, J., Lee, P.A., Dyar, M.D., Sklute, E.C., and Taylor, E. (2018) Ice-covered chemosynthetic ecosystems: Mineral availability and microbiological accessibility (ICE-MAMBA). *Lunar Planet. Sci. XLIX*, Lunar Planet. Inst., Houston, (abstr.) #1361.
520. Helbert, J., Maturilli, A., Dyar, M.D., Ferrari, S., Müller, N., and Smrekar, S. (2018) Orbital spectroscopy of the surface of Venus. *Lunar Planet. Sci. XLIX*, Lunar Planet. Inst., Houston, (abstr.) #1219.
521. Mullen, T., Parente, M., and Dyar, M.D. (2018) Domain adversarial neural networks applied to laser-induced breakdown spectroscopy. *Lunar Planet. Sci. XLIX*, Lunar Planet. Inst., Houston, (abstr.) #1182.
522. Mullen, T., Dyar, M.D., Parente, M., and Breitenfeld, L. (2018) Improving matching accuracy in Raman spectroscopy by quantifying the wavenumber shift in Raman spectroscopy between instruments. *Lunar Planet. Sci. XLIX*, Lunar Planet. Inst., Houston, (abstr.) #1185.

523. Lepore, K.H., Dyar, M.D., and Remi, S. (2018) SuperLIBS: A high-capacity laser-induced breakdown spectroscopy system analogous to SuperCam Mars 2020. *Lunar Planet. Sci. XLIX*, Lunar Planet. Inst., Houston, (abstr.) #1179.
524. Sklute, E.C., Kashyap, S., Wang, P., Tague, T.J. Jr., Dyar, M.D., and Holden, J.F. (2018) FTIR and Raman spectroscopic analysis of nanophase iron (oxyhydr)oxides bioreduced by hyperthermophilic archaea. *Lunar Planet. Sci. XLIX*, Lunar Planet. Inst., Houston, (abstr.) #1153.
525. King, J.L., Watts, J.C., Dyar, M.D., Bleacher, J., McAdam, A., Hurowitz, J., and Young, K. (2018) Comparison of univariate and multivariate calibration methods for geological trace elements with handheld XRF. *Lunar Planet. Sci. XLIX*, Lunar Planet. Inst., Houston, (abstr.) #1176.
526. King, J.L., Watts, J.C., Dyar, M.D., Bleacher, J., McAdam, A., Hurowitz, J., and Young, K. (2018) Preliminary comparison of handheld XRF spectrometers for geological univariate calibrations. *Lunar Planet. Sci. XLIX*, Lunar Planet. Inst., Houston, (abstr.) #1172.
527. Watts, J.C., King, J.L., Dyar, M.D., Ytsma, C., Bleacher, J., McAdam, A., Hurowitz, J., and Young, K. (2018) Filter selectioin for analysis of geological samples with handheld Bruker Tracer XRF. *Lunar Planet. Sci. XLIX*, Lunar Planet. Inst., Houston, (abstr.) #1169.
528. Kashyap, S., Sklute, E., Ross, L., Emerson, D., Tague, T.J. Jr., Wang, P., Holden, J.F., and Dyar, M.D. (2018) Spectroscopic characterization of natural biogenic iron (oxyhydr)oxides from freshwater and marine environments. *Lunar Planet. Sci. XLIX*, Lunar Planet. Inst., Houston, (abstr.) #1130.
529. Lane, M.D., Allain, J.P., Cahill, K.S., Clark, R.N., Cloutis, E.A., Dyar, M.D., Helbert, J., Hendrix, A.R., Holsclaw, G., Osterloo, M., Pearson, N., Savin, D.W., and the TREX team. Toolbox for research and exploration (TREX): The fine particle spectral library. *Lunar Planet. Sci. XLIX*, Lunar Planet. Inst., Houston, (abstr.) #1098.
530. McCanta, M.C., Dyar, M.D., Breitenfeld, L., and Lanzirotti, A. (2018) Mapping ferric iron variation in lunar glass beads: Observing changing oxidation conditions in situ. *Lunar Planet. Sci. XLIX*, Lunar Planet. Inst., Houston, (abstr.) #1073.
531. McCanta, M.C., Dyar, M.D., Steven, C., Gunter, M., and Lanzirotti, A. (2018) In situ measurements of Fe^{3+} in pyroxene using x-ray absorption spectroscopy using an oriented crystal calibration to refine geothermobarometric calculations. *Lunar Planet. Sci. XLIX*, Lunar Planet. Inst., Houston, (abstr.) #1074.
532. Dyar, M.D., McCanta, M.C., Lanzirotti, A., Gunter, M., Steve, C., Breitenfeld, L., and Wagoner, C. (2018) Orientation dependence of vanadium x-ray absorption spectra: Implications for studies of V valence and resultant fugacity. *Lunar Planet. Sci. XLIX*, Lunar Planet. Inst., Houston, (abstr.) #1067.
533. Sklute, E.S., Kashyap, S., Wang, P., Tague, T.Jr., Dyar, M.D., and Holden, J.F. (2018) Effects of surrounding medium (fluid vs. air) on spectral properties of nanophase iron (oxyhydr)oxides. *Lunar Planet. Sci. XLIX*, Lunar Planet. Inst., Houston, (abstr.) #1064.
534. Breitenfeld, L.B., Dyar, M.D., Tokle, L., and Robertson, K. (2018) Predicting ilmenite-geikielite composition using Raman spectroscopy. *Lunar Planet. Sci. XLIX*, Lunar Planet. Inst., Houston, (abstr.) #1072.
535. Levy, J.S., Fassett, C.I., Rader, L.X., King, I.R/. Chaffey, P.M., Wagoner, C.M., Hanlon, A.E., Watters, J.L., Kreslabsky, M.A., Holt, J.W., Russell, A.T., and Dyar, M.D. (2018) Distribution and characteristics of boulder halos at high latitudes on Mars: Reworking of sediment and ice indicates boulders outlast the craters that excavate them. *Lunar Planet. Sci. XLIX*, Lunar Planet. Inst., Houston, (abstr.) #1093.
536. Cohen, B.A., Petro, N.E., Lawrence, S.J., Dyar, M.D., Elardo, S.M., Grinspoon, D.H., Hiesinger, H., Liu, Y., McCanta, M.C., Norman, M.D., Schwenzer, S.P., Swindle, T.D., vander Bogert, C.H., and Wiens, R.C. (2018) CURIE: Constrainging solar system bombardment using in situ radiometric dating. *Lunar Planet. Sci. XLIX*, Lunar Planet. Inst., Houston, (abstr.) #1029.

537. Widemann, T., Marcq, E., Tsang, C., Mueller, N., Kappel, D., Helbert, J., and Dyar, M.D. (2018) The Venus Emissivity Mapper — Investigating the atmospheric structure and dynamics of Venus' polar region. *Lunar Planet. Sci. XLIX*, Lunar Planet. Inst., Houston, (abstr.) #2386.
538. Breitenfeld, L.B., and Dyar, M.D. (2018) Calculating mineral Raman Coefficients using a diamond reference. *GeoRaman-8*, p. 26.
539. Breitenfeld, L.B., and Dyar, M.D. (2018) Effect of grain size on Raman signal of silicates. *GeoRaman-8*, p. 121.
540. Dyar, M.D., and Breitenfeld, L.B. (2018) Predicting pyroxene composition with Raman spectroscopy through use of machine learning approaches. *GeoRaman-8*, p. 30.
541. Dyar, M.D., Helbert, J., Maturilli, A., Walter, I., Widemnn, T., Marcq, E., Ferrar, S., D'Amore, M., Muller, N., and Srekar, S. (2018) Venus surface oxidation and weathering as viewed from orbit with six-window VNIR spectroscopy. *VEXAG 15*, Abstract #8015.
542. Helbert, J., Dyar, D., Walter, I., Wendler, D., Widemann, T., Marcq, E., Guignan, G., Maturilli, A., Ferrari, S., Mueller, N., Kappel, D., D'Amore, M., Boerner, A., Tsang, C., Arnold, G., Smreekar, S., and Ghail, R. (2018) The Venus Emissivity Mapper (VEM) — Obtaining global mineralogy of Venus from orbit. *VEXAG 15*, Abstract #8023.
543. Lepore, K., and Dyar, M.D. (2019) Temporal changes in LIBS spectra observed using time-series collection protocols. *LPSC L*, Abstract #1095.
544. Watts, J.C., King, J., Mulkahey, C., Tremblay, C., and Dyar, M.D. (2019) Preliminary assessment of the effect of bulk composition on accuracy of Olympus Delta pXRF analyses. *LPSC L*, Abstract #1074.
545. Ytsma, C.R., and Dyar, M.D. (2019) Updated hydrogen, lithium, boron, carbon, and sulfur prediction accuracies with LIBS under vacuum, Earth, and martian atmospheres. *LPSC L*, Abstract #1081.
546. Izenburg, N.R., and Dyar, M.D (2019) VEXAG Venus Exploration documents 2019 update. *LPSC L*, Abstract #1083.
547. Lepore, K., Ytsma, C., and Dyar, M.D. (2019) Comparisons among laser-induced breakdown spectra from ChemCam, ChemLIBS, and SuperLIBS. *LPSC L*, Abstract #1103.
548. McCanta, M.C., and Dyar, M.D. (2019) Effects of oxidation and shock on pyroxene spectral features. *LPSC L*, Abstract #1383.
549. Ytsma, C.R., Hurowitz, J., and Dyar, M.D. (2019) LIBS and PIXL Prediction accuracies for Ni, Mn, S, and mMajor elements: A comparative study using the same standards. *LPSC L*, Abstract #1080.
550. Dyar, M.D., Ytsma, C.R., and Lepore K. (2019) Standards for geochemical aAnalysis of major, minor, and trace elements in rock powders. *LPSC L*, Abstract #1396.
551. Burbine, T.H., Wallace, S.M., and Dyar M.D. (2019) Applying the Bus-DeMeo asteroid taxonomy to meteorite spectra. *LPSC L*, Abstract #1655.
552. Breitenfeld, L.B., Dyar, M.D., Tremblay, C. (2019) Quantification of mineral abundances in binary mixtures using Raman spectroscopy and multivariate analysis. *LPSC L*, Abstract #1754.
553. Rollosson, L.M., Michaud, D.D., Ytsma, C.R., and Dyar, M.D. (2019) Accuracy of univariate analysis of major, minor, and trace elements in doped samples using SciAps Z-300 portable LIBS, *LPSC L*, Abstract #1077.
554. Michaud, D.D., Rollosson, L.M., Ytsma, C.R., and Dyar, M.D. (2019) Limits of detection for minor and trace elements using SciAps Z-300 Portable LIBS. *LPSC L*, Abstract #1079.
555. Wallace, S.M., Burbine, T.H., Sheldon, D, and Dyar, M.D. (2019) Machine learning applied to asteroid taxonomy based on reflectance spectroscopy: An objective method. *LPSC L*, Abstract #1097.
556. Roberts, S.E., Sheffer, A.A., McCanta, M.C., Dyar, M.D., and Sklute, E.C (2019) Investigating redox change during impacts. *LPSC L*, Abstract #1285.

557. Sklute, E.C., Taylor, E.C., Mikuchi, J.A., Dyar, M.D., and Lee, P.A. (2019) Preliminary FTIR of bioreduction products from the halotolerant and psychrotolerant Shewanella strain, BF02, an important astrobiological analogue microbe. *LPSC L*, Abstract #1430.
558. Glotch, T.D., Ye, C., Young, J.M., Londsley, D.H., Nekvasil, H., Dyar, M.D., and Sklute, E.C. (2019) Spectroscopy of synthetic pigeonite standards. *LPSC L*, Abstract #2420.
559. Steven, C.J., Dyar, M.D., McCanta, M.C., Lanzarotti, A., Leight, C., Wagoer, C., Breitenfeld, L.B., and Gunter, M.E. (2019) Toward quantifying oxygen fugacity in Solar System materials: In situ multivalent element analyses in pyroxene. *LPSC L*, Abstract #1393.
560. Orlando, T.M., Clendenen, A.R., Schieber, G.L., Jones, B.M., Loutzenhiser, P.D., Aleksandrov, A.B., Hibbitts, C.A., and Dyar, M.D. (2019) Formation, transport, and release of molecular water on and within lunar materials. *LPSC L*, Abstract #2267.
561. Helbert, J., Dyar, D., Walter, I., Rosas-Ortiz, Y., Widemann, T., Marcq, E., Guignan, G., MAturilli, A., Varatharajan, I., Ferrari, S., Mueller, N., Kappel, D., D'Amore, M., Boerner, A., Tsang, C., Arnold, G., Smrekar, S, and Ghail, R. (2019) The Venus Emissivity Mapper — Obtaining Global Mineralogy of Venus from Orbit on the ESA EnVision and NASA VERITAS Missions to Venus. *LPSC L*, Abstract #2046.

Theses Supervised:

Reich, D.R. (M.S., University of Oregon, 1989) Geology and Petrology of the Mt. Emily Volcanic Center.
Hull, C.D. (Ph.D., University of Oregon, 1990) Multicomponent Chemical Equilibrium Modeling of Fluids and U-Th Geochronology of Minerals in Geothermal Systems.
Harrell, M.D. (Honors College, B.A., University of Oregon, 1991) *In situ* Alteration of a Rock from the Earth's Mantle
Moeller, K. J. (M.S., University of Oregon, 1991) Crystal Chemistry of Chlorites from Metapelites.
Grant, C. G. (Ph.D., 1995, Chemistry, University of Oregon) Sources of Experimental and Analytical Error in Measurements of the Mössbauer Effect in Amphibole.
Taylor, M.E. (M.A., West Chester University, 1996) Crystal Chemistry of Iron in Tourmaline.
Voci, Christopher (M.A., West Chester University, 1996) Pb Stability in Pyromorphite from Landfills.
Stefanis, M. (B.A., Mount Holyoke College, 1999) An Interpretation of the Rocks at the Mars Pathfinder Landing Site.
Polyak, D.E. (B.A., Mount Holyoke College, 1999) Crystal Chemistry of Iron in Plagioclase from Four Heavenly Bodies.
Blackwell, M.A. (B.A., Mount Holyoke College, 2000) Recoil-free Fraction Effects in Amphibole.
Lowe, E.W. (B.A., Mount Holyoke College, 2000) Distribution Coefficients for Fe^{3+} and Fe^{2+} in Metapelites from Western Maine.
Cartwright, B.M. (M.S., University of Massachusetts, 2003) Plagioclase Fe^{3+}/Fe^{2+} Correlation with Magma Oxygen Fugacity in a Volcanic Succession: The Atascosa Mountains, South-central Arizona. Co-supervised with Sheila Seaman.
Makuch, L.B. (B.A., University of Massachusetts, 2002) The Ares Project. Honors College.
Therkelsen, J.B. (B.A., Amherst College, 2002) Shock-induced changes in redox state of experimentally shocked plagioclase, pyroxene, and olivine.
Peek, K.M. (B.A., Mount Holyoke College, 2002) The disruption of an icy satellite and the evolution of the resulting debris ring. A formation scenario for Saturn's rings.
Dickson, J. (B.A., Hampshire College, 2002) Water on Mars: A synthesis of hydrologic features on the surface of Mars.
Daane, A.R. (B.A., Mount Holyoke College, 2004) Brightness and color variations in the hot pulsating horizontal branch star PG1627+017.
Hunter, M.O. (B.A., Mount Holyoke College, 2004) Pacific Equatorial Current systems during the waning of the 2002-2003 El Niño.

O'Connor, V. (B.A., Smith College, 2005) Comparative crystal chemistry of hydrous iron sulfates from different terrestrial environments.
Dopfel, E. (B.A., Mount Holyoke College, 2006) The chemical activators of cathodoluminescence in jadeite.
Sklute, E.C. (B.A., Mount Holyoke College, 2006) Mössbauer spectroscopy of synthetic olivine across the Fe-Mg solid solution.
Rothstein, Y. (B.A., Mount Holyoke College, 2006) Spectroscopy of jarosite and implications for the mineralogy of Mars.
Howenstine, J. (B.A., University of Massachusetts, 2006) Analysis of depth-diameter relationship of martian craters.
Bendersky, C. (B.A., Mount Holyoke College, 2007) The onset of thermal metamorphism in enstatite chondrites.
Walker, C.A. (B.A., Mount Holyoke College, 2007) Variations of solar wind parameters over a solar cycle: Expectations for NASA's Solar Terrestrial Relations Observatory (STEREO) Mission.
Graham, S. (B.A., Mount Holyoke College, 2007) GPS geodetic constraints on the November 21, 2004 Mw 6.3 earthquake off the northwest coast of Dominica: implications for in situ volatile solubilities and eruptions dynamics.
Barkley, M. (B.A., Mount Holyoke College, 2007) The effects of F-OH^- substitution on the crystal structure of pegmatitic topaz.
Cadieux, Sarah Beth (B.A., Mount Holyoke College, 2008) Carbon-isotope stratigraphy of Upper Cretaceous deposits of the Dalmatian Island of Brač, Croatia.
Langford, Amy (B.A., Mount Holyoke College, 2008) Unbiased search for molecular outflows in the Taurus Molecular Cloud.
Emerson, Erica (B.A., Mount Holyoke College, 2008) Analysis of iron oxidation in garnets.
Tucker, Jonathan (B.A., Amherst College, 2009) Calibrating ChemCam: Preparing to Probe the Red Planet.
Knutson, J.K. (B.A., Mount Holyoke College, 2010) Exploring biotite iron transformation by the hyperthermophilic archaeon Pyrobaculum Islandicum.
Barbieri, Lindsay (B.A., Hampshire College, 2010) Deciphering Late-Amazonian climate change on Mars using evidence preserved in gully fan stratigraphy.
Bell, S. (B.A., Amherst College, 2011) Fresh lunar crater ejecta as revealed by the Miniature radio Frequency (Mini-RF) instrument on the Lunar Reconnaissance Orbiter.
Ozanne, M.V. (B.A. Mount Holyoke College, 2012) Comparison of shrunken regression methods for major elemental analysis of rocks using laser-induced breakdown spectroscopy (LIBS).
DeVeaux, M.L. (B.A. Mount Holyoke College, 2012) Evaluation of statistical methods for classification of laser-induced breakdown spectroscopy (LIBS) data.
Williams, Molly (B.A., Mount Holyoke College, 2012) Characterizing Fe(III) transformation in a deep-sea hyperthermophilic archaeon.
Kashyap, Srishti (B.A., Mount Holyoke College, 2013) Isolating and characterizing an Fe(III) transforming deep sea thermophilic archaeon.
Breitenfeld, Laura (B.A., Mount Holyoke College, 2017) Predicting olivine composition using Raman spectroscopy through band shift and multivariate nnalyses.
Ytsma, Caroline (B.A. Smith College, 2018) Univariate and multivariate quantification of hydrogen, lithium, boron, carbon, and sulfur under vacuum and in Earth and Mars atmospheres using laser-induced breakdown spectroscopy.
Carey, CJ (Ph.D., University of Massachusetts, 2018) Graph construction for manifold discovery.
Boucher, Thomas (Ph.D., University of Massachusetts, 2018) Transfer learning with mixtures of manifolds.

Graduate Committees:
McCanta, Molly (Ph.D., Brown University, 2004)

Buczkowski, Debra (Ph.D., University of Massachusetts, 2006)
Keskula-Snyder, Anna (Ph.D., University of Massachusetts, 2006)
Klima, Rachel (Ph.D., Brown University, 2007)
Amy Stander (MS, URI, 2013)
Tommy Boucher (Ph.D., UMass, 2018 Computer Science)
C.J. Carey (Ph.D., UMass, 2017, Computer Science)
S. Giguere (Ph.D., UMass, current student, Computer Science)
S. Kashyap (Ph.D., UMass, current student, Microbiology)

EXTERNAL GRANT:

PREVIOUS FUNDING:

American Chemical Society, Petroleum Research Fund:
"Cation Ordering in Synthetic Trioctahedral Micas"
$18,000 funded, 7/1/87-8/31/89
$4,500 supplement, 5/1/88-9/30/88
$2,500 supplement, 5/1/89-7/1/89
"Detailed Crystal Chemistry of Iron-Bearing Phyllosilicates"
$40,000 funded, 5/1/91-8/31/93
$3,000 supplement, 6/1/91-9/30/91

National Science Foundation, Earth Sciences Division:
"Crystal Chemistry and Petrogenesis of Biotites from Pelitic Schists"
$60,000 funded, 7/1/87-6/30/90
"Crystal Chemistry of Metapelitic Minerals in a Petrologic Context"
$50,226 funded, 1/1/89-12/31/90
"Crystal Chemistry of Hydrogen and Oxygen in Common Phyllosilicate Minerals"
$61,774 funded, 1/1/92-12/31/93
“Development of Standards for Light Element Analysis in Geological Materials: Collaborative Research"
$ 21,639 funded, 6/1/93-12/31/95
"The Boron Budget in High-Grade Pelitic Metamorphic Rocks: How, When, and Where does the Boron Go?" (Joint with C.V. Guidotti and E.S. Grew)
$56,333 funded for period 1/1/96-12/31/97
"Hydrogen Partitioning and Fe^{3+} Exchange in Mantle Minerals: Effects on Mechanical Behavior - Collaborative Research" (Joint with S.J. Mackwell)
$142,997 funded for period 11/1/93 to 5/31/98
$5,000 supplement funded for 5/1/94 to 9/1/94
"Redox Processes in Rio Grande Rift and Colorado Plateau Xenoliths: Collaborative Research" (Joint with A.V. McGuire)
$55,598 funded for period 6/1/94-5/31/98
$7,000 supplement funded for 5/1/95 to 9/1/95
“Synchrotron MicroXANES Study of Iron Redox in Mantle Phases”
$60,000 funded for period 8/15/98 - 2/28/01
“R.U.I.: Acquisition of a New Mössbauer spectrometer”
$49,840 funded for period from 3/1/99 - 2/28/01
“R.U.I.: Collaborative Research: Chemical Equilibria Involving Iron and Hydrogen in Metapelites from Western Maine”
$27,468 funded for period from 8/1/99 - 7/31/01
“RUI: Acquisition of a Scanning Electron Microscope at Mount Holyoke College”
$226,560 funded for period from 6/1/02-5/30/03

"RUI: Collaborative Research: Hydrogen and Ferric Iron in Felsic Melts"
(collaborative with Sheila Seaman, University of Massachusetts)
$86,000 funded for period from 1/1/03-12/31/06
"RUI: Collaborative Research: Improvements in the Application of the Mössbauer Effect to Studies of Minerals"
(collaborative with Martha Schaefer, LSU)
$76,939 funded for period from 1/1/05-12/31/08
"Redox Ratios by Fe-XANES**"**
(collaborative with M. Gunter and A. Lanzirotti)
$104,897 funded for period from 6/1/08-5/31/11
"Effects of Composition and Cooling Rate on Fe XANES Glass Calibrations"
(Collaborative with Molly McCanta at Tufts University)
$115,363 funded to MHC for period from 8/1/12 – 7/31/15

National Science Foundation, Division of Computation and Data-Enabled Science and Engineering:
"Transfer Learning for Chemical Analyses from Laser-Induced Breakdown Spectroscopy"
(Sridhar Mahadevan, UMass, Co-I)
$141,129 to MHC for period from 9/1/13 – 8/31/15

National Science Foundation, Division of Undergraduate Education:
"Undergraduate Research Program in Materials Science"
$14,500 funded, 5/1/88-9/30/88
"Undergraduate Research Program in Materials Science"
$36,600 funded, 5/1/89-12/31/89
"Equipment for Program Improvement in Mineralogy/Petrology"
$45,000 funded, 1/1/89-12/31/89
$40,000 match from University of Oregon
$7,500 match from I.B.M. and Novell
"Support for Development of Minerals and Mineralogy: A Three-Dimensional Approach"
$75,000 funded for period from 3/1/00 - 2/28/02
"A Modular, Inquiry-Based Regional Approach to Introductory Laboratories"
(S. Good, C.G. Fisher, R.M. Busch, T.M. Lutz, L. Srogi, and C.G. Wiswall, Co-I's) NSF grant DUE-9850923, $40,800 funded, 6/1/98-5/31/2000.
"An Integrative Curriculum in Earth, Human, and Environmental Sciences
(Joint with L. Savoy, M.J. Markley, A. Werner, M.A. McMenamin, S. Dunn, and T. Millete)
$170,000 funded for period from 1/1/00 - 6/30/05
"Support for Development of Minerals and Mineralogy: A Three-Dimensional Approach"
$417,244 funded for period from 3/1/02 – 2/28/08
"An Integrative Curriculum in Planetary Science"
(C.M. Hamilton, T. Burbine, co-Is)
$91,900 funded for period from 9/1/05 – 8/31/07
"Scaffolding Effective Practice for Use of Animations in Teaching Mineralogy and Physical Geology"
(M. Gunter and L. Wenk, Co-I's)
$150,000 funded for period from 1/1/09 -12/31/10
"Building Analytical Competence for Geoscience Students through use of Spectroscopic Tools"
(Collaborative with John B. Brady and Eileen McGowan)
$73,375 funded to MHC for period 8/15/12-7/31/15

National Science Foundation Scholarships in Science, Technology, Engineering, and Mathematics
"Improving Recruitment and Retention of Transfer Students to STEM Majors at Mount Holyoke College"
(Sarah Bacon and Becky Packard, Co-Is)

$600,000 for period from 1/1/12-12/31/16

Packard Foundation
"Earth and Environmental Sciences in California and the Southwest" (Joint with A. Ellison, L. Savoy, and T. Millette)
$200,000 funded for period from 1/1/00 - 12/31/02

Tektronix Foundation:
"Request for Upgrade to Mössbauer Spectroscopy Laboratory"
$4,000, 1987; $6,000, 1988; $10,000, 1989

NASA, Cosmochemistry Division:
"Synchrotron microFTIR characterization of hydrogen in nominally anhydrous minerals in martian materials."
$68,000 funded for period from 1/1/01 - 12/31/02
"Ferric Iron and Hydrogen in Mars Minerals"
$45,000 funded for period from 1/1/03 - 12/31/03
"Acquisition of a 4.5K Mössbauer Spectrometer"
$35,345 funded for period from 1/1/05 to 12/31/06

NASA, Exobiology Program:
"Biogenic iron oxide transformations by thermophilic and mesophilic iron-reducing microbes"
James Holden, University of Massachusetts, PI
$208,316 to MHC for period from 4/1/14-3/31/18

NASA, Mars Fundamental Research Program:
"Temperature Dependence and Resolution of Fundamental Mössbauer Parameters in Mars-Analog Minerals"
$150,000 funded for period from 10/1/02 – 9/30/06
"Taking Apart the Rocks of Mars" (C. Pieters, P.I., J. Bishop, J. Sunshine, T. Hiroi, Co-Is)
NNG04GB53G
$60,000 funded for period from 12/31/03 – 11/30/06
"Analysis and Characterization of Sulfates and Sulfides Using Multiple Spectral Techniques (M. Lane, P.I., J.L. Bishop, Co-I)
$31,000 funded for period from 1/1/05-12/31/06
"Temperature Dependence and Resolution of Fundamental Mössbauer Parameters in Mars-Analog Minerals"
(collaborative with M. Schaefer, LSU)
$90,000 funded for period from 3/1/06-2/28/09
"Mineral Standards and Technique Development for Laser-Induced Breakdown Spectroscopy"
$375,000 funded for period from 3/1/06-2/28/09
"Formation of Magnetic Minerals on Mars by Alteration of Nanophase Ferric Oxides/Oxyhydroxides"
(Janice Bishop, SETI/Ames, PI)
$30,000 funded for period from 3/1/06-2/28/09
"Further Analysis and Characterization of Sulfates and Sulfides Using Multiple Spectral Techniques"
(collaborative with Melissa Lane, Planetary Science Institute (PI), and Janice Bishop, SETI)
$32,000 funded for period from 3/1/06-2/28/09
"Characterizing the Rocks of Mars through Integrated Spectroscopy"
(collaborative with C. Pieters (PI), J. Bishop, M. Lane, T. Hiroi, J. Sunshine)
$60,000 to MHC for period from 3/1/07 – 2/28/11
"Analysis and Characterization of Phosphates Using Multiple Spectral Techniques"

(collaborative with Melissa Lane (PI), Planetary Science Institute, and Janice Bishop, SETI)
$45,947 funded for period from 3/1/08-2/28/12

"The State of Sulfur on Mars: Understanding the Interrelationships Among the Crystal Structure, Chemistry, and Spectroscopy of Sulfates and Sulfides "
(collaborative with Melissa Lane (PI), Planetary Science Institute, and Janice Bishop, SETI)
$97,754 funded to MHC for period from 6/1/10-5/31/13

"Technique Development for Laser-Induced Breakdown Spectroscopy: Calibration, Classification, and Light Element Analysis"
(collaborative with Sam Clegg and Roger Wiens, LANL, and Martha Schaefer)
$719,000 funded for period from 3/1/09 – 5/30/14

"Effects of Shock Metamorphism on Phyllosilicate Spectroscopy"
(Joseph Michalski, P.I.)
$67,941 funded to MHC for period from 6/1/10-5/31/14

"Impact History and Meteoritic Contributions to the Martian Upper Crust"
(collaborative with Caleb Fassett, PI)
$261,888 funded to MHC for period 6/1/14-5/31/18

"Transfer learning for chemical analyses from laser-induced breakdown spectroscopy on the surface of Mars"
(collaborative with Sridhar Mahadavean)
$445,093 funded to MHC for period 11/29-14-11/30/17

NASA, Lunar Advanced Science and Exploration Research Program:

"Thermodynamics, VIS-IR Spectroscopy, and Mapping of Adsorbed Water on the Moon"
(K. Hibbitts, PI)
$33,920 to MHC for period from 6/1/08 – 5/31/09

"Pyroxene Spectroscopy as a Tool to Probe the Composition and Thermal History of the Lunar Surface"
(Rachel Klima, PI)
$104,914 to MHC for period from 1/1/10 – 5/31/13

"The Stability and Transport of Water on the Moon"
(Karl Hibbitts, P.I.)
$106,614 funded to MHC for period from 9/1/11-6/30/15

"Solar Wind Induced Production of Hydroxyl and Water on the Moon"
(Thomas Orlando, PI)
$9,313 to MHC for period from 9/1/11-6/30/15

NASA, Mars Science Laboratory Participating Scientist Program:

"Enhancing Science Return from ChemCam through Laboratory and Statistical Analyses and Integration with APXS"
$476,885 for period from 2/15/12-12/31/16

NASA, Lunar Science Institute Program:

"The Moon as Cornerstone to the Terrestrial Planets: The Formative Years"
C.M. Pieters, PI, Brown University
$135,000 funded to MHC for period from 4/9/09 – 4/8/14

NASA Planetary Geology and Geophysics Program:

"Integrated Spectroscopy of Pyroxenes: Composition, Structure, and Thermal History"
(Rachel Klima, PI)
$32,711 to MHC for period from 8/5/11-8/4/14

"Pyroxene Spectroscopy, Composition, Structure, and Thermal History"
(Rachel Klima, PI)

$91,313 to MHC for period from 6/1/13 – 5/31/16

NASA Solar System Workings Program:
"SuperCam-Analog Laser-induced Breakdown Spectrometer at Mount Holyoke College"
$445,095 for period 10/1/16-9/30/18

CURRENT FUNDING:

NASA, Solar System Exploration and Research Virtual Institute Program:
"Remote, In Situ, and Synchrotron Studies for Science and Exploration"
Tim Glotch, Stony Brook Univ., PI (**Dyar is Deputy PI**)
$777,256 to MHC for period from 1/1/14-12/31/18
"Volatiles, Regolith and Thermal Investigations Consortium for Exploration and Science (VORTICES)"
Ben Bussey, APL, PI
$51,998 to PSI for period from 1/1/14-12/31/18
"Environment and Evolution of Exploration Destinations: Science and Engineering Synergism"
Carle Pieters, Brown Univ., PI
$135,600 to MHC for period from 1/1/14-12/31/18
"TREX: Toolbox for Research and Exploration"
Amanda Hendrix, PSI, PI
$5,483,517 to PSI 6/1/17 – 5/31/22

NASA, Exobiology Program:
"ICE-MAMBA Ice-covered Chemosynthetic Ecosystems: Mineral Availability and MicroBiological Accessibility"
Jill Mikuchi, Univ. of Tennessee, PI
$208,316 to PSI for period from 1/22/17-1/21/20
"Fe(III) Oxide Reduction by a Hyperthermophillic Crenaraeon: Novel Mechanisms and Detection"
James Holden, Univ. of Massachusetts, Amherst, PI
$230, 236 to Planetary Science Institute for period from 10/1/18 – 9/30/21

NASA Emerging Worlds Program:
"Volatile Adsorption onto Primitive Grains for Understanding the Formation of the Early Solar System"
Karl Hibbitts, PI
$13,858 to PSI for period from 3/1/5-2/28/18

NASA Solar System Workings Program:
"Oxidation State of Lunar Glasses: Implications for Surface and Eruptive Processes on the Moon"
Molly McCanta, PI
$136,530 to PSI for period from 10/1/16-3/30/19
"Towards Quantifying Oxygen Fugacity in Solar System Materials: In Situ Multivalent Element Analyses in Pyroxene"
Molly McCanta, PI
$267,184 to Dyar for period from 10/1/18 – 9/30/21

NASA Planetary Data Archiving, Restoration, and Tools:
"Advanced XAS Calibration Tools for In Situ Analysis of Redox States of Fe, Ti, Mn, Cr, V, and Eu in Extraterrestrial Glasses"
$208,997 to PSI for period from 1/15/17-1/14/20

NSF Information Integration and Informatics

"Collaborative Research: Deep Learning for Spectroscopy"
Collaborative with Sridhar Mahadevan and Mario Parente
$373,793 to MHC for period from 4/1/16-3/31/20

NSF Petrology and Geochemistry:
"Refining Geothermobarometry in Pyroxenes using In Situ Measurements of Fe^{3+}"
$172,000 fto MHC or period from 7/1/18 – 6/30/2101

NSF Planetary Astronomy:
"Formation, Stability, and Detection of Amorphous Ferric Sulfate Salts on Mars"
Elizabeth Sklute, PI
$232,273 to MHC for period from 10/1/18 – 9/30/21

EXHIBIT B

Previous Four Years of Expert Testimony for Melinda Darby Dyar, Ph.D.

Dr. Melinda Darby Dyar has not testified as an expert at trial or by deposition during the previous four years.